MCEER

EARTHQUAKE ENGINEERING TO EXTREME EVENTS

ISSN 1520-295X

Experimental Investigation of Full-Scale Two-Story Steel Plate Shear Walls with Reduced Beam Section Connections

by

Bing Qu, Michel Bruneau, Chih-Han Lin and Keh-Chyuan Tsai

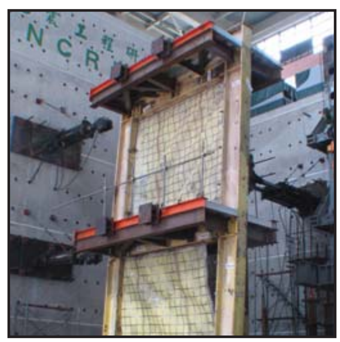

Technical Report MCEER-08-0010

March 17, 2008

This research was conducted at the University at Buffalo, State University of New York and was supported primarily by the Earthquake Engineering Research Centers Program of the National Science Foundation under award number EEC 9701471.

NOTICE

MCEER
EARTHQUAKE ENGINEERING TO EXTREME EVENTS

Experimental Investigation of Full-Scale Two-Story Steel Plate Shear Walls with Reduced Beam Section Connections

by

B. Qu,[1] M. Bruneau,[2] C-H. Lin[3] and K-C. Tsai[4]

Publication Date: March 17, 2008
Submittal Date: March 1, 2008

Technical Report MCEER-08-0010

Task Number 10.2.1

NSF Master Contract Number EEC 9701471

1 Assistant Professor, Department of Civil and Environmental Engineering, California Polytechnic State University; Former Graduate Student, Department of Civil, Structural, and Environmental Engineering, University at Buffalo, State University of New York
2 Professor, Department of Civil, Structural, and Environmental Engineering, University at Buffalo, State University of New York
3 Assistant Research Fellow, National Center for Research on Earthquake Engineering
4 Director, National Center for Research on Earthquake Engineering, and Professor, National Taiwan University

MCEER
University at Buffalo, State University of New York
Red Jacket Quadrangle, Buffalo, NY 14261
Phone: (716) 645-3391; Fax (716) 645-3399
E-mail: *mceer@buffalo.edu*; WWW Site: *http://mceer.buffalo.edu*

Preface

The Multidisciplinary Center for Earthquake Engineering Research (MCEER) is a national center of excellence in advanced technology applications that is dedicated to the reduction of earthquake losses nationwide. Headquartered at the University at Buffalo, State University of New York, the Center was originally established by the National Science Foundation in 1986, as the National Center for Earthquake Engineering Research (NCEER).

Comprising a consortium of researchers from numerous disciplines and institutions throughout the United States, the Center's mission is to reduce earthquake losses through research and the application of advanced technologies that improve engineering, pre-earthquake planning and post-earthquake recovery strategies. Toward this end, the Center coordinates a nationwide program of multidisciplinary team research, education and outreach activities.

MCEER's research is conducted under the sponsorship of two major federal agencies: the National Science Foundation (NSF) and the Federal Highway Administration (FHWA), and the State of New York. Significant support is derived from the Federal Emergency Management Agency (FEMA), other state governments, academic institutions, foreign governments and private industry.

MCEER's NSF-sponsored research objectives are twofold: to increase resilience by developing seismic evaluation and rehabilitation strategies for the post-disaster facilities and systems (hospitals, electrical and water lifelines, and bridges and highways) that society expects to be operational following an earthquake; and to further enhance resilience by developing improved emergency management capabilities to ensure an effective response and recovery following the earthquake (see the figure below).

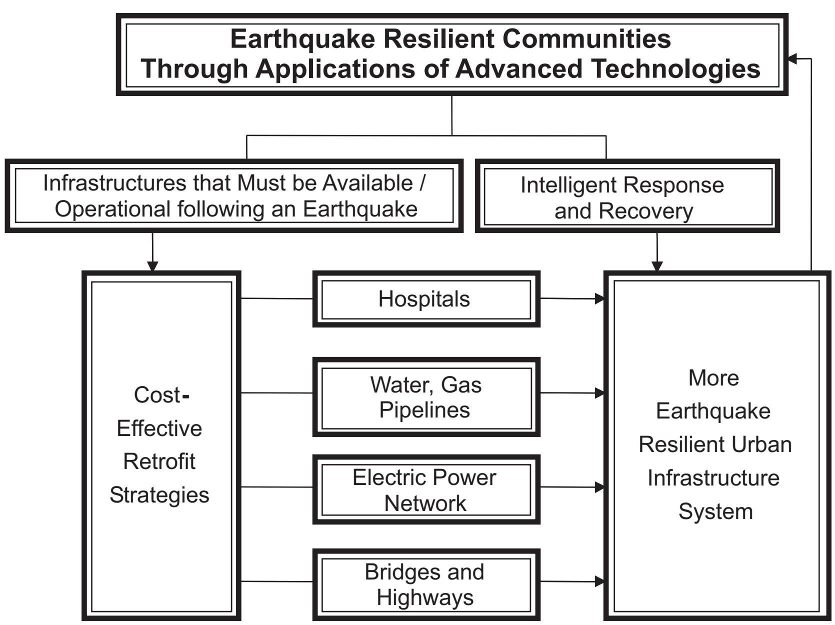

A cross-program activity focuses on the establishment of an effective experimental and analytical network to facilitate the exchange of information between researchers located in various institutions across the country. These are complemented by, and integrated with, other MCEER activities in education, outreach, technology transfer, and industry partnerships.

This report describes a two-phase experimental research program on Steel Plate Shear Walls (SPSWs), conducted in collaboration with the National Center for Research on Earthquake Engineering (NCREE) in Taipei, Taiwan. The research project investigated the replaceability of infill panels following an earthquake, the behavior of a repaired SPSW in a subsequent earthquake, and the seismic performance of intermediate beams. The test specimen was a two-story SPSW that had an intermediate composite beam with reduced beam section (RBS) connections. In Phase I, the specimen was pseudodynamically tested and subjected to three ground motions of progressively decreasing intensity. The buckled panels were replaced by new panels prior to subjecting the specimen to a subsequent pseudodynamic test and cyclic test to failure in Phase II. The results showed that replacing the buckled infill panels was a viable option that would provide adequate resistance against future earthquakes. The repaired SPSW performed well during the subsequent earthquake and dissipated a similar amount of energy without causing severe damage to the boundary frame or exhibiting overall strength degradation.

ABSTRACT

Steel Plate Shear Walls (SPSWs) consist of infill steel panels surrounded by boundary frame members. These infill panels are allowed to buckle in shear and subsequently form diagonal tension field actions to resist the lateral loads applied on the structure. Research conducted since the early 1980s has shown that this type of system can exhibit high initial stiffness, behave in a ductile manner, and dissipate significant amounts of hysteretic energy, which make it a suitable option for the design of new buildings as well as for the retrofit of existing constructions. However, some impediments still exist that may limit the widespread acceptance of this structural system. For example, no research has directly addressed the replaceability of infill steel panels following an earthquake, and uncertainties remain regarding the seismic behavior of intermediate beams in a multi-story SPSW. Intermediate beams are those to which steel plates are welded above and below, by opposition to anchor beams at the top and bottom levels that have steel plates only below or above.

The work presented in this report experimentally investigates the above issues with regards to SPSW performance. A two-phase experimental program was conducted on a full-scale two-story SPSW with reduced beam section connections and composite floors. In Phase I, the specimen was pseudodynamically tested, subjected to three ground motions of progressively decreasing intensity. The buckled panels were replaced by new panels prior to subjecting the specimen to a subsequent pseudodynamic test and cyclic test to failure in Phase II.

It is shown that the repaired specimen can survive and dissipate significant amounts of hysteretic energy in a subsequent earthquake without severe damage to the boundary frame or overall strength degradation. It is also found that the specimen had exceptional redundancy and exhibited stable force-displacement behavior up to the story drifts of 5.2 and 5.0% at the first and second story, respectively. Experimental results from pseudodynamic and cyclic tests, respectively, are compared to the seismic performance predictions obtained from a dual strip model using tension only strips and a monotonic pushover analysis using a three-dimensional finite element model, and good agreement is observed.

ACKNOWLEDGEMENTS

Sincere Thanks to the fine people at the National Center for Research on Earthquake Engineering (NCREE), located in Taipei, Taiwan, Republic of China, especially Professor Keh-Chyuan Tsai and his research assistants Mr. Chih-Han Lin and Mr. Ying-Cheng Lin for facilitating the experimental portion of the research described in this report. The writers are also grateful to China Steel, who provided the construction materials for the specimens.

This work was financially supported in part by the Earthquake Engineering Research Centers Program of the US National Science Foundation under Award Number ECC-9701471 to the Multidisciplinary Center for Earthquake Engineering Research (MCEER), and in part by the Taiwan National Science Council and NCREE. All sponsors are gratefully acknowledged. However, any opinions, findings, conclusions, and recommendations presented in this document are those of the writers and do not necessarily reflect the views of the sponsors.

TABLE OF CONTENTS

TABLE OF CONTENTS (cont'd)

TABLE OF CONTENTS (cont'd)

TABLE OF CONTENTS (cont'd)

LIST OF FIGURES

FIGURE	TITLE	PAGE

LIST OF FIGURES (cont'd)

LIST OF FIGURES (cont'd)

LIST OF FIGURES (cont'd)

LIST OF FIGURES (cont'd)

LIST OF FIGURES (cont'd)

LIST OF TABLES

NOTATIONS

A_b	cross-section area of beam
A_c	cross-section area of column
E	young's modulus
H	story height
I_c	moment of inertia of column
L	bay width
t	thickness of infill panel
α	infill tension field inclination angle
$\varepsilon_{\ln}^{pl}$	logarithmic strain
σ_{true}	Cauchy stress

ABBREVIATIONS

AISC	American Institute of Steel Construction
ATC	Applied Technology Council
CSA	Canadian Standards Association
FEMA	Federal Emergency Management Agency
HBE	Horizontal Boundary Element
MCEER	Multidisciplinary Center for Earthquake Engineering Research (Buffalo, NY)
NCREE	National Center for Research on Earthquake Engineering (Taipei, Taiwan)
PGA	Peak Ground Acceleration
RBS	Reduced Beam Section
SPSW	Steel Plate Shear Wall
UB	University at Buffalo
VBE	Vertical Boundary Element

SECTION 1

INTRODUCTION

1.1 General

Steel Plate Shear Walls (SPSWs), which consist of infill steel panels surrounded by columns, called Vertical Boundary Elements (VBEs), and beams, called Horizontal Boundary Elements (HBEs) have been used as lateral force resisting system in a large number of building structures in the United States, Canada, Mexico, Japan, Taiwan and other countries.

Early designs of SPSW infill panels only allowed for elastic behavior, or shear yielding in the post-elastic range, an approach that typically resulted in the selection of relatively thick or heavily-stiffened infill panels. These designs, while resulting in a stiffer structure that would reduce displacement demand as compared to the bare steel frame structure during seismic events, would also induce relatively large infill panel yield forces on the boundary frame members, resulting in substantial amounts of steel used and expensive detailing.

Researchers on the behavior of SPSWs in the early 1980s (Thorburn *et al.* 1983) proposed the use of relatively thinner plates for the infill panels. Such thin infill panels are allowed to buckle in shear and subsequently form diagonal tension field actions to resist the lateral loads applied on the structure. Significant research contributions by others since then, investigating behavior of SPSWs using the monotonic and cyclic loading and shaking table tests, have shown that this type of structural system can exhibit high initial stiffness, behave in a ductile manner, and dissipate significant amounts of hysteretic energy, which make it a suitable option for the design of new buildings as well as for the retrofit of existing constructions (Thorburn *et al.*1983; Tromposch and Kulak 1987, Driver *et al.* 1997; Rezai 1999, Lubell *et al.* 2000, Berman and Bruneau 2003, and Vian and Bruneau 2005). In addition, analytical research on SPSWs has also validated useful models for the design and analysis of this lateral load resisting system (Thorburn *et al.*1983; Elgaaly *et al.*1993; Driver *et al.* 1997; Berman and Bruneau 2003).

As a result of the above research, design procedures for SPSWs are provided by the CSA Limit States Design of Steel Structures (CSA 2000) and the AISC Seismic Provisions for Structural Steel Buildings (AISC 2005). Innovative SPSW designs have also been proposed and experimentally validated to expand the range of applicability of SPSWs (Berman and Bruneau 2003; Vian and Bruneau 2005).

However, some impediments still exist that may limit the widespread acceptance of this system. For example, no research has directly addressed the replaceability of infill steel panels following an earthquake, and there remains uncertainties regarding the seismic behavior of HBEs of SPSWs. The latter problem was addressed by Vian and Bruneau (2005) and Lopez Garcia and Bruneau (2006), resulting in useful models for design of anchor HBEs (i.e. those HBEs at the ground and roof levels of SPSWs). However, more detailed experimental information about seismic behavior intermediate HBE (intermediate HBEs are those to which are welded steel plates above and below, by opposition to anchor HBEs that have steel plates only below or above) remains missing, particularly for those HBEs having reduced beam section (RBS) connections.

1.2 Scope and Objectives

This report describes an experimental research program conducted to investigate the replaceability of infill panels and the seismic behavior of intermediate HBEs – issues that impact the performance of SPSWs.

First, in collaboration with the National Center for Research on Earthquake Engineering (NCREE) in Taipei, Taiwan, a two-phase experimental program was conducted to test a two-story SPSW specimen having an intermediate composite beam with RBS connections. The testing program also investigated how to replace the infill panels of the SPSW after a severe earthquake and how the repaired SPSW would behave in a second equally severe earthquake.

Next, analytical studies using both a simple model (called the strip model) and a 3D finite element (FE) model were conducted to replicate the SPSW behavior observed from tests.

1.3 Outline of Report

Section 2 contains a brief overview of past experimental research related to this structural system in applications to provide earthquake resistance.

Section 3 describes design of the tested specimen from a prototype steel plate shear wall. Following this, details on the test setup are given along with relevant descriptions and results of sample coupon testing. Finally, the instrumentation layout is described.

Section 4 presents results of the experimental program. The determination of loading protocol and the methods of load application are presented, followed by force versus displacement hysteresis plots, photos of accumulated damage, and related descriptions.

Section 5 describes the analytical model development and results of analytical investigations of the experimental results. Both the strip model and the 3D finite element (FE) model are considered. Effectiveness of the developed models is also discussed.

Conclusions based on the information presented in the previous sections are made in Section 6 and recommendations for future research are given.

SECTION 2

REVIEW OF PAST EXPERIMENTAL RESEARCH ON STEEL PLATE SHEAR WALLS

2.1 Introduction

Prior to key research performed in the 1980s (Thorburn *et al.* 1983), designs of SPSW infill panels only allowed for elastic behavior, or shear yielding in the post-elastic range. This design concept typically resulted in selection of relatively thick or heavily-stiffened infill panels. While resulting in a stiffer structure that would reduce displacement demand as compared to the bare steel frame structure during seismic events, these designs would induce relatively large infill panel yield forces on the boundary frame members, resulting in substantial amounts of steel used and expensive detailing. Numerous experimental and analytical investigations conducted since 1980s have demonstrated that a SPSW having unstiffened thin infill panels allowed to buckle in shear and subsequently form a diagonal tension field absorbing input energy, can be an effective and economical option for new buildings as well as for the retrofit of existing constructions in earthquake-prone regions. While extensive reviews of past research can be found in the literature (i.e. Berman and Bruneau 2003, Vian and Bruneau 2005, Sabelli and Bruneau 2007, to name a few), some work relevant to the work presented here is summarized below, with more emphasis on experimental research on large scale SPSWs.

2.2 Thorburn, Kulak, and Montgomery (1983)

Based on the theory of diagonal tension field actions first proposed by Wagner (1931), Thorburn *et al.* (1983) investigated the postbuckling strength of SPSWs and developed two analytical models to represent unstiffened thin infill panels that resist lateral loads by the formation of tension field actions. In both cases, contribution to total lateral strength from the compressive stresses in the infill panels were neglected because it was assumed that plate buckles at a low load and displacement level. In addition, it was assumed that the columns were continuous over the whole height of the wall, to which the beams were connected using simple connections (i.e. "pin" connections).

The first model, an equivalent brace model used to provide the story stiffness of a panel, represents the infill panels as a single diagonal tension brace at each story. Based on elastic strain energy formulation, analytical expressions were provided for the area of this equivalent brace member for two limiting cases of column stiffness, namely, infinitely rigid against bending and completely flexible.

The second model proposed by Thorburn *et al.* (1983) is strip model (also known as a multi-strip model), in which each infill panel is represented by a series of inclined pin-ended only members, as shown in figure 2-1, that have a cross-sectional area equal to strip spacing times the panel thickness.

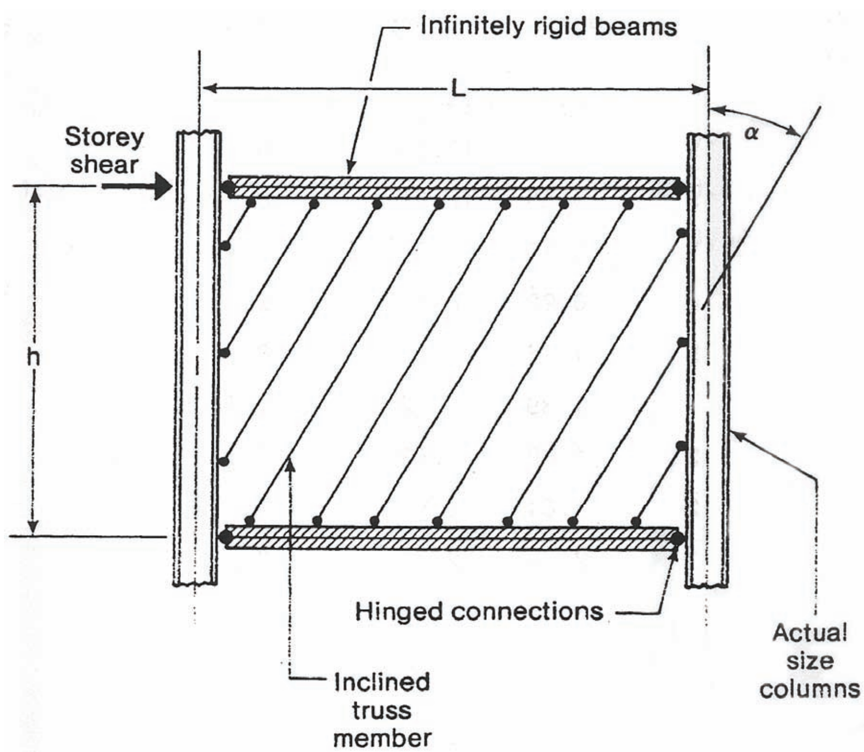

FIGURE 2-1 Schematic of Strip Model (Thorburn *et al.* 1983)

It was found that a minimum of ten strips is required at each story to adequately replicate the behavior of the wall. Using the principle of least work, the inclination angle for the strip, denoted as α, and equal to that of the tension field can be determined for the infinitely rigid column case, as,

$$\tan^4 \alpha = \left[\frac{1 + \frac{L \cdot t}{2 \cdot A_c}}{1 + \frac{H \cdot t}{A_b}} \right] \tag{2-1}$$

where H is the story height; L is the bay width; t is the infill panel thickness; and A_b and A_c are cross section areas of the beam and column, respectively.

2.3 Timler and Kulak (1983)

Based on the work by Thorbrrn *et al.* (1983), Timler and Kulak (1983) considered the effects of column flexibility and revised equation (2-1):

$$\tan^4 \alpha = \left[\frac{1 + \frac{L \cdot t}{2 \cdot A_c}}{1 + H \cdot t \cdot \left(\frac{1}{A_b} + \frac{H^3}{360 \cdot I_c \cdot L} \right)} \right] \tag{2-2}$$

where I_c is the moment of inertia of column, and all other terms were defined previously. This equation appears in both the Canadian CSA-S16-01 Standard (CSA 2000) and the 2005 AISC Seismic Provisions (AISC 2005) for design of SPSWs.

Timler and Kulak also conducted a test on a large-scale SPSW to verify the analytical work of Thorburn *et al.* (1983). A SPSW specimen, shown in figure2-2, consisting of 5mm thick infill panels was tested under quasi-static cyclic loading. The bay dimensions were 3750 mm wide by 2500 mm high. Simple beam-to-column connections were used. Beams and columns were W310x129 and W460x144 respectively. No gravity loads were applied to the specimen.

The angle of inclination of the tension field along the centerline of the panel was found to vary from 44° to 56°. The maximum load attained was 5395 kN. Failure of the specimen resulted from tearing of the weld used to connect the infill plate to the fish plate, and it was concluded that, if this had been avoided, the specimen could have resisted a larger ultimate load.

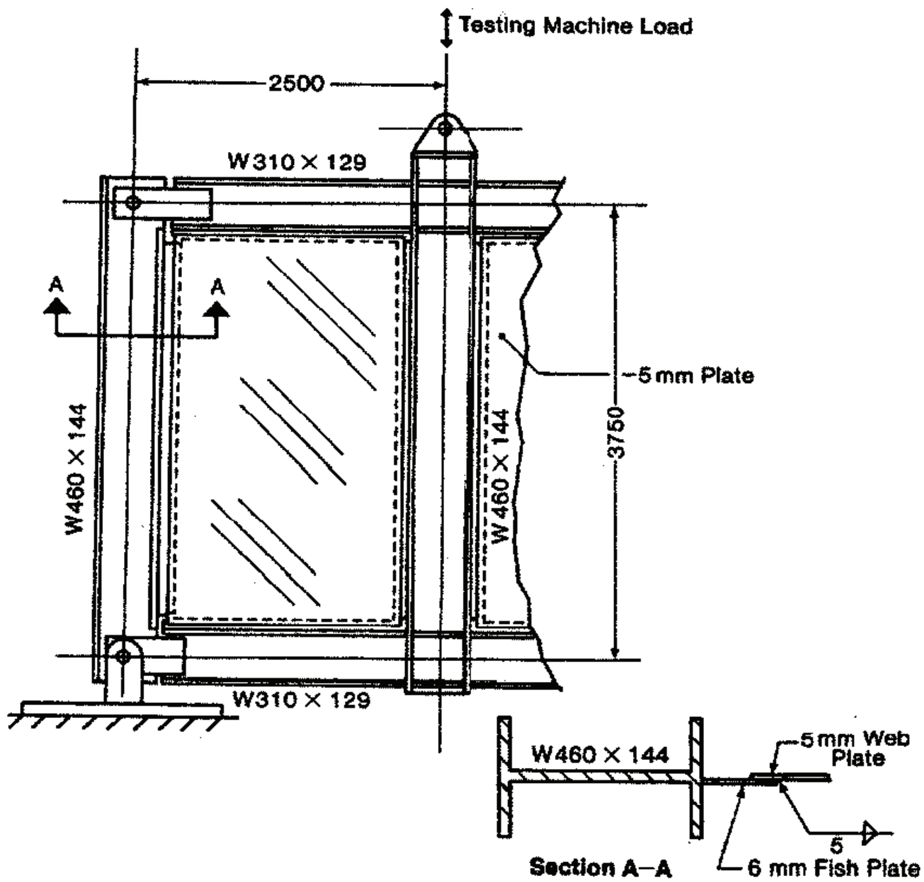

FIGURE 2-2 Schematic of Test Specimen (Timler and Kulak 1983)

2.4 Driver, Kulak, Kennedy and Elwi (1997)

Driver *et al.* (1997) tested a large-scale four-story SPSW with unstiffened infill panels and moment-resisting beam-to-column connections as shown in figure 2-3 using a sequence of loading intended to simulate a severe seismic event. Gravity loads were applied to each column and cyclic in-plane horizontal loads were applied at each floor level. The cyclic deflection amplitudes were gradually increased according to the recommendations outlined in ATC-24 (ATC 1992) until failure. The test specimen was able to resist increasingly higher loads in each successive cycle until a deflection of five times the deflection corresponding to the point of first significant yielding, after which degradation of the load-carrying capacity was gradual and stable. The cycle in which the peak capacity occurred coincided approximately to that in which plate tore and local column flange buckling began to take place in the lowest story. Prior to failure of the specimen, the lowest story reached nine times its yield deflection. The test specimen proved to be initially very stiff, showed excellent ductility and energy dissipation characteristics, and exhibited stable behavior at very large deformations and after many cycles of loading.

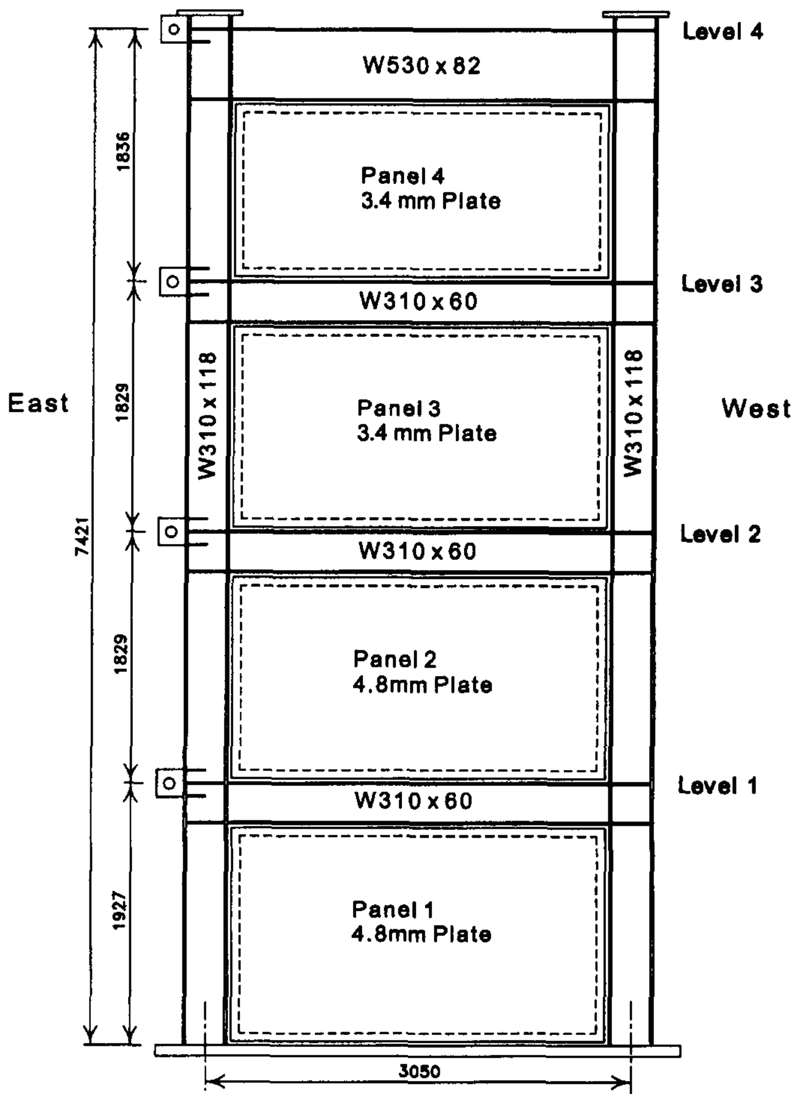

FIGURE 2-3 Schematic of Test Specimen-North Elevation (Driver *et al.* 1997)

2.5 Berman and Bruneau (2005)

Berman and Bruneau (2005) conducted quasi-static cyclic testing on three SPSW specimens having light gauge cold-formed steel for the infill panels. Two specimens using flat infill panels and one specimen using type B corrugated steel deck were tested subjected to ATC-24 loading protocol. Test setup is shown in figure 2-4. Boundary frame members were designed to remain elastic. Beams had flexible connections to the columns. In two of the three specimens, epoxy was used as an attempt to provide an alternative way to connect infill panels to the fishplates for retrofit instance where welding fumes are unacceptable to occupants. Epoxied connection proved ineffective for the flat plate case, but worked for the corrugated panel.

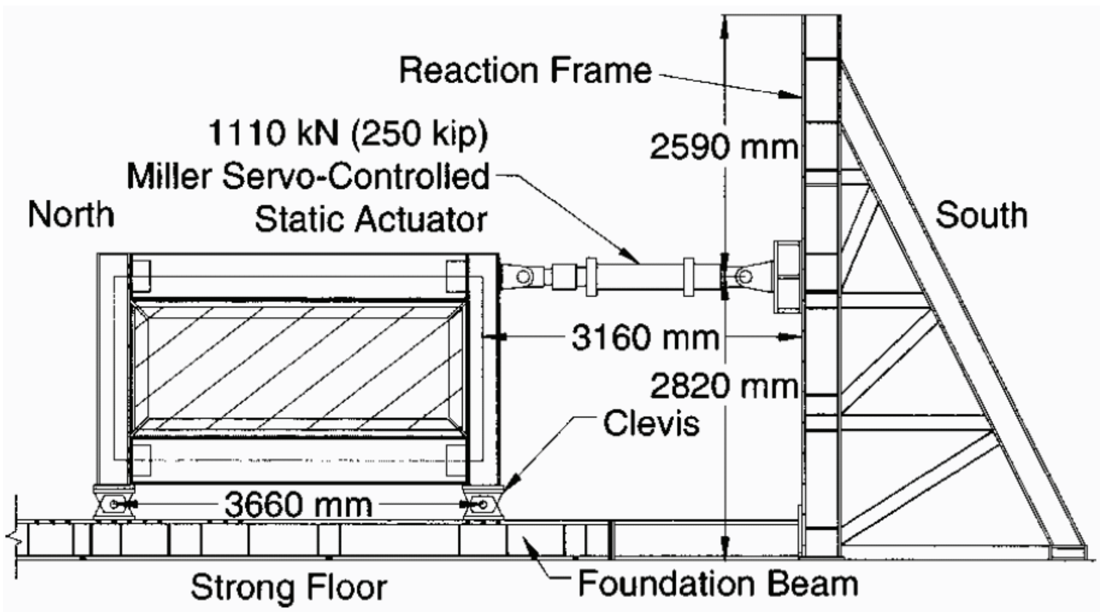

FIGURE 2-4 Schematic of Testing Setup (Berman and Bruneau 2005)

From the hysteresis curves and monotonic results of pushover analysis using strip model, it was found the corrugated infill panel contributed over 90% to the total initial stiffness and this specimen exhibited unsymmetric hysteresis loops since the tension field action only developed in the direction of the corrugations, a behavior similar to that a braced frame with single slender brace (Bruneau *et al.* 1998). To achieve symmetric system behavior, the researchers recommended two walls with opposed orientation of corrugations be used.

The specimen using flat infill panel welded to boundary frame members reached a ductility ratio of 12 and drift of 3.7%. Reasonable agreement was observed in the initial stiffness and base shear strength through the comparison between experimental and monotonic pushover results. The flat infill panel contributed approximately 90% of the initial stiffness of the system.

2.6 Lin and Tsai (2004)

Lin and Tsai (2004) explored two solutions to reduce the out-of-plane deformations of the infill panels that typically develop when the tension fields are fully formed. The first option considered is tube restrainers placed on both sides of the infill panels. Two specimens with 2 tubes and 3 tubes, as shown in figures 2-5 and 2-6 respectively, were studied. An additional specimen of the other option utilized a concrete panel adjacent to the infill steel panel to reduce panel buckling as shown in figure 2-7. In all cases, the specimens were tested under quasi-static cyclic loading scheme.

The similarities of infill panels and boundary frame members in the SPSW specimens made it possible to have a direct comparison of the test results between the restrained panel by Lin and Tsai (2004), and solid panel by Vian and Bruneau (2005). It was found the maximum base shear of these specimen using restrained systems was an average of 4% higher than the unstiffened solid panel specimen; while the elastic stiffness was an average of 15% higher. These approaches using the restrainer systems therefore provided a nonsignificant improvement to energy dissipation and hysteresis loops exhibited by the unstiffened solid panel specimen, while the out-of-plane panel buckling amplitude was reduced.

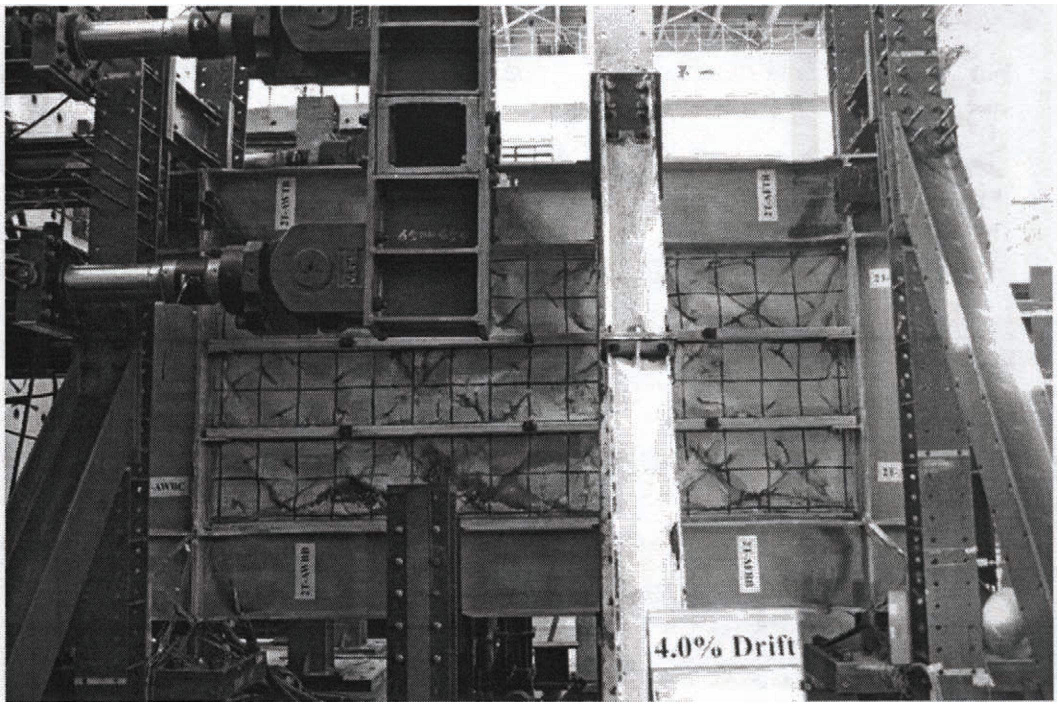

FIGURE 2-5 Specimen 2T Test at 4% Drift (Lin and Tsai 2004)

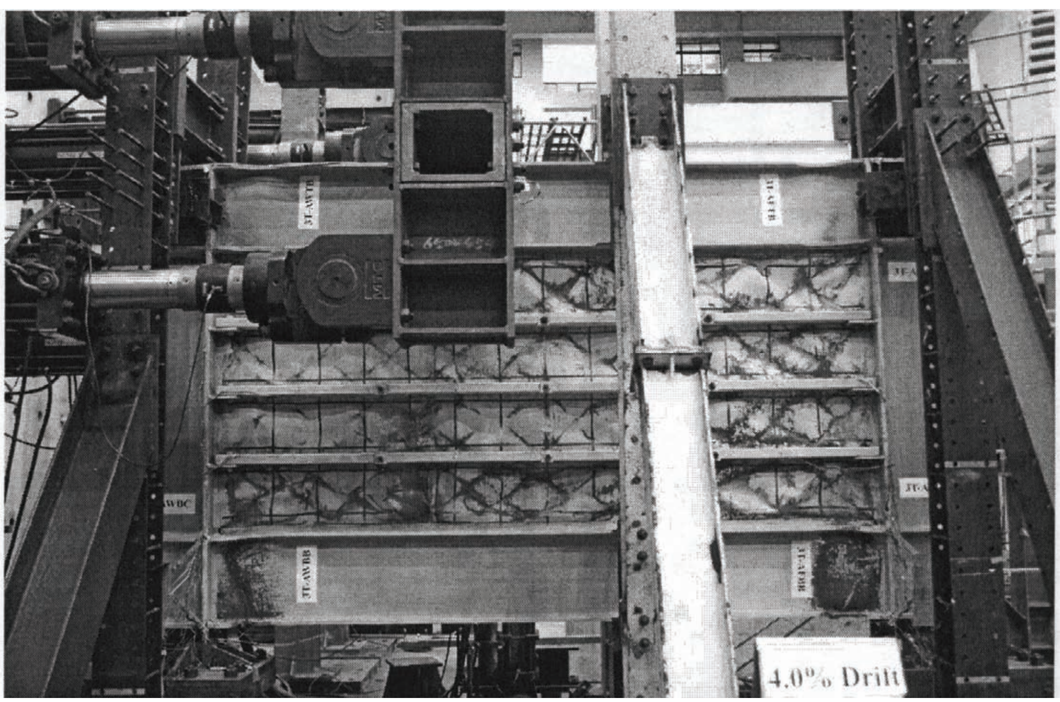

FIGURE 2-6 Specimen 3T Test at 4% Drift (Lin and Tsai 2004)

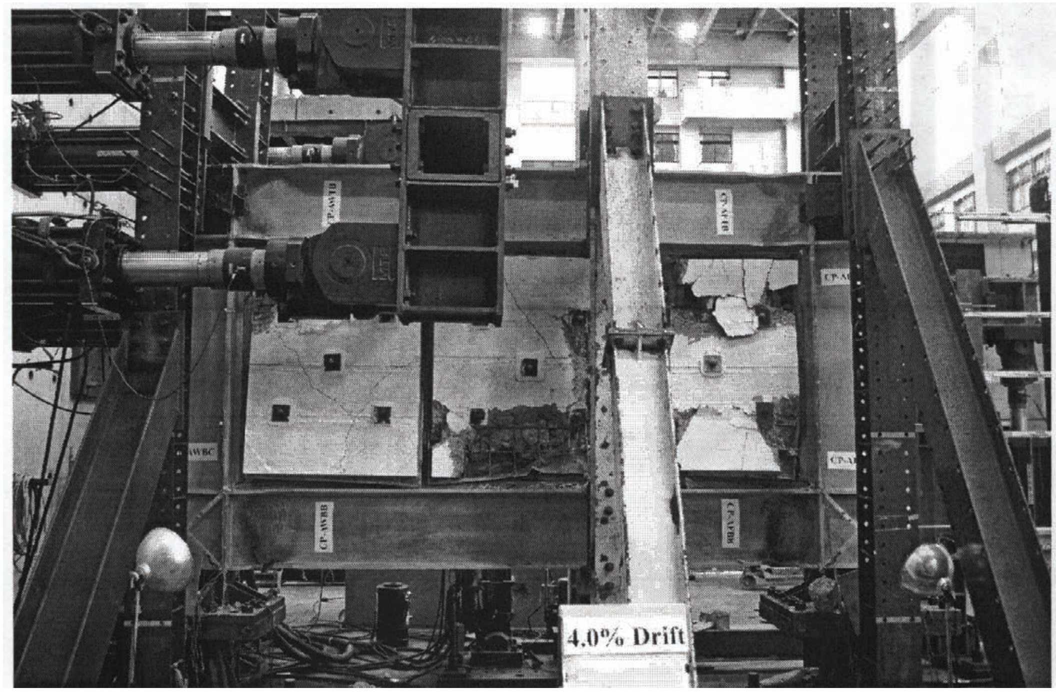

FIGURE 2-7 Specimen CP Test at 4% Drift (Lin and Tsai 2004)

2.7 Vian and Bruneau (2005)

Two variations on the solid fill panel system that allow for the passage of utilities through the plane of the wall were introduced in the study by Vian and Bruneau (2005), as shown in figures 2-8 and 2-9 respectively. One system accomplishes this goal using unstiffened panel perforations, which, it was shown, in addition to allowing utility pass-through, may be used to reduce the strength and stiffness of a solid panel wall to levels required in a design when thinner plate is unavailable. Another system preserves the general strength and stiffness of a solid SPSW panel, while allowing utility passage through a reinforced cutout that transmits panel forces to the boundary frame.

FE analysis was used to investigate the overall behavior of the tested specimens, and aid in defining design displacement limits for ductile performance of the perforated panel system. Based on the test results and analytical investigation, recommendations were presented for the ductile design of SPSW anchor beams and perforated panel systems.

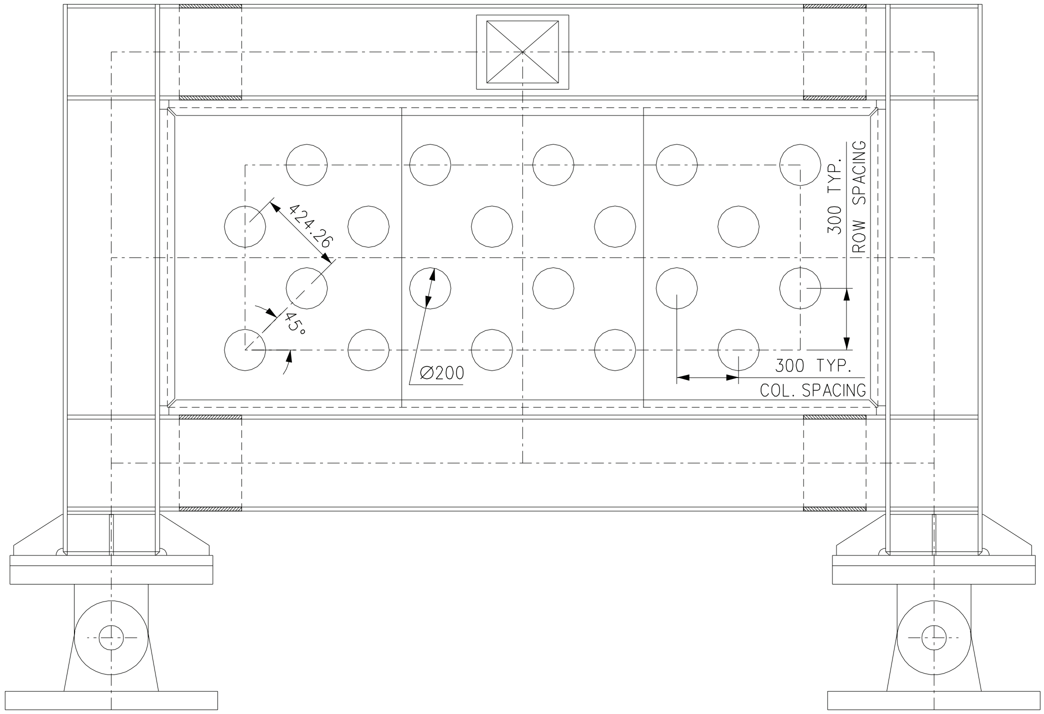

FIGURE 2-8 Specimen P (Vian and Bruneau 2005)

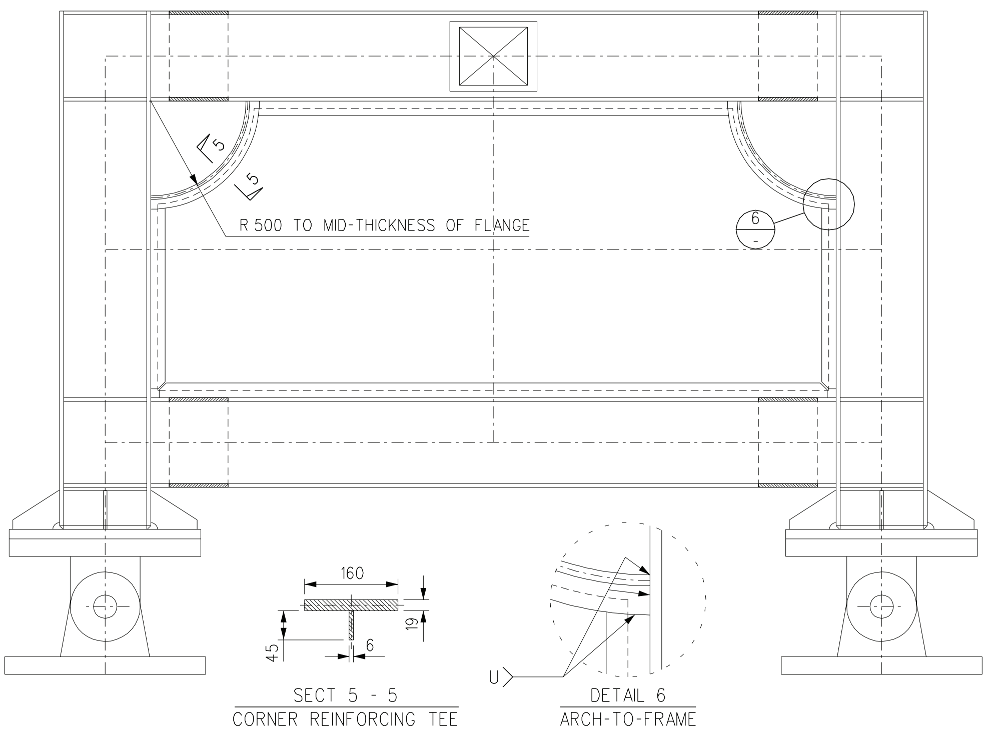

FIGURE 2-9 Specimen CR (Vian and Bruneau 2005)

2.8 Jalali and Sazgari (2006)

Jalali and Sazgari (2006) performed theoretical and experimental post-buckling study on SPSWs. In the first part of their research, the available theoretical relations based on strip model were improved and used to predict the yield displacement and yield strength of a steel panel. The second part described experimental results of a small scale SPSW consisting of 300mmx500mm infill panel and boundary frame using simply connections. The specimen was tested under cyclic loading in order to evaluate the force-displacement relation and post-buckling behavior of the specimen. The test setup was shown in figure 2-10.

It was found the infill panels surrounded by boundary frame members can be able to display ductile behavior. The drifts corresponding to the yielding and rupture in the panel were 1.7% and 5% respectively. The FE analysis of the test specimen accurately predicted the pre-yielding and post-buckling behavior of the steel panel and showed good agreement with the experimental results.

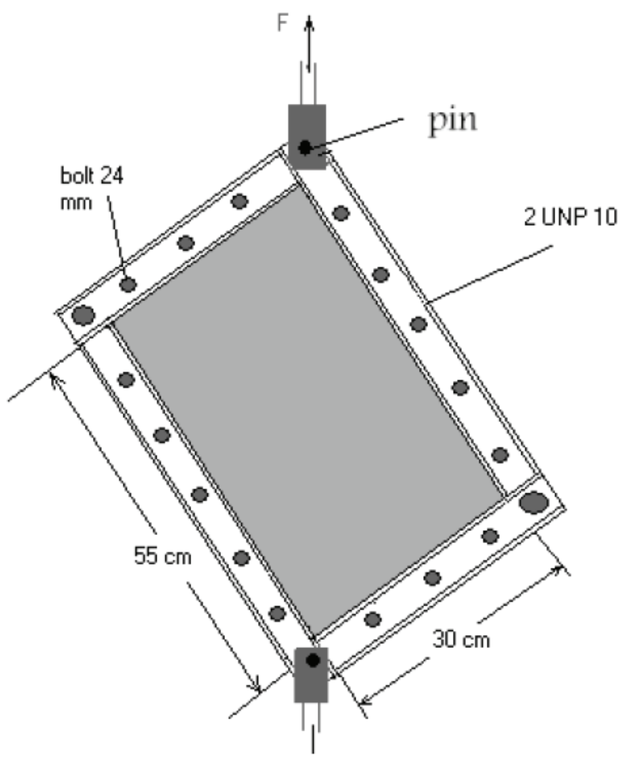

FIGURE 2-10 Test Setup (Jalali and Sazgari 2006)

In the analytical study on the SPSW, several modes of the infill panel were considered, which is necessary for the post-buckling analysis to capture the real behavior of the specimen. Jalali and Sazgari also examined the strain distribution along the strip element. According to the FE results, the observed strain distribution along each strip element was not uniform and the distribution can be approximated as parabolic distribution. The strain at the both ends of the yielded strip is about 5 to 20 times the strain at the middle of the strip.

2.9 Park, Kwack, Jeon, Kim and Choi (2007)

Park *et al*. (2007) investigated the behavior of SPSW with unstiffened thin infill panels. Five one-third specimens of one-bay three-story prototype SPSW were tested under cyclic lateral loading. The primary test parameters included the thickness of infill panels and the strength and compactness of columns. The columns were either compact (SC type) or noncompact (WC type). For the three specimens of SC type, the thicknesses of the infill panels were 2 mm, 4 mm and 6 mm, respectively. For the two specimens of SC type, the thicknesses of the infill panels were 4 mm and 6 mm, respectively. The specimens were fixed at the column bases; later supports were placed to prevent out-of-plane displacement of the boundary frame; and in-plane cyclic loads were applied at the roof level as shown in figure 2-11.

Local tearing failures in the infill panels resulting from the repeatedly orthogonal tension fields were observed in all specimens. Local buckling occurred in columns of the WC specimens, resulting in a reduction of stiffness and strength of the specimen. The SC specimens exhibited good deformation and energy absorption capacity although fractures were observed at the column base and beam-to-column connections.

The researchers classified the SPSW deformation modes as shear-dominated behavior and flexure-dominated behavior respectively. The walls with thin plates show shear dominated behavior, whereas the walls with relatively thick plates show the flexure-dominated behavior. The researchers concluded the shear-dominated walls have better deformation capacity than the flexure-dominated walls, since infill panels yielded early across the wall height and plastic hinges were developed at frame members by moment-frame actions in shear-dominated walls. Based on simple free body diagram, an evaluation method for the SPSW deformation mode was proposed.

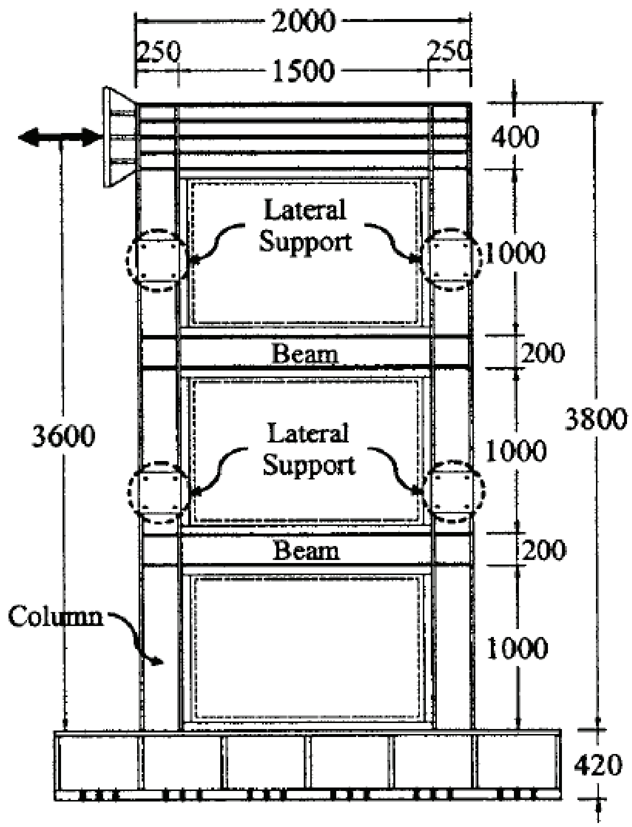

FIGURE 2-11 Dimension of the Specimen (Park *et al.* 2007)

In addition, analytical models were developed for the SPSW specimens. The initial stiffnesses from testing were compared with those from FE analyses. It was found the numerical analyses overestimated the initial stiffnesses of the SPSW specimens by 10% to 30%.

Furthermore, simplified free body diagrams for evaluating strength of columns at the first story to ensure ductile behavior of SPSWs, were proposed and preliminary examinations were made on the specimens using these free body diagrams. However, those free body diagrams incorrectly neglected the effects from boundary frame moment resisting action.

SECTION 3

EXPERIMENTAL PROGRAM DESIGN AND SETUP

3.1 Introduction

As discussed earlier, at the time of this writing, no research had directly addressed the replaceability of the infill panels in SPSWs following an earthquake. There also remained uncertainties regarding the seismic behavior of intermediate HBEs of SPSWs. To address these issues, a two-phase testing program was developed to test a full-scale SPSW. This section first describes design of the SPSW specimen. The specimen had two stories to allow investigations of the seismic behavior of intermediate HBE. The infill panels, which buckled and substantially yielded during the Phase I tests, were replaced by new panels and subjected to the Phase II tests to investigate the replaceability of the infill panels and seismic performance of the so-repaired SPSWs. Following a discussion of the specimen design, specimen fabrication procedure is presented. Next, the complete experimental setup and description of the instrumentation are given. Last, material properties from coupon tests are provided.

3.2 Design of Test Specimen

Selection of the test specimen was done such that representative SPSW frame aspect ratio and infill plate thicknesses could be obtained. A two-story steel building prototype was considered, for which the SPSW test specimen provided part of the lateral force resisting system. For the prototype structure described below, seismic loads were calculated using the equivalent lateral force procedure and the structural components (i.e. infill panels and boundary frame) were sized to resist the corresponding earthquake forces. Limitations of the equipment available for the testing were also considered.

3.2.1 Description and Design Loads of the Prototype Structure

The prototype structure is a two-story steel frame building with plan dimensions of 40 meters in the east-west direction and 32 meters in the north-south direction. The floor plan is shown in figure 3-1. Heights of the first and second story measured from HBE centerlines are respectively 4014 mm and 3952 mm. In the north-south direction (the direction of primary interest) there are two single-bay SPSWs that act as the primary lateral load resisting system as shown in the figure 3-1. The bay width of each SPSW is 4000 mm measured from column centerlines.

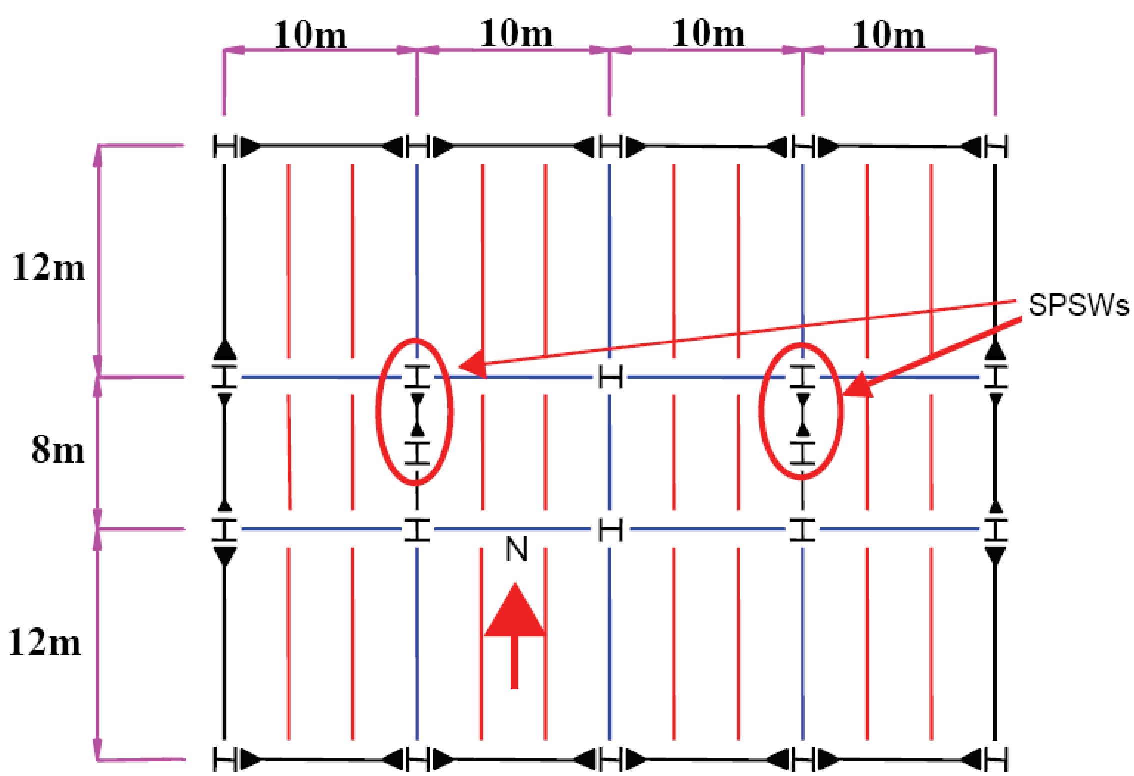

FIGURE 3-1 Plan View of Prototype Structure

Gravity loads determined from the prototype structure and a portion of the design live loads were used as the active seismic weight. The equivalent lateral force procedure of FEMA 450 (FEMA 2003) was used to calculate the design base shear. The corresponding base shear tributary to each SPSW in the prototype structure was approximately 2011 kN (equivalent lateral forces of 667.4 kN and 1343.6 kN applied at the first and second story respectively). Note that the calculation of base shear applied to each SPSW neglected the stiffness of the moment frames along the north-south directions (i.e. assuming all the lateral forces on the prototype structure to be resisted by the SPSW system since the moment frames were assumed to have a small stiffness relative to those SPSWs) as well as the effect of torsional response in plan. This provided a reasonable basis to design plate sizes.

3.2.2 Specimen Design Procedure

Boundary frame members of the specimen were specified to be A572 Gr.50 steel members while the infills were specified be SS400 steel panels, which is similar to ASTM A36 steel (Kuan 2005). For the obtained equivalent lateral forces, design of the specimen was done per the following procedure:

Step 1: Assume inclination angles of infill tension fields at the first and second story respectively.

Step 2: Assume that 75% of the story shears are resisted by the infill panels and calculate the corresponding required plate thickness at each story using the following equation:

$$t_{wi} = \frac{0.75V_i}{0.5 f_{ypi} L \sin 2\alpha_i} \tag{3-1}$$

where V_i is the story shear; f_{ypi} is the yield stress of the infill panel of each story; L is the bay width of the wall; and α_i is the infill tension field inclination angle at each story.

Step 3: Assume the size for the boundary frame members.

Step 4: Calculate the inclination angles of the infill tension fields per the equation provided in the AISC Seismic Provisions. If the calculated angles are close to those assumed in step 1, continue the design. Otherwise, return to step 1 and modify the assumed angles.

Step 5: Calculate the vertical component of the infill panel yield forces acting along the HBEs, ω_{ybi}, according to the following equation:

$$\omega_{ybi} = f_{ypi} t_{wi} \left(\cos\alpha_i\right)^2 \tag{3-2}$$

Step 6: Design the RBS connections at the ends of HBEs per the requirements of FEMA 350, considering the vertical uniform loads determined from (3-2).

Step 7: Perform a pushover analysis on a strip model of the wall to obtain the design forces of boundary frame members.

Step 8: Check the adequacy of the boundary frame members using LRFD beam-column design equations. If all the members are adequate and not overdesigned, continue the design. Otherwise, return to Step 3 and modify the size of the assumed members.

Step 9: Check whether or not the overall system strength (including the contributions of boundary frame members and infill panels) obtained from pushover analysis is greater than and close to the design base shear. If so, end the design process. Otherwise, return to Step 3 and modify the size of the assumed members.

3.2.3 Infill Panels

Based on the design procedure described in the previous section, the minimum required thicknesses of the infill panels at the first and second story were determined to be 2mm and 3mm respectively. The China Steel Company provided infill panels of measured thicknesses equivalent to 2mm and 3mm for the first and second story, respectively. Their yield strengths were respectively determined to be 335 MPa and 338 MPa from uniaxial tension tests of the plate coupons. Detailed data from coupon tests are presented in Section 3.6. Since widths of the available steel plates were less than the bay width of the specimen, the infill panel at each story was obtained by welding several steel plates. More detailed information about the fabrication of infill panels is introduced in Section 3.3.2.

After the Phase I tests, the buckled infill panels were removed by flame cut and new panels of same specification were installed for the Phase II tests. These were measured to be 3.2 mm and 2.3 mm thick with yield strengths of 310 MPa and 285 MPa at the first and second story, respectively. The measured differences of plate thickness and yield stresses for Phases I and II are within the tolerances for such plates and steel grade.

3.2.4 Boundary Frame Members

After establishing centerline dimensions of the frame and determining the infill panel thicknesses, design of the boundary frame members surrounding the infill panels was done with the objective of keeping the beams and columns elastic under the maximum loading, except for plastic hinges at the VBE bases and at the ends of HBEs which are necessary to develop the expected plastic mechanism. Pushover analyses on strip models of the tested specimens were conducted using SAP 2000 to determine the maximum moments, shear forces, and axial forces in the boundary frame members. The infill panels were modeled as elasto-perfectly plastic materials based on uniaxial tension tests of the plate coupons. Plastic hinges accounting for the interaction of axial force and flexure were defined at the ends of HBEs and VBE bases. The nominal flexural strengths at the ends of HBEs were obtained accounting for the flange reduction presented in the next section. The design resulted in the selection of H532x314x25x40 VBEs continuous over two stories, and H446x302x13x21, H350x252x11x19, and H458x306x17x27 HBEs at the top, intermediate and bottom levels, respectively. The names of Taiwan designation H shapes (corresponding to United States designation W shapes) reflect their depth, flange width, as well as web and flange thicknesses. Figure 3-2 shows the boundary frame, overall dimensions, and section sizes. Note that additional details illustrated in the figure will be described in a later section. Plastic strength of the system from pushover analysis was checked using SAP2000 to ensure that it was adequate to resist the lateral design forces.

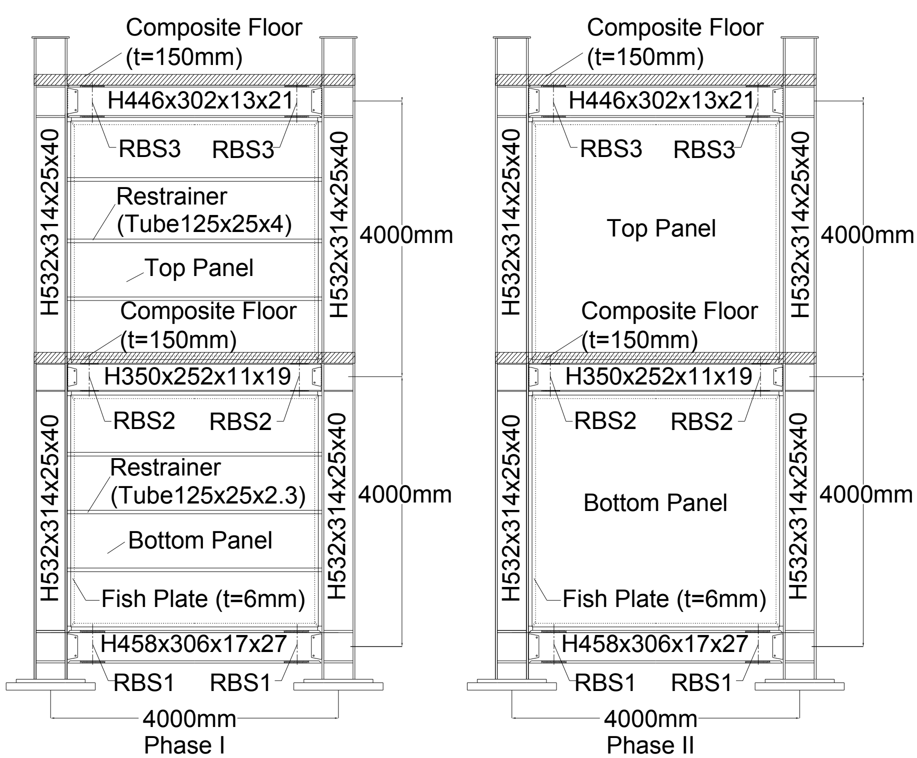

FIGURE 3-2 Schematic of Specimens

3.2.5 RBS Connections

Vian and Bruneau (2005) demonstrated that, for the given tension field forces, application of RBS connections at HBE ends can achieve optimum designs of HBEs (i.e. resulting in HBEs of smaller cross-sections), particularly for those HBEs at the ground and roof levels (i.e. anchor HBEs). In addition, this type of connections is expected to ensure the ductile behavior of SPSW. The RBS connections were designed to comply with the existing sizing requirements, including the limit of maximum beam flange width reduction of 50 percent (FEMA 2000). The designed RBS plastic moment reduction ratios were 0.655, 0.674, and 0.651 for the HBEs at the bottom, intermediate, and top levels, respectively. The schematic of RBS connections is illustrated in figure 3-3.

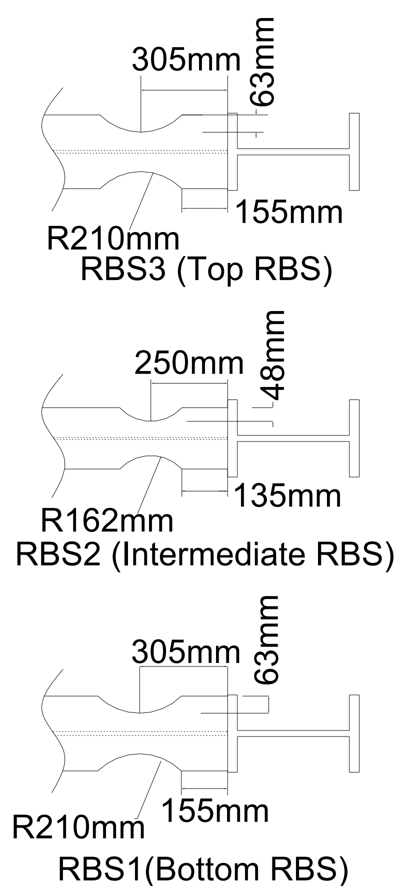

FIGURE 3-3 Schematic of RBS Connections

3.2.6 Infill Plate-to-Boundary Frame Connections

"Fish plates" were used along the boundary frame members to connect the infill panels. Thickness of the fish plate was determined to be 6.0 mm which was thicker (and of higher yield strength) than the SS400 infill panels. The fish plate was attached to beam and column flanges using fillet welds on both sides of the plate as shown in figure 3-4. The corner detail chosen was similar to the Modified Detail B recommended by Schumacher *et al.* (1999), as shown in figure 3-5. Note that the infill panels for the Phase I tests were welded on one side of the fish plates and the new panels installed for the Phase II tests were welded on the other side (after removing the Phase I panels).

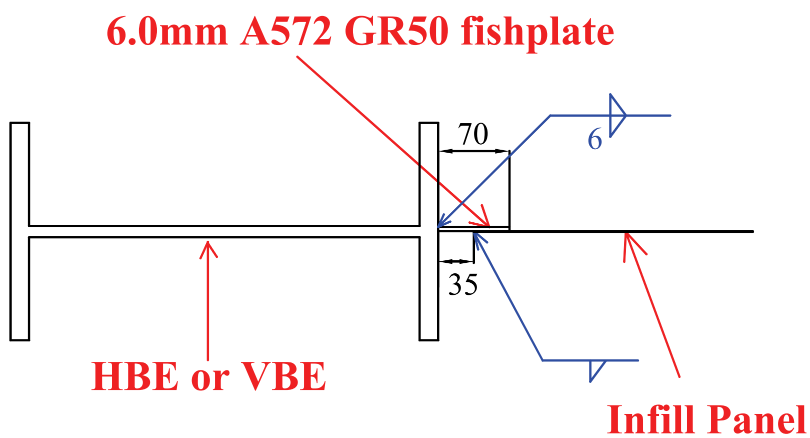

FIGURE 3-4 Fishplate and Panel Section Details

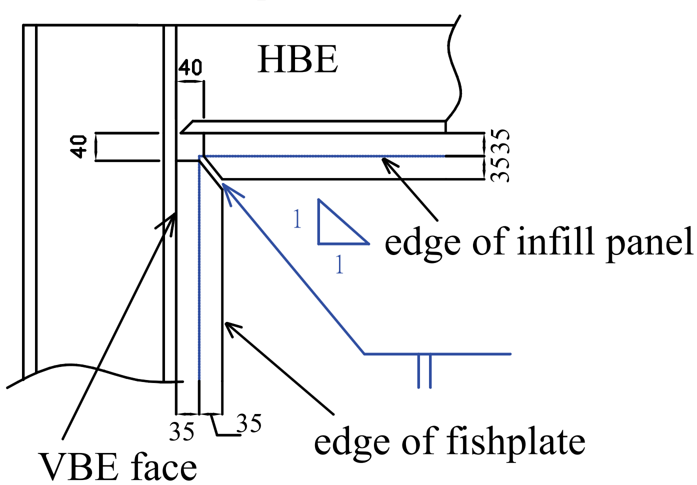

FIGURE 3-5 Fishplate Corner Detail

3.2.7 Slabs and Floor Trusses

Composite slabs, having a 3W-0.92t corrugated steel deck per Taiwan designation, which is equivalent to a 3 inch composite gauge 20 deck (James River Steel 2004), were designed to be 150 mm thick from the top of the composite slab to the bottom flute and 2480 mm wide at floor levels. Floor trusses, consisting of WT members (as part of the floor slab system) as shown in figure 3-6, were used to transfer in-plane loads to the specimen at floor levels.

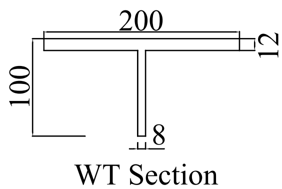

(a)

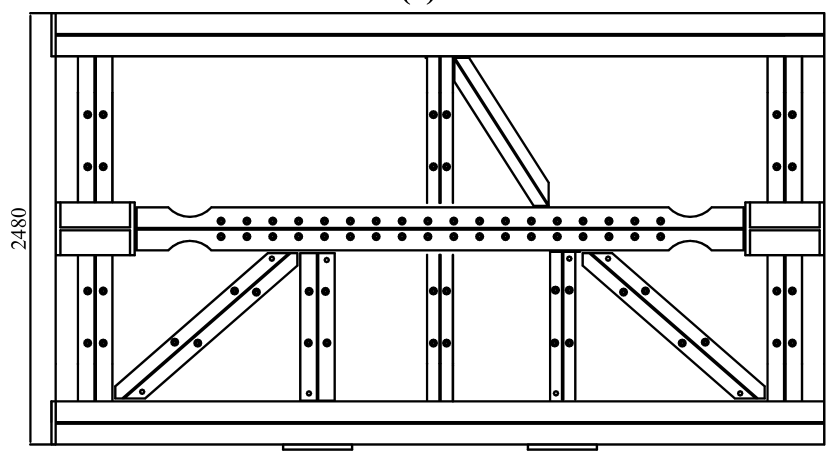

(b)

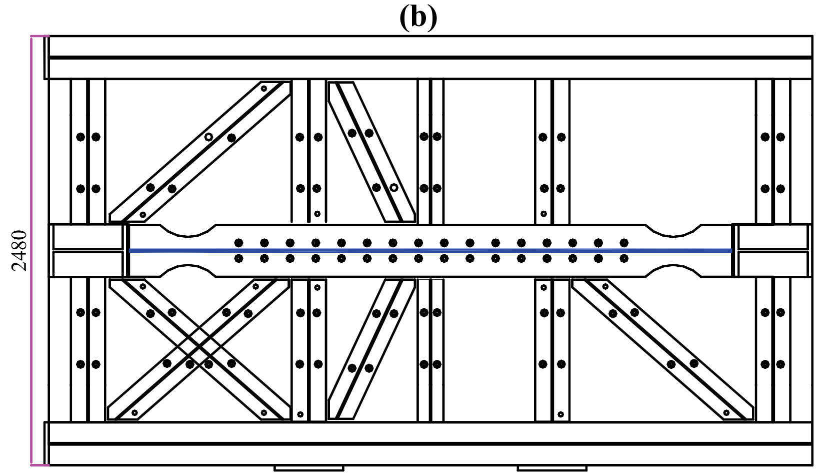

(c)

FIGURE 3-6 Ancillary Trusses (a) WT Section (b) 1st Floor (c) 2nd Floor

3.2.8 Restrainers

In the Phase I tests, the infill panels were laterally restrained at regular intervals by horizontal restrainers added solely to minimize the amplitude of the out-of-plane buckling displacements of the infill panels that typically develop in SPSWs at large inelastic drifts. According to the restrainer design procedure proposed by Tsai *et al.*

(2006), rectangular tubes of 125x75x4 and 125x75x2.3 were placed at quarter points of the first and second story respectively as shown in figure 3-2. The names of Taiwan designation rectangular tubes (corresponding to US designation rectangular HHS) reflect their depth, width, as well as wall thickness. Note that no restrainers were utilized in the Phase II tests.

3.3 Fabrication Procedure

For fabrication of the specimen, the boundary frame was firstly constructed. Next, the infill panels at the first and second story were built by first welding segments of steel plates together (using full penetrate "seam" welds) and then welding the resulting plate to the boundary frame. Finally, the concrete slabs and floor trusses were constructed. The following sections present detailed information about this fabrication procedure.

3.3.1 Fabrication of Boundary Frame

Many steps in the fabrication of the boundary frame members, including cutting of the reduced beam flanges in HBEs, welding of the continuity plates to the VBEs, and welding of the fish plates to the boundary frame members, were conducted in the shop. Those structural components were then sent to the laboratory for construction. The VBEs were firstly erected and fixed to the strong floor using anchor bolts at their bases (figure 3-7). After that, top, intermediate, and bottom HBEs were lifted and welded to the VBEs (figure 3-8).

FIGURE 3-7 VBE Erection (Photo Courtesy of C.H.Lin and K.C.Tsai, NCREE)

FIGURE 3-8 Installation of HBEs
(Photo Courtesy of C.H.Lin and K.C.Tsai, NCREE)

3.3.2 Fabrication of Infill Panels

As mentioned earlier, the needed infill panels are 3468 mm wide, which is greater than the width of the available steel plates. To build the infill panels, small segments of steel plates were welded for the first-story and second-story infill panels, respectively. Those small plate segments were manually welded by the fabricator using E7018 electrodes and full penetration welds as shown in figure 3-9.

To control the quality of welds, the boundary frame was laid down on the strong floor and the assembled infill panels were welded to the fish plates along the boundary frame members. During this welding process, the infill panels were supported using temporary restrainers to prevent excessive out-of-plane deflection. The above procedures are illustrated in figures 3-9 to 3-12. After welding the infill panels to boundary frame, the specimen was erected and fixed to the strong floor.

FIGURE 3-9 Manual Welds along Small Plate Segment Edges
(Photo Courtesy of C.H.Lin and K.C.Tsai, NCREE)

FIGURE 3-10 Assembled Infill Panels
(Photo Courtesy of C.H.Lin and K.C.Tsai, NCREE)

FIGURE 3-11 Restrainers in the Frame
(Photo Courtesy of C.H.Lin and K.C.Tsai, NCREE)

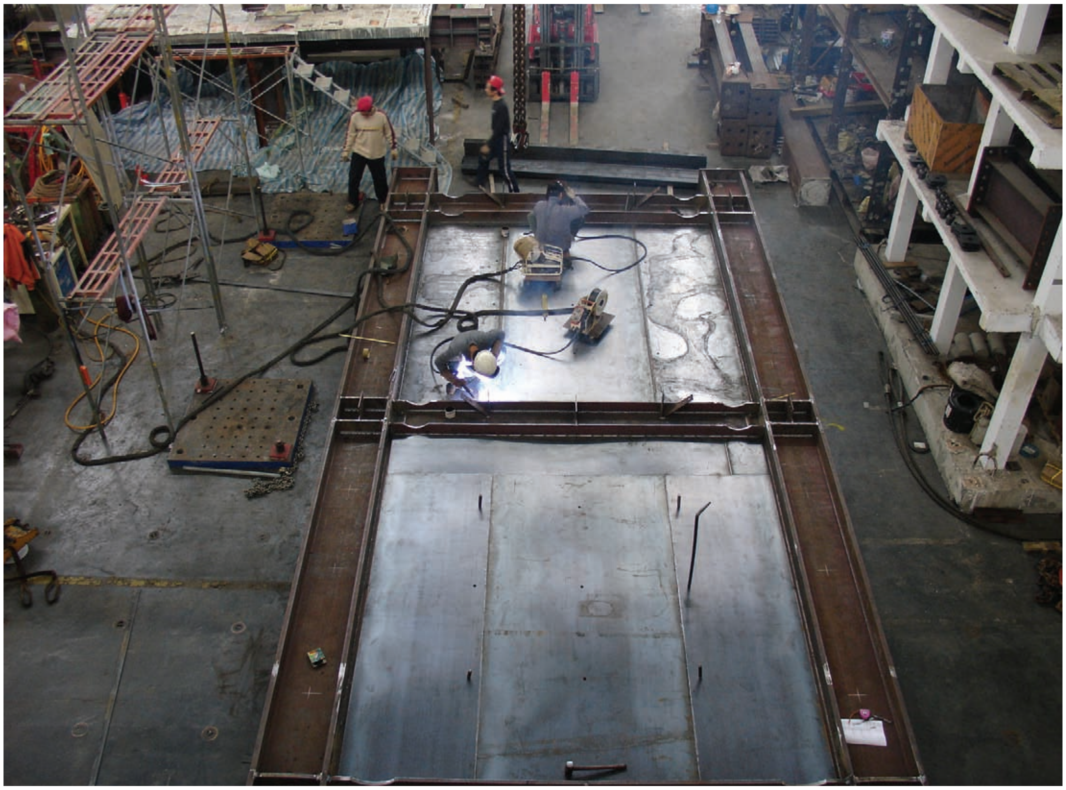

FIGURE 3-12 Welding Infill Panels to Boundary Frame (Photo Courtesy of C.H.Lin and K.C.Tsai, NCREE)

3.3.3 Fabrication of Concrete Slabs

The next step in fabrication of the specimen was construction of the composite slabs. The floor trusses which were used to transfer the lateral forces of actuators to the specimen were installed to the specimen at floor levels followed by the installation of corrugated steel decks. Self consolidating concrete was then cast into the steel decks. Figures 3-13 and 3-14 show the construction process of the slab.

FIGURE 3-13 Corrugated Steel Deck
(Photo Courtesy of C.H.Lin and K.C.Tsai, NCREE)

FIGURE 3-14 Casting Concrete Slab
(Photo Courtesy of C.H.Lin and K.C.Tsai, NCREE)

3.4 Test Setup

The test setup details are described in this section. Note that the loading protocol and observations of test results are presented in the Section 4.

3.4.1 NCREE Laboratory and Test Setup

The experimental phase of this research project was conducted in collaboration with NCREE in Taipei, Taiwan. The NCREE laboratory has experience and equipments to perform pseudodynamic and quasi-static cyclic testing on large-scale specimen, and the capabilities to apply the large lateral force required for this specimen.

The NCREE's reinforced concrete reaction wall and strong floor facility for large-scale structural testing, illustrated in figure 3-15 (NCREE 2002), was used for this purpose. The reaction wall consists of two parallel 1200 mm thick reinforced and post-tensioned concrete walls, separated by a distance of 2600 mm, and tied together by 400 mm thick reinforced concrete ribs spaced at 3000 mm. Plan view and elevation of the test setup for this testing are illustrated in figures 3-16 and 3-17, respectively.

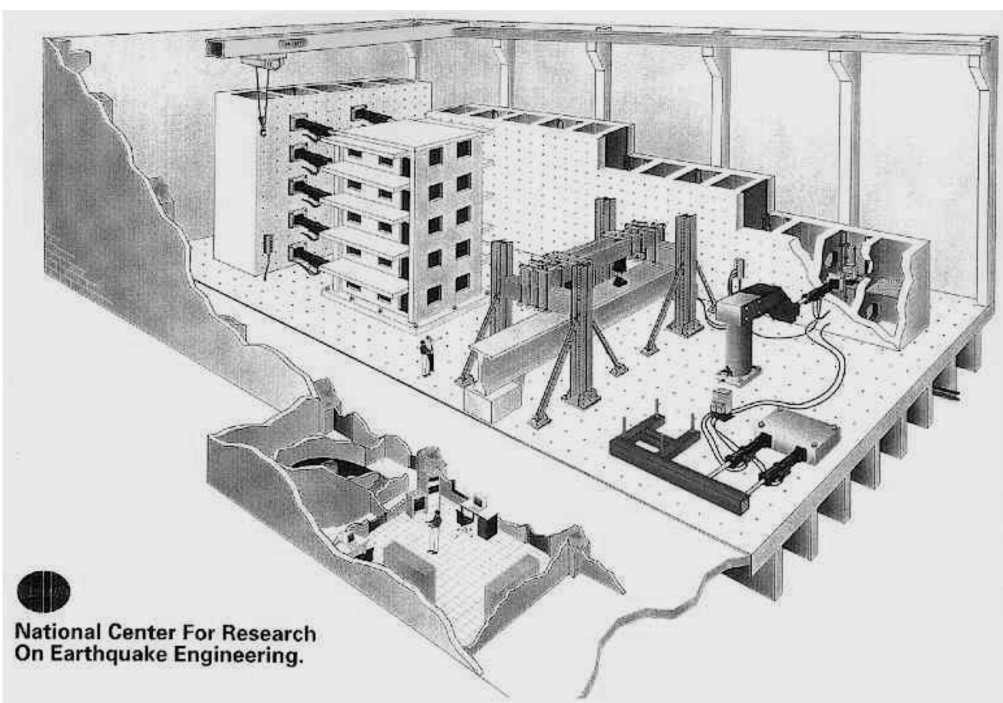

FIGURE 3-15 NCREE Reaction Wall and Strong Floor Layout (NCREE 2002)

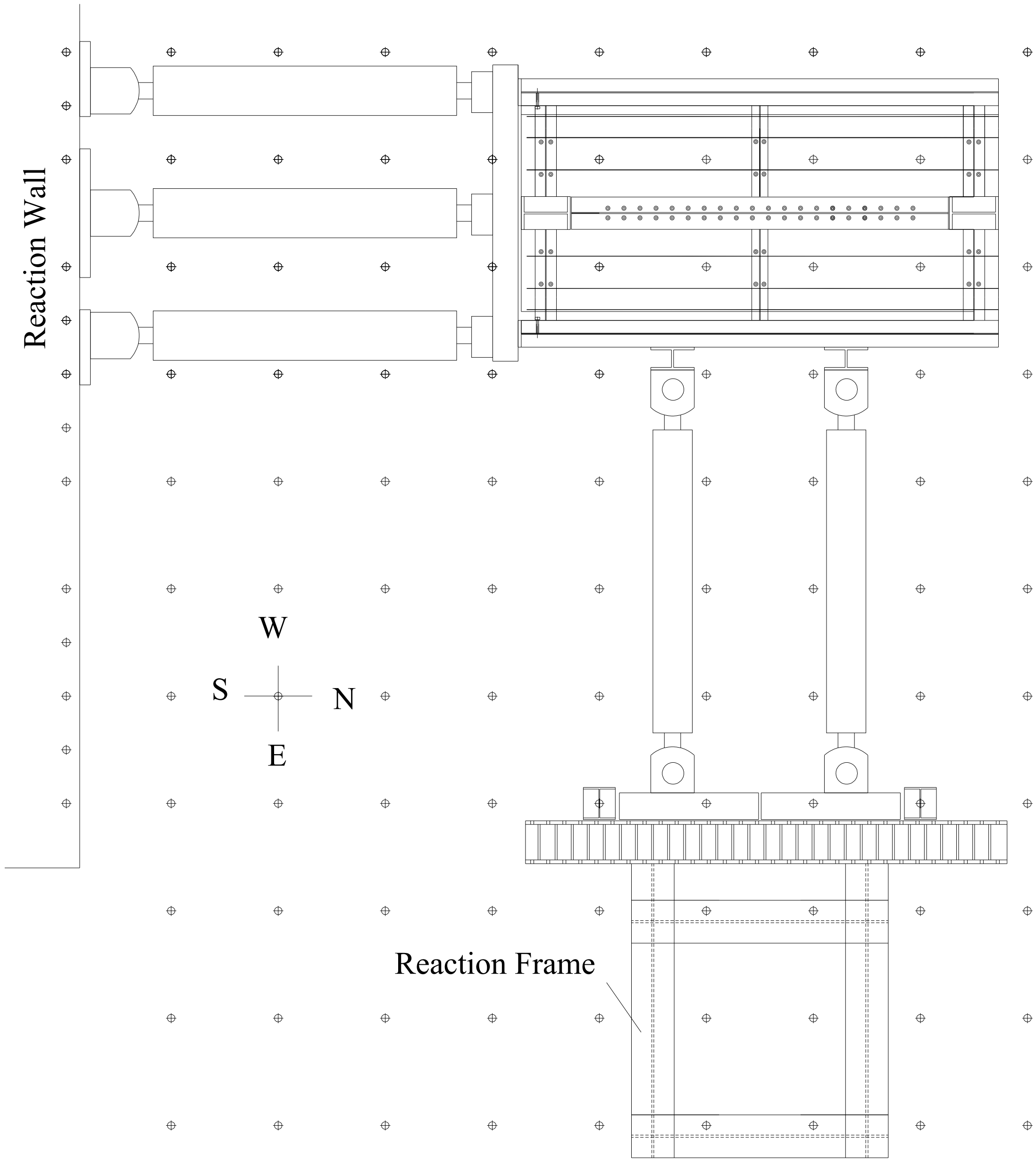

FIGURE 3-16 Plan View of Test Setup

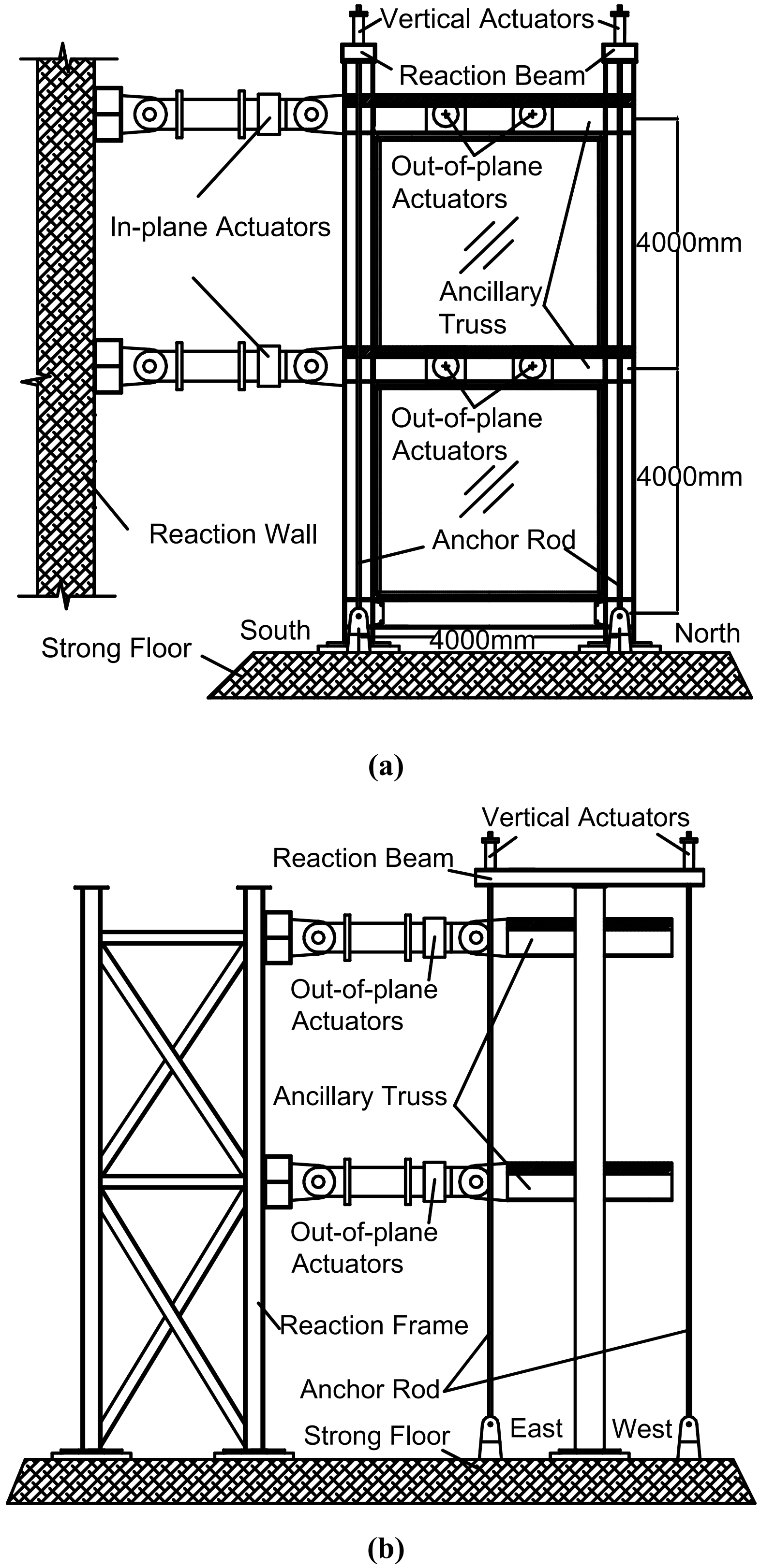

FIGURE 3-17 Elevation of Test Setup (a) in-plane (b) out-of-plane

3.4.2 Specimen Mounting

Base plates 100 mm thick were fastened to the strong floor using high strength, post-tensioned rods. Then, the 50-mm-thick VBE end plates were attached to the base plates using eighteen M30 A490 high strength bolts to provide sufficient base shear strength.

3.4.3 Actuator Mounting

In-plane (north-south) servo controlled hydraulic actuators were mounted between the specimen and reaction wall as shown in figures 3-16 and 3-17(a). Three actuators with an individual load capacity of 1000 kN and an available stroke of 500mm were employed to apply in-plane loading on the specimen at each story. Floor trusses (as part of the floor slab system) were used to transfer the in-plane loads to the specimen at the floor levels.

A vertical load of 1400 kN was applied by a reaction beam at the top of each column to simulate the gravity loads that would be present in the prototype structure. Each reaction beam transferred the load exerted by two vertical actuators mounted between the reaction beam and anchor rods pinned to the strong floor.

3.4.4 Lateral Supports

To avoid out-of-plane (east-west) displacements of the SPSW, lateral bracing was provided at floor levels through the use of two hydraulic actuators mounted between the edge of the floor (floor truss) and a reaction frame as shown in figures 3-16 and 3-17(b). Those actuators were pinned at each end and acted as out-of-plane rollers, allowing development of the expected specimen deformations. Note that large out-of-plane forces were not expected in this testing.

3.5 Instrumentation

Behavior of the boundary frame as well as infill panels during testing was measured in a number of ways as described below. A total of 203 data acquisition channels were used to collect experimental data. In addition, five video cameras were used to record the global behavior of the specimen and the local behavior of the RBS connections and infill panels.

3.5.1 Frame Behavior

3.5.1.1 Strains in Frame Members

Uniaxial strain gauges were placed at quarter points of the story height on the flange of each column and center of the reduced flange of each beam as shown in figure 3-18. Assuming that plane sections remain plane, this arrangement allows for measurement of average axial strains and curvature at a cross-section, which can be used to calculate axial load and moment, respectively, at that location. Rosette strain gauges were placed at 1/4 and 3/4 points of the story height on the web of each column (one on each side of the web) so that the principal stresses at these locations could be obtained.

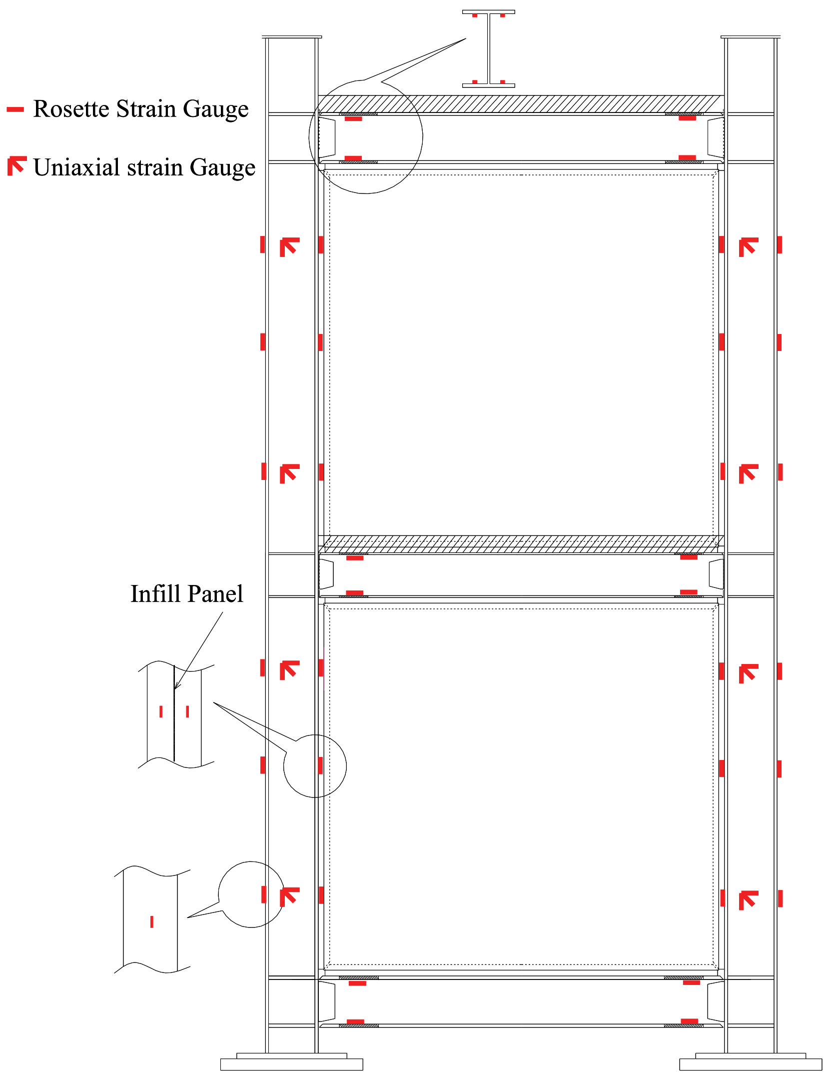

FIGURE 3-18 Strain Gauges on the SPSW

3.5.1.2 Frame/Specimen Displacement

Tiltmeters were placed at various locations as shown in figure 3-19 on the boundary frame to obtain in-plane rotations of these parts. Dial meters were placed at column base to monitor the relative displacement between the column bases and strong floor caused by possible slippage of the specimen on the strong floor under in-plane loading.

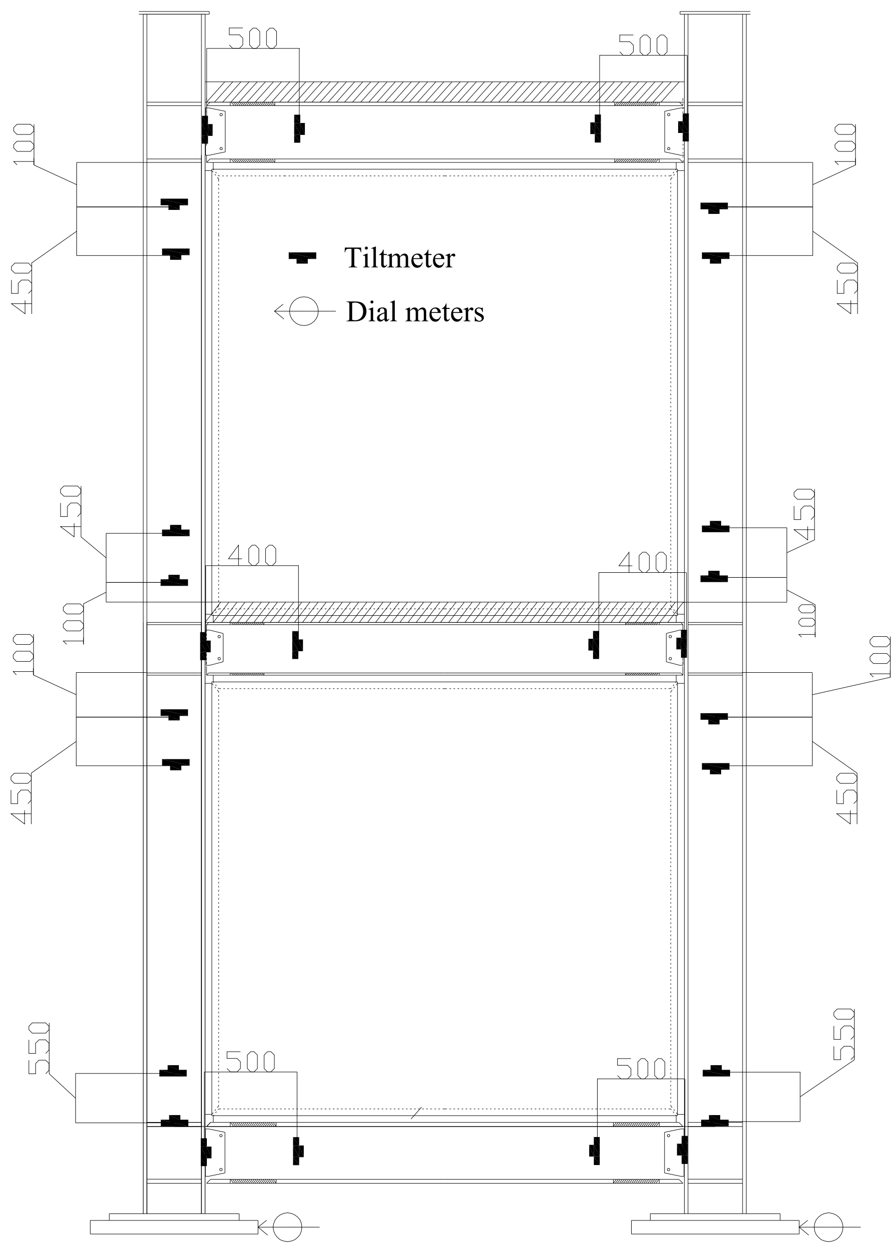

FIGURE 3-19 Tiltmeters and Dial Meters on the SPSW

Magnetostrictive transducers (Temposonics) were placed at the north ends of the intermediate and top HBEs as shown in figure 3-20, respectively, to obtain the floor displacements and correspondingly determine the story drift histories during testing.

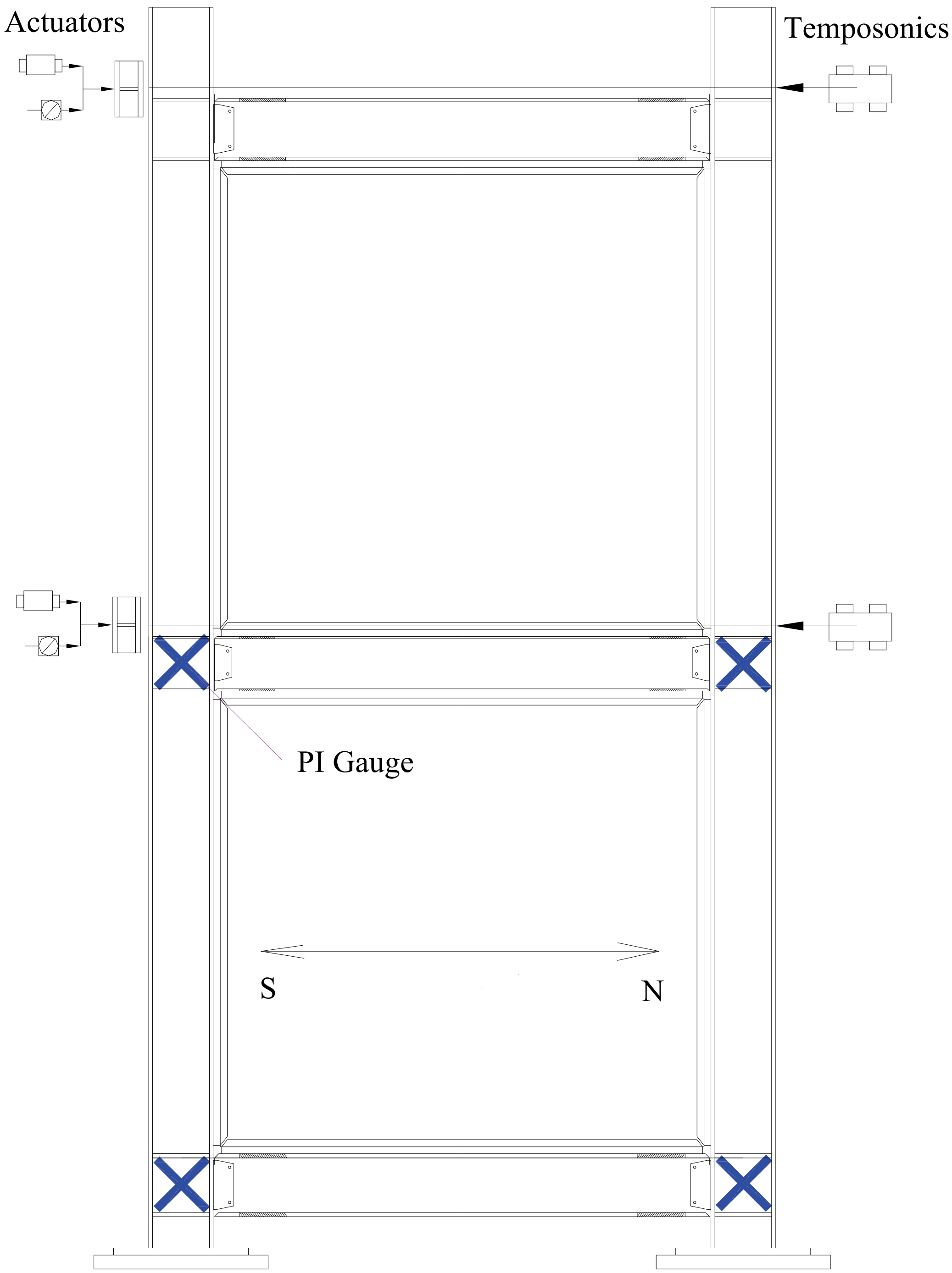

FIGURE 3-20 Temposonics on the SPSW

3.5.1.3 Panel Zone Deformation Measurements

For measuring the deformations of the panel zones, PI gauges were respectively placed at the panel zones of intermediate and bottom HBE-to-VBE connections as shown in figure 3-20. A PI gauge device consists of an aluminum bar, one end pinned at a corner of the panel zone and the other end slotted to allow movement but guidance along the diagonal, while there is a piece of metal, bent in a semi-circular "omega" shape, which measures displacement via a calibrated strain gage, as this omega shape opens or closes (Vian and Bruneau 2005).

3.5.2 Panel Behavior

Linearly variable displacement transformeters (LVDTs) were placed across the panels at an angle of 41degrees from the vertical to obtain the diagonal elongation of the infill panels as shown in figure 3-21 (12 LVDTs for each story, i.e. six on each side of the infill panel).

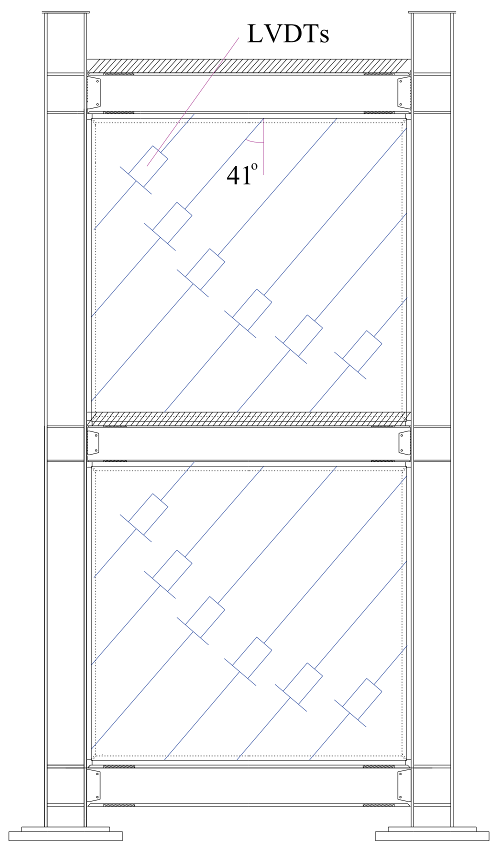

FIGURE 3-21 LVDTs on the SPSW

3.6 Material Tests

Compressive strength of the concrete used in slabs was determined to be 27.5 MPa from cylinder tests conducted 14 days after casting. Coupons of the boundary frame members as well as infill panels were tested in a universal testing machine to determine the material strengths. Strains were recorded using an MTS electro-mechanical extensometer as shown in figure 3-22.

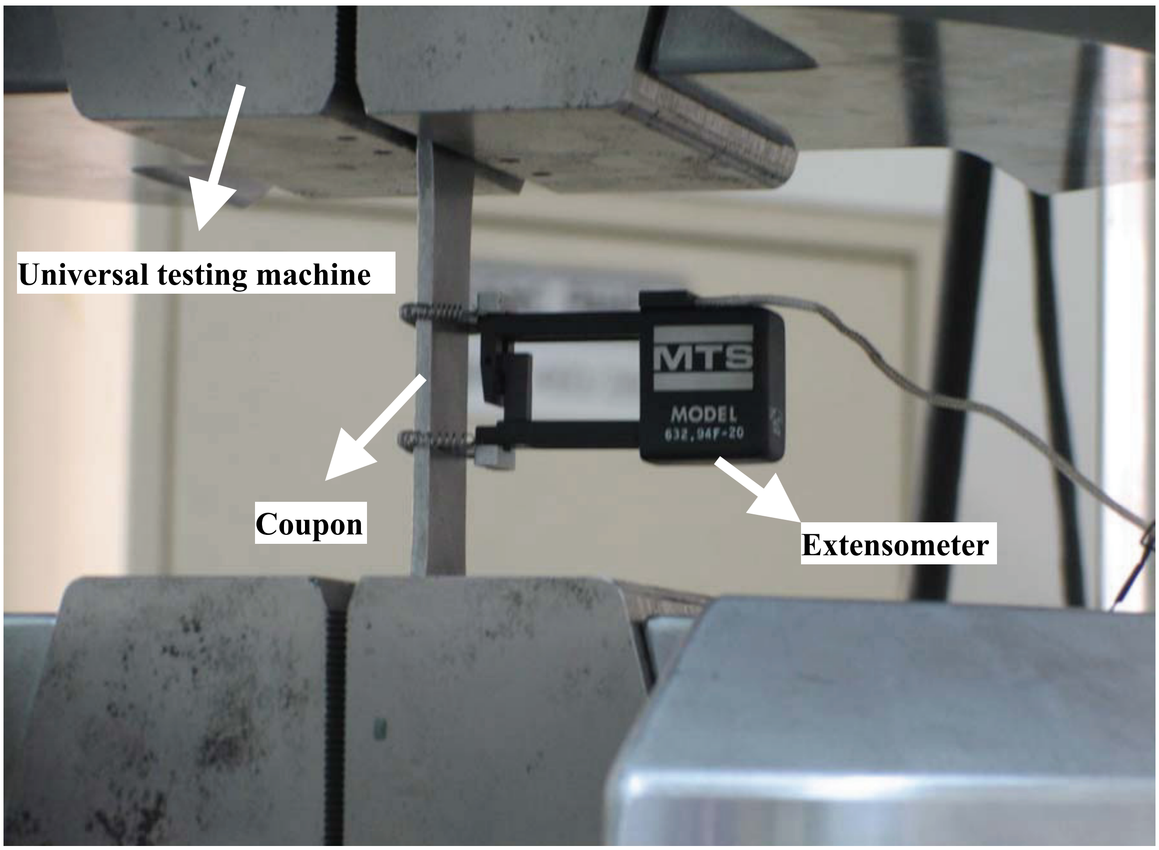

FIGURE 3-22 Coupon Test Setup

The tested coupons were cut along rolling direction of the plates. Considering that tension fields typically develop along the diagonal direction in infill panels, coupons cut at an angle of 45 degree to the rolling direction from the Phase II infill panels were also tested. The results of coupon tests for the boundary frame members and infill panels are summarized in tables 3-1 and 3-2. Stress vs. strain curves of the tested coupons are presented in figures 3-23 to 3-27. As shown, all plates displayed ductile behavior. The infill panel coupons cut along the rolling direction and those at the 45-degree direction have similar yield and ultimate strengths.

TABLE 3-1 Material Properties of Boundary Frame Members

Coupon Description	Nominal thickness (mm)	Actual thickness (mm)	Yield strength* (MPa)	Ultimate strength (MPa)
Bottom HBE flange	27	28	335	496
Bottom HBE web	17	19	290	500
Intermediate HBE flange	19	19	470	589
Intermediate HBE web	11	12	475	608
Top HBE flange	21	22	350	519
Top HBE web	13	13	290	467
VBE flange	40	40	357	548
VBE web	25	25	370	505

*the lower yield strength obtained from testing

TABLE 3-2 Material Properties of Infill Panels

Coupon ID	Phase	Story	Nominal thickness (mm)	Actual thickness (mm)	Yield strength (MPa)	Ultimate strength (MPa)
1	I	1F	3	3.0	338	482
2	I	2F	2	2.0	335	412
3*	II	1F	3	3.2	312	425
4	II	1F	3	3.2	308	445
5*	II	2F	2	2.3	290	360
6	II	2F	2	2.3	280	376

*cut along 45º direction to the rolling direction

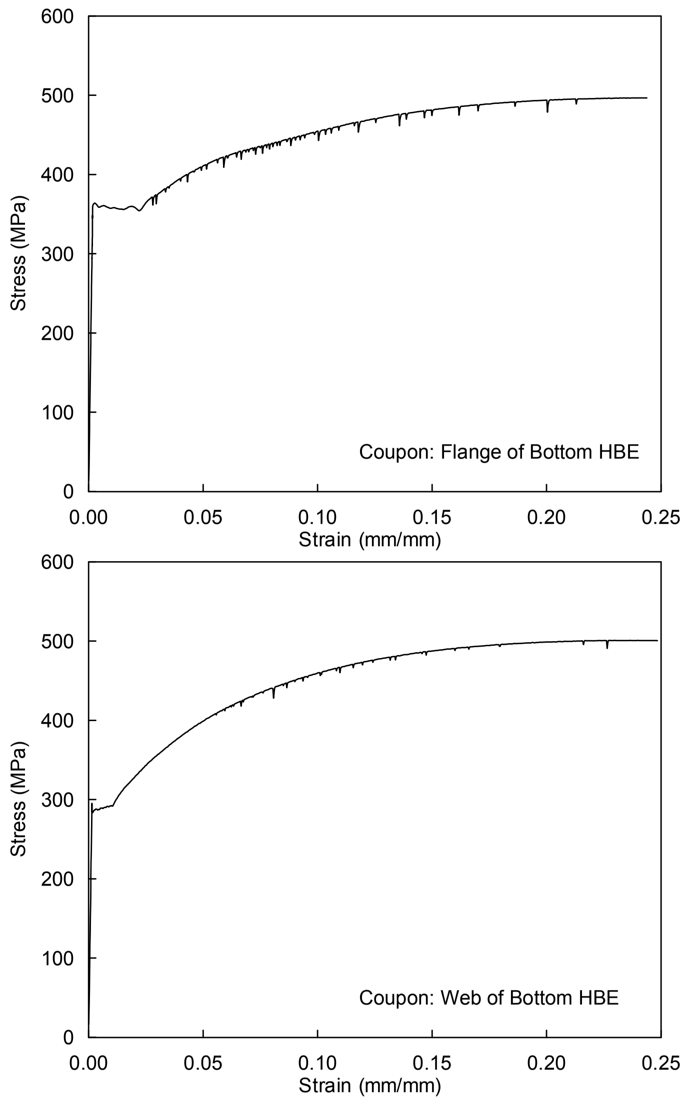

FIGURE 3-23 Stress vs. Strain Curves of Bottom HBE

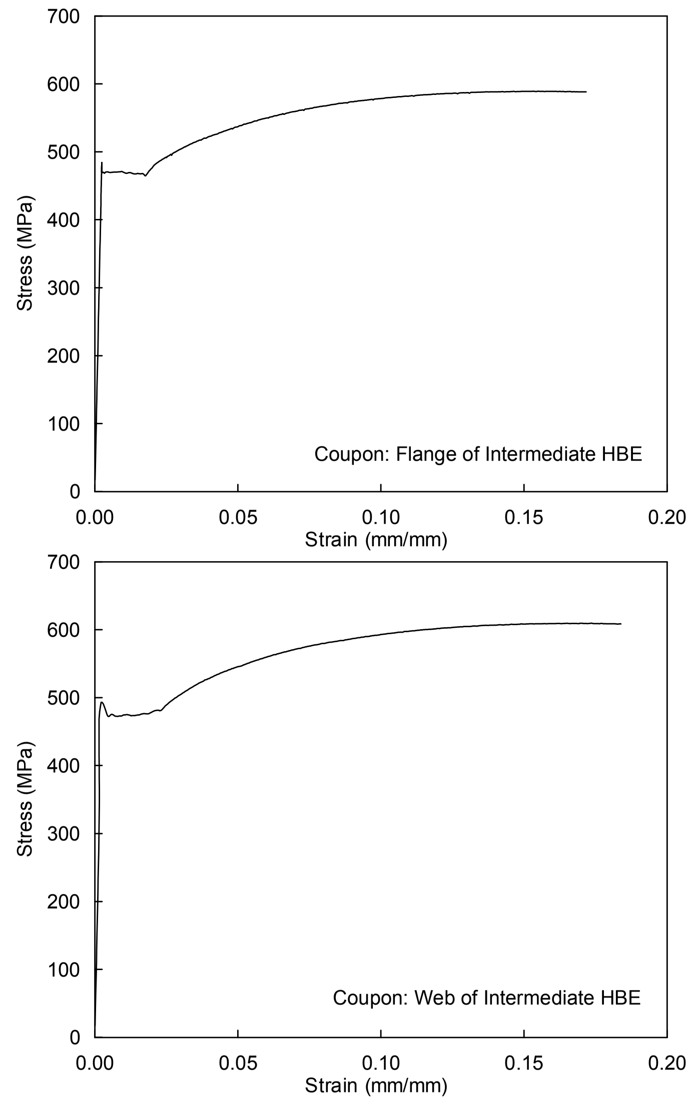

FIGURE 3-24 Stress vs. Strain Curves of Intermediate HBE

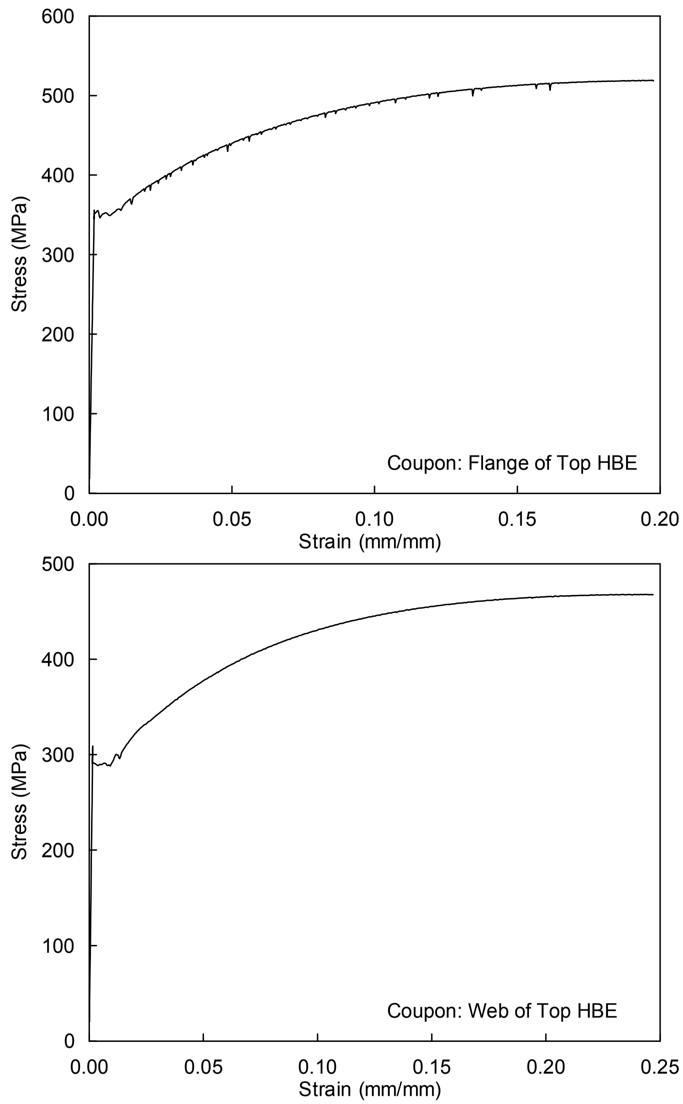

FIGURE 3-25 Stress vs. Strain Curves of Top HBE

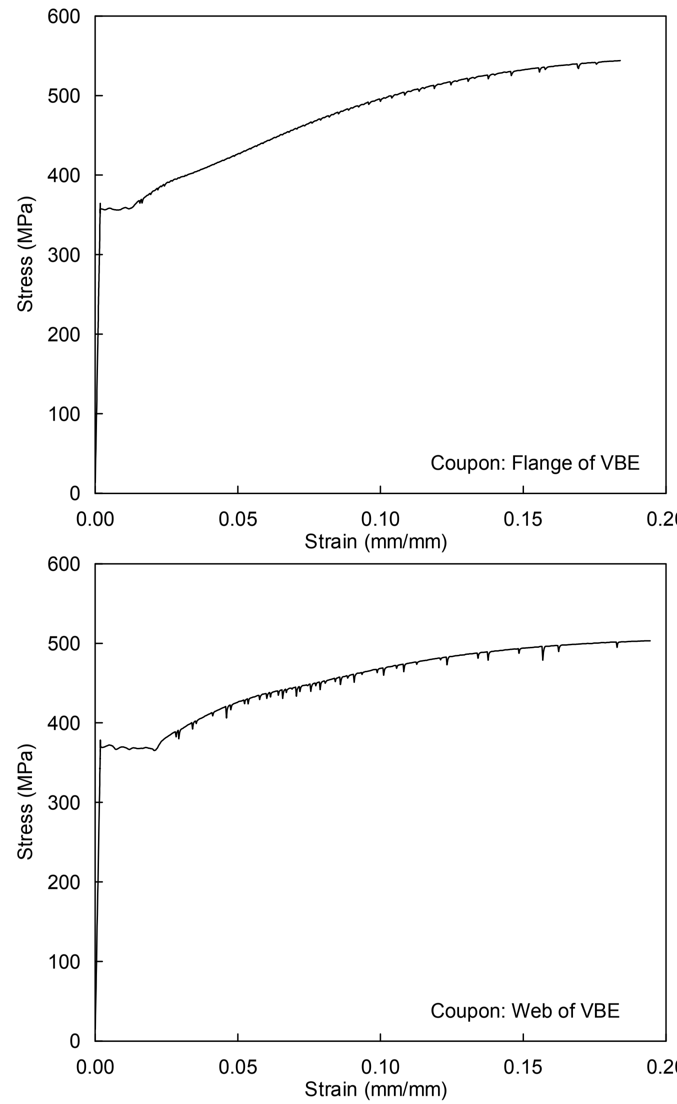

FIGURE 3-26 Stress vs. Strain Curves of VBE

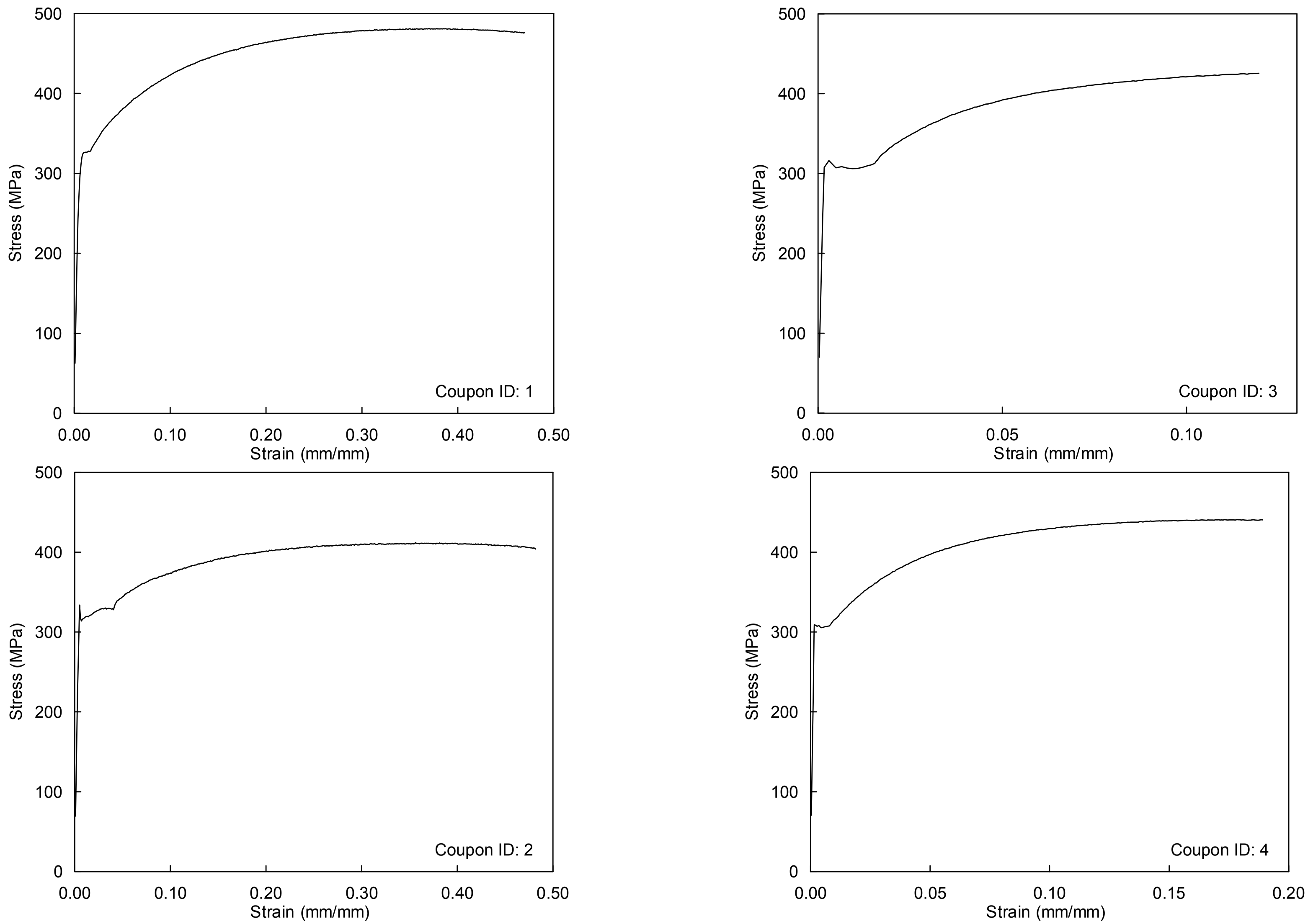

FIGURE 3-27 Stress vs. Strain Curves of Infill Panel Coupons

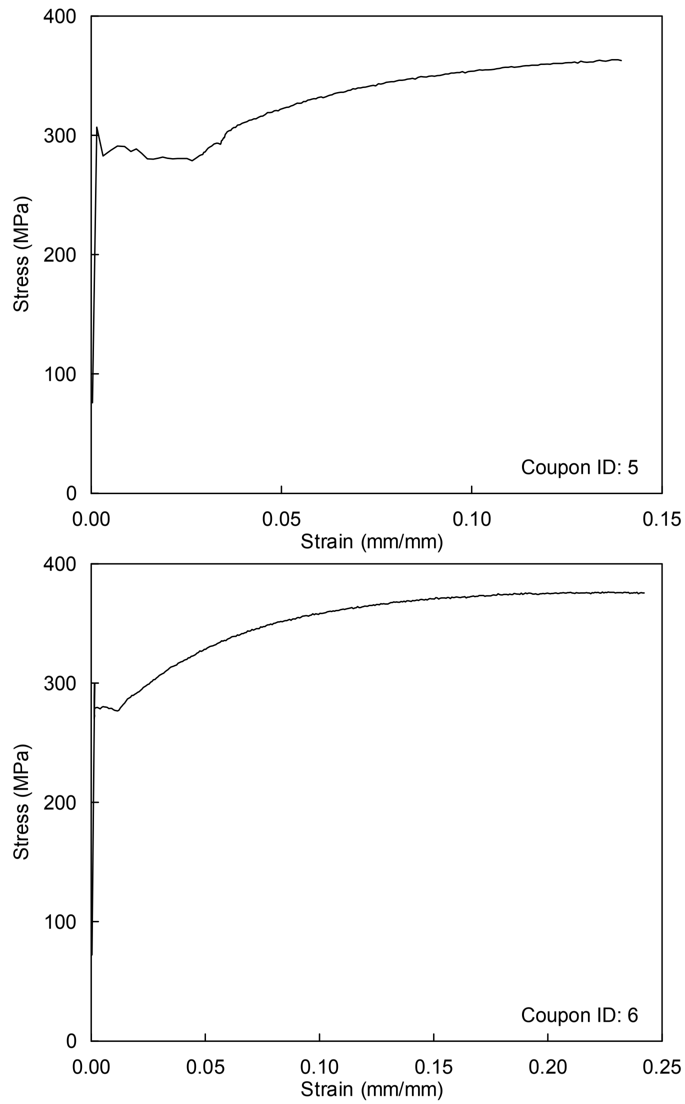

FIGURE 3-27 (Cont'd) Stress vs. Strain Curves of Infill Panel Coupons

SECTION 4

EXPERIMENTAL PROGRAM RESULTS AND OBSERVATIONS

4.1 Introduction

As introduced in Section 3, a two-phase experimental program was developed to test a full-scale two-story SPSW specimen with RBS connections to address the replaceability of infill panels following an earthquake, the behavior of the repaired SPSW in a subsequent earthquake, and the seismic performance of the intermediate HBE. This section focuses on the behavior of the specimen in the Phase II tests to experimentally address the above issues. However, for comparison purpose and completeness, a number of key observations from the Phase I tests are also provided.

Note that the Phase I tests were entirely the responsibility of NCREE, as part of this MCEER/NCREE collaborative research program on SPSWs. In fact, early tests conducted at low amplitudes for the purpose of preliminary determination of the specimen properties revealed deficiency in the test setup. The entire experimental schedule had to be adjusted consequently. Participation of the author in this collaborative program focused entirely on the activities after the Phase I tests (i.e. started from the replacement of infill panels as part of the Phase II testing program). However, direct observation was possible at the midways of the Phase I tests. More information about the Phase I tests is presented in Tsai *et al.* (2006). However, since the behaviors observed in the Phase II tests are dependent on some of the characteristics observed in Phase I, the substantial part of this section is devoted to repeating the information presented in Tsai *et al.* (2006).

The following sections first introduce the pseudodynamic testing method used in the tests along with the earthquake and cyclic loading programs. Following this discussion, qualitative and quantitative observations regarding the specimen performance during both linear and nonlinear behaviors are presented. The infill panel replacement between the Phase I and Phase II tests and some remedy work conduced to correct premature damage that occurred in the specimen during testing are also presented.

4.2 Phase I Tests

As reviewed in Section 2, most of the previous experimental research on full-scale (and large-scale) SPSWs was conducted using the quasi-static testing method. However, the cyclic displacement histories applied on the tested specimens in those investigations may not necessarily correspond to the inertial force effects on the prototype structures of those specimens in an actual earthquake. To have a better understanding of the seismic behavior of SPSW system, the specimen described in Section 3 was tested using the pseudodynamic testing procedure in the Phase I tests. The following briefly describes this testing method and the earthquake time histories used in this investigation, followed by the seismic responses of the specimen obtained in each test of this phase. Then, observations regarding behavior of the specimen made during the tests are presented.

4.2.1 Pseudodynamic Testing Procedure and Ground Motions

The pseudodynamic sub-structural testing technique was adopted in this study for the purpose of obtaining the seismic response of the entire prototype structure described in Section 3 through testing the considered sub-structural assembly (i.e. the SPSW). Using this approach, the SPSW specimen, which was the primary lateral force resisting system of the prototype structure of interest, was physically tested, while the rest of the 3D prototype structure shown in figure 3-1 including the moment frame acting in the other principal direction of the building were numerically modeled in the computer. The equilibrium and displacement compatibility conditions between the experimental and analytical sub-structures were enforced by the loading system. Descriptions of the theory underlying the well-known pseudodynamic analysis method are available in the literature (Tsai *et al.* 2006) and not reported here.

In this research, the computer program package PISA3D developed by NCREE was used as the control and analysis engine to model the above mentioned sub-structural assemblies and determine the corresponding inertia forces. To be able to initiate the pseudodynamic test, initial stiffness must be entered in the computer program. In this case, the stiffness was obtained through preliminary testing the wall in the elastic range. The tests were webcast to the public through http://exp.ncree.org/spsw/.

The pseudodynamic testing method requires that the specimen be subjected to an earthquake excitation. Therefore, selection of a specific ground motion is necessary to calculate structural response in the analysis and control engine (i.e. PISA 3D as mentioned earlier). In this study, the ground acceleration history of the 1999 Chi-Chi earthquake recorded at the station TCU082EW was chosen to be representative of the large earthquake excitation having a long return period likely to occur in Taiwan.

The original record of the above earthquake is a 35-second ground acceleration history. To obtain the structural response during the earthquake as well as that right after the earthquake (i.e. free vibration response of the structure), a 15-second period of time with no ground acceleration was artificially added at the end of the abovementioned 35-second record, resulting in a 50-second ground acceleration record for the entire tests.

The ground acceleration record was scaled so that the spectral acceleration (5% damping) associated with the first mode period determined from the eigenvalue analysis was equivalent to that for a 2500-year return period design response spectra. Accordingly, the scaled earthquake record has a peak ground acceleration (PGA) of 0.63g and a peak pseudo-acceleration (PSa) response of 1.85 g at the fundamental period of 0.52 second for the prototype structure as shown in figure 4-1.

In order to investigate the seismic behavior of the wall in a severe earthquake as well as during large aftershocks, the SPSW specimen as tested under three pseudodynamic sequences using the above earthquake record scaled up to levels of excitations representative of seismic hazards having 2, 10, and 50% probabilities of exceedances in 50 years, subjecting the SPSW specimen to earthquakes of progressively decreasing intensity.

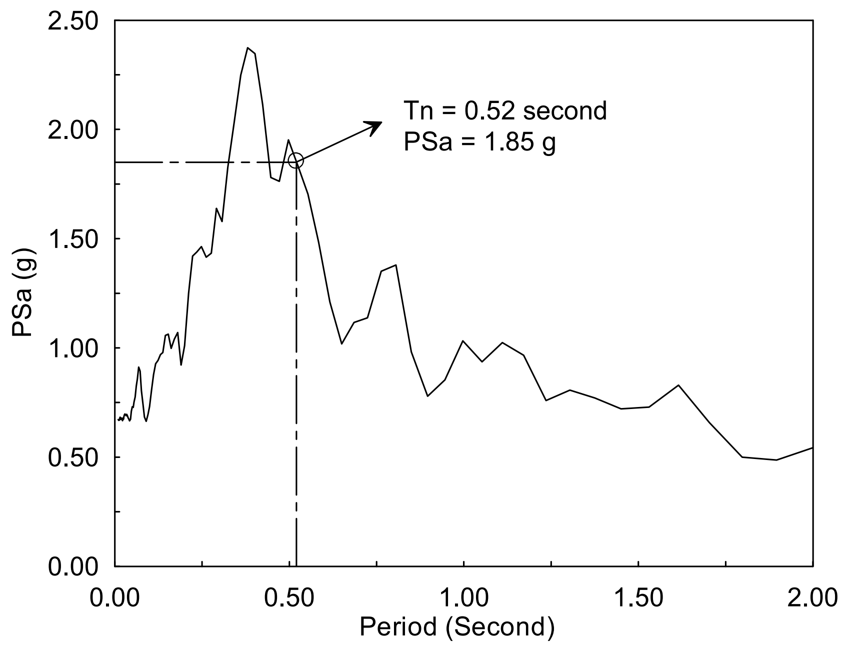

FIGURE 4-1 PSa Spectrum of the Chi-Chi Earthquake (2% in 50 Yrs and 5% Damping)

4.2.2 Specimen Responses

Before the pesudodynamic tests could be successfully conducted, some problems encountered in the early stage of the Phase I tests. In the first two tests using the earthquake having a probability of exceedance in 50 years, unexpected failures were encountered in the intermediate concrete slab and the south VBE base. The specimen was strengthened twice as described later. After that, the third test on the SPSW specimen was conducted using the earthquake having a probability of exceedance in 50 years. Then, Tests 4 and 5 simulated the aftershocks of decreasing magnitudes. Therefore, a total of 5 tests were conducted in Phase I as summarized in table 4-1.

TABLE 4-1 Summary of the Phase I Tests

Test ID	Stoppage time step (sec)	Hazard level in 50 yrs (%)	Testing Date
1	9.5	2	Oct. 7, 2005
2	24	2	Nov. 7, 2005
3	50	2	Feb. 8, 2006
4	50	10	Feb.9, 2006
5	50	50	Feb. 10, 2006

Note that, although some observations made during Tests 1 and 2 are presented in the following sections, the results of these two tests are not compared here since those two tests did not generate complete testing data due to the premature failures.

For convenience, the ground motion inputs, displacement histories at floor levels, story shear responses, recorded in Tests 3, 4 and 5 are shown in figures 4-3, 4-5 and 4-7, respectively. It should be noted that in this report, the displacement and story drifts designated as "+" or "-" refer to loading in the north and south direction (i.e. pushing away from or pulling towards the reaction wall, recalling the test set up illustrated in Section 3), respectively. Hystereses obtained from Tests 3, 4 and 5 are presented in figures 4-2, 4-4 and 4-6, respectively. Generally, the SPSW specimen behaved satisfactorily as expected in Tests 3, 4 and 5. As shown, the SPSW specimen experienced a strong earthquake was able to dissipate certain amounts of hysteretic energy in a severe aftershock and exhibited essentially elastic behavior when the intensity of the earthquake loads decreased.

For comparison purpose, the maximum drift and story shear force responses of Tests 3, 4, and 5 are summarized in table 4-2.

TABLE 4-2 Summary of the Maximum Response of the Phase I tests

Tests	PGA (g)	Story	Positive Loading		Negative Loading	
			Story shear (kN)	Story drift (%)	Story shear (kN)	Story drift (%)
Test 3	0.67	1F	3960	2.60	-3856	-1.85
		2F	2501	2.30	-2526	-1.47
Test 4	0.53	1F	3478	2.00	-3287	-1.73
		2F	1940	1.76	-2393	-1.48
Test 5	0.22	1F	1396	1.19	-1228	-0.47
		2F	814	1.13	-1025	-0.48

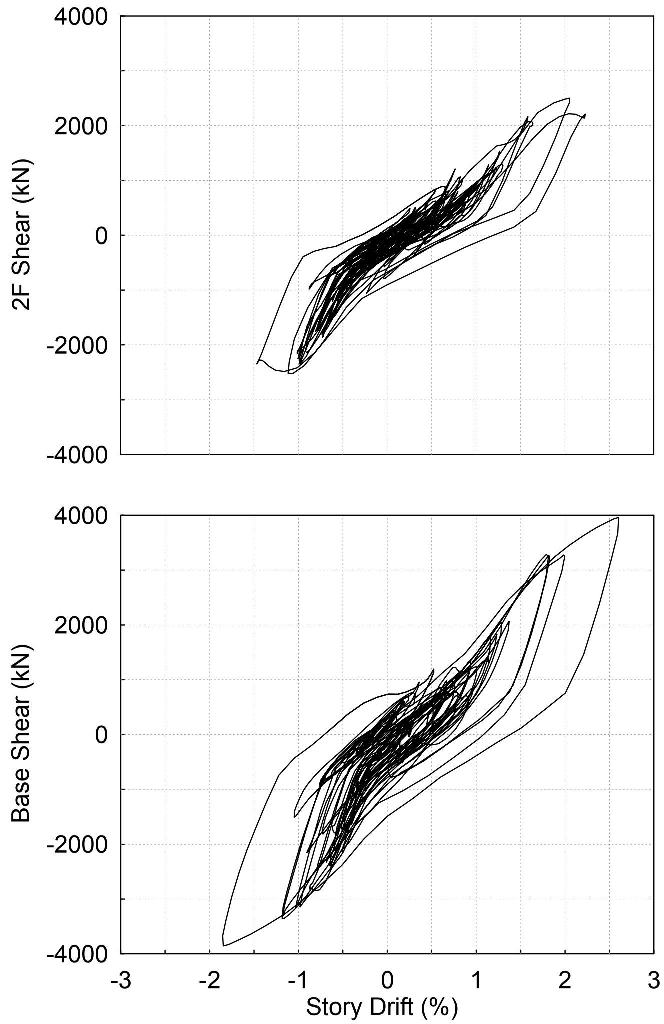

FIGURE 4-2 Hystereses of Test 3

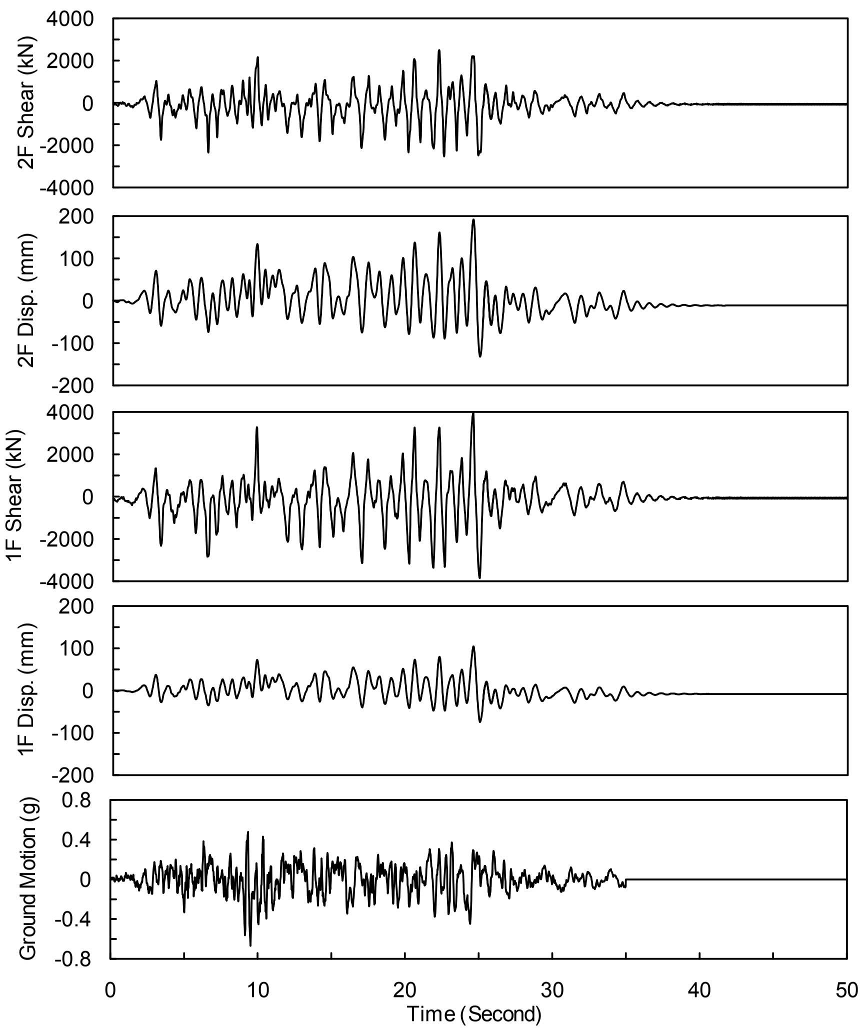

FIGURE 4-3 Ground Motion and Specimen Responses of Test 3

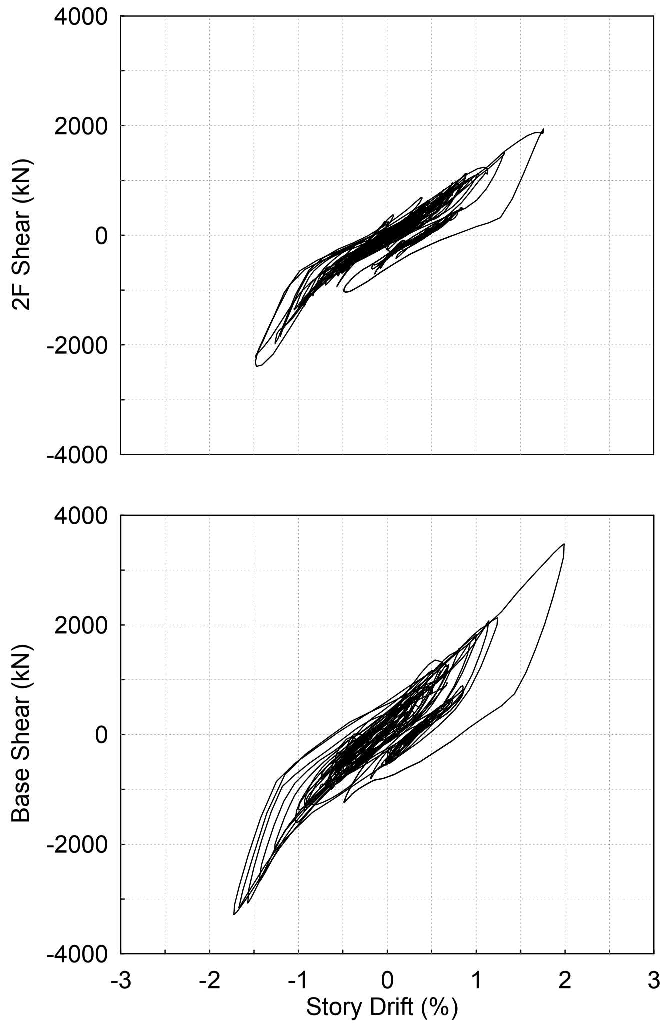

FIGURE 4-4 Hystereses of Test 4

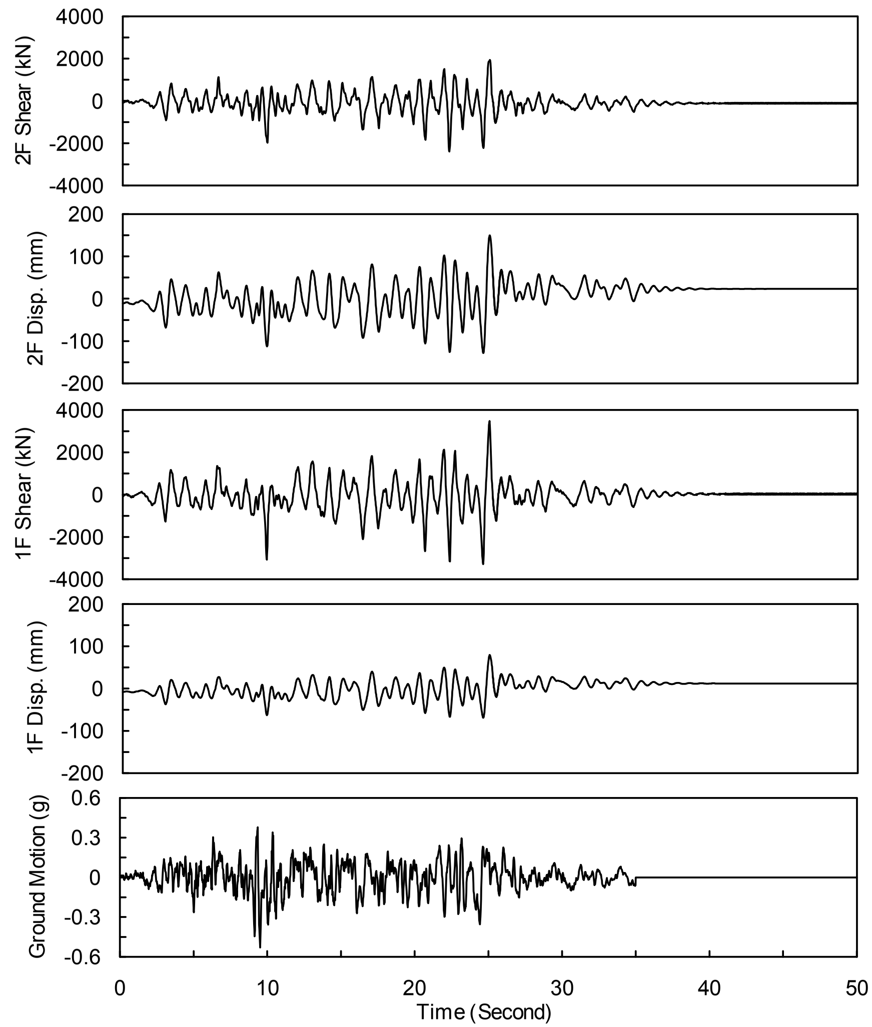

FIGURE 4-5 Ground Motion and Specimen Responses of Test 4

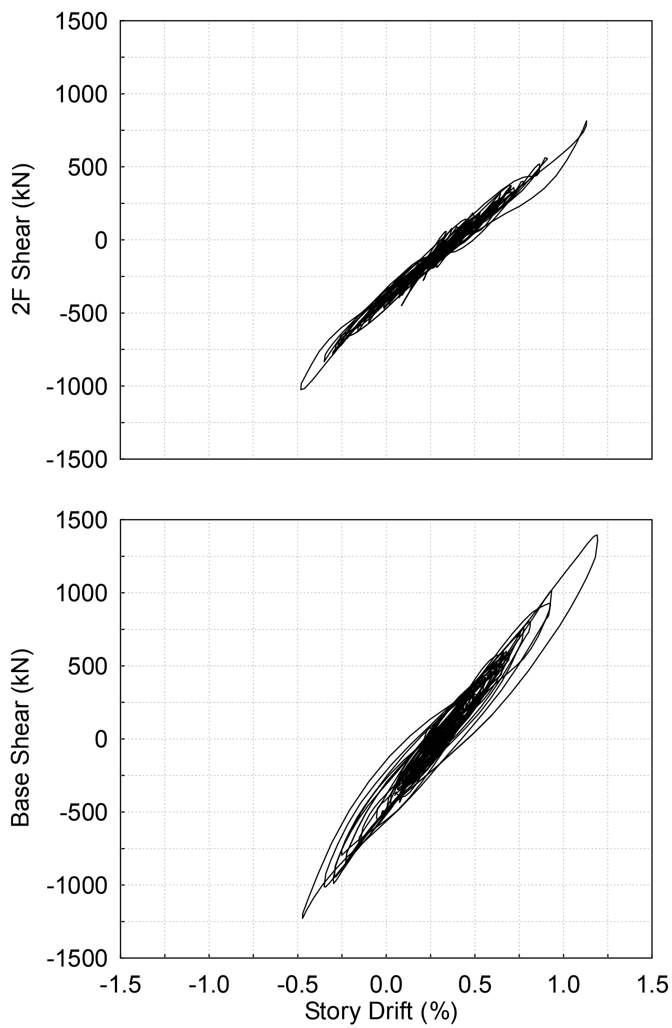

FIGURE 4-6 Hystereses of Test 5

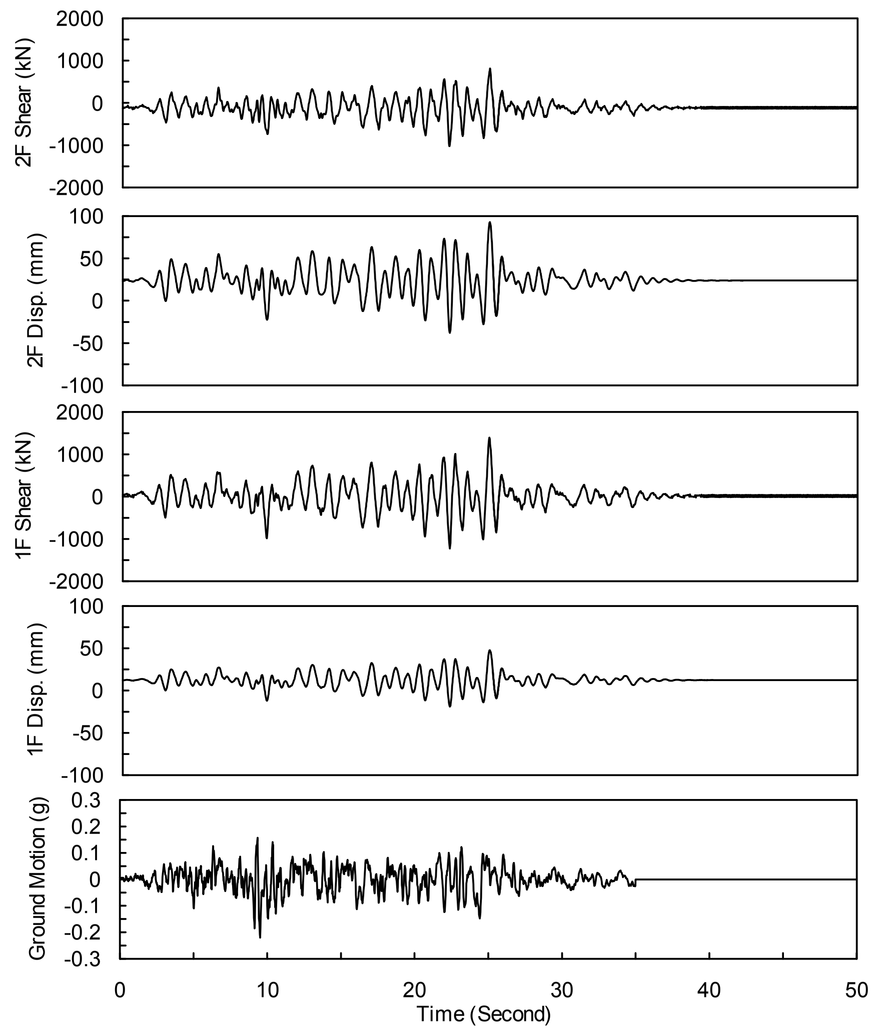

FIGURE 4-7 Ground Motion and Specimen Responses of Test 5

4.2.3 Experimental Observations of Phase I

4.2.3.1 Phase I-Test 1

The first test of Phase I was conducted using the Chi-Chi earthquake scaled to represent a hazard level having a 2% probability of exceedance in 50 years as described earlier. The gravity load of 1400 kN was first applied at the top of each VBE. An inspection of the infill panels revealed that no visible plate buckling occurred. Then, the pseudodynamic loads were applied on the specimen.

The test proceeded smoothly until 9.00 seconds from the beginning of the ground motion (recognizing that the experimental time scale is different from the excitation time scale in the pseudodynamic test procedure), when several pinging sounds were heard coming from the west side of the intermediate concrete slab. Inspection of that slab revealed that a crack along its longitudinal direction (i.e. along the north-south direction) developed adjacent to the south column, as shown in figure 4-8. The above mentioned crack propagated along the slab above the intermediate HBE, as shown in figure 4-9, when testing continued on the specimen.

At 9.50 seconds from the beginning of the ground motion, the longitudinal crack opened substantially in the intermediate HBE slab as shown in figure 4-10, resulting in a failure of loading transfer mechanism. Although the infill panels and boundary frame members exhibited mostly linear behavior (i.e. no visible plate buckling and whitewash flaking were observed during the test), the load path in the specimen had changed significantly from the intended design and the damage on the slab made it impractical to continue testing.

The above failure was primarily due to the insufficient longitudinal shear strength of the intermediate concrete slab. In addition, as previously shown in figure 3-6, the west side of the intermediate floor trusses had less truss members than the south side. This layout compromised the in-plane loading transfer capability of the west-side intermediate floor.

To repair the in-plane loading transfer system, instead of replacing the slab, the specimen was unloaded to its original position and additional diagonal members were added to the intermediate floor truss to enhance the existing loading transfer capacity as shown in figure 4-11. In order to limit the impacts of the resulting floor truss on the behavior of the RBS connections in the intermediate HBE, the newly added truss members were connected to the intermediate HBE outside the RBS region as shown in figure 4-12.

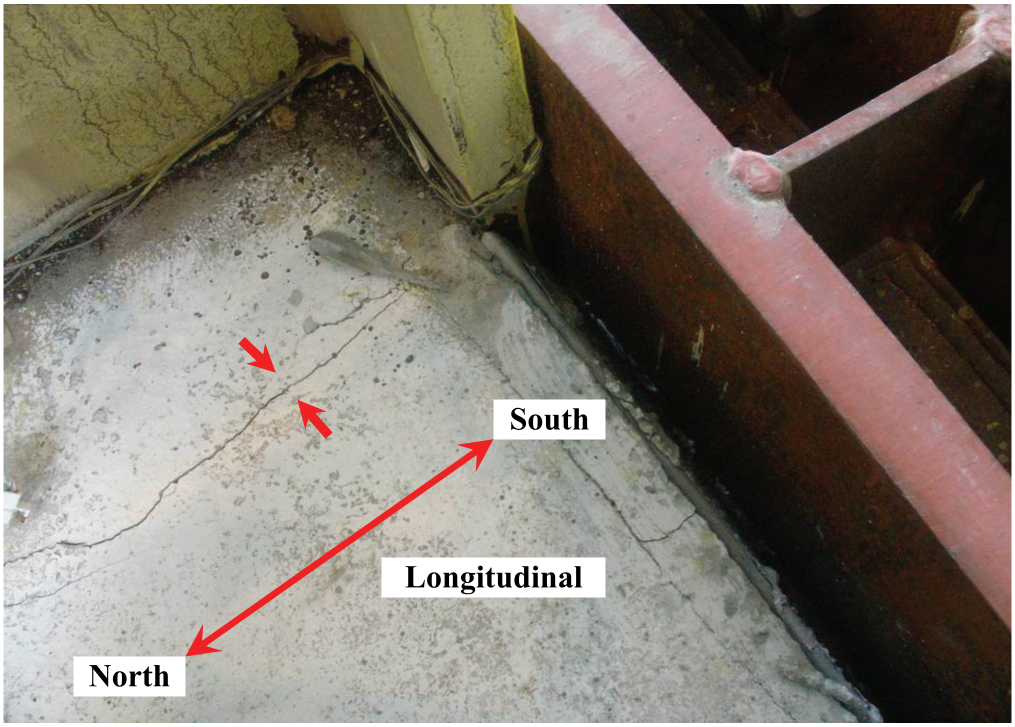

FIGURE 4-8 Onset of the Crack in Intermediate Concrete Slab (Photo Courtesy of C.H.Lin and K.C.Tsai, NCREE)

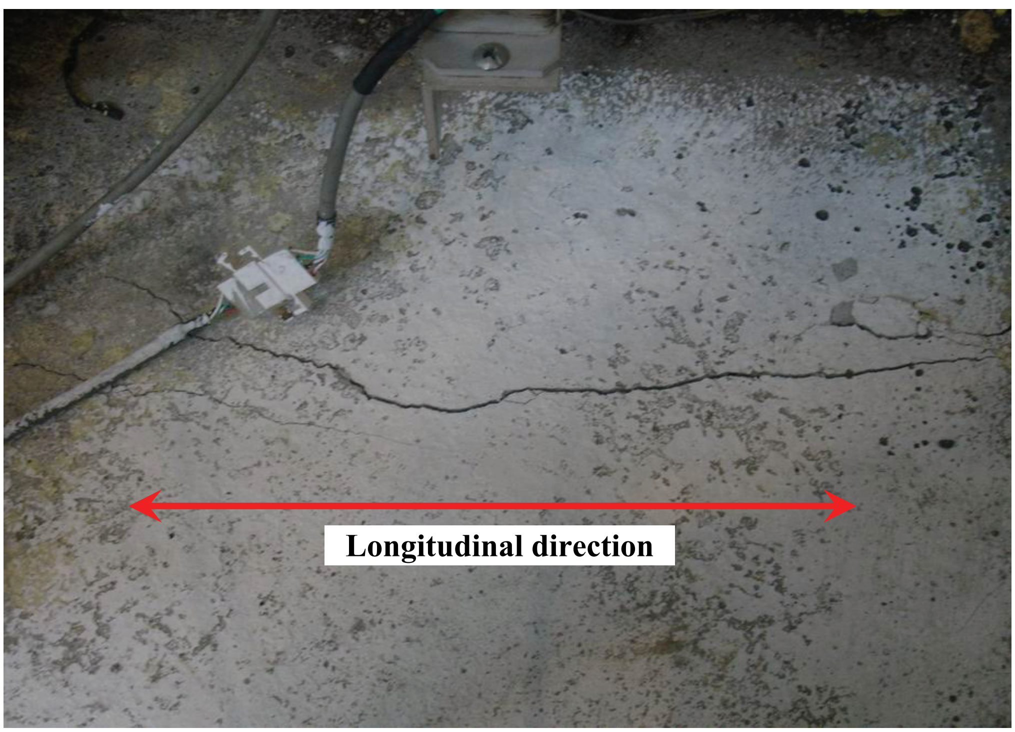

FIGURE 4-9 Propagation of the Crack in Intermediate Concrete Slab (Photo Courtesy of C.H.Lin and K.C.Tsai, NCREE)

(a) Crack along the Intermediate HBE

(b) Crack at the South End of the Intermediate HBE

FIGURE 4-10 Penetration of the Crack in Intermediate Concrete Slab (Photo Courtesy of C.H.Lin and K.C.Tsai, NCREE)

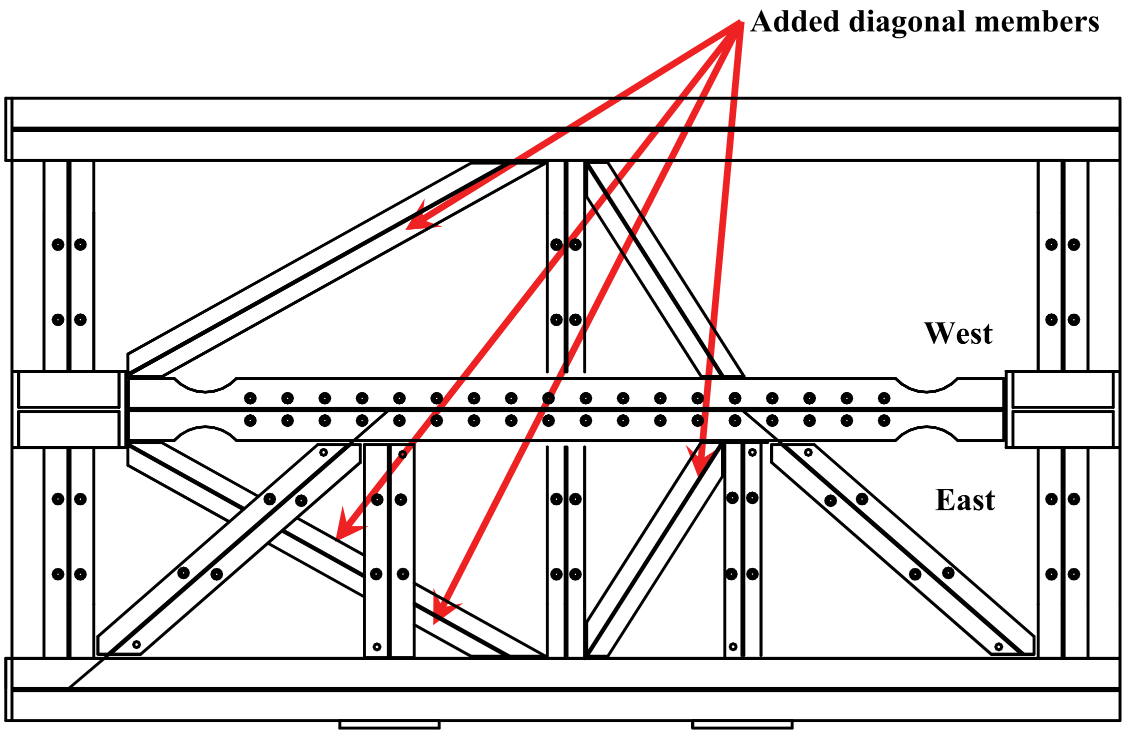

FIGURE 4-11 Layout of the Intermediate Floor Truss Strengthened after Test 1

FIGURE 4-12 Typical Floor-Truss-Member-to-Intermediate-HBE Connection

4.2.3.2 Phase I-Test 2

After doing the above strengthening work, Test 2 was conducted using the same loading program as Test 1. Visible buckling and yielding of the infill panels was observed as the story drift increased in Test 2, along with audible pinging sounds when the panel fold that developed in the previous loading cycles reoriented themselves. The boundary frame members behaved similarly to Test 3 (described in greater length in the next section) to 24 seconds from the beginning of the ground motion, when the anchor bolts used to fix the south VBE base fractured followed by a significant slip deformation of the intermediate concrete slab from the corrugated steel deck. The test was then stopped.

The specimen was relocated to its original position. At that point, the cracked intermediate concrete slab was removed and a new slab was reconstructed as shown in figure 4-14. In addition, the west side of the intermediate floor truss was further strengthened by adding more members to provide a larger load transfer capacity as shown in figure 4-13. The fractured anchor bolts at the south VBE base were replaced by new ones and the south and north VBE bases were further strengthened by welding the VBE end plates to anchor plates connected to the strong floor.

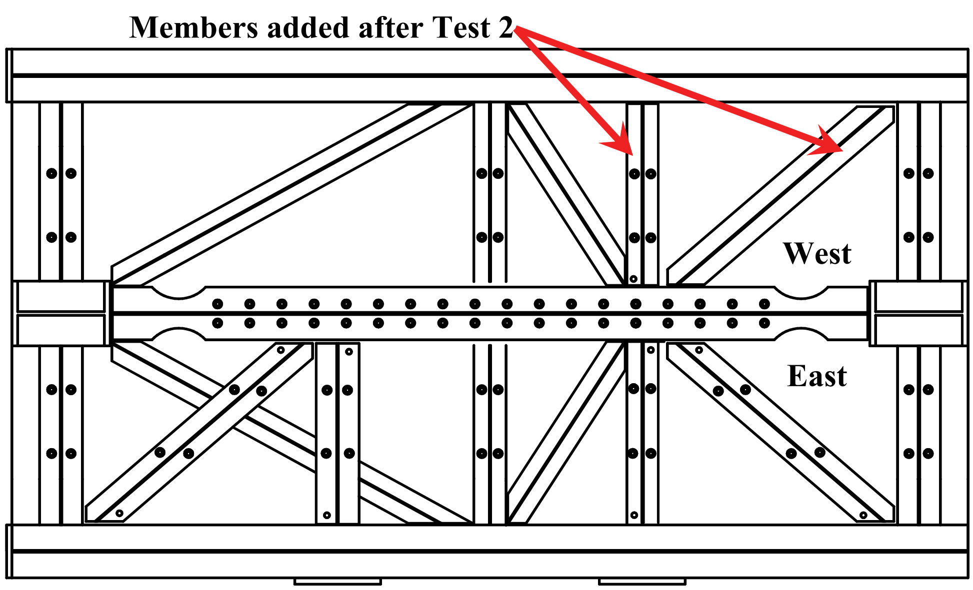

FIGURE 4-13 Layout of the Intermediate Floor Truss Strengthened after Test 1

(a) Installment of New Shear Studs

(b) Rebar Layout of the Intermediate Slab

FIGURE 4-14 Reconstruction of the Intermediate Slab
(Photo Courtesy of C.H.Lin and K.C.Tsai, NCREE)

4.2.3.3 Phase I-Test 3

After proper curing of the concrete used to repair the intermediate concrete slab (such that it could develop its expected strength, Test 3 was conducted restarting from the beginning of the same pseudodynamic loading history as for Tests 1 and 2.

Elastic buckling of the panel and linear force-displacement behavior were observed during the early stage of this test. Yielding of the infill panels (as usually indicated by the whitewash flaking) were observed after the test proceeded to 6.68 seconds from the beginning of the earthquake excitation. Flaking of whitewash was noted along the tension field direction in a number of locations on the infill panels as shown in figure 4-15.

By 9.97 seconds from the beginning of the ground motion, when a base shear of approximately 3284 kN had been imparted on the specimen, previously observed yielding of infill panels along the tension field inclination directions as shown in figure 4-15 was spread across the infill panels followed by initiation of some panel tears, presumably resulting from low cycle fatigue at the ridge of buckles, as shown in figures 4-16. The infill panels remained slightly buckled when the specimen was returned to zero displacement as shown in figure 4-17.

At 20.70 seconds from the beginning of the ground motion (before the specimen experienced the peak response), the test was paused and an inspection was made on the specimen. As a result of cyclic infill panel yielding, infill panel tears previously observed, as shown in figure 4-16 further developed as shown in figure 4-18.

As the test proceeded, the specimen experienced the peak story drift responses of 2.6 and 2.2% at the first and second story, respectively. Yield lines were also observed in a number of locations in the boundary frame members. Web of the intermediate HBE yielded significantly over their entire beam depth in the RBS region, as shown in figure 4-19a. This yielding behavior suggests the presence of substantial shear force and axial force developed in the beam. Visible yield lines were observed on the bottom flanges of the intermediate HBE. Interestingly, as shown in figure 4-19b, these yielding lines on the bottom flange of the intermediate HBE spread over the half of the reduced flange region close to the VBE face rather than concentrating at the center of the RBS region (i.e. where the flange is reduced the most).

The yielding behavior of the top HBE was quite similar to the intermediate HBE, but to a lesser degree, as shown in figure 4-20. However, different from the top and intermediate HBEs, no prominent yielding was observed in the bottom HBE since plastic hinges developed at the VBE bases mostly above the bottom HBE (as indicated by the VBE yielding pattern described below). Only a limited number of yield lines appeared on the web of the bottom HBE, over the RBS region, as shown in figure 4-21.

Significant flaking of the whitewash was observed on the VBE flanges at the north and south VBE bases as shown in figure 4-23 while yielding, but to a of lower degree, was seen to have developed on the VBE webs, as shown in figure 4-22.

The testing was eventually concluded at 50 seconds from the beginning of the ground motion. Throughout the test, no in-span plastic hinge was observed in the HBEs at all levels. Welds used to connect the infill plate segments (as mentioned in Section 3) in the panel interior remained intact. No other yielding lines were visible along the VBE height, indicating that, as intended, the VBEs behaved primarily in the elastic range except at their bases.

FIGURE 4-15 Yield Lines across the Infill Panel

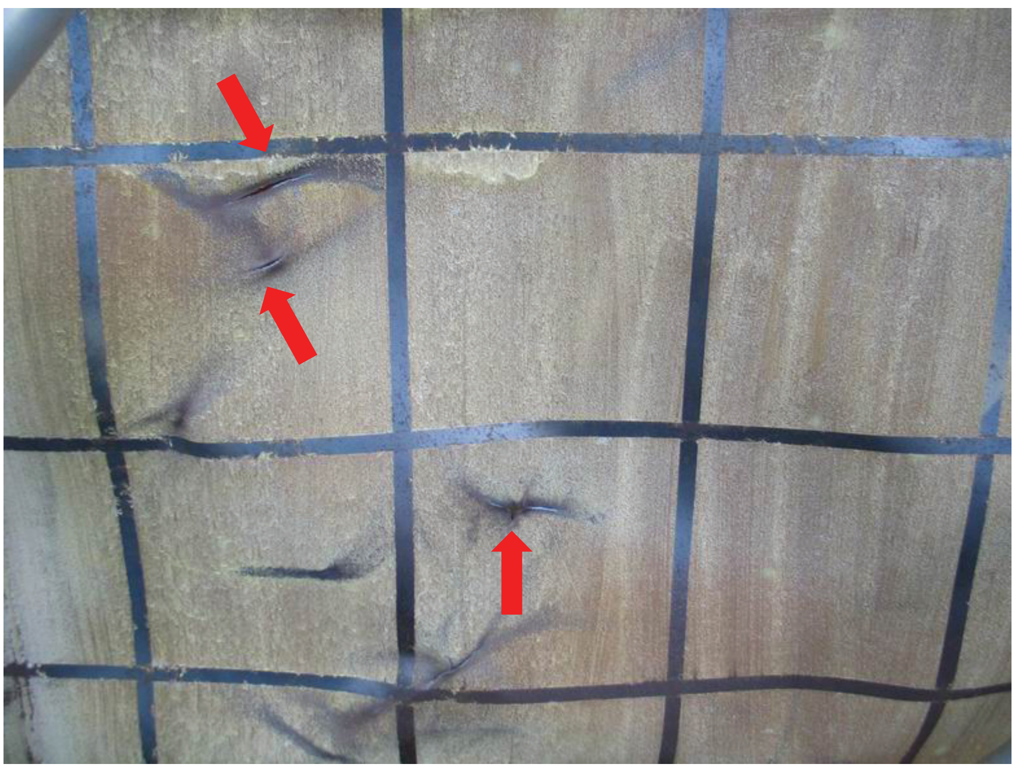

FIGURE 4-16 Initiation of the Panel Tear

(a) The First Story

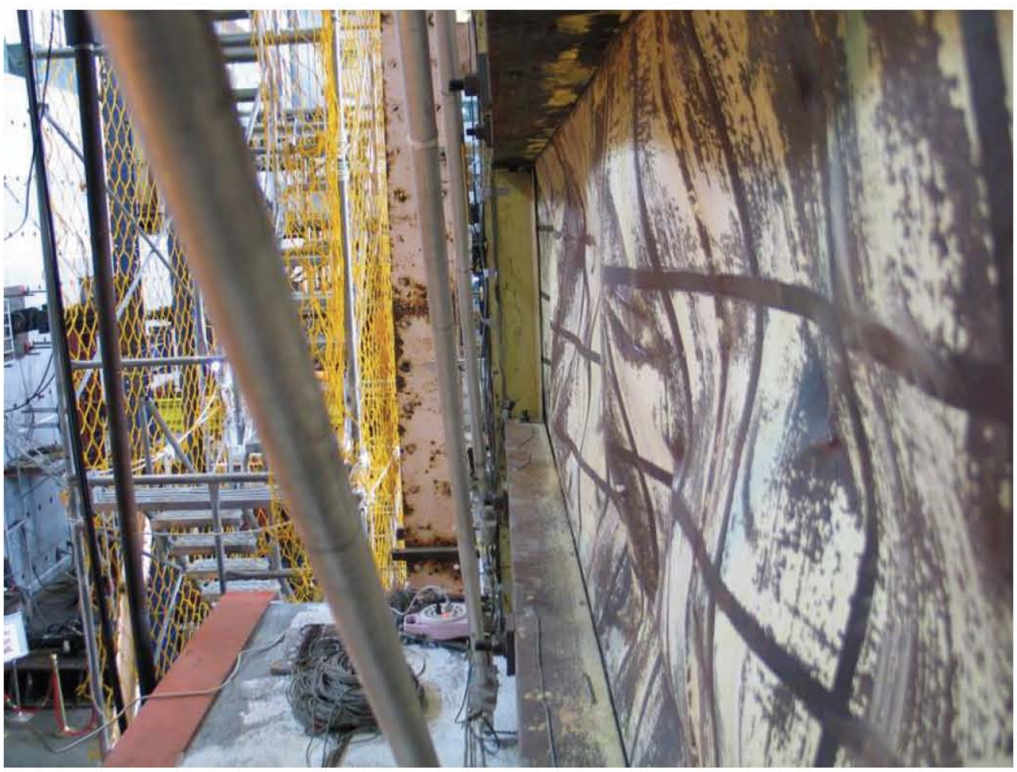

(b) The Second Story

FIGURE 4-17 Buckled Panels at the Neutral Position of the Specimen

(a) Overall View of Panel Tear

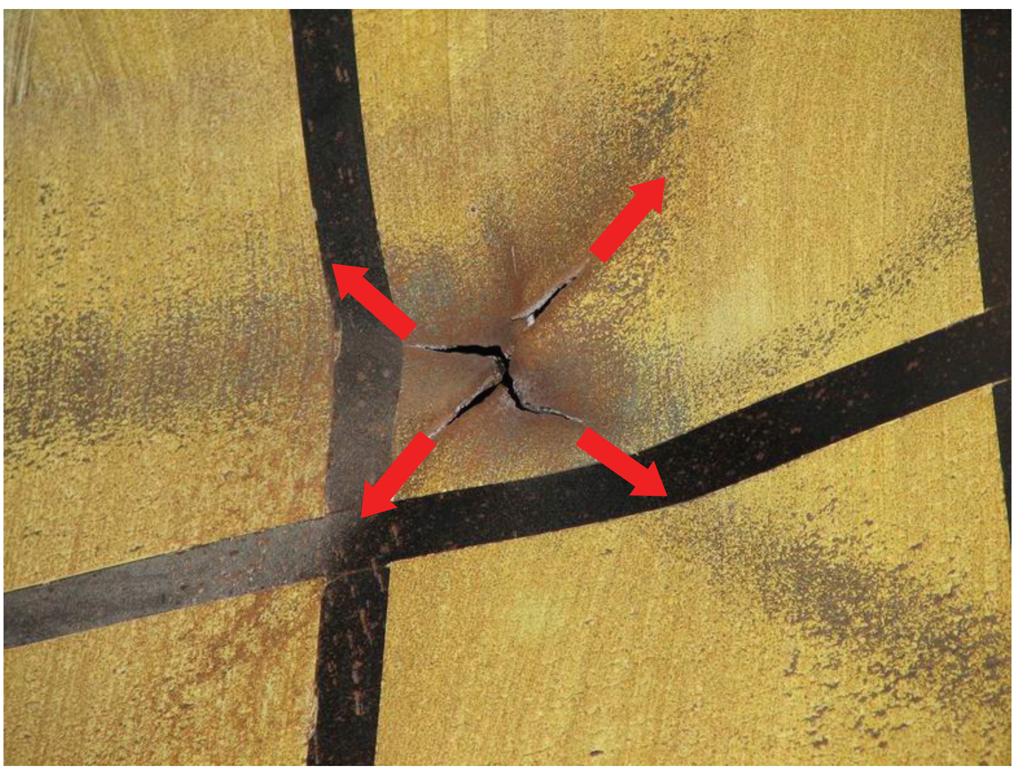

(b) Detail of Panel Tear

FIGURE 4-18 Panel Tear in Test 3

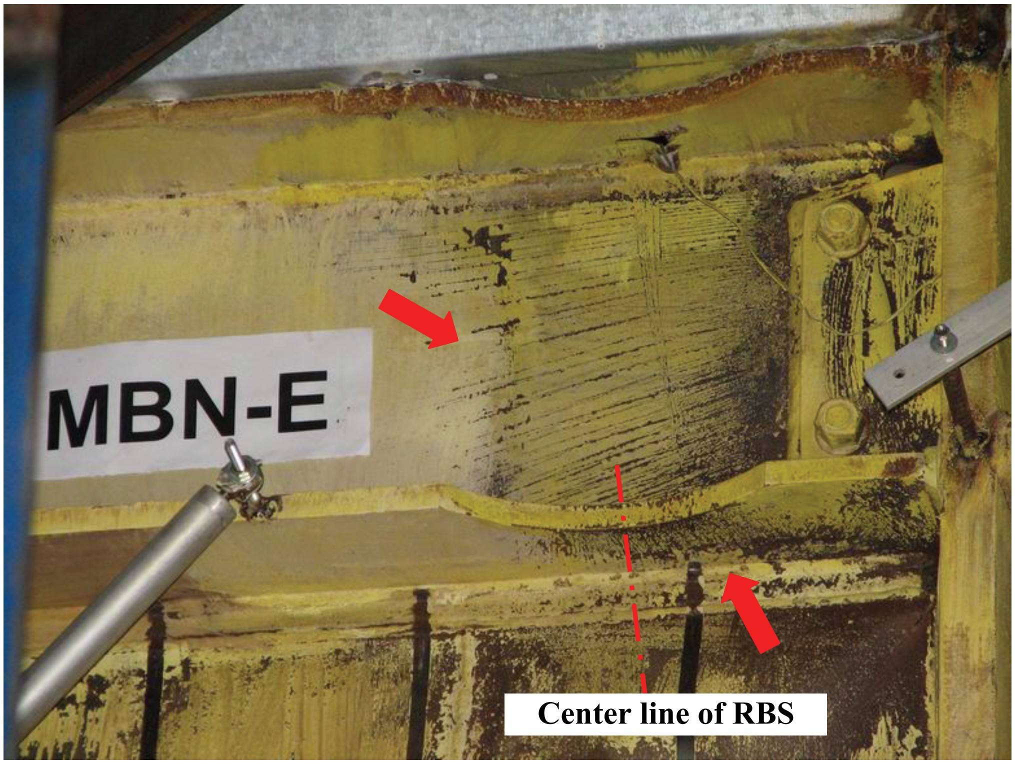

(a) North End of the Intermediate HBE

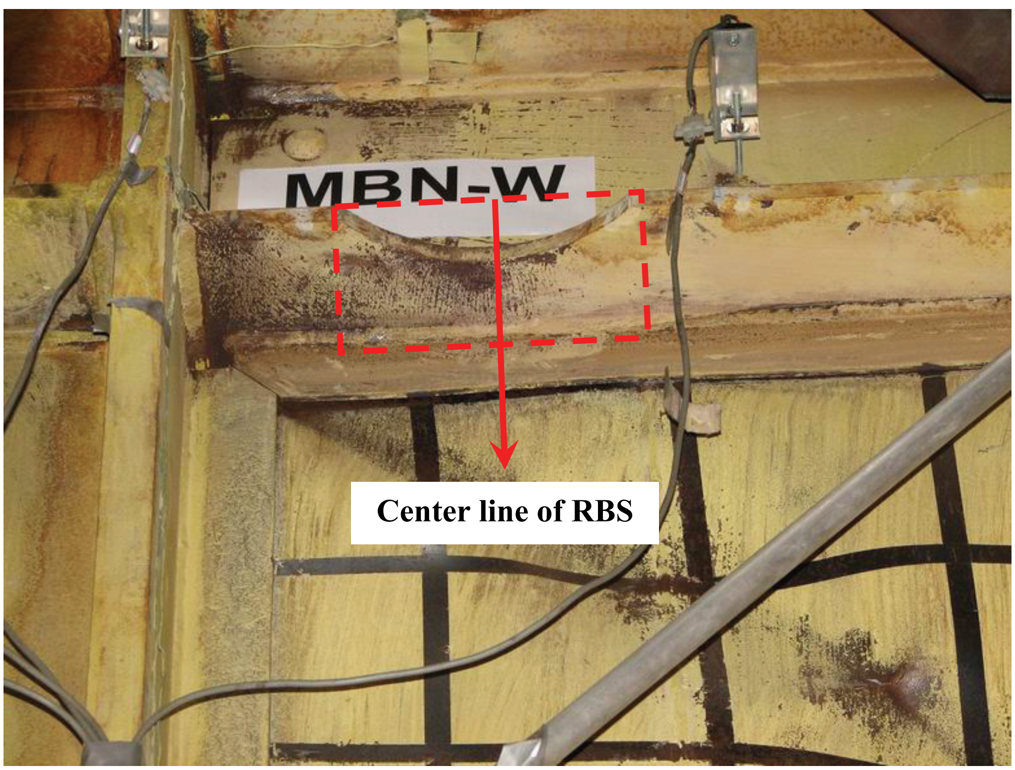

(b) South End of the Intermediate HBE

FIGURE 4-19 Yielding Pattern of the Intermediate HBE in Test 3

(a) Web Yielding at the North End of the Top HBE

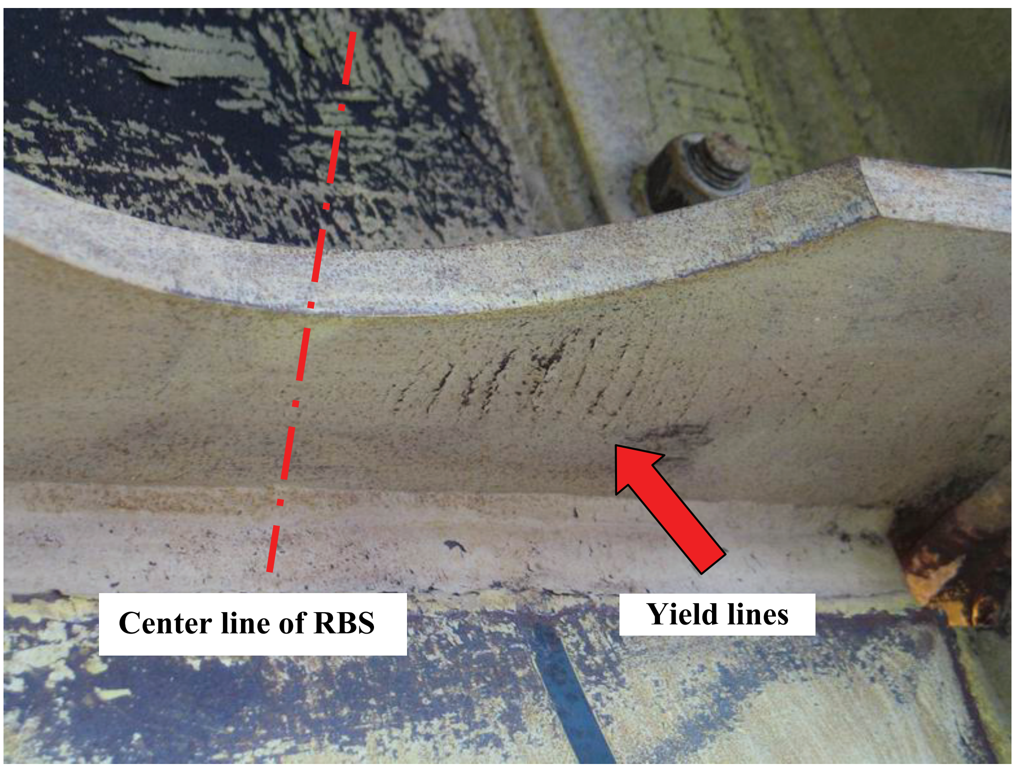

(b) Flange Yielding at the North End of the Top HBE – East Side

FIGURE 4-20 Yielding Pattern of the Top HBE in Test 3

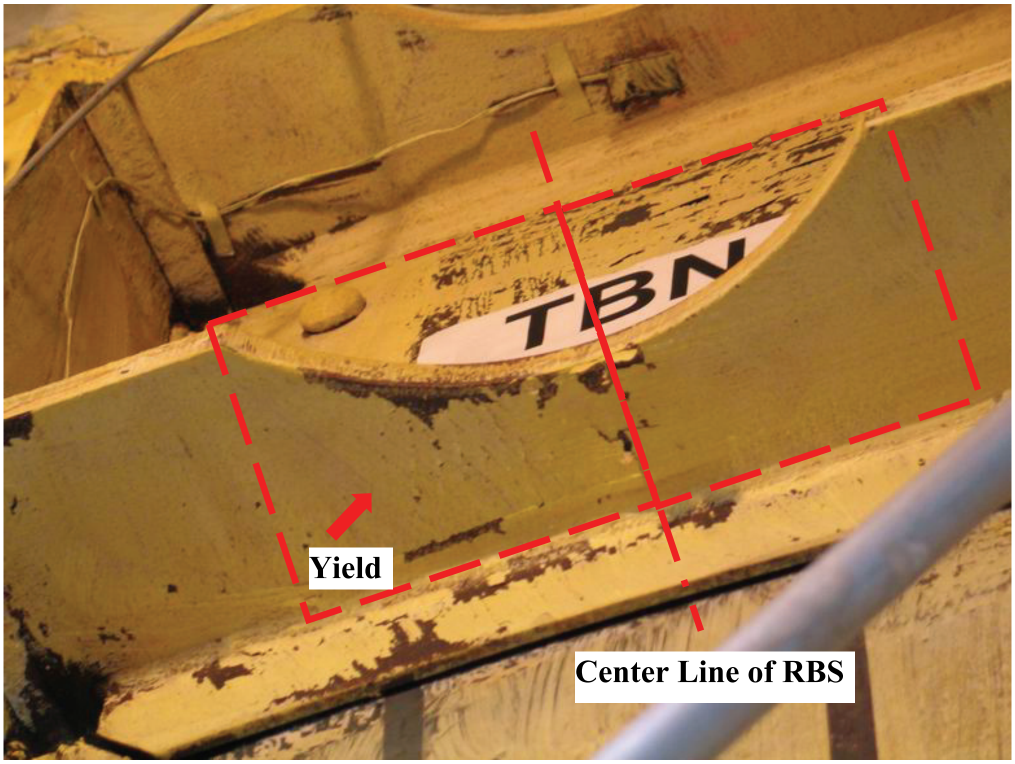

(c) Flange Yielding at the North End of the Top HBE – West Side

FIGURE 4-20 (Cont'd) Yielding Pattern of the Top HBE in Test 3

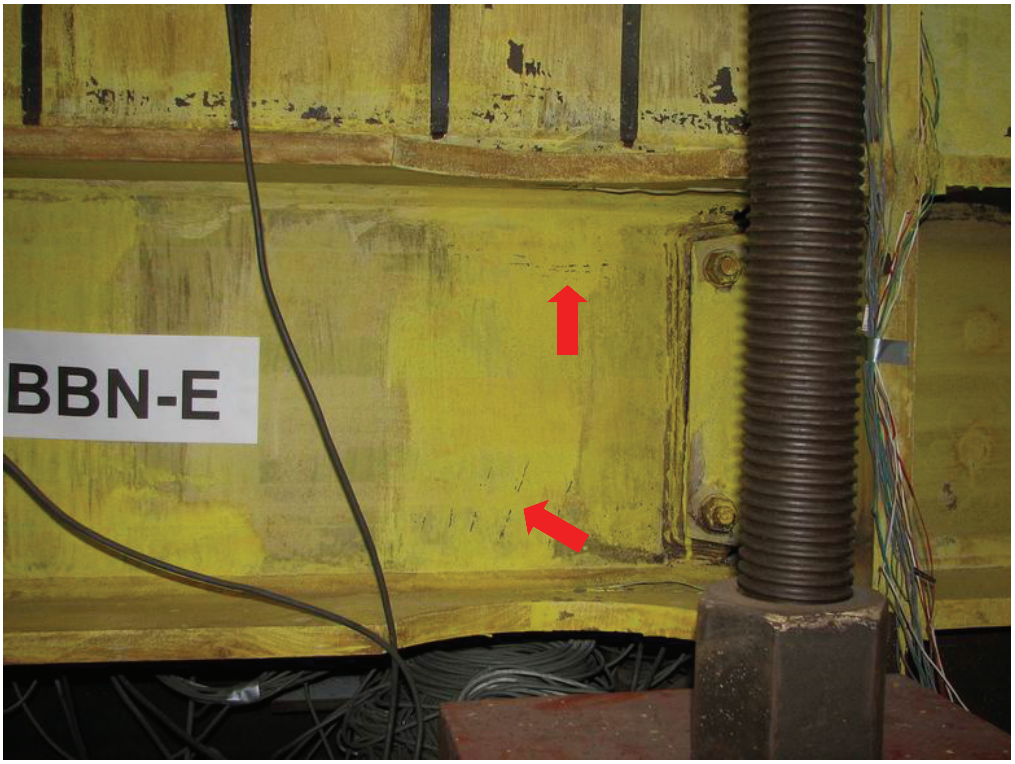

(a) North End of the Bottom HBE – East Side

(b) North End of the Bottom HBE – West Side

FIGURE 4-21 Yielding Pattern of the Bottom HBE in Test 3

(c) South End of the Bottom HBE – East Side

(d) South End of the Bottom HBE – West Side

FIGURE 4-21 (Cont'd) Yielding Pattern of the Bottom HBE in Test 3

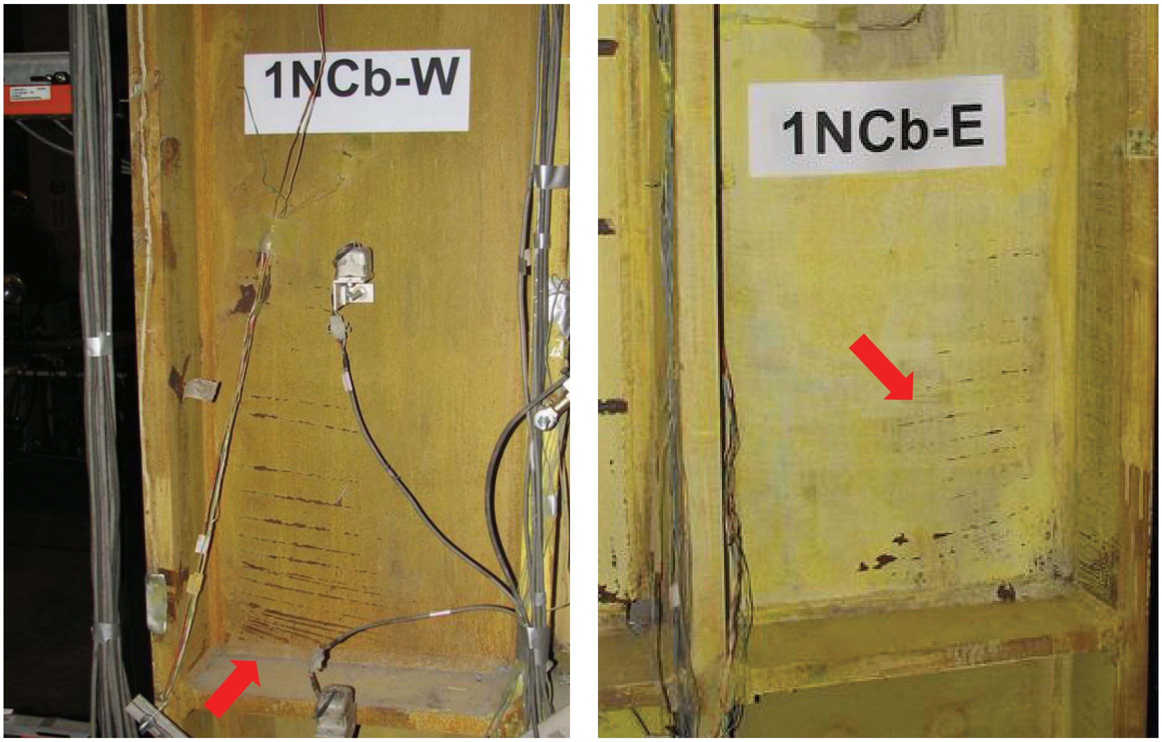

(a) West Side (b) East Side

FIGURE 4-22 VBE Web Yielding Pattern at the North VBE Base in Test 3

(a) South VBE Base (b) North VBE Base

FIGURE 4-23 VBE Flange Yielding Pattern at the Column Bases in Test 3

4.2.3.4 Phase I-Test 4

The next stage of the Phase I tests included testing the SPSW specimen using the Chi-Chi earthquake record (TCU08-EW) scaled to a level representative of a seismic hazard having a 10% probability of exceedance in 50 years, to investigate how the SPSW would behave in a subsequent larger aftershock.

The same gravity load of 1400 kN as used in previous tests was applied at the top of each VBE followed by the application of pseudodynamic earthquake loads. The test was paused for inspections at 17.15 seconds, 22.38 seconds, 24.68 seconds, and 25.17 seconds from the beginning of the ground motion.

In the early stage of this test, there was no audible buckling sound from the infill panel. As the test progressed, audible buckling sounds (which came from the alternating tension field orientation during reversed loading cycles as observed in the previous tests) began and the magnitude of the buckling waves grew remarkably.

At 25.17 seconds from the beginning of the earthquake excitation, fractures were observed at the lower north corner of the first-story infill panel, as shown in figure 4-24. Those fractures initiated at the toes of the fillet welds connecting the infill panels to the fish plates. After further inspection, the other corners of the infill panels at the first and second story were found to have similar fractures. All those fractures were less than 25 mm in length throughout the test and did not affect the story shear strength of the wall.

The infill panel tears observed in the prior tests continued to propagate as the test proceeded. Figure 4-25 shows the worst tear, which was approximately 250 mm in length in the first-story infill panel, at the end of this test. During this test, the extent of visible yielding increased at the RBS connections of all levels and at the VBE bases, while no fractures were found in the boundary frame members. No strength degradation was observed during the test.

FIGURE 4-24 Fractures at the Corner of the First-Story Infill Panel

FIGURE 4-25 Panel Tear in the First-Story Infill Panel (at the End of Test 4)

4.2.3.5 Phase I-Test 5

The last test of Phase I was conducted using the Chi-Chi earthquake record (TCU08-EW) scaled to a level representative of a seismic hazard having a 50% probability of exceedance in 50 years, to investigate how the SPSW would behave in a subsequent smaller aftershock.

The test was paused at 17.15 seconds and 25.18 seconds from the beginning of the earthquake. There was little yielding in the tests, as reflected by the fact that the story shear vs. drift behavior of the specimen remained virtually linear as shown in figure 4-6. Throughout this test, no fractures were observed on the boundary frame members and the infill panel damages observed previously did not progress to a higher degree of severity.

4.3 Infill Panel Replacement

At the end of the Phase I tests, the residual story drifts were 0.31 and 0.29% at the first and second story, respectively; and no fracture was found in the boundary frame, which was deemed to be in satisfactory condition, allowing for the replacement of infill panels for the subsequent phase of testing. It took a crew of three technicians 2-1/2 days to complete the infill panel replacement.

As shown in figure 4-26, the buckled plates were cut along the fish plates as well as along the horizontal lines at the quarter points of story height. Some of the cutout buckled panel, and the specimen and fish plate details after removing the infill panels are shown in figures 4-27 and 4-28, respectively.

New infills were installed into the structural frame of the specimen by welding along the fish plates as shown in figure 4-29. These panel segments (approximately 1200mm x 4000mm) were then connected together, first by tack welding at a number of points along their edges to keep them aligned, and then by continuous full penetration welds along their edges, as shown in figure 4-30. The infill panels of the Phase I tests were welded on one side of the fish plates and those of the Phase II tests were welded to the other side as shown in figure 4-31. The so-repaired specimen before the Phase II tests is shown in figure 4-32.

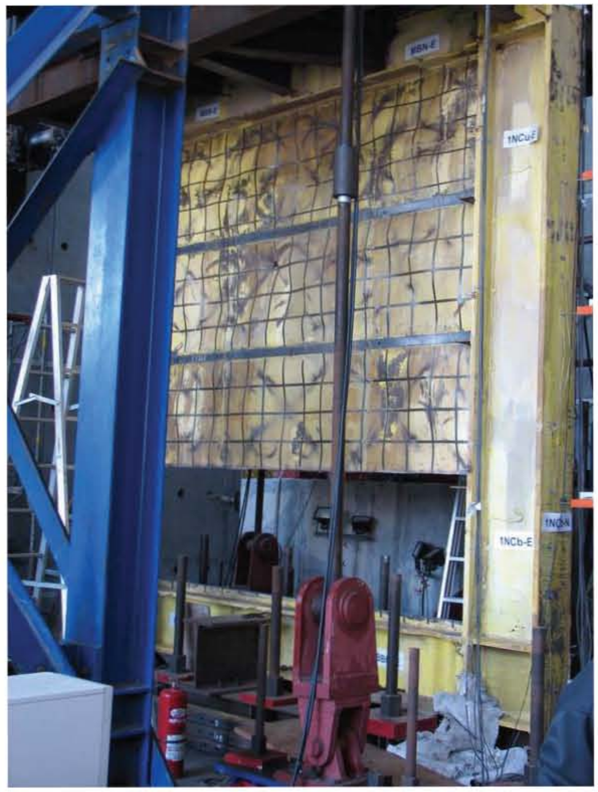

FIGURE 4-26 Specimen during the Infill Panel Removal

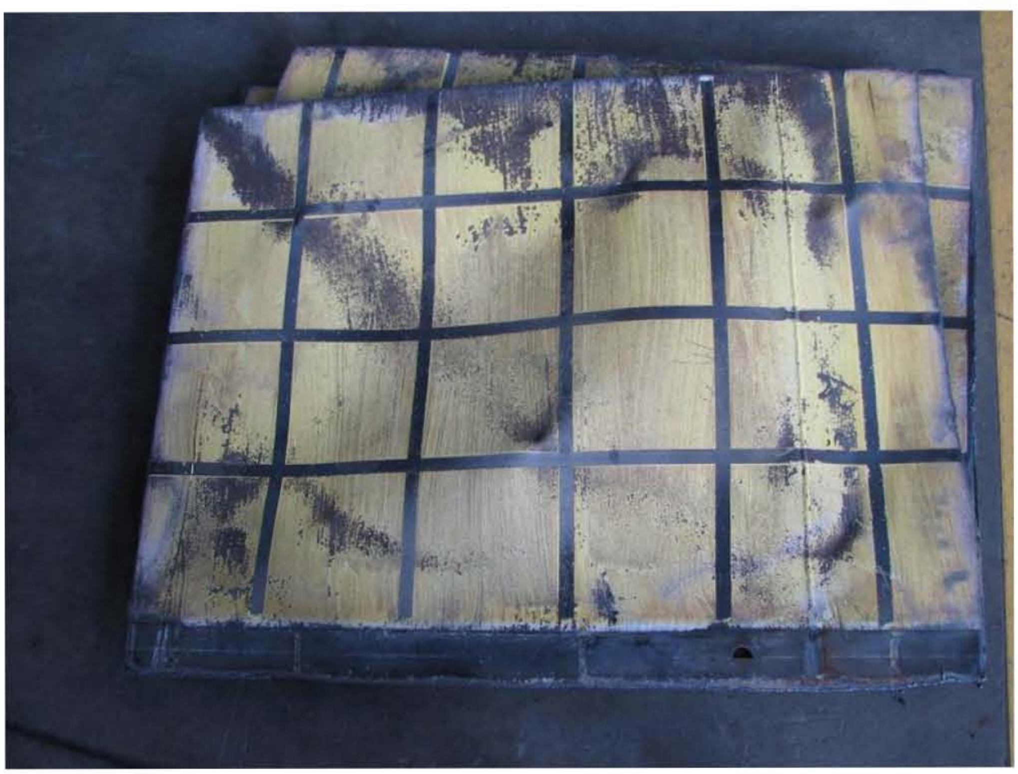

FIGURE 4-27 Cutout Buckled Panels

(a) Overall View of the Specimen

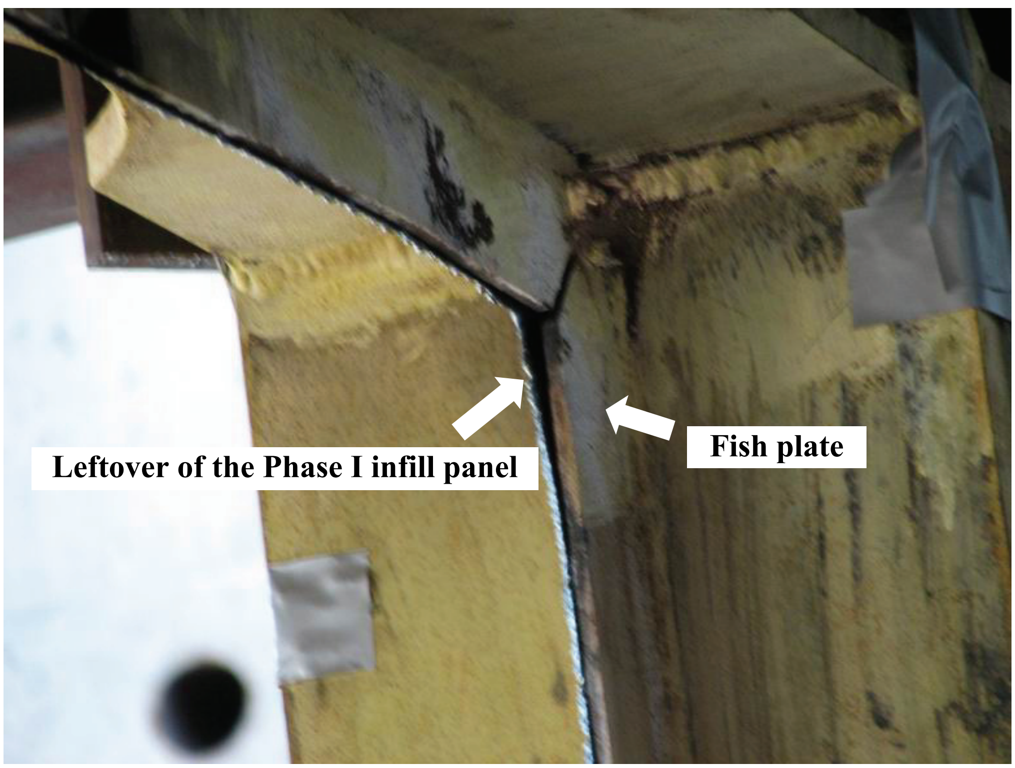

(b) Detail of the Fish Plates

FIGURE 4-28 Specimen after the Infill Panel Removal

(a) the Second Story (b) the First Story

FIGURE 4-29 New Panel Installation

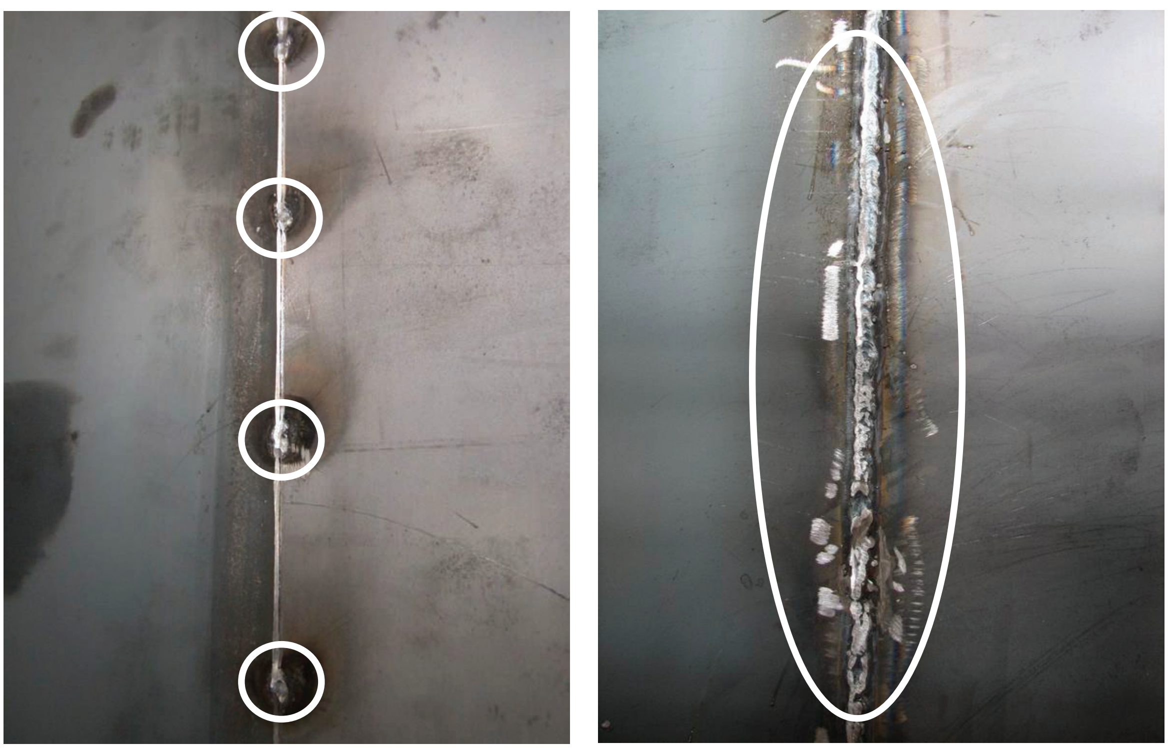

(a) Tack Welds (b) Final Continuous Welds

FIGURE 4-30 Welds in New Panels Interior

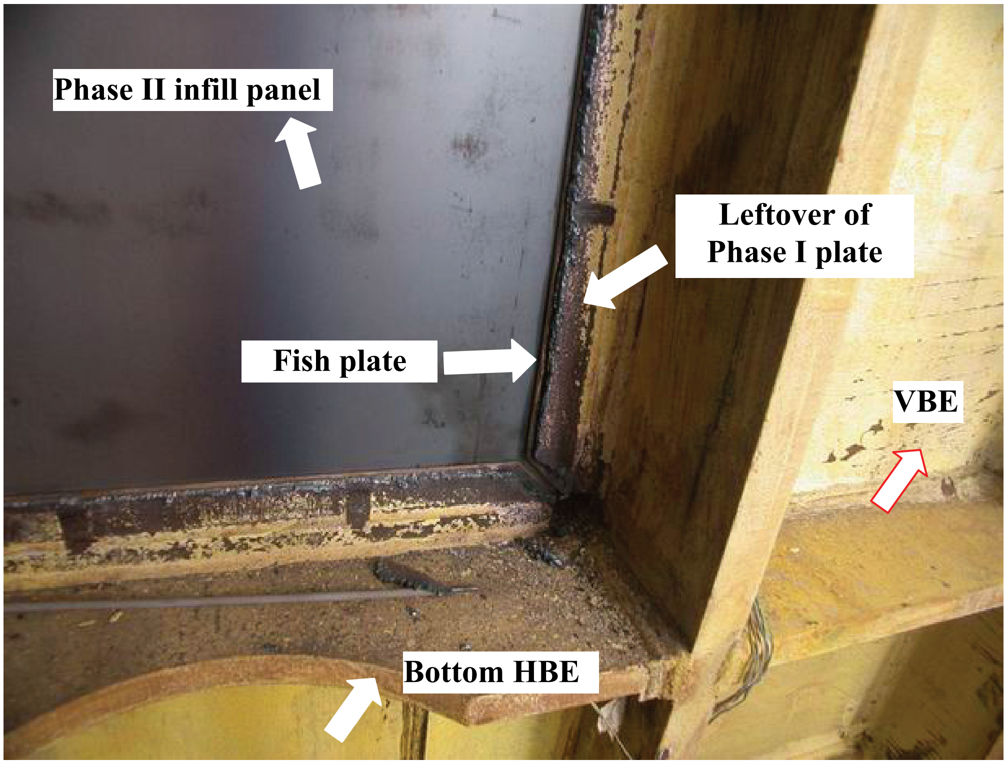

FIGURE 4-31 Detail of Fish Plates after the Infill Panel Installation

FIGURE 4-32 Specimen prior Phase II Tests

4.4 Phase II Tests

The objective of the Phase II tests is to experimentally address the ultimate behavior of the intermediate HBE of the wall and the performance of the repaired SPSW in a new earthquake. For those purposes, the specimen was tested under pseudodynamic loads followed by cyclic loads to failure. The following describes the loading programs, observation, and test results of the Phase II tests

4.4.1 Loading Programs

In order to investigate how the repaired SPSW specimen would behave in a second earthquake in the first stage of Phase II, the specimen was tested under the pseudodynamic loads corresponding to the Chi-Chi earthquake record (TCU082-EW) scaled to a seismic hazard having a 2% probability of exceedance in 50 years (i.e. equivalent to the first earthquake record considered in the Phase I tests). For convenience, hystereses obtained from the Phase II pseudodynamic test is presented in figure 4-33. The corresponding ground motion inputs, displacement histories at floor levels, story shear responses, recorded in the test is shown in figure 4-34.

The next stage of the Phase II tests involved cyclic tests of the SPSW specimen to investigate the ultimate behavior of the intermediate HBE and the cyclic behavior and ultimate capacity of the wall. A displacement-controlled scheme was selected for the cyclic test. Because the first mode response dominated the global response of the SPSW in the prior pseudodynamic test (although some higher mode effects were observed) and to allow testing both stories even if failure progressively develops at one of the two stories, a displacement constraint was exerted to ensure that the in-plane actuators displaced in a ratio corresponding to a first mode of response throughout the entire test.

Table 4-3 shows the story drift history applied during the cyclic testing of the first and second story respectively. Since the specimen was pulled (to the south) to the maximum actuator stroke when the peak story drifts reached -3.2% and -3.0% at the first and second story respectively, the applied displacement history became unsymmetrical beyond that point, in that the peak story drifts due to loading toward the south were kept at -3.2% and -3.0% at the first and second story respectively in all subsequent cycles while increasing displacements were still applied in the other direction. The hysteretic curves progressively obtained from the Phase II cyclic test are shown in figure 4-35.

TABLE 4-3 Cyclic Story Drift Histories

Displacement step	Number of cycles	Cumulative number of cycles	1F		2F	
			Positive drift (%)	Negative drift (%)	Positive drift (%)	Negative drift (%)
1	2	2	1.2	-1.2	1.0	-1.0
2	2	4	2.4	-2.4	2.0	-2.0
3	2	6	3.0	-3.0	2.5	-2.5
4	2	8	3.2	-3.2	3.0	-3.0
5	2	10	3.7	-3.2	3.5	-3.0
6	2	12	4.3	-3.2	4.0	-3.0
7	2	14	4.8	-3.2	4.5	-3.0
8	0.25	14.25	5.2	-[a]	5.0	-[a]

[a]Not applicable.

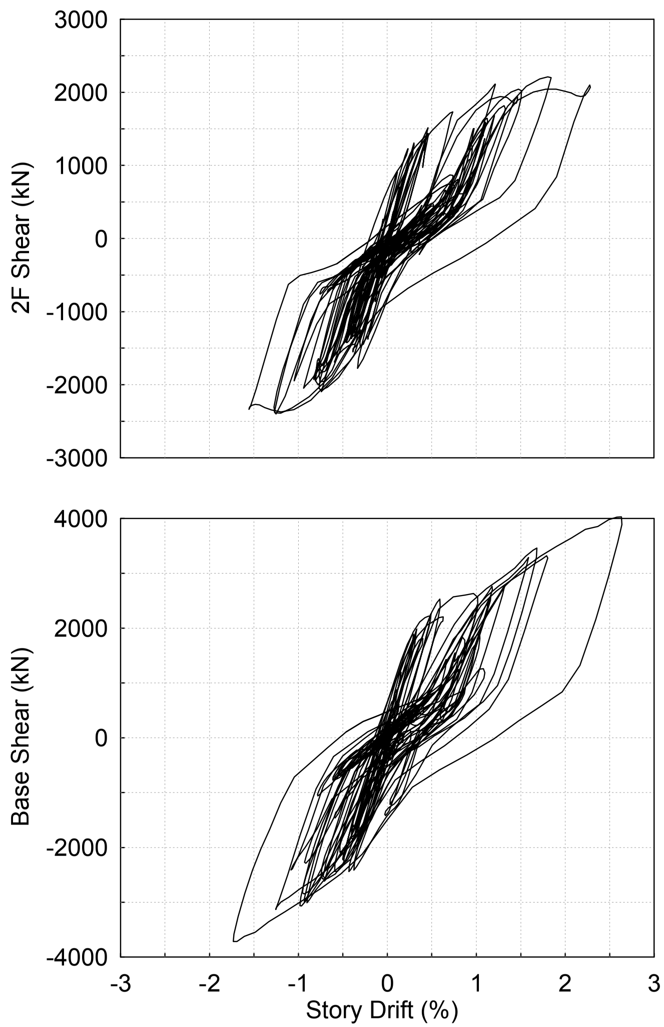

FIGURE 4-33 Hystereses of the Phase II Pseudodynamic Test

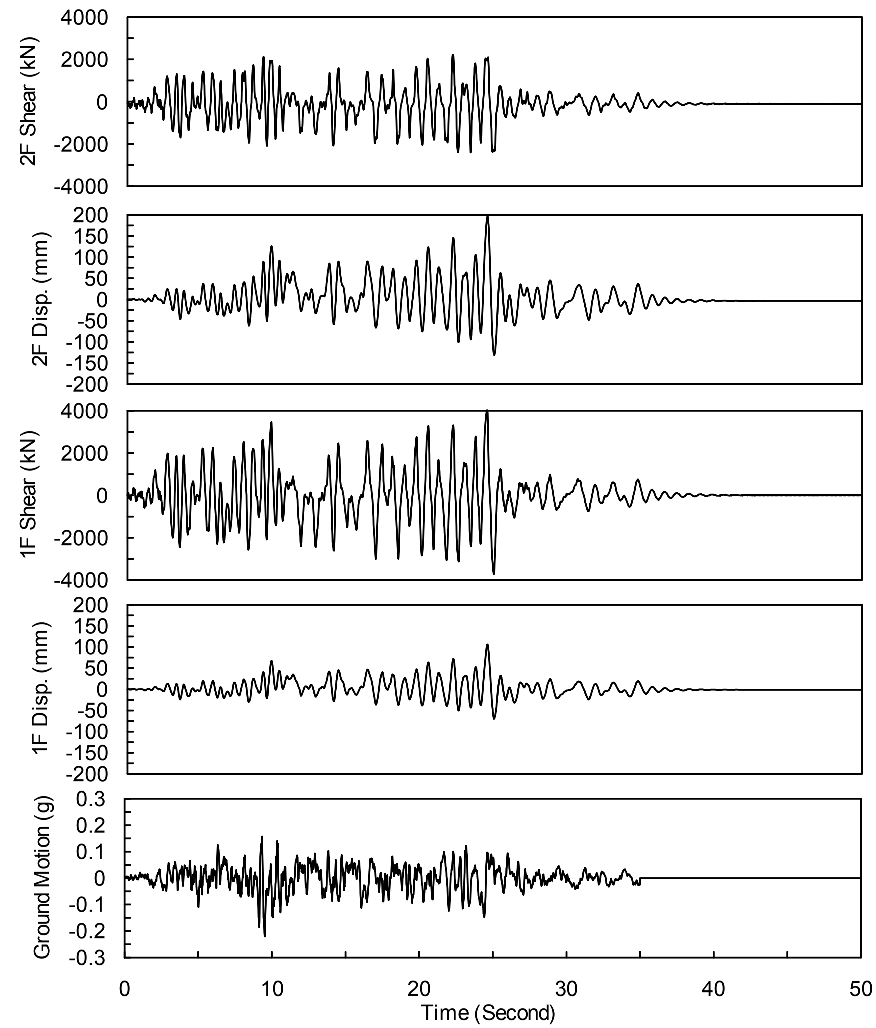

FIGURE 4-34 Ground Motion and Specimen Responses of the Phase II Pseudodynamic Test

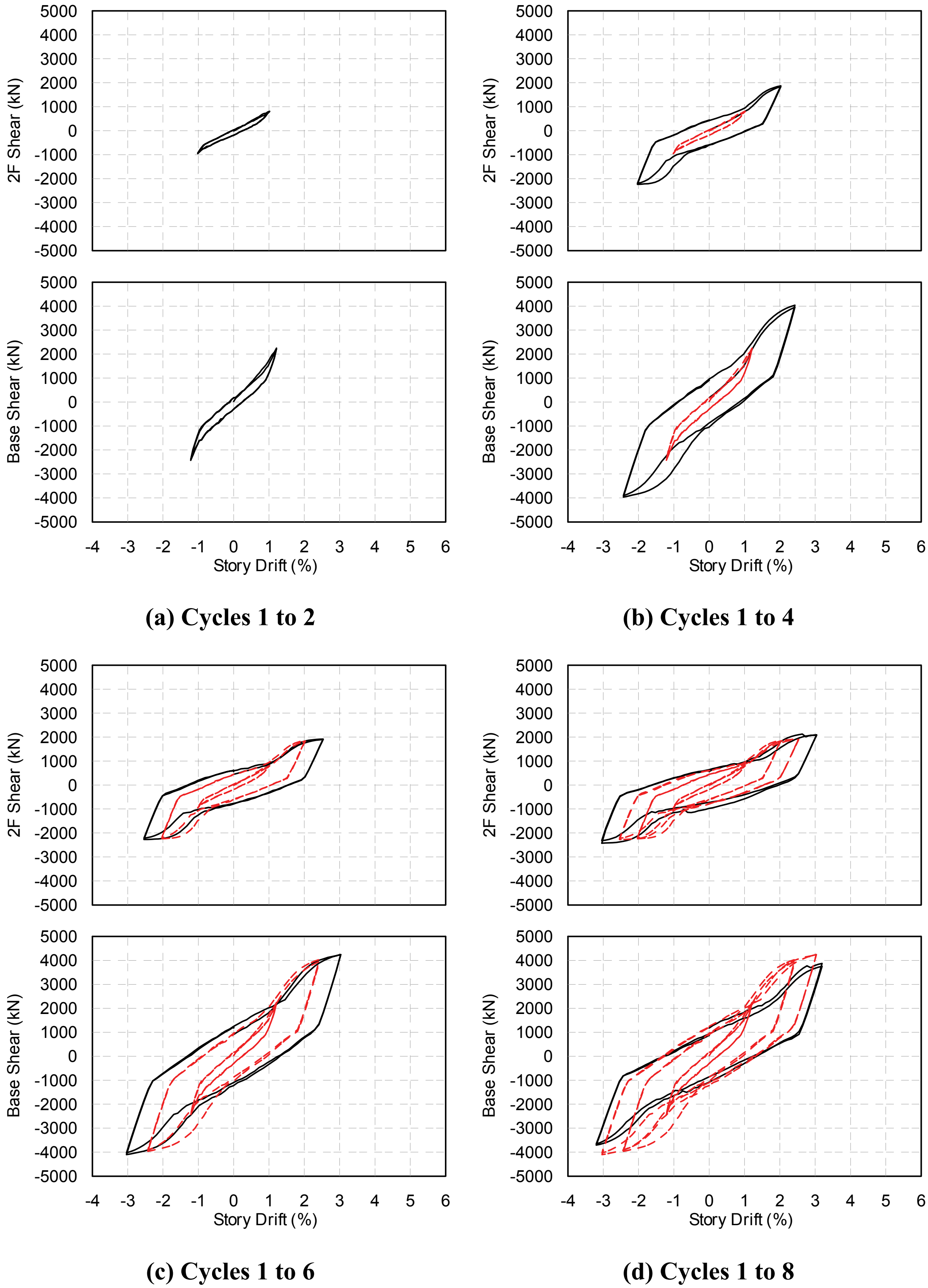

FIGURE 4-35 Progressive Hystereses of the Phase II Cycle Test

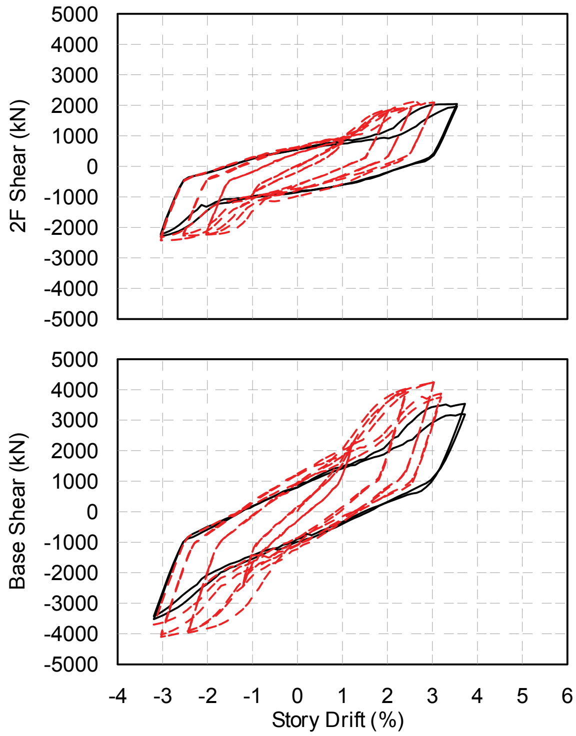

(e) Cycles 1 to 10

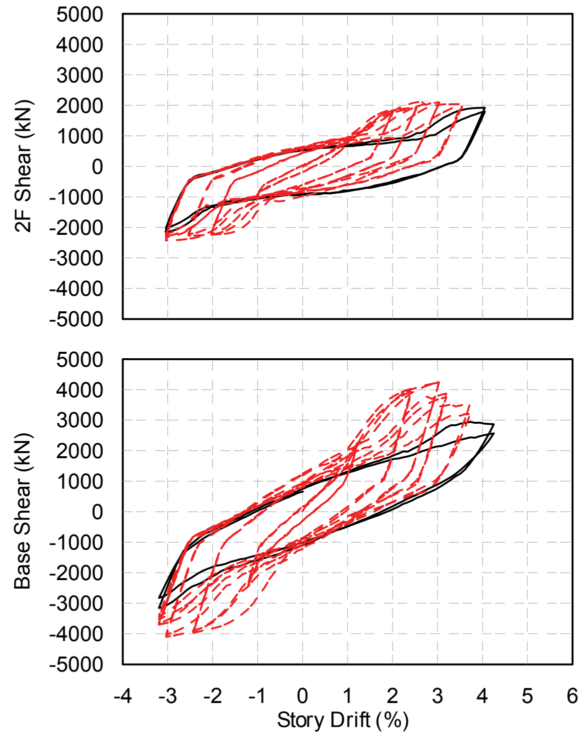

(f) Cycles 1 to 12

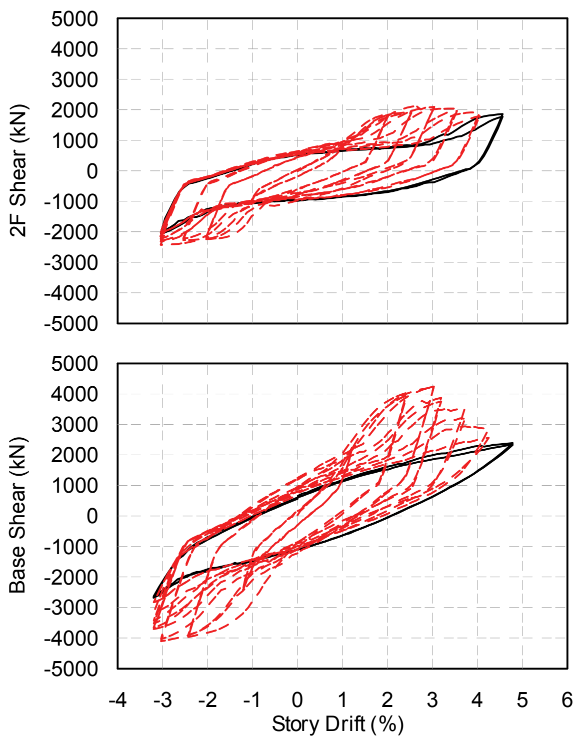

(g) Cycles 1 to 14

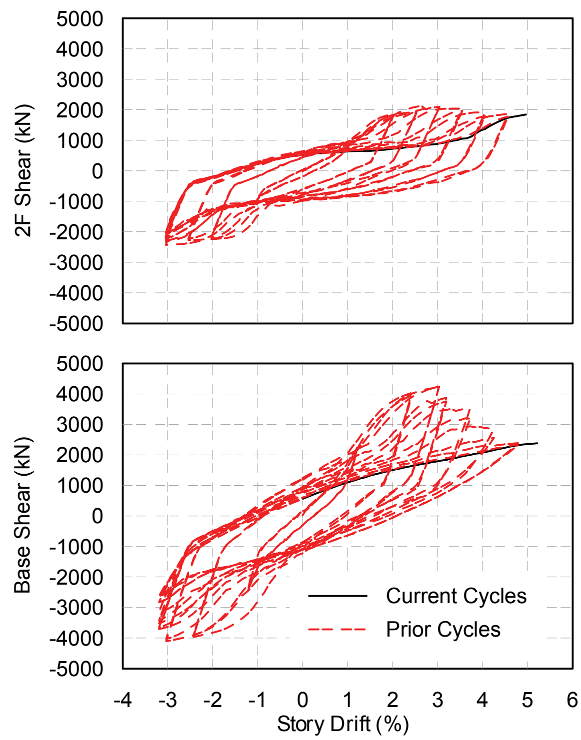

(h) Cycles 1 to 14+

FIGURE 4-35 (Cont'd) Progressive Hystereses of the Phase II Cycle Test

4.4.2 Experimental Observation of the Phase II Tests

4.4.2.1 Phase II Pseudodynamic Test

Starting the earthquake record at 0 second, there was very little yielding/buckling during the early stage of this test, as reflected by the fact that the story shear vs. story drifts behavior of the specimen remained virtually linear. The specimen remained elastic all the way until the time of 4.16 seconds from the beginning of the earthquake excitation.

As the test proceeded, there had been audible buckling sound from the infill panels and visible elastic buckling of the panels was observed as shown in figure 4-36.

As the test was further progressed, the buckling sound grew louder and the magnitude of buckling waves on the infill panels increased as shown in figure 4-37. Yielding of the first-story infill panel started from the lower north corner and then spread across the panel interior. Yield was also apparent in the second-story infill panel, but to a lesser degree. Figure 4-38 shows an early stage of the yielding along one yield line of the infill panels.

For the time between 5.00 seconds and 12.00 seconds from the beginning of the earthquake excitation, the characteristic diagonal tension fields, as represented by the formation of panel folds shown in figure 4-39, were detected in both stories. When the SPSW specimen reached higher story drifts, more waves were seen over the infill panels. From the square grid painted over the whitewash on the infill panels it is apparent that the buckling waves, and hence the tension field, were oriented at approximately 45º from vertical. In addition, loud noises were heard as the panel reoriented its tension field and buckle waves upon reversal of the loading direction. After unloading to the original position of the specimen, as shown in figure 4-40 residual buckles were visible in a complex surface geometry that did not favor any particular orientation of the buckles in either direction of loading (contrary to what was shown in figure 4-39 at large drifts). This phenomenon indicated that the infill panels had undergone significant plastic elongations and could not "fit" its original place without buckling.

At 19.84 seconds from the beginning of the ground motion, i.e. a point before the SPSW specimen experienced the maximum story drift response, the test was paused and the specimen was visually inspected. Yielding of infill panels had become more evident in both stories. As a result of the cyclic infill panel yielding, small plate tears had occurred in the specimens. Besides the typical tears at sharp buckle ridge in the panel interior as shown in figure 4-41, which are similar to those observed in the Phase I tests, tears were also found along the welds connecting the infill panels to the fish plates. Figure 4-42 shows the plate tears along the VBE and HBE respectively. These plate tears did not propagate severely during the subsequent loading steps and were considered to have a negligible effect on the overall behavior. Yield of the RBS connections of the intermediate and top HBEs became more pronounced following the same pattern described earlier (see figures 4-19 and 4-20). More importantly, a vertical fracture initiated at the bottom of the shear tab at the north end of the intermediate HBE as shows in figure 4-43. However, no reduction in story shear strength was observed.

Testing then resumed, and the specimen reached its maximum deformation (i.e. story drifts of 2.6% and 2.3% at the first and second story respectively). Several loud bangs were heard from the specimen. Another inspection made at 25.26 seconds from the beginning of the earthquake revealed that cracks developed in a number of locations in the concrete slabs of the specimen. However, those cracks did not propagate, resulting in no impact on the floor capacity of transfer the loads to the SPSW specimen and no reduction in story shear strength. Figure 4-44 shows a typical crack in the slab at intermediate level. The abovementioned cracks at the shear tab of the intermediate HBE further progressed, but to a limited degree. Figure 4-45 shows the progressive crack propagation (i.e. the crack respectively observed at 19.84 seconds, 22.75 seconds and 25.26 seconds from the beginning of the ground motions).

The testing eventually concluded at 50 seconds from the beginning of the earthquake excitation. Throughout the test, no in-span plastic hinge was observed in the HBEs at all levels. Welds connecting the small infill plate segments in the panel interior remained intact. The maximum amplitude of infill panel buckles was larger than that of the Phase I specimen, in which the infill panels were restrained at the quarter story heights. Similar to the Phase I tests, no other yielding lines were visible along the VBE height, indicating that, as intended, the VBEs behaved primarily in the elastic range except at their bases.

(a) The First Story (b) The Second Story

FIGURE 4-36 Onset of Elastic Buckling of Infill Panels

(a) The First Story (b) The Second Story

FIGURE 4-37 Developed Elastic Buckling of Infill Panels

(a) Lower North Corner of The First-Story Panel

(b) Upper North Corner of The Second-Story Panel

FIGURE 4-38 Typical Yield Lines across the Infill Panels

(a) The First Story **(b) The Second Story**

FIGURE 4-39 Characteristic Diagonal Tension Field Folds

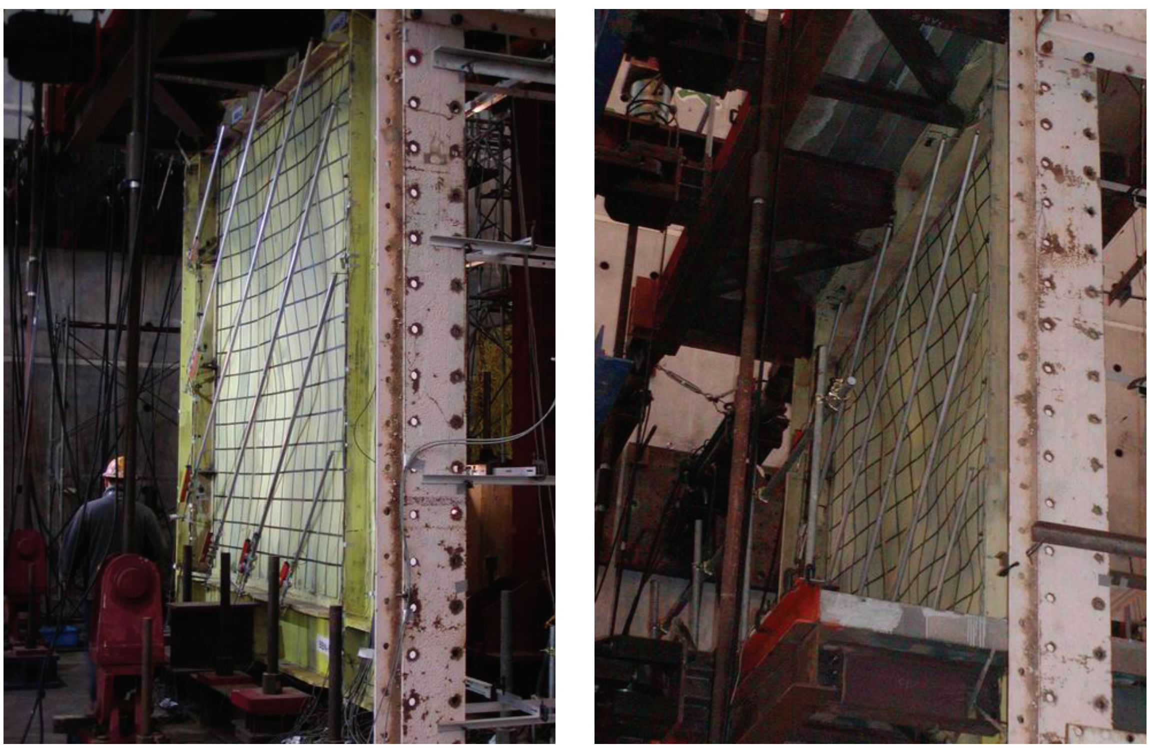

(a) The First Story **(b) The Second Story**

FIGURE 4-40 Residual Buckles of Infill Panels

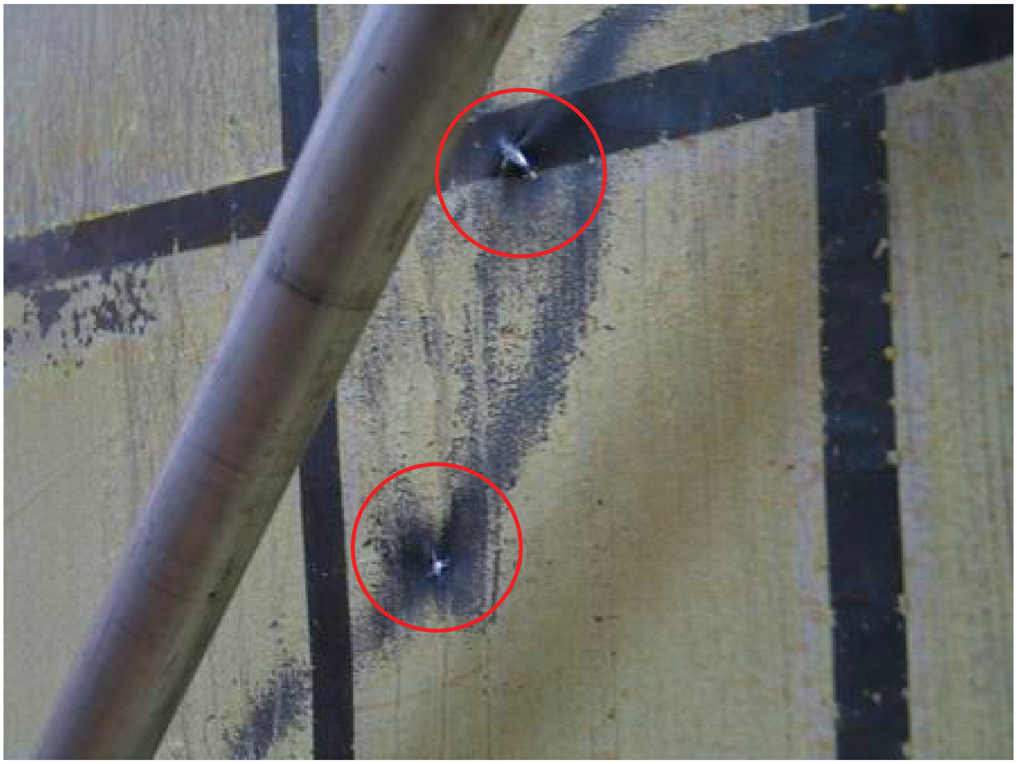

FIGURE 4-41 Tears in the Panel Interior of the Phase II Specimen

(a) Along HBE **(b) Along VBE**

FIGURE 4-42 Panel Tears along Boundary Frame Members

(a) Overview of the Fracture at the Shear Tab

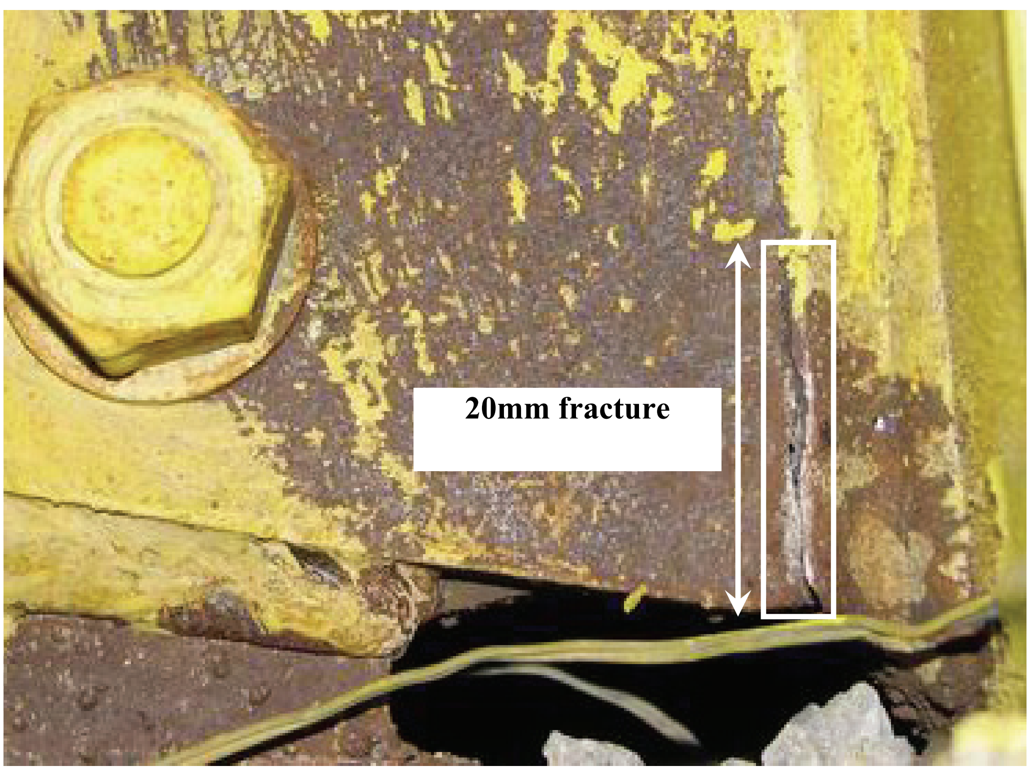

(a) Detail of the Fracture at the Shear Tab

FIGURE 4-43 Formation of the Crack at the Bottom of the Shear Tab at the North End of the Intermediate HBE

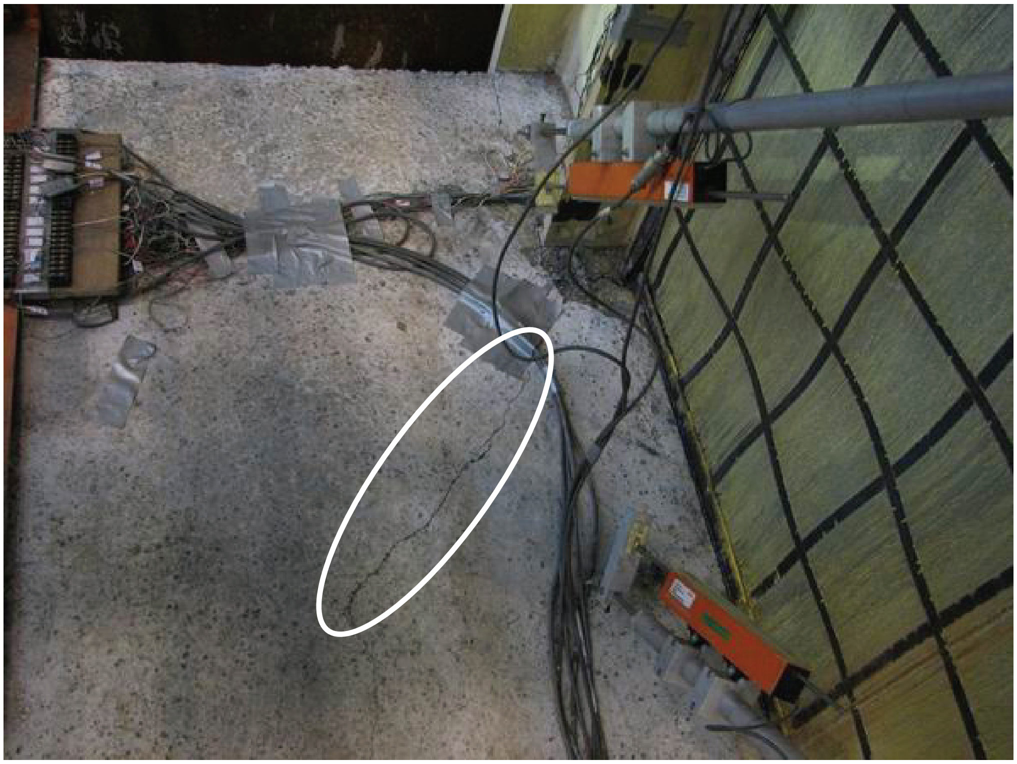

FIGURE 4-44 Cracks in the Intermediate Slab

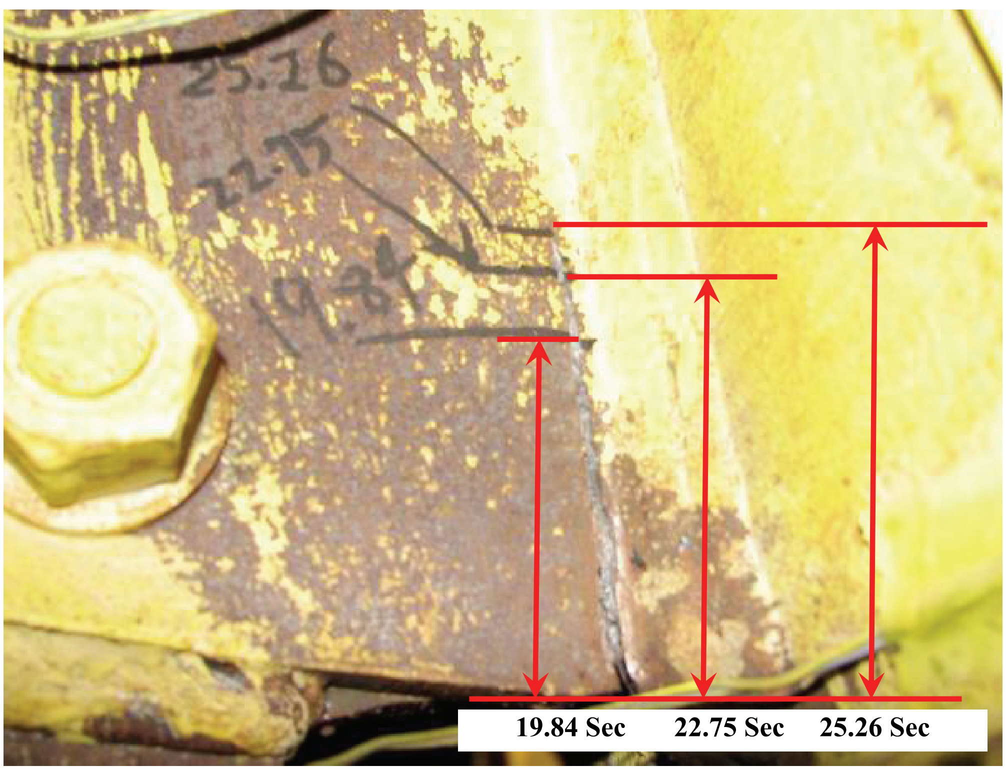

FIGURE 4-45 Development of the Fracture at the Bottom of the Shear Tab at the North End of the Intermediate HBE

4.4.2.2 Phase II Cyclic Test

The next stage of the Phase II tests involved cyclic test of the SPSW specimen to investigate the ultimate behavior of the intermediate HBE and the cyclic behavior and ultimate capacity of the SPSW specimen.

As mentioned earlier, the boundary frame members were still in good condition after the Phase II pseudodynamic test, except for a small visible fracture at the bottom of the shear tab at the north end of the intermediate beam. To correct this limited damage and get a better assessment of the possible ultimate capacity of the wall, the damaged shear tab was replaced by a new one installed on the other side of the beam web (as shown in figure 4-46) prior to the Phase II cyclic test.

A displacement-controlled scheme was selected for this cyclic test. The story drift histories presented in table 4-3 were applied to the specimen. The following describes the performance in this test.

During the first 6 loading cycles, the specimen exhibited ductile performance up to the maximum story drifts of 3.0 and 2.5% at the first and second story respectively. The existing yield patterns of the boundary frame members became considerably more pronounced. However no fractures were observed in them. Audible buckling of the infill panels was observed in all cycles. Increased yielding was noted in the infill panels at both stories. Fractures at the lower corners of the second-story infill panel grew slightly as shown in figure 4-47. In addition, vertical plate tear was observed at the upper north corner of the first-story infill panel as shown in figure 4-48.

At the onset of Cycle 7, a vertical fracture developed at the bottom part of the new shear tab at the north end of the intermediate HBE as shown in figure 4-49 (i.e. similar to the one observed in the Phase II pseudodynamic test). Additionally, horizontal cracks were observed to initiate from the weld access hole and propagate into the web at the intersection and beam web and beam flange as shown in figure 4-50. When the specimen was pushed in the north direction to the story drifts of 2.8% and 2.6% at the first and second story respectively in this cycle, the above mentioned vertical fracture penetrated along the shear tab at the north end of the intermediate HBE. This unexpected failure resulted in story shear reductions of 76 kN and 83 kN at the first and second story respectively. A similar fracture developed along the shear tab at the south end of the intermediate HBE when the specimen was pulled in the south direction (i.e. towards the reaction wall) in this cycle.

Rupture of the shear tabs triggered fractures of HBE bottom flanges at the ends of the intermediate HBE. When the specimen reached the maximum story drifts of 3.2% and 3.0% at the first and second story respectively, in Cycle 8, cracks initiated at the ends of the bottom flange of the intermediate HBE as shown in figure 4-51. However, those fractures did not propagate further in this cycle.

During Cycle 9, when the specimen was loaded in the north direction to story drifts of 3.7% and 3.5% at the first and second story, respectively, the bottom flange at the north end of the intermediate HBE fractured as shown in figure 4-52a. However, no fracture developed in the reduced beam flange regions of the intermediate HBE. Similar fracture was also observed in the HBE bottom flange at the south end of the intermediate HBE when the SPSW specimen was loaded in the south direction to story drifts of 3.2% and 3.0% respectively, as shown in figure 4-52b. Excessive deformations due to the ruptures in HBE flanges worsened the plate tears in the upper north corner of the first-story infill panel in Cycle 10 as shown in figure 4-53. The lateral load capacity of the specimen first-story panel declined gradually and in a stable manner during the remaining loading cycles. However, since the test was conducted using displacement control, testing could proceed to further investigate behavior, particularly of the undamaged second story.

During Cycles 11 and 12, pinging sounds were heard from the specimen. A further inspection revealed that fractures developed to a length of 800 mm along the welds connecting the infill panels and the fish plates along the north VBE as shown in figure 4-54. In the meanwhile, the plate tears and weld ruptures at the upper north corner of the first story infill panel gradually propagated to a length of 900 mm as shown in figure 4-55.

By Cycles 13, fractures at the upper north corner of the first-story infill panel propagated over a length of 2500 mm as shown in figure 4-56. During Cycle 14, the first-story panel was almost torn away from the intermediate HBE as shown in figure 4-57. As a result, the base shear strength of that panel dropped to 2387 kN. Note that up to the peak drifts of 4.8% and 4.5% at the first and second story respectively, the second story had not suffered significant loss of strength and no fractures were observed either in the fish plates connecting to the infill panel to HBEs and VBEs, or in the top HBE itself.

In Cycle 14+, the test concluded at the maximum story drifts of 5.2% and 5.0% at the first and second story, respectively. Testing stopped when a sudden failure occurred in the load transfer mechanism. Subsequent inspection revealed that ruptures occurred in the floor truss members of the top slab. Figure 4-58 illustrates the locations of fractured members and figure 4-59 shows the typical failures of those members. Note that those fractures were sudden and were accompanied by a large release of energy transferred from floor truss to the concrete slab, resulting in a fatal longitudinal crack along the top concrete slab, as shown in figure 4-60. Figure 4-61a shows the relative displacement of the west part of the failed concrete slab, where more steel transfer members fractured relative to the east side. Figures 4-61b and 4-61c, taken after the concrete slab was chipped , show the rebar fractures and the deformation of the shear studs in the slab.

FIGURE 4-46 Repaired Shear Tab at the North End of Intermediate HBE

(a) Onset of the Panel Tear

(b) Development of the Panel Tear

FIGURE 4-47 Panel Tear at the Lower Corners of the Second-Story Infill Panel

FIGURE 4-48 Vertical Plate Tear at the Upper North Corner of the First-Story Infill Panel

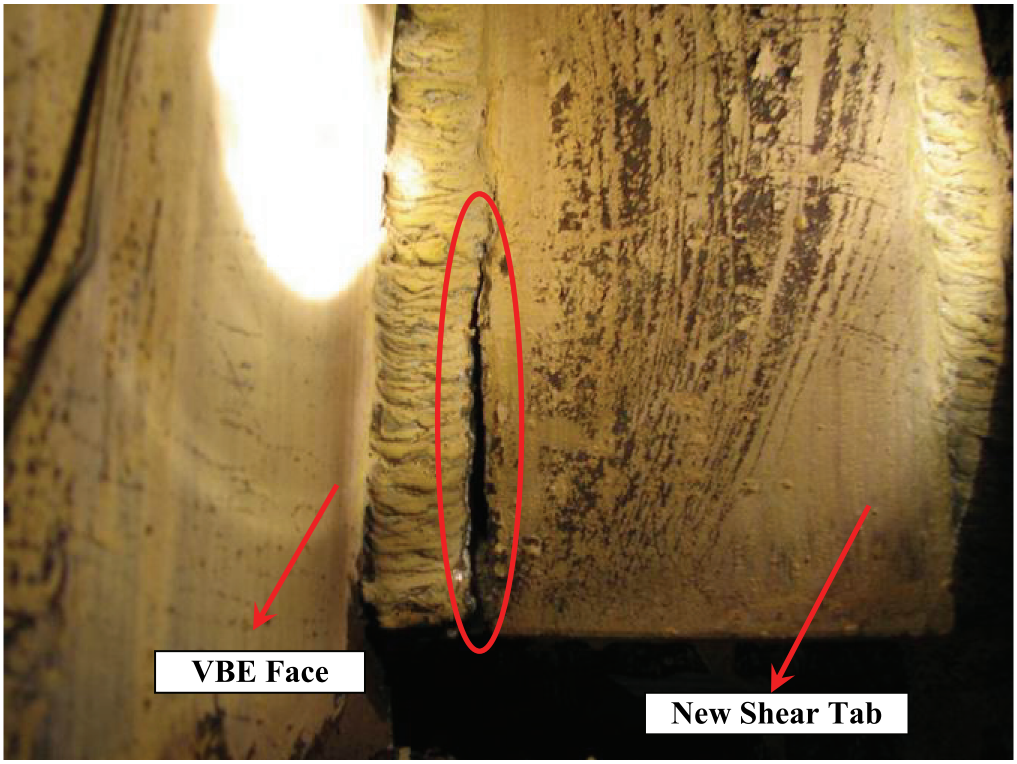

FIGURE 4-49 Vertical Fracture Developed at the Bottom Part of the Shear Tab at the North End of the Intermediate HBE (During Cycle 7)

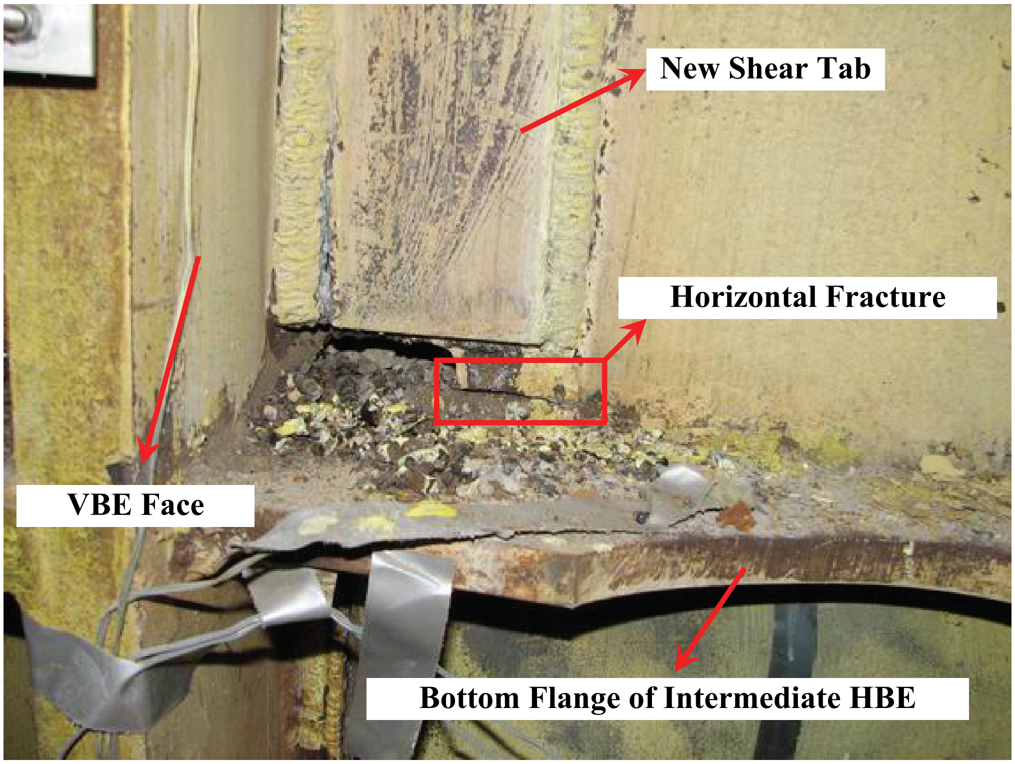

(a) At the Bottom Edge of the Intermediate HBE Web

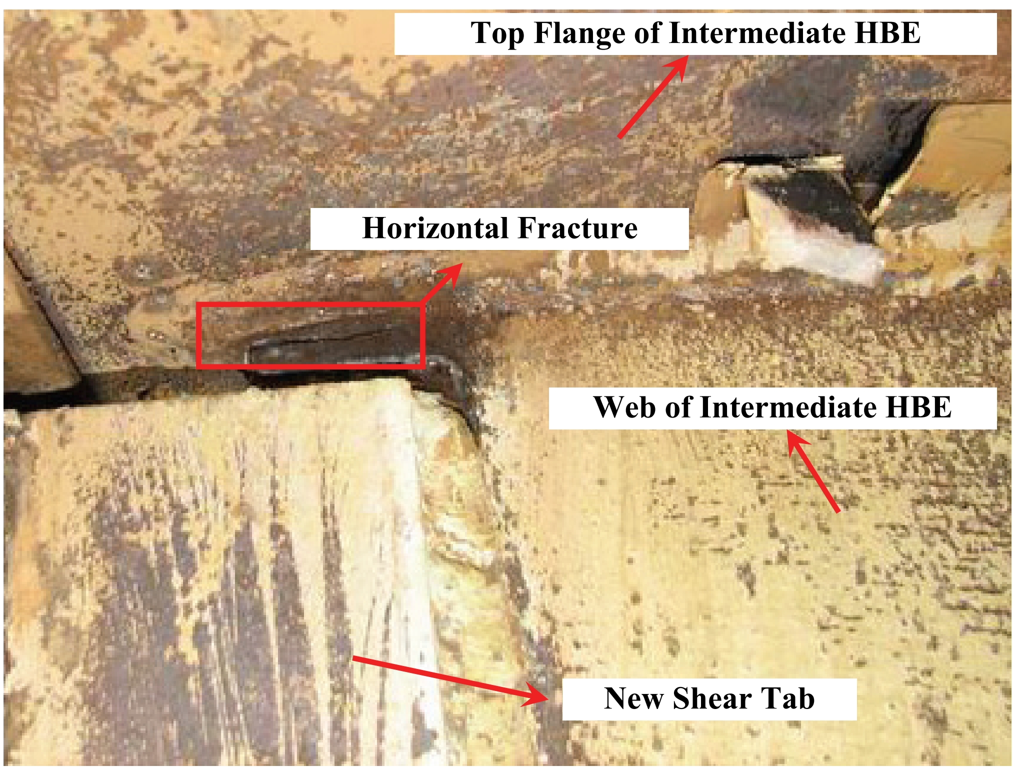

(b) At the Top Edge of the Intermediate HBE Web

FIGURE 4-50 Horizontal Fracture along the Edge of the Intermediate HBE Web

(a) At the North End of the Intermediate HBE

(b) At the South End of the Intermediate HBE

FIGURE 4-51 Onset of the Bottom Flange Fractures at the Ends of the Intermediate HBE (During Cycle 8)

(a) At the North End of the Intermediate HBE

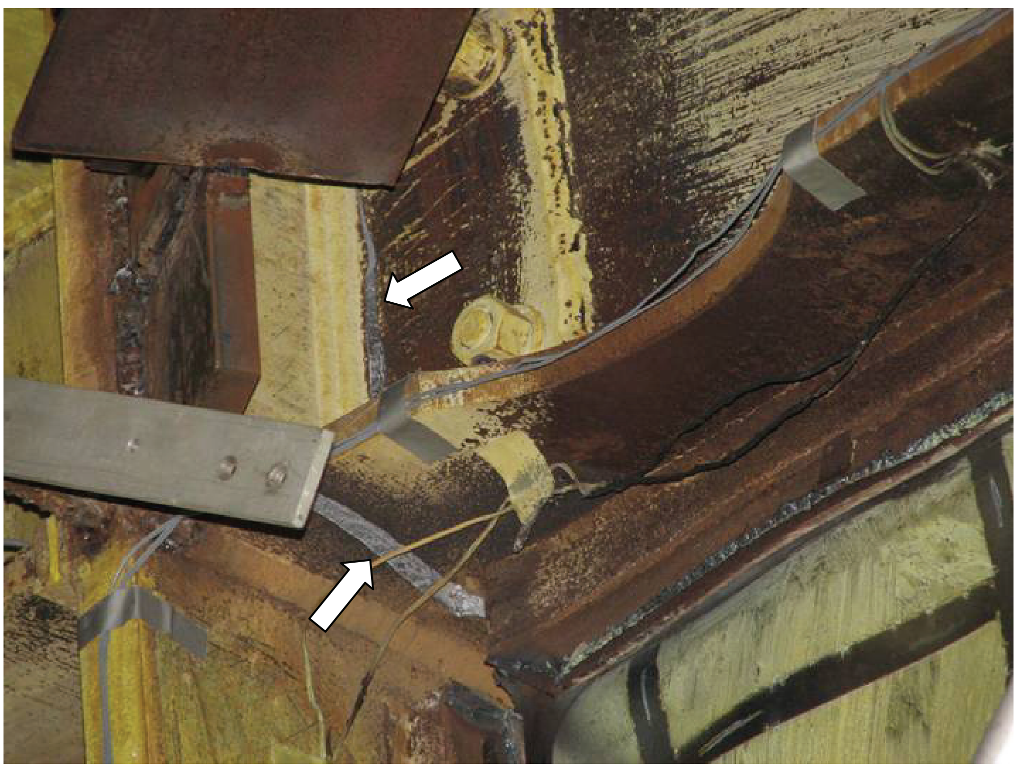

(b) At the South End of the Intermediate HBE

FIGURE 4-52 Bottom Flange Fractures at the Ends of the Intermediate HBE

FIGURE 4-53 Plate Tear at the Upper North Corner of the First-Story Infill Panel (During Cycle 10)

FIGURE 4-54 Failures of the Welds Connecting the First-Story Infill Panel to the Fish Plate Along the North VBE

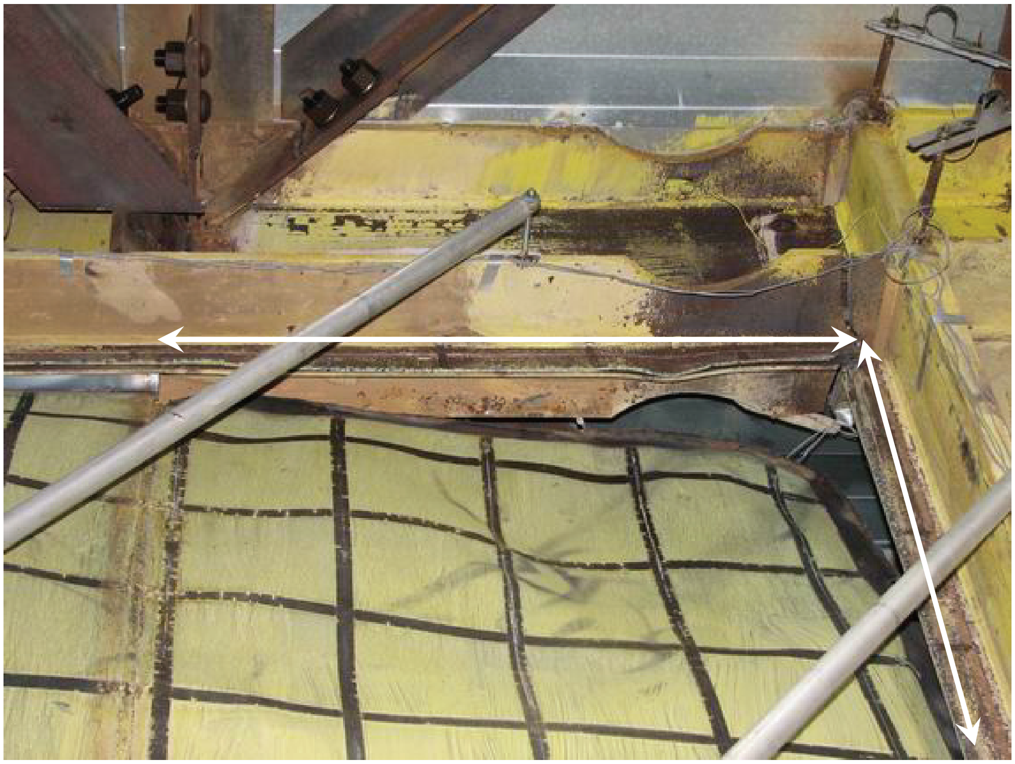

FIGURE 4-55 Plate Tear at the Upper North Corner of the First-Story Infill Panel (During Cycles 11 and 12)

FIGURE 4-56 Plate Tear at the Upper North Corner of the First-Story Infill Panel (During Cycle 13)

FIGURE 4-57 Plate Tear at the Upper North Corner of the First-Story Infill Panel (During Cycle 14)

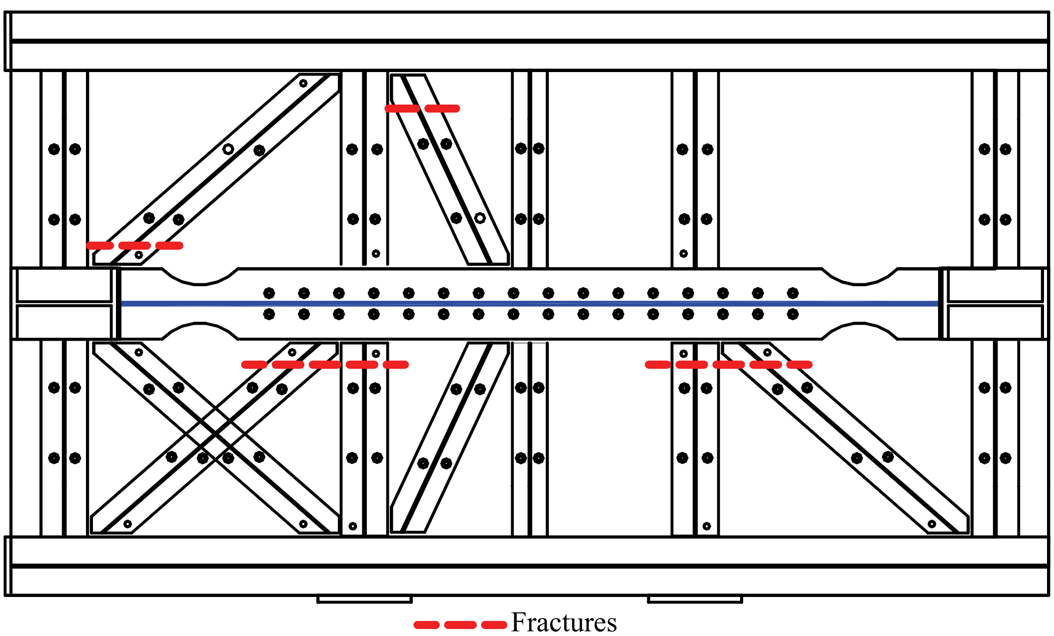

FIGURE 4-58 Failed Members in the Top Floor Truss

(a) Fractures of the Truss Members Connected to the Middle of the Top HBE

(b) Fractures of the Truss Member Connected to the End of the Top HBE

FIGURE 4-59 Typical Failures of the Top Floor Truss Members

(c) Excessive Rotation of the Connecting Plates

FIGURE 4-59 (Cont'd)Typical Failures of the Top Floor Truss Members

FIGURE 4-60 Crack in the Top Concrete Slab

(a) Slip of the Failed Top Concrete Slab

(b) Fractured Rebar in the Top Concrete Slab

FIGURE 4-61 Failures in the Top Concrete Slab

(c) Deformed Shear Stud in the Top Concrete Slab

FIGURE 4-61 (Cont'd) Failures in the Top Concrete Slab

4.4.3 Discussion of the Phase II Test Results

4.4.3.1 Phase II Pseudodynamic Test

Generally, the repaired SPSW specimen behaved satisfactorily as expected. The Phase II tests provided valuable data to evaluate the seismic performance of a multi-story SPSW repaired by replacing the infill panels buckled in a prior sever earthquake and subsequent aftershocks.

As mentioned earlier, the earthquake excitation used in the Phase II pseudodynamic test is the same as that used in Test 3 of Phase I. Therefore, comparing the hysteretic curves obtained from these two tests provides an opportunity to address the replaceability of infill panels in SPSWs. Such a comparison is illustrated in figure 4-62. As shown, the two specimens are found to behave similarly under the same strong ground motion. At first glance, the initial stiffness of the repaired specimen (Phase II) appears to be higher than that of the original one. However, this is only because the results shown for the Phase I specimen are those obtained after the specimen was repaired due to the unexpected failures in Tests 1 and 2 of Phase I, as mentioned earlier. Therefore the infill panels had already experienced some inelastic deformation before these unexpected failures occurred. As such, it is expected that the infill pate in Test 3 of Phase I would not be dissipating hysteretic energy up to the maximum drifts ever experienced in Tests 1 and 2, which is consistent with what is observed in figure 4-62.

Also shown in figure 4-62, in the Phase II pseudodynamic test, both the first and second story exhibited stable force-displacement behavior, with some pinching of the hysteretic loops as the magnitude of story drifts increased, particularly after the development of a small crack along the bottom of the shear tab at the north end of the intermediate beam at the story drifts of 2.6% and 2.3% at the first and second story respectively.

Figure 4-63 shows the diagonal elongation of infill panels obtained from the LVDTs placed across the infill panels. As shown, the elongation of the infill panel at each story is uniform along the diagonal direction enriched by the really superposed strain history for each separate strip, indicating the formation of a well distributed tension fields for the specimen under the earthquake excitation.

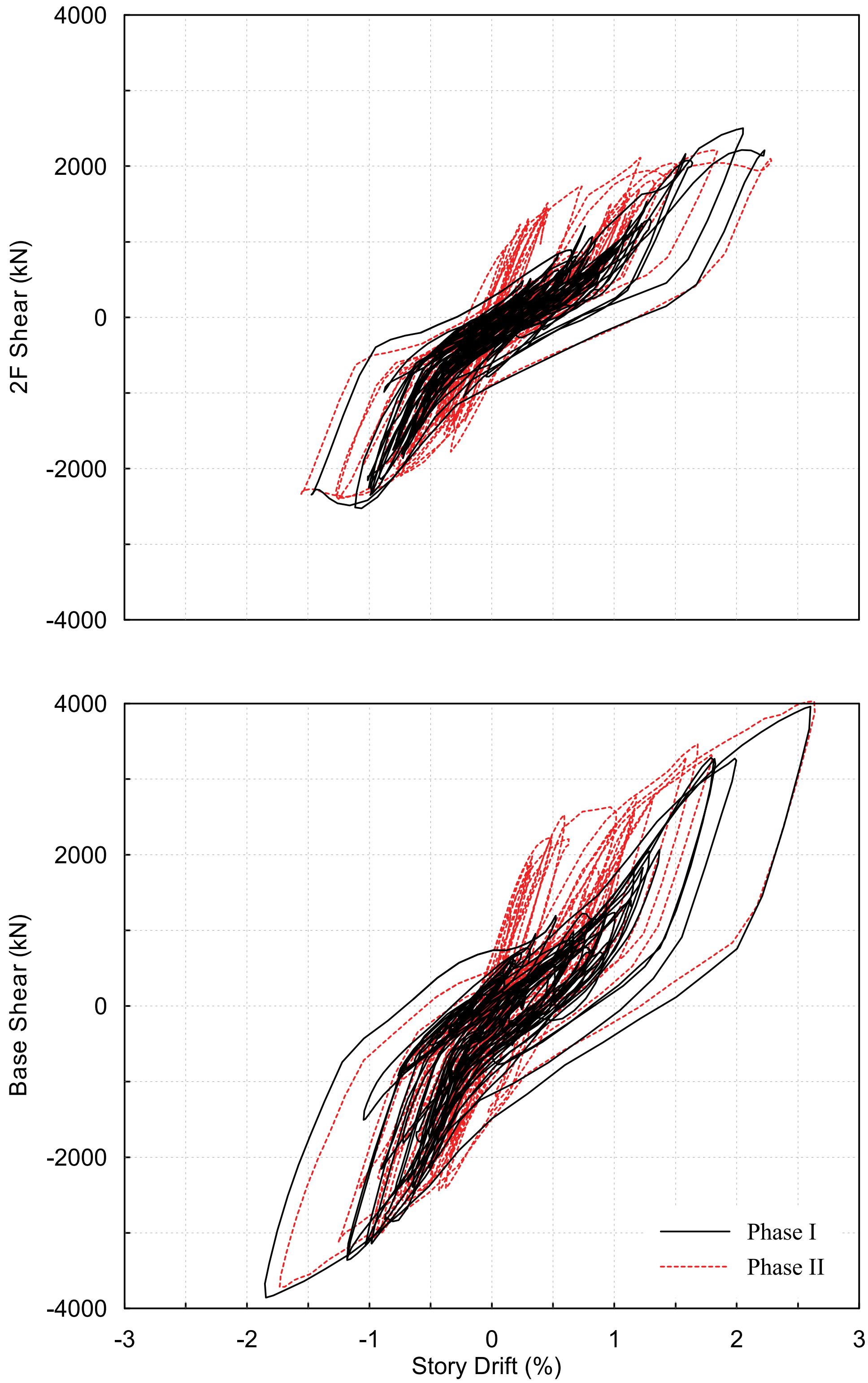

FIGURE 4-62 Hystereses of Phase I and Phase II

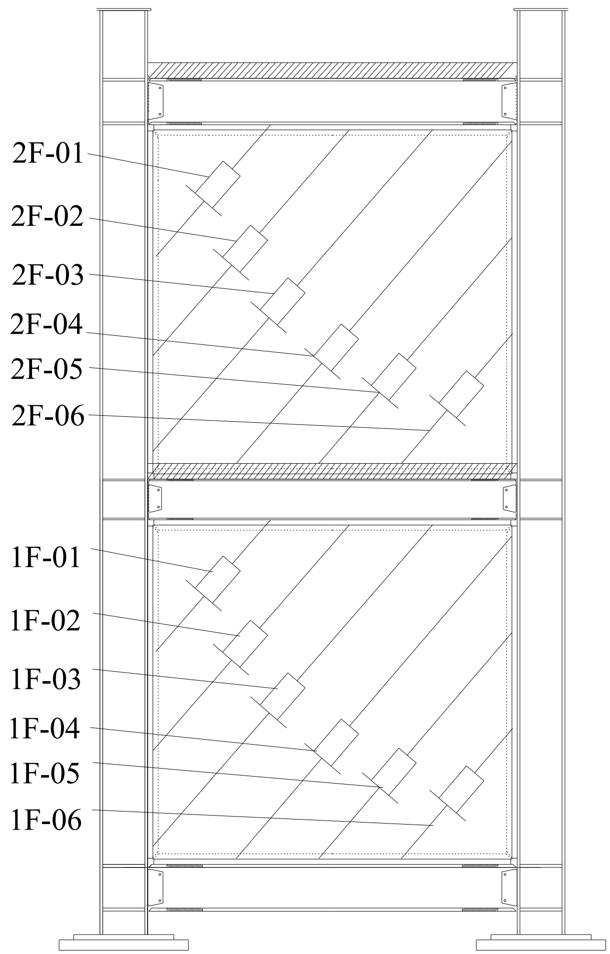

(a) Layout of Strips

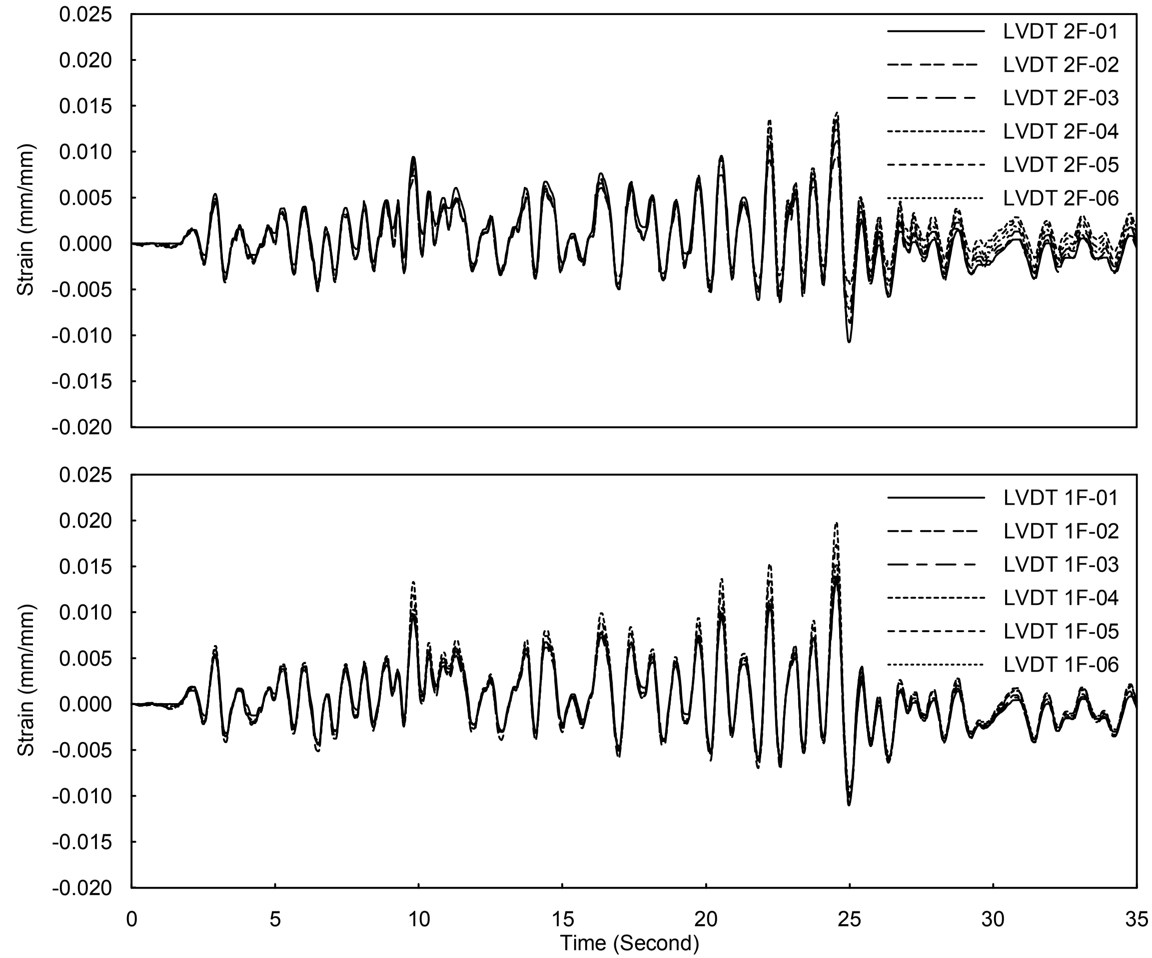

(b) Strip Elongation Comparisons

FIGURE 4-63 Diagonal Elongation of the Infill Panel

4.4.3.2 Phase II Cyclic Test

The Phase II cyclic test provided an opportunity to further investigate the ultimate behavior of the SPSW, in particular of its intermediate HBE, as well as to determine the final failure modes for this specimen. The hysteretic curves progressively obtained at various stages throughout the Phase II cyclic test are shown in figure 4-35.

Comparing the hysteretic curves in figure 4-35 to those from shown in figure 4-33, it is observed the initial stiffness of the SPSW specimen in the Phase II cyclic test was smaller than that in the Phase II pseudodynamic test. Again, in a way similar to what was mentioned in Section 4.4.3.1 when comparing the Phase I and II pseudodynamic tests, the reason for this observation is that the Phase II pseudodynamic test stretched the infill panels up to story drifts of 2.6% and 2.3% at the first and second story, respectively, resulting in the pinching hysteretic loops in the Phase II cyclic test up to those story drifts. Larger drift was required for the infill panels to continue a new to the system stiffness and strength.

As shown in figure 4-35, strength of the wall gradually decreased as the ruptures described in Section 4.4.2.2 occurred in the specimen. However, the SPSW exhibited stable force-displacement behavior and provided a significant energy dissipation capacity, exhibiting substantial redundancy of this system. Compared to the base shear strength, the second-story shear strength reduced to a lesser degree before total failure of the load transfer mechanism since the fractures concentrated in the intermediate HBE and the first-story infill panel, even as the second-story infill panel could be subjected to larger drifts by virtue of the displacement-controlled testing procedure.

4.5 Summary

This section describes the observations and testing results of a two-phase experimental program of a full-scale two-story SPSW specimen with RBS connections, which was developed to experimentally address the replaceability of infill panels following an earthquake as well as the behavior of the repaired SPSW in a subsequent earthquake and the seismic performance of the intermediate HBE.

The pseudodynamic tests show that a SPSW repaired by replacing the infill panels buckled in a prior earthquake by new ones can be a viable option to provide adequate resistance to the lateral loads imparted on this structure during new seismic excitations (note that possible undesirable aesthetic issues related to residual story drifts from the first earthquake prior to repair are beyond the scope of this work). The repaired SPSW behaved quite similarly to the original one. Testing showed that the repaired SPSW can survive and dissipate a similar amount of energy in the subsequent earthquake without severe damage to the boundary frame and without overall strength degradation.

Results from the Phase II cyclic test also allowed to investigate the ultimate displacement capacity of the SPSW specimen. Though the hysteretic curves were pinched at the low story drift levels due to the inelastic deformations that the infill panels experienced during the previous pseudodynamic test, and even though the strength of the SPSW dropped as the ends of the intermediate beam fractured at drifts in excess of 3% which is expected to occur during severe earthquakes, the SPSW specimen exhibited stable force-displacement behavior and provided a significant energy dissipation capacity, exhibiting substantial system redundancy.

The VBEs and the top and bottom HBEs, as well as top and bottom RBS connections performed as intended. However, the intermediate HBE failed unexpectedly. The ends of the intermediate HBE having RBS connections ultimately developed fractures in the shear tabs followed by fractures at the end of the bottom beam flanges. No fractures developed in the reduced beam flange region. Further investigation is required to clarify the local behavior of intermediate HBE in SPSW, to develop a better understanding of how such intermediate HBE should be designed.

SECTION 5

ANALYTICAL MODELLING OF TESTED SPECIMEN

5.1 Introduction

This section presents the modeling and analysis conducted to simulate the experimental specimen performance using the commercially available finite element (FE) software package ABAQUS/Standard (HKS 2002). For this purpose, a dual strip model and a 3D FE model were developed for the specimen subjected to pseudodynamic earthquake loads and cyclic loads, respectively. The following describes the selection of element types, boundary conditions, material properties, and loading inputs for those two numerical models. Results are also presented for each model followed by discussions on the effectiveness of the models.

5.2 Simulation Using Dual Strip Model

Noting that beam-column and truss elements are commonly available in typical software packages and nonlinear analysis using such elements is universally efficient (particularly for the structures under iterative loads), it is decided to first model the tested specimen using those simple elements to investigate the specimen behavior under earthquake loads. Strip model was employed for this purpose. This section discusses the modeling assumptions and adequacy of the model.

5.2.1 Model Development

5.2.1.1 General Description of Strip Model

As mentioned in Section 2, a simplified analytical model for analyzing SPSWs, known as strip model, was originally presented by Thorburn *et al.* (1983). The strip model assumes that the lateral load resistance of a SPSW is primarily achieved through the formation of diagonal tension field actions after the infill panels buckle. Generally speaking, buckling of the infill panels occurs at relatively low story drifts in SPSWs because the width and height of the infill panels are much larger than their thickness, and some initial imperfection inevitably exists within the panel. Capturing these behaviors, Thorburn *et al.* (1983) modeled the tension field in a SPSW as a series of discrete pin-ended strips inclined with the same orientation as the tension field, as shown in figure 5-1. This procedure assumes that the compression strength of the panel in the orthogonal direction is negligible and that the angle of inclination of the tension field can be reasonably predicted. The strips are assigned an area equal to the plate thickness multiplied by the width of the strip. Based on this model, the diagonal strips and boundary frames can be respectively modeled using truss and beam-column elements in conventional analysis packages, making this approach practical in typical structural design environments.

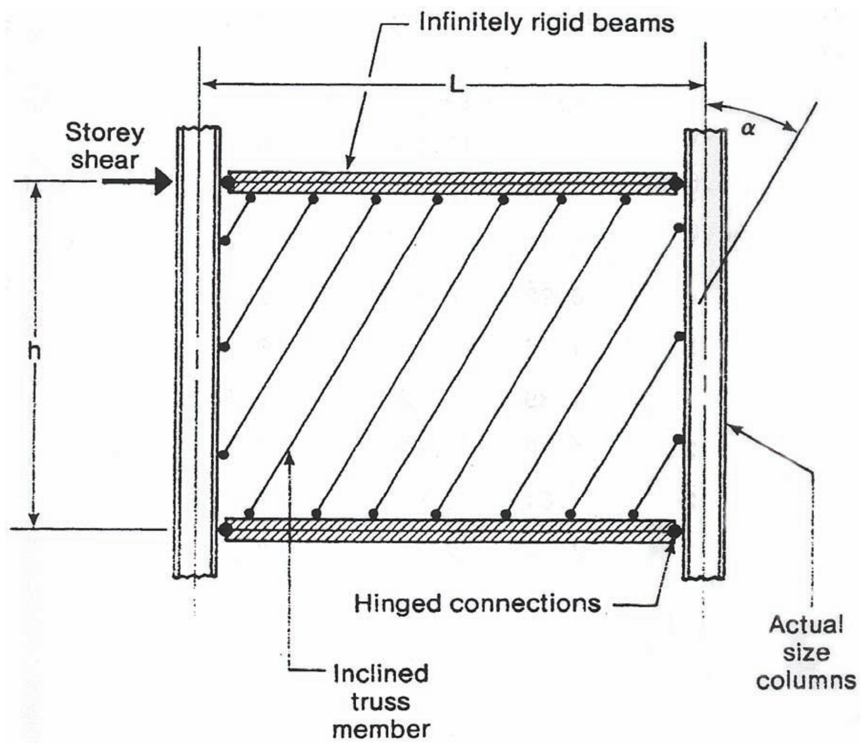

FIGURE 5-1 Original Strip Model (From Thorburn *et al.* 1983)

Monotonic pushover analyses on strip models have been widely conducted and the plastic strength of SPSWs obtained from those analysis have been validated by the results of the previous physical tests on single-story as well as multistory SPSW specimens by Timler and Kulak (1983), Tromposch and Kulak (1987), Driver *et al.* (1997) and Berman and Bruneau (2003).

The pesudodynamic tests described in Section 4 have affords the first opportunity to evaluate the adequacy of the strip model for modeling SPSWs under a time-history of seismic response. During seismic events, the infill panels of SPSWs can develop diagonal tension field actions to resist the lateral forces due to earthquakes. The inclination of tension field depends on the acting direction of the earthquake forces. When the earthquake-induced displacements applied on the wall reverse from one direction to the other direction, the tension field inclination also reorients.

However, the conventional strip model shown in figure 5-1, which is developed for monotonic pushover analysis to determine the ultimate strength of the wall, can only capture the tension field in one direction. To account for reorientation of the tension field in SPSWs under the reversed cyclic loading history from earthquakes, it is proposed to represent the infill panel of a SPSW as two series of discrete pin-ended strips, as shown in figure 5-2. Those two sets of strips have the same inclined angle to vertical but act in opposed directions and can be developed following the procedure described below.

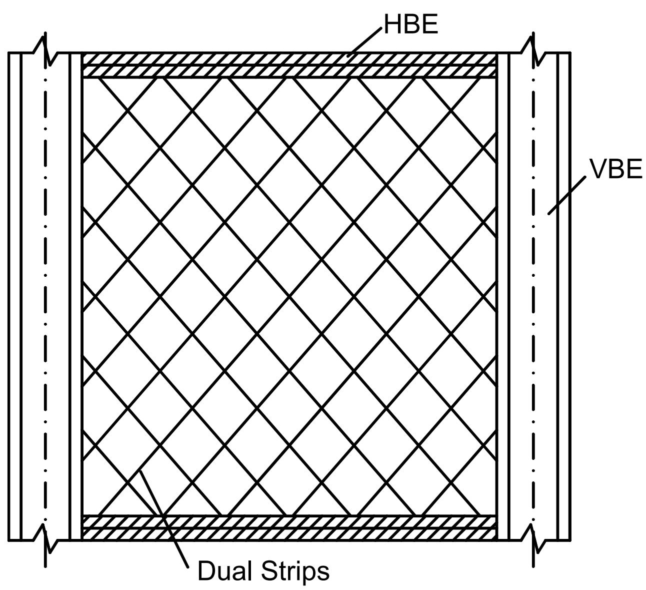

FIGURE 5-2 Schematic of Dual Strip Model

5.2.1.2 Geometry Definition and Simplification

The graphical user interface program ABAQUS/CAE, was used to define the geometry of the dual strip model of the tested SPSW specimen. In this package, the boundary frame members and infill strips were defined as different "parts" in the preprocessor of the software package. All those parts were later connected through displacement constraints, which impose deformation compatibility even when the connected parts do not have nodes in common.

Line elements were used for both the boundary frame members and infill strips. The elements for the boundary frame members were located at the centerline of those members. Fifteen strips were used to represent each infill panel in each direction. The boundary frame members and strips were meshed with beam-column elements and truss elements, respectively, properties of which are described in the next section.

Following the manual layout of basic geometry, profile geometry information was defined in the property module of ABAQUS/CAE. Profiles including the wide flange cross-sections, are provided in ABAQUS/CAE. Users can provide detailed geometry information (e.g. width, depth, and plate thickness) to define a cross-section and then assign the properties of that cross-section (e.g. cross-section area) to the corresponding structural members. However, limitations exist in using this procedure, namely, (i) geometries of the cross-section profile assigned to a structural member have to be constant along that member, which indicates that further steps are necessary for structural members having gradually variable cross-sections (e.g. reduced flange segments); and (ii) constant material properties have to be assigned to each cross-section profile, which means some special assumptions or equivalent procedures must be used for those composite cross-sections that have various material properties (e.g. elastic-plastic behavior and young's modulus) in different segments of the cross-sections.

To overcome the first limitation, each HBE was divided into five segments as shown in figure 5-3 (i.e. the segments with and without reduced beam flanges). Profiles defined for the non-reduced beam cross-sections were assigned to those segments outside the RBS regions.

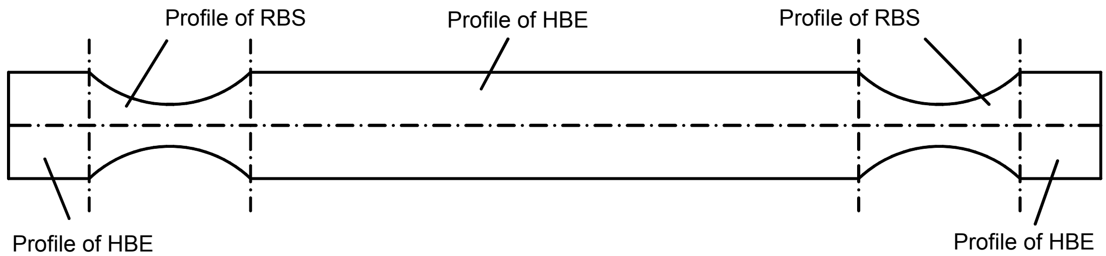

FIGURE 5-3 HBE Profile Assignments

For those segments with reduced beam flanges, the arc cutouts of the RBS regions were simplified as rectangular cutoffs as shown in figure 5-4 in this investigation. The length and width of the approximate reduced beam flange using rectangular cutoffs were respectively equal to the length and minimum width of the original reduced beam flange, recognizing that this is a somewhat more severe reduction than the actual RBS used. Note that Lee (2006) demonstrated that this simplification provides reasonable predictions for global responses of the structures.

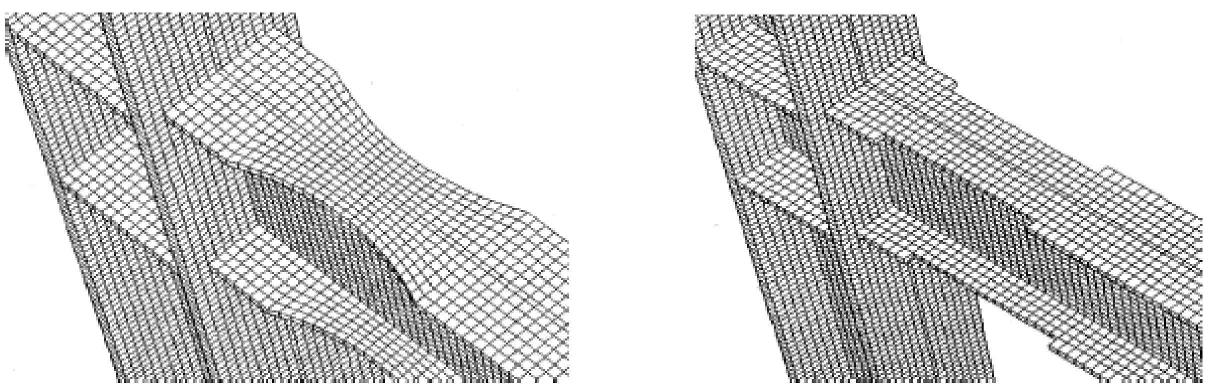

FIGURE 5-4 Simplification of RBS Connection (from Lee 2006)

In addition, to consider the contribution of the concrete slabs to the global behavior of the SPSW specimen, the thicknesses of the top flanges of the intermediate and top HBEs were increased to provide the same positive plastic cross-section moments as the real composite beam cross-sections as shown in figure 5-5. Note that the composite action was incorrectly considered by the above procedure in negative flexure case, for which tension is resulted in the concrete slab. However, this approximation would have negligible impacts on simulation of global behavior of the SPSW specimen as demonstrated by the results presented later. Also note that this procedure was not necessary for the bottom HBE since that beam has no concrete slab.

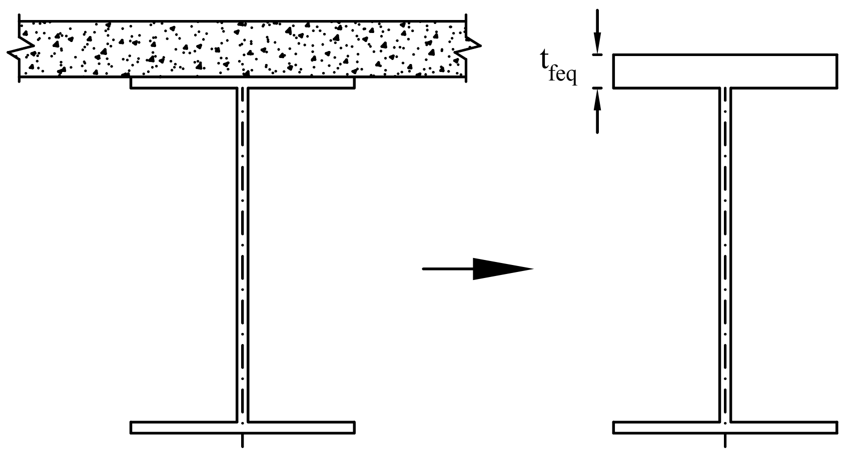

FIGURE 5-5 Simplification of Concrete Slab

For VBEs, the as-built cross-sectional dimensions were used to determine their profile geometries.

With respect to modeling the infill panels, the main issue was selection of the inclination angle of the diagonal strips corresponding to the inclination angle of the tension field. A method of estimating this angle based on the principle of least work was derived by Thorburn *et al.* (1983) and later refined by Timler and Kulak (1983). The derivation was similar to that of Kuhn *et al.* (1952), which, in turn, was based on the theory of pure diagonal tension originally developed by Wagner (1931).

According to Timler and Kulak (1983), the angle of inclination, α, for SPSWs having pin-ended beams can be estimated using equation (2-2), which has been adopted by the AISC Seismic Provisions and the CSA S16 Standard for design of SPSWs. Timler and Kulak demonstrated that reasonable agreement was obtained between the predicted values and those measured in the infill panels of their tested specimens.

However, there are considerable added complexities in extending their equation for use in SPSWs having moment resisting HBE-to-VBE connections. This arises because the story shear is shared in a complex interaction between the moment resisting boundary frame and the diagonal tension field, resulting in difficulties in formulating the internal work. Rezai (1999) demonstrated that for SPSWs of typical proportions, the angle of inclination would not be expected to differ from 45 by more than a few degrees and neither the wall strength nor the infill panel stresses are markedly sensitive to the angle of the tension field. Thus, for expediency, the tension field angle estimated using equation (2-2) was adopted in this investigation. Accordingly, each strip was assigned an area equal to the actual plate thickness multiplied by the width of the strip.

5.2.1.3 Element Selection and Mesh Generation

Truss elements (ABAQUS element T3D2) and beam elements (ABAQUS element B31) were used to represent the infill panel strips and boundary frame members, respectively.

T3D2 is a two-node truss element. Each node has three translational degrees of freedom (u_x, u_y, and u_z). B31 is a two-node linear beam element which allows for transverse shear deformation and can be used for thick ("stout") as well as slender beams. Each node at the end of the element has six degrees of freedom: three translational (u_x, u_y, and u_z) and three rotational (θ_x, θ_y, and θ_z). ABAQUS assumes that the transverse shear behavior of B31 is independent of the response of the beam cross-section to bending. B31 can also be subjected to large axial strains, which make it suitable to consider the beam-column behavior of HBEs and VBEs.

A total of 125 elements were used for each VBE. A total of 70 elements (10 elements for each reduced beam flange segment, 30 elements for the segment between the RBS regions, and 10 elements for each segment outside the RBS region) were used to model each HBE. Infill panels at each story were represented by thirty strips (fifteen strips in each direction).

5.2.1.4 Material Properties

As mentioned earlier, the profiles defined in ABAQUS/CAE for line elements have to have uniform material properties across the whole cross-section.

The coupon test results described in Section 3 indicated that the material properties (e.g. yield and ultimate strengths) of the webs and flanges are different in the HBE and VBE cross-sections. However, given that flange strength defines almost entirely the plastic moment of a wide flange cross-section (compared to the web strength), and thus has more impact on global strength of the SPSW, the flange material properties were used for the HBE and VBE cross-sections.

For the infill panels with strips oriented in both directions, to capture the wall behavior under reversed cyclic responses, the behavior of each strip was modeled similar to that of a slender brace having a very large slenderness (e.g. in excess of 200) in a concentrically braced frame, for which the compression strength of the strip is negligible. To account for this behavior, a tension-only material property, as shown in figure 5-6, was assigned to the infill panel strips.

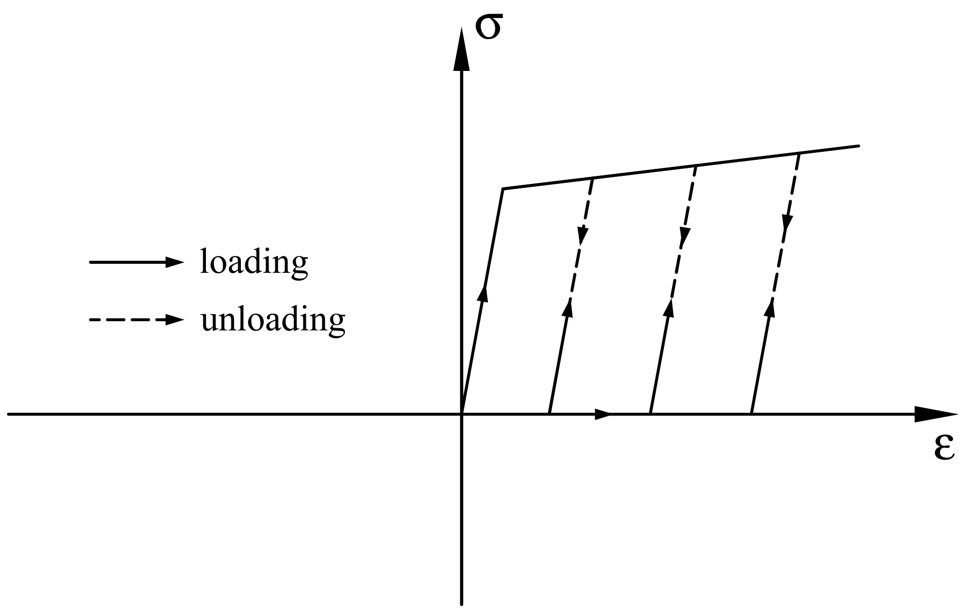

FIGURE 5-6 Tension-Only Material Property

Note that the nominal strain-stress relationships obtained from the coupon tests were transformed into the "true" strain-stress relationship for analysis purpose (as required by ABAQUS) and the corresponding procedures will be described in detail later. A von Mises yield surface was adopted as the yield criterion for all members.

5.2.1.5 Boundary and Initial Conditions and Loading

The VBEs, HBEs, and infill strips were connected using a displacement constraint (i.e. the ABAQUS constraint: tie) in the interaction module of ABAQUS/CAE.

The boundary frame was fixed at the column bases to replicate the test conditions. Boundary conditions preventing the out-of-plane displacements were imposed at floor levels. In the initial loading step, the full gravity load of 1400 kN was applied to the top of the VBEs. This magnitude is equal to the target gravity load used in the physical test.

To validate the above mentioned model developed to predict the nonlinear behavior of the SPSW specimen under earthquake load, the floor displacement histories recorded during the Phase II pseudodynamic test as shown in figure 5-7 were applied at the floor levels of the model. Thus, a displacement-controlled approach was essentially used in this simulation. It is expected to assess the adequacy of the model through comparing the story shear responses from the physical test with those from simulations.

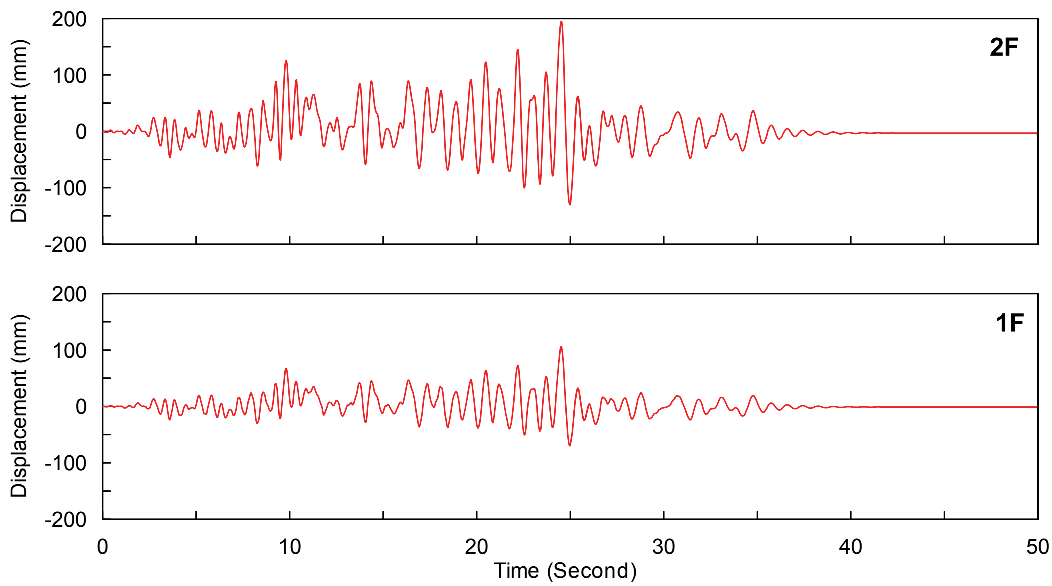

FIGURE 5-7 Displacement Inputs

5.2.2 Comparison with Test Results

Analysis using the dual strip model shown in figure 5-8a was carried out to compare the results with the tested SPSW behavior observed during the Phase II pseudodynamic test. Figure 5-9 compares the hysteretic curves obtained analytically and experimentally. As shown, the global behavior of the SPSW specimen can be satisfactorily predicted by the dual strip model although a number of effects were neglected in this model. Note that no calibration was done in the analysis (i.e. it is a blind prediction). In addition, the simulation captures an important aspect of SPSW infill panel behavior, namely that after unloading, the once-yielded infill strips can yield again only upon greater story drifts.).

5.2.3 Effects of Strip Numbers

Another dual strip model representing each infill panel as twenty-five strips in each direction, as shown in figure 5-8b, was developed to investigate the effects of numbers of strips on the simulation results, although the abovementioned model using fifteen strips was found to adequately capture the global experimental response. Figure 5-10 compares the hysteretic curves obtained from the dual strip models using twenty-five and fifteen strips. As shown, there is no distinguishable difference between the results from both models, which confirms that further increasing the number of strips beyond the number originally considered does not significantly improve the accuracy of the results.

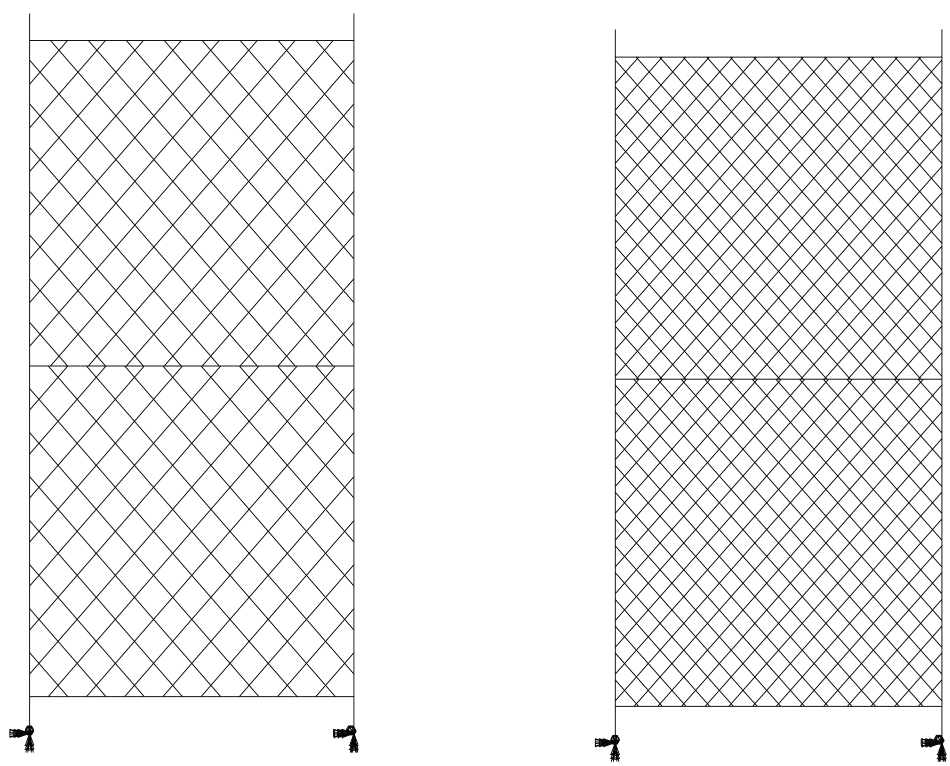

(a) Model Using 15 Strips **(b) Model Using 25 Strips**

FIGURE 5-8 Dual Strip Models

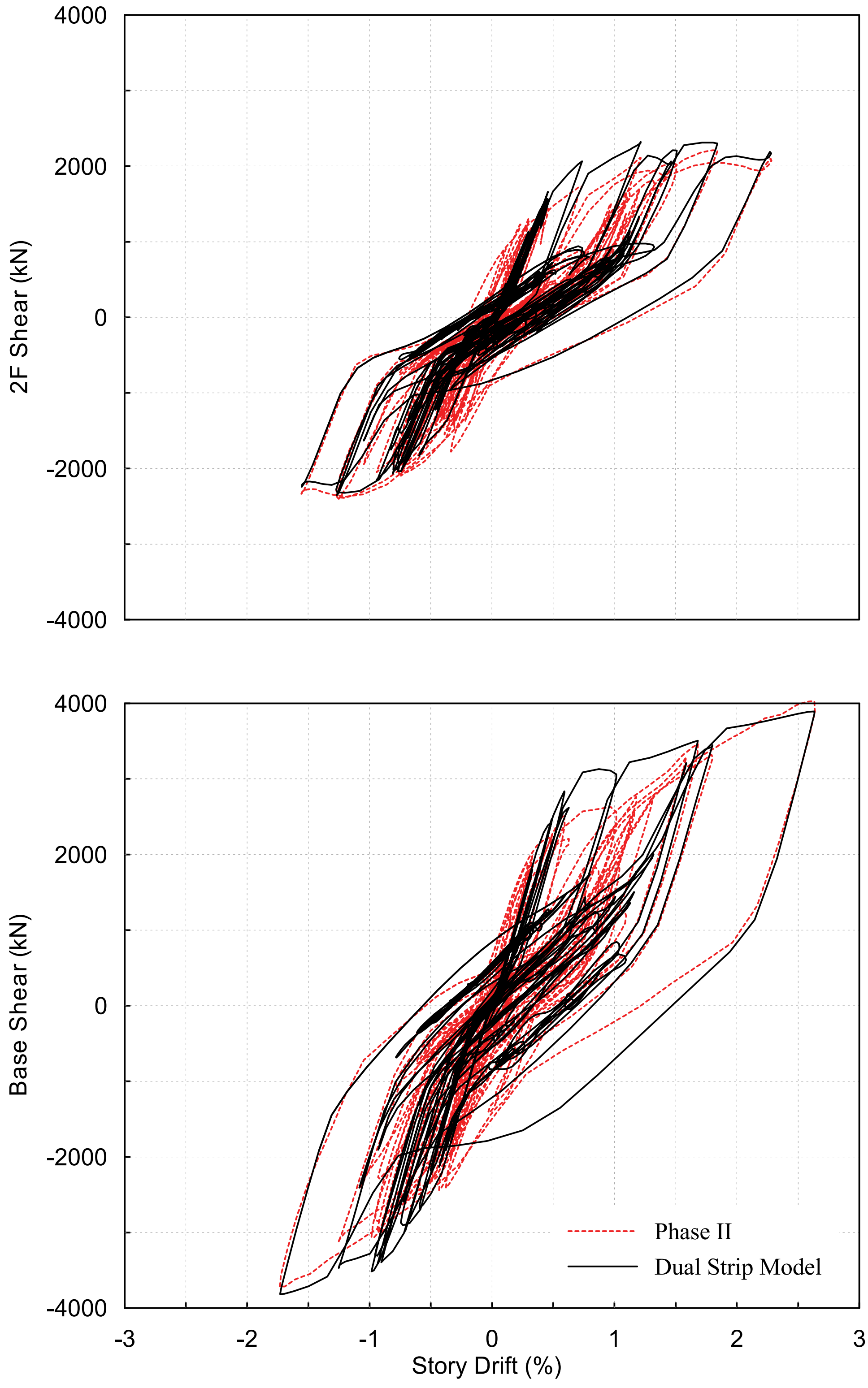

FIGURE 5-9 Hystereses from the Dual Strip Model and the Phase II Pseudodynamic Test

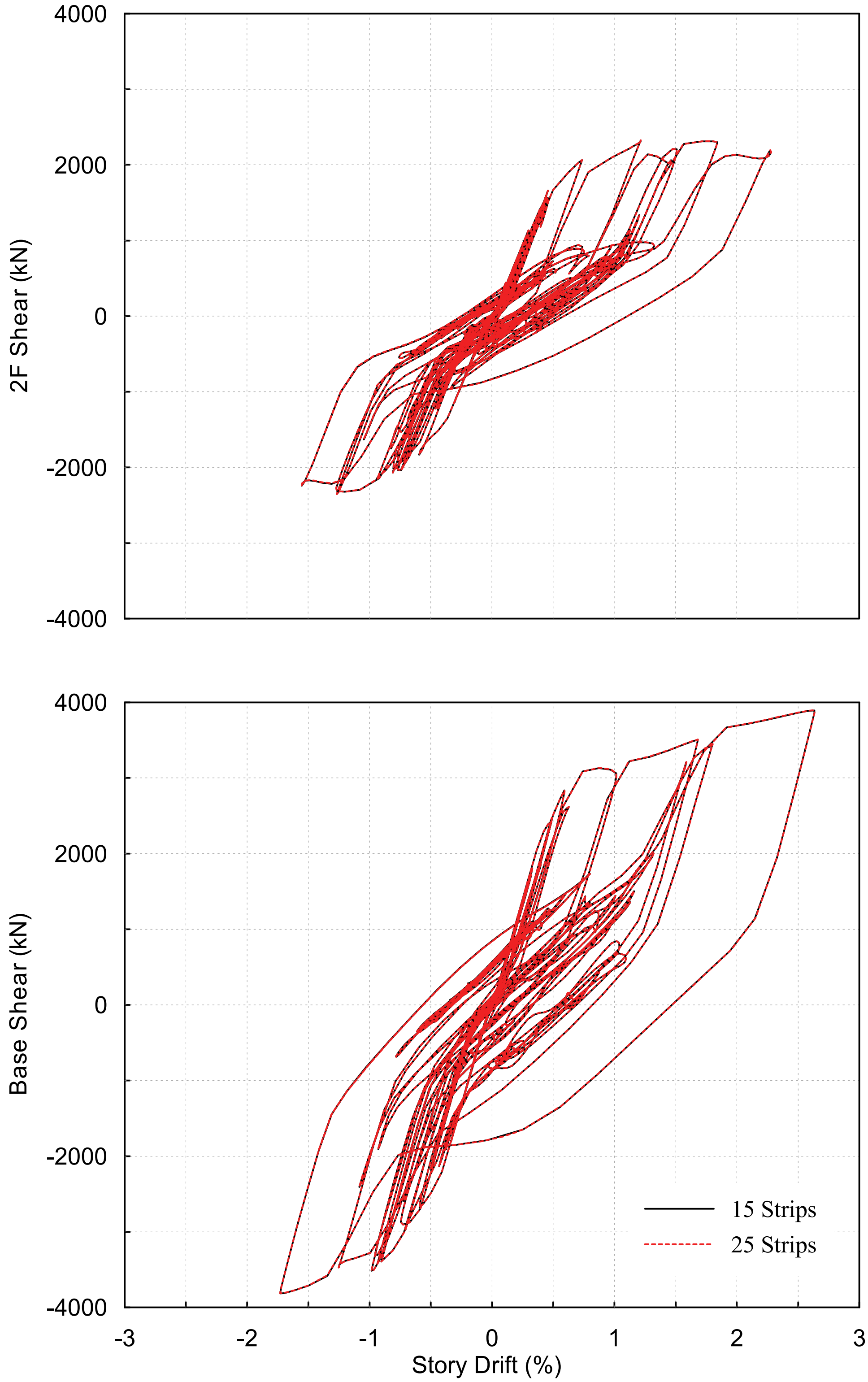

FIGURE 5-10 Comparison of Hystereses from the Dual Strip Models Using Different Numbers of Strips

5.3 Simulation Using 3D Finite Element Model

Although the aforementioned simplified dual strip models provide reasonable predictions for behavior of the tested specimen, infill panel shear buckling and some other local plastic behaviors observed in the boundary frame during testing are not best investigated by the dual strip model. To take into account those effects and further assess the global behavior of the SPSW specimen, a 3D FE model, which explicitly models each frame member as built-up cross-sections of plate elements (rather than one-dimensional idealizations) was further developed as described below.

Vian and Bruneau (2005) demonstrated that although the entire cyclic response of SPSWs can be replicated using 3D FE models, the monotonic response obtained from a monotonic pushover analysis using such a model can adequately capture the behavior of the wall at the peak story drifts of a cyclic test – hence only the monotonic analysis was conducted here to compare the results of the Phase II cyclic test.

5.3.1 Description of Model

5.3.1.1 Geometry Definition and Mesh Generation

The graphical user interface program ABAQUS/CAE, was also used to define the geometry of the 3D FE model. Similar to the dual strip model, "parts" were defined in terms of net geometry only and were specified the element types to be used in the analysis. The final model consists of different "parts", with the interaction between those parts defined through displacement constraint (i.e. ABAQUS interaction: Tie), which impose deformation compatibility. Note that the parts connected through the above constraints may not have nodes in common along their common boundary. ABAQUS impose the boundary displacement of one part, which is defined as master, to the other part, which is defined as slave, to ensure the deformation compatibility between the two pieces.

The connection tab, i.e. "fish plate", used in the experiments to connect the infill panels to the surrounding boundary frame, was neglected in this FE modeling. Instead, a direct connection was assumed to take place between the two structural elements, an approximation whose effects on analysis results were found to be negligible (Driver *et al.* 1997). Note that the other members of the specimen including HBEs, VBEs, concrete slabs and floor trusses were all considered in the 3D FE model.

The floor truss members were meshed using truss elements (ABAQUS element: T3D2, which was descried earlier) and the other segments of the FE model were meshed with quadrilateral shell elements having properties described in the next section. All plate elements were located at the mid-thickness of the physical elements they represent. Following the manual layout of basic geometry, the mesh was generated by a module within ABAQUS/CAE. Different segments of the model (i.e. webs and flanges of frame members and infill panels) were meshed using the "structured meshing technique" in ABAQUS/CAE. A total of 30,553 elements were used for the 3D FE model shown in figure 5-13a. Note that relatively fine meshes were generated over the RBS segments of HBEs and regions along panel edges.

5.3.1.2 Element Selection (S4R Shells)

The infill panels and boundary frame members were modeled using the four-node S4R element, a general purpose, doubly-curved shell, with reduced integration. Each node has six degrees of freedom: three translational (u_x, u_y, u_z) and three rotational (θ_x, θ_y, θ_z). Transverse shear deformation is allowed for by the use of thick shell theory as the thickness increases, or become discrete Kirchhoff thin shell elements, with transverse shear deformation becoming very small, as the thickness decreases (HKS 2002).

The S4R element accounts for finite member strains and large rotations, and allows for change in thickness. It is therefore suitable for large-strain analysis involving materials with a nonzero effective Poisson's ratio, as well as applications in which geometric and material nonlinearities are anticipated, as cross-sectional properties are calculated by numerical integration using seven Gaussian integration points through the shell thickness.

The S4R element also use a reduced integration scheme, with just a single integration point at the center of the shell. This scheme can provide more accurate results and significantly reduce run time compared with fully integrated elements, especially in 3D problems, if the elements are not distorted. However, under certain loading conditions, a phenomenon in which singular spurious energy modes are present, known as "hourglass", may occur. Mesh size refinement and distributing concentrated loads in the model over multiple nodes are ways of reducing the possibility of this effect. Moreover, an artificial stiffness is added by ABAQUS to both the membrane and bending terms of the shell stiffness formulation to counteract this phenomenon. While the user may explicitly define the values of these terms, the default values are typically sufficient to control "hourglass". The accumulation of strain energy dissipated by hourglass control over the history of SPSW analysis was negligible, as demonstrated by Vian and Bruneau (2005).

5.3.1.3 Boundary Conditions

Fixed boundary conditions were applied to all degrees of freedom of the nodes at the base of the specimen, to replicate the fully fixed VBE bases. The out-of-plane resistance provided by the lateral supports at the floor levels of the specimen during the experiments was modeled by fixing displacements in that direction. To do so, the exterior nodes of the elements around the perimeter of the concrete slabs were restrained against movement in the out-of-plane direction.

5.3.1.4 Initial Conditions

The initial shape of each infill panel of the specimen was not recorded, although some visible deviation from perfect flatness was observed prior to the Phase II cyclic test. These imperfections help precipitate the global panel buckling during the test, which is not detrimental in itself.

A linear eigenvalue buckling analysis was performed to determine the first three buckling modes of each infill panel prior to the monotonic pushover analysis on the FE model. Then, the artificial panel deformations (as described later) were introduced based on the buckling modes and applied as the initial condition of the specimen infill panels using the imperfection command within ABAQUS/Standard.

When analyses were conducted without using the above procedure, the panel would remain flat, incorrectly carrying the load via panel shear until either shear yielding occurs, or bifurcation shear buckling occurs, then transmitting the load via tension field actions. This did not agree with experimental observations, where, due to panel imperfections, shear buckling occurred almost immediately under very low lateral loads, (and was both audible and visible). Therefore, the introduction of initial imperfections into the analytical model was deemed appropriate and necessary to capture the observed experimental behavior.

In addition, the full gravity load of 1400 kN was applied to the top of the VBEs prior to the monotonic pushover analysis of the FE model. This magnitude is equal to the target gravity load used in the physical test.

5.3.1.5 Material Properties

ABAQUS/Standard performs calculations for element behavior based on "true" stress (Cauchy stress) and logarithmic strain, σ_{true} and $\varepsilon_{\ln}^{pl}$, respectively. Therefore, coupon test data based on the nominal values, as described in Section 3, (i.e. those based on the original geometry of the coupon for isotropic material), were converted to those measures for input by the following simple relations (HKS 2002):

$$\sigma_{true} = \sigma_{nom} \cdot \left(1 + \varepsilon_{nom}\right) \tag{5-1}$$

$$\varepsilon_{\ln}^{pl} = \ln\left(1 + \varepsilon_{nom}\right) - \frac{\sigma_{true}}{E} \tag{5-2}$$

Using pairs of ($\varepsilon_{\ln}^{pl}$, σ_{true}) data points, all steel structural subassemblages were modeled as being of an isotropic material with a simple elastoplastic constitutive behavior. A von Mises yield surface was selected as the yield criterion.

The unconfined concrete model was used for the concrete slab on the basis of the compressive strength measured from cylinder tests. In addition, as mentioned earlier, the trusses at floor levels were also modeled in this 3D FE model. However, no coupon tests were conducted to collect the specified material properties of those truss members.

Considering those members were not expected to provide significantly useful information with regards to the observed overall specimen behavior, an elasto-perfectly plastic material property based on their nominal strength (i.e. A572 Gr.50) was assumed in this investigation.

5.3.1.6 Loading of the FE Model

During the Phase II cyclic test, a displacement controlled loading scheme was applied to the specimen through the actuators at floor levels. For the reasons presented in Section 4, the specimen was loaded to displace per a shape corresponding to the first mode of response. For determination of the lateral loads to be used in the monotonic pushover analysis, relationship of the story drift ratio versus the peak drifts of the first story in the positive loading cycles obtained from the test is illustrated in figure 5-11. As shown, the story drift ratio remained about 0.84 up to a first-story drift of 3% and became approximately 0.94 subsequently. To best capture the tested specimen response at the peak story drifts in the positive loading cycles, it was decided to load the FE model accordingly, i.e. using a displacement-controlled scheme in proportion to the story drift ratio of 0.84 until the first story reached a story drift of 3% and a story drift ratio of 0.94 thereafter.

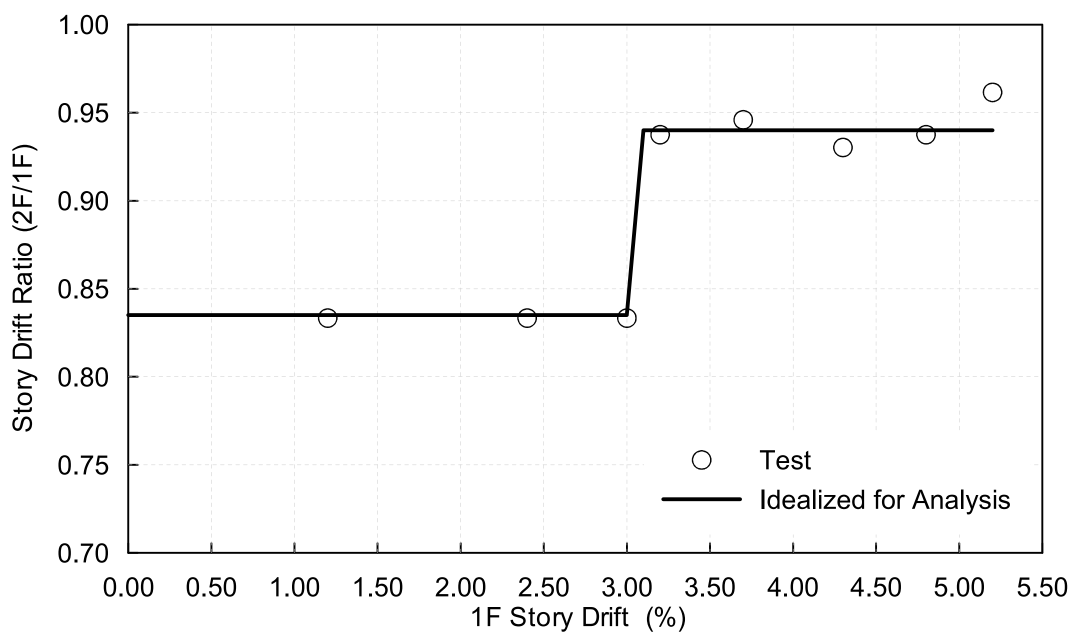

FIGURE 5-11 Displacement Constraint

5.3.1.7 Nonlinear Problem Solution

The displacement loading history was applied to the model as a static load, since the testing was carried out in a slow, quasi-static manner. Therefore, dynamic effects were not considered in the model. However, the inherent instability of panel shear buckling creates some challenges to overcome during the problem solution. The S4R shell elements described above allowed for the use of large deformation (geometric nonlinear) analysis, with element formulations updated as the model deforms, to the current deformed configuration, for use in the subsequent increment. The nonlinear material properties discussed earlier provide additional complexity to the solution. ABAQUS contains time incrementation and solution stabilization techniques, briefly summarized below, to overcome these challenges and perform a robust analysis.

ABAQUS/Standard solves nonlinear problems using the Newton method. The nonlinear solution response curve is calculated by specifying the loading as a function of "time" (artificial in the case here, as it is a slow, quasi-static loading) and incrementing the time to obtain nonlinear response (HKS 2002). The approximate equilibrium configuration is calculated at the end of each time increment, a task that may take several iterations to converge. ABAQUS uses an automatic incrementation control scheme for efficient calculation of a solution after the program is supplied with an initial time increment.

Solution difficulties presented by the localized instability discussed above were minimized by using the "STABILIZE" option within ABAQUS/Standard, which provides an automatic addition of volume-proportional damping to the model during a nonlinear static analysis. Since this option is used for a static and not dynamic analysis, an artificial mass matrix is introduced into the model and an additional damping force term is added to the model's global equilibrium equations (HKS 2002). Vian and Bruneau (2005) demonstrated that the default for this option in ABAQUS/CAE provides reasonable results for analysis of SPSWs with different infill panel layouts and therefore those default configurations were used in this investigation.

5.3.2 Results of Analyses

The FE model meshes as well as the physical specimen are shown together in figure 5-14. The first three eigen-buckling models for each infill panel of the specimen are shown in figure 5-13. An amplitude of 2% of the specified infill panel thickness was assigned to the infill panel nodal displacements for the first mode to serve as initial imperfections. To account for the reduced impacts of higher buckling modes on the initial imperfection of infill panels, 1.6% and 1.28% of the infill panel thickness (i.e. 80% and 64% of that used for the first mode) were introduced as initial imperfections of the second and third modes, respectively. Those three sets of initial imperfections were superimposed to produce the initial deformed shape of the model prior to analysis.

Although the initial imperfection imposed in the FE model was smaller than the observed infill panel deformation of the specimen before the Phase II cyclic test, comparable infill panel shear buckling and formation of the diagonal tension fields, as well as SPSW strengths were observed in the simulation, as shown in figure 5-15. The pushover curves obtained from the 3D FE model are compared with the hysteretic curves obtained from the physical testing in figure 5-15.

It is observed that the story shears from the FE analysis are greater than those obtained from the cyclic test prior to 2.6 and 2.3% story drifts at the first and second story, respectively. This is principally because the specimen was loaded into the inelastic range in the prior Phase II pseudodynamic test, resulting in the partial absence of infill panel tension fields at low story drift levels. However, the story shears obtained from FE analysis agree well with those obtained from the Phase II cyclic test at story drifts exceeding the maximum story drifts of 2.6 and 2.3% at the first and second story respectively reached in the Phase II pseudodynamic test. After story drifts of 3% and 2.5% at the first and second story respectively, the story shears from the cyclic tests are smaller than those from FE analysis due to the ruptures in the intermediate HBE and failures of the welds connecting the infill panels to fish plates. Note that fracture behavior of structural assemblages of the physical specimen was not included in the analytical model.

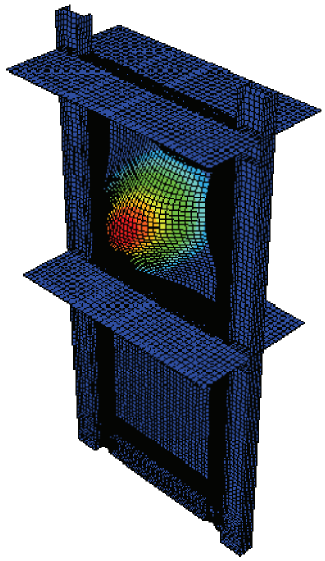

(a) 1st mode of 2F Panel

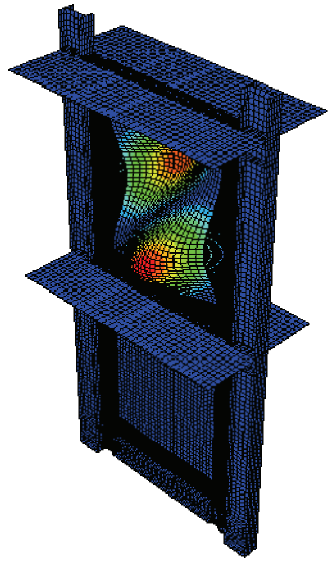

(b) 2nd mode of 2F Panel

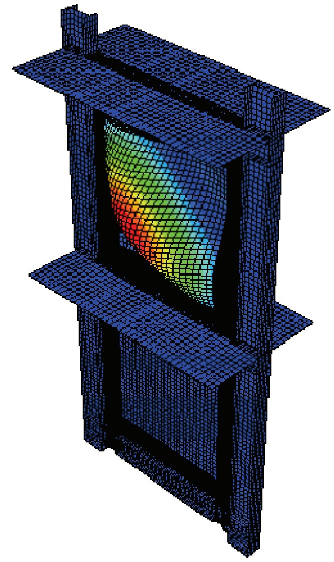

(c) 3rd mode of 2F Panel

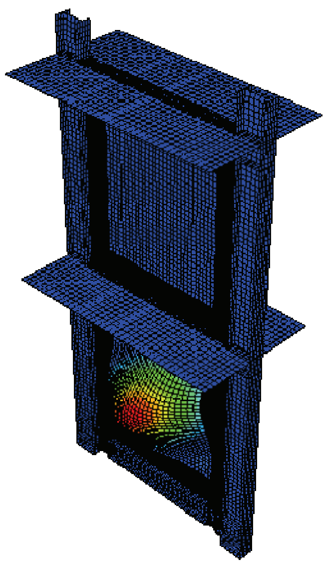

(d) 1st mode of 1F Panel

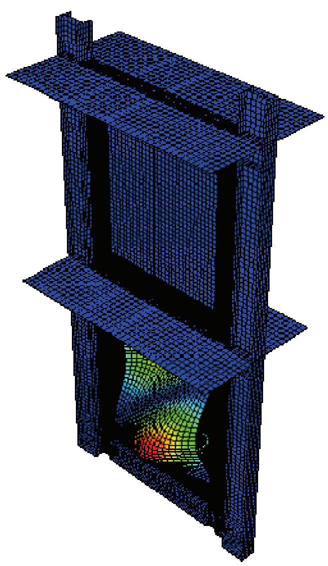

(e) 2nd mode of 1F Panel

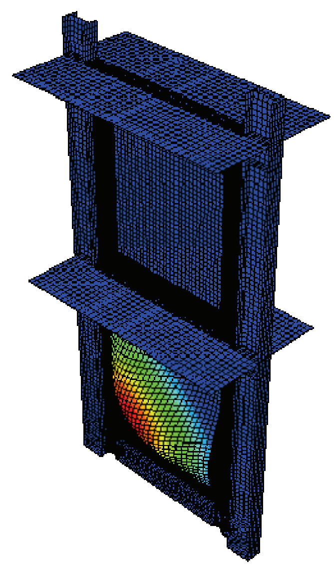

(f) 3rd mode of 1F Panel

FIGURE 5-12 Buckling Modes of 3D FE Model

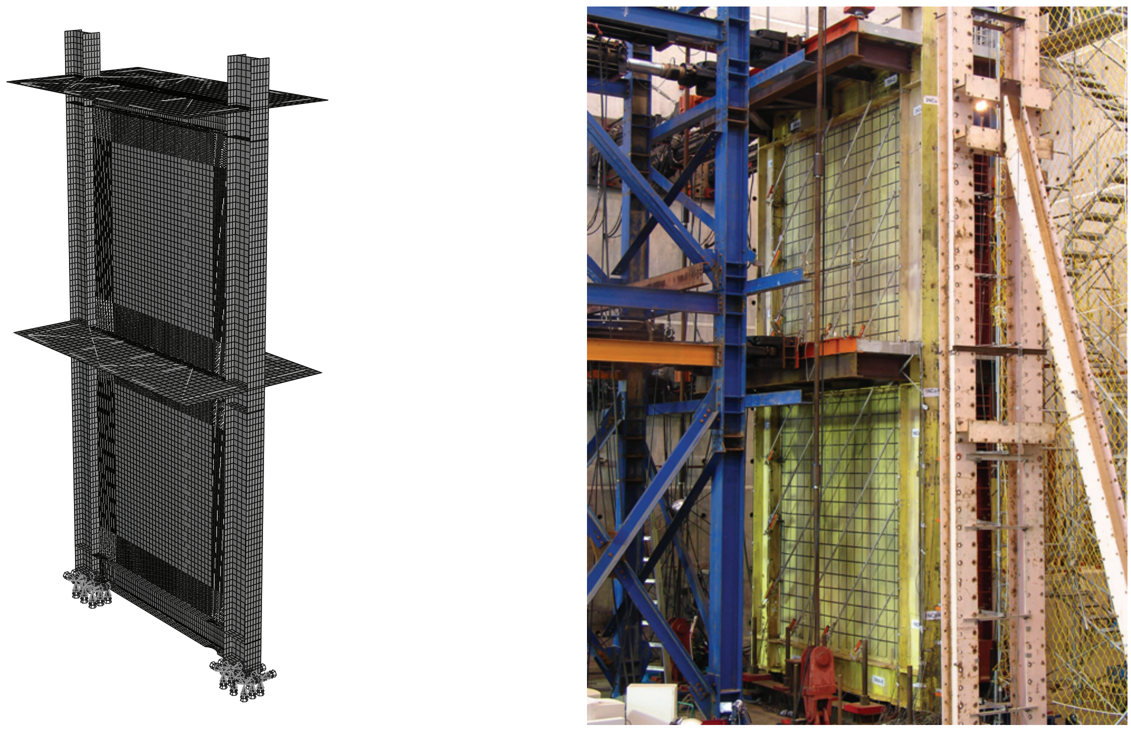

(a) Mesh of the 3D FE Model **(b) Physical Specimen**

FIGURE 5-13 FE Model and Specimen

(b) Tension Field in the 3D Model **(b) Tension Field in the Specimen**

FIGURE 5-14 Tension Fields in the FE Model and Specimen

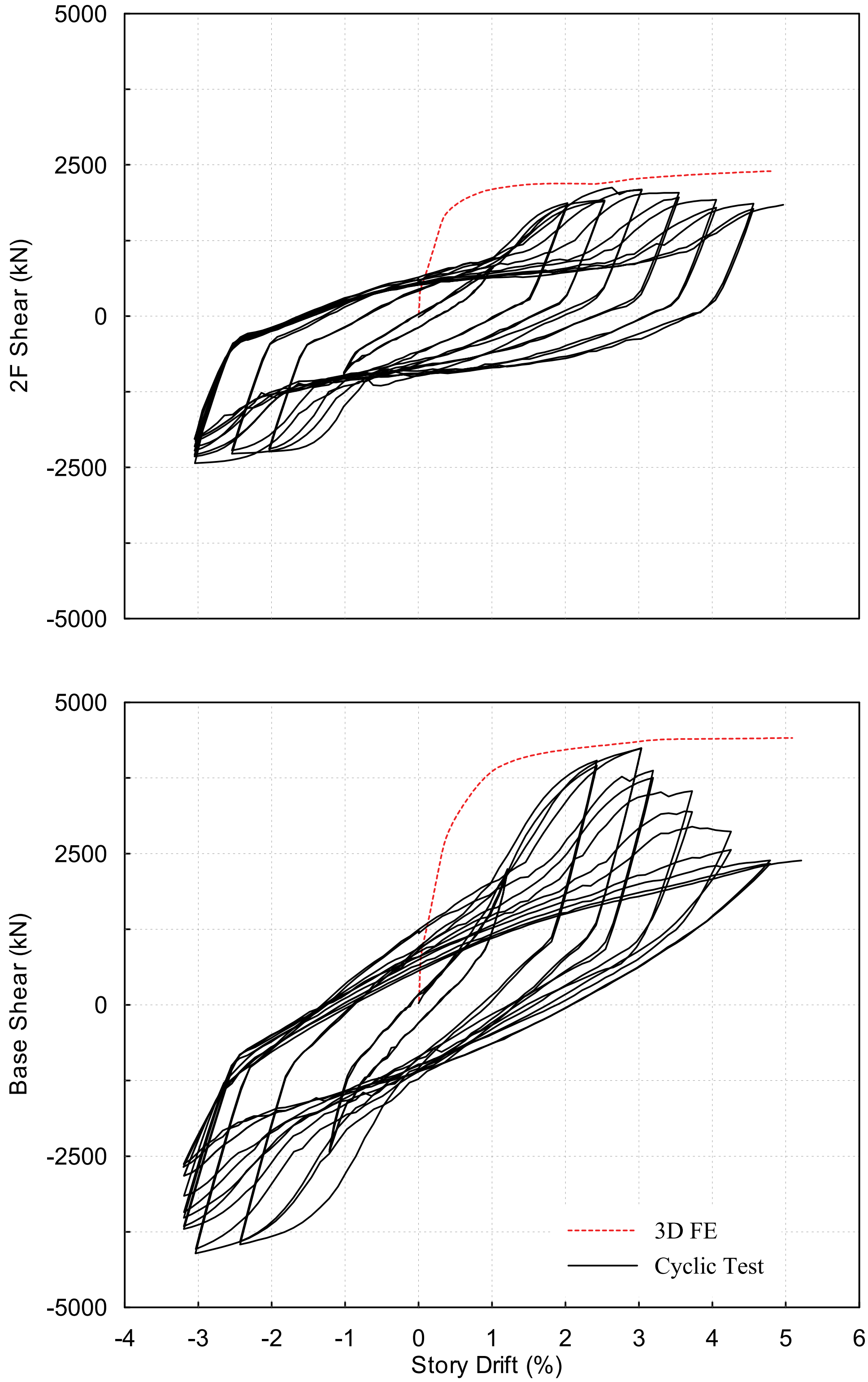

FIGURE 5-15 Monotonic Pushover Curves and Hystereses of the Phase II Cyclic Test

5.4 Summary

The FE analysis software package ABAQUS/Standard was used to perform nonlinear analysis of models of the tested SPSW specimen described in the previous two sections. Two analytical models, namely, the dual strip model and the 3D FE model, were respectively considered.

The dual strip model discretely represented the infill panels using tension-only strips and was analyzed under pseudodynamic loads recorded from the Phase II pseudodynamic test. This model was found to accurately predict the global nonlinear behavior of SPSW under earthquake loads, as demonstrated by comparison with the experimental results of the Phase II pseudodynamic test.

The 3D FE model, which explicitly modeled each frame member as built-up cross-sections of plate elements, was used to perform analysis under monotonic loads. The overall behavior and ultimate strength of the wall were shown to be equally well predicted by this model when comparing with the experimental results from the Phase II cyclic test, suggesting the modeling assumptions and model development procedure utilized in this case are appropriate for modeling other SPSW problems.

SECTION 6

SUMMARY, CONCLUSIONS, AND RECOMMENDATIONS FOR FUTURE RESEARCH

6.1 Summary and Conclusions

In this report, a full scale two-story SPSW specimen with RBS connections and composite floors was designed and tested, to experimentally address the replaceability of infill panels following an earthquake, the behavior of the repaired SPSW in a subsequent earthquake, and the seismic performance of the intermediate HBE.

The specimen was first pseudodynamically tested, subjected to three ground motions of progressively decreasing intensity. The buckled panels were then replaced by new panels prior to re-testing the specimen for the same pseudodynamic loads. The repaired SPSW specimen behaved satisfactorily in that second earthquake quite similarly to the original one. Subsequent cyclic test of the SPSW specimen investigated the ultimate behavior of the intermediate HBE and the cyclic behavior and ultimate capacity of the SPSW. Although hysteretic curves were pinched at low story drift levels (due to the inelastic deformations that the infill panels experienced during the pseudodynamic tests), the SPSW structure exhibited stable force-displacement behavior and provided a significant energy dissipation capacity, exhibiting substantial redundancy. However, the ends of the intermediate HBE having RBS connections ultimately developed fractures in the shear tabs followed by fractures at the end of the bottom beam flanges. No fractures developed in the reduced beam flange region. This revealed that HBE yielding/failure behavior was different from that of beams in a conventional moment frame due to the presence of internal forces.

The testing showed that, in SPSWs, replacing the infill panels buckled in a prior earthquake by new ones can be a viable option to provide adequate resistance to future seismic excitations. It also showed that the repaired SPSW can survive and dissipate a similar amount of energy in the subsequent earthquake without severe damage to the boundary frame and without overall strength degradation.

The FE analysis software package ABAQUS/Standard was used to perform nonlinear analysis of models of the tested SPSW to replicate the observed behavior of the specimen. A dual strip model used to discretely represent the infill panels using tension-only strips, and to analyze the global behavior of the SPSW under pseudodynamic loads, was found accurate to predict the nonlinear behavior of the SPSW under earthquake loads. A 3D FE model used to rigorously model all parts of the tested specimen and analyze its behavior under monotonic (pushover) loads captured well the ultimate strength of the SPSW when comparing with the experimental results and allowed to investigate local behavior of boundary frame members in the future.

6.2 Recommendations for Future Research

The testing conducted has shown that the pattern of yielding in the RBS details of SPSW is different from that in the RBS connections of conventional steel moment frame. It would be important to investigate the reasons for these difference in observed yielding behavior and to develop an improved capacity design procedure for HBEs to better ensure the ductile performance of SPSWs.

SECTION 7

REFERENCES

AISC. (2005), "Seismic Provisions for Structural Steel Buildings." American Institute of Steel Construction, Chicago, Illinois.

ATC (1992), "Guidelines for Cyclic Seismic Testing of Components of Steel Structures." Report No.24 Applied Technology Council, Redwood City, CA.

Berman, J. W. and Bruneau, M. (2003), "Experimental Investigation of Light-Gauge Steel Plate Shear Walls for the Seismic Retrofit Of Buildings. " Technical Report MCEER-03-0001, Multidisciplinary Center for Earthquake Engineering Research, Buffalo, N.Y., May 2, 2003.

Berman, J. W. and Bruneau, M. (2005), "Experimental Investigation of Light-Gauge Steel Plate Shear Walls." Journal of Structural Engineering, ASCE, Vol. 131, No. 2, pp. 259-267.

Bruneau, M., Uang, C-M, Whittaker, A.S. (1998), "Ductile Design of Steel Structures." McGraw-Hill, New York.

Canadian Standards Association (CSA). (2000), "Limit States Design of Steel Structures." CAN/CSA S16-01. Willowdale, Ontario, Canada.

Driver, R. G., Kulak, G. L., Kennedy, D. J. L., and Elwi, A. E. (1997), "Seismic Behavior of Steel Plate Shear Walls. " Structural Engineering Report 215, University of Alberta, Department of Civil and Environmental Engineering, February 1997.

Elgaaly, M., Caccese, V., and Du, C. (1993), "Postbuckling Behavior of Steel-Plate Shear Walls Under Cyclic Loads", Journal of Structural Engineering, ASCE, Vol. 119, No. 2, Feb. 1993, pp. 588-605.

FEMA (2000), "FEMA 350: Recommended Seismic Design Criteria for New Steel Moment-Frame Buildings." SAC Joint Venture for the Federal Emergency Management Agency, Washington, D.C.

FEMA (2004), "FEMA 450: NEHRP Recommended Provisions For Seismic Regulations For New Buildings And Other Structures." Building Seismic Safety Council for the Federal Emergency Management Agency, Washington, D.C.

Hibbitt, Karlsson, and Sorenson, Inc. (HKS) (2002), "ABAQUS/Standard Users Manual." Version 6.3, Hibbitt, Karlsson, and Sorenson, Inc., Pawtucket, Rhode Island.

James River Steel Inc. (2004), "Composite Floor Decks" <http://www.jamesriversteel.com/comp3.htm>.

Jalali, A., and Sazgari, A. (2006), "Experimental and Theoretical Post-Buckling Study of Steel Shear Walls" Proceeding of the 4th International Conference on Earthquake Engineering, Paper No. 114, Taipei, Taiwan.

Kuan, M.L. (2005), "Discussion on ASTM A36 and CNS SS400." < http://www.twce.org.tw/info/%A7%DE%AEv%B3%F8/367-3-1.htm> (in Chinese).

Kuhn, P., Peterson, J.P., and Levin, L.R. (1952), "A Summary of Diagonal Tension. Part I: Methods and Analysis." Technical Note 2661, National Advisory Committee for Aeronautics, Washington, D.C.

Lee, C.H. (2006), "Approximate Analytical Evaluation of Elastic Story Drift of Steel Moment Frames with Radius-Cut Reduced Beam Section" Proceeding of the 4th International Conference on Earthquake Engineering, Paper No. 48, Taipei, Taiwan.

Lin, Y.C. and Tsai, K.C. (2004), "Seismic Responses of Steel Shear Wall Constructed with Restrainers" (in Chinese) Technical Report NCREE-04-015, National Center for Research on Earthquake Engineering, Taipei, Taiwan, R.O.C., September 2004.

Lopez-Garcia, D. and Bruneau, M. (2006), "Seismic Behavior of Intermediate beams in Steel Plate Shear Walls", Proceeding of the 8th U.S. National Conference on Earthquake Engineering, Paper No.1089, San Francisco, CA.

Lubell, A.S., Prion, H.G.L., Ventura, C.E., and Rezai, M. (2000), "Unstiffened Steel Plate Shear Wall Performance under Cyclic Loading." Journal of Structural Engineering, Vol.126, No.4, pp.453-460.

NCREE (2002), "Reaction Wall & Strong Floor Test System" NCREE Laboratory Experimental Facilities, <http://www.ncree.gov.tw/eng/3_lab/facility/Facilities2.htm> (February 19, 2003).

Park, H.G., Kwack, J.H., Jeon, S.W., Kim, W.K., and Choi, I.R. (2007), "Framed Steel Plate Wall Behavior under Cyclic Later Loading", Journal of Structural Engineering, Vol.133, No.3, pp.378-388.

Rezia, M., (1999), "Seismic Behavior of Steel Plate Shear Walls by Shake Table Testing", Ph.D. Dissertation, University of British Columbia, Vancouver, British Columbia, Canada.

Sabelli, R., and Bruneau, M. (2007), "Steel Plate Shear Walls (AISC Design Guide).", American Institute of Steel Construction, Chicago, Illinois.

Schumacher, A., Grondin, G.Y., and Kulak, G.L. (1999), "Connection of Infill Panels in Steel Plate Shear Walls", Canadian Journal of Civil Engineering, Vol. 26, No. 5, pp. 549-563.

Timler, P. A. and Kulak, G. L. (1983), "Experimental Study of Steel Plate Shear Walls." Structural Engineering Report No. 114, Department of Civil Engineering, The University of Alberta, Edmonton, Alberta, November 1983.

Thorburn, L. Jane, Kulak, G. L., and Montgomery, C. J. (1983), "Analysis of Steel Plate Shear Walls." Structural Engineering Report No. 107, Department of Civil Engineering, The University of Alberta, Edmonton, Alberta, May 1983.

Tromposch, E.W., and Kulak, G.L. (1987), "Cyclic and Static Behaviour of Thin Panel Steel Plate Shear Walls", Structural Engineering Report No. 145, Department of Civil Engineering, University of Alberta, Edmonton, Alberta, Canada.

Tsai, K.C., Lin, C.H., Lin,Y.C., Hsieh, W.D., and Qu, B. (2006), "Substructural Hybrid Tests of A Full Scale Two-story Steel Plate Shear Wall." Technical Report NCREE-06-017, National Center for Research on Earthquake Engineering. Taipei, Taiwan.(in Chinese).

Vian D. and Bruneau M.(2005), "Steel Plate Shear Walls for Seismic Design and Retrofit of Building Structure", Technical Report MCEER-05-0010, Multidisciplinary Center for Earthquake Engineering Research, Buffalo, N.Y.

Wagner, H. (1931), "Flat Sheet Metal Girders with Very Thin Webs, Part III: Sheet Metal Girders with Spars Resistant to Bending – The Stress in Uprights – Diagonal Tension Fields." Technical Memorandum No.606, National Advisory Committee for Aeronautics, Washington, D.C.

MCEER Technical Reports

MCEER publishes technical reports on a variety of subjects written by authors funded through MCEER. These reports are available from both MCEER Publications and the National Technical Information Service (NTIS). Requests for reports should be directed to MCEER Publications, MCEER, University at Buffalo, State University of New York, Red Jacket Quadrangle, Buffalo, New York 14261. Reports can also be requested through NTIS, 5285 Port Royal Road, Springfield, Virginia 22161. NTIS accession numbers are shown in parenthesis, if available.

NCEER-87-0001 "First-Year Program in Research, Education and Technology Transfer," 3/5/87, (PB88-134275, A04, MF-A01).

NCEER-87-0002 "Experimental Evaluation of Instantaneous Optimal Algorithms for Structural Control," by R.C. Lin, T.T. Soong and A.M. Reinhorn, 4/20/87, (PB88-134341, A04, MF-A01).

NCEER-87-0003 "Experimentation Using the Earthquake Simulation Facilities at University at Buffalo," by A.M. Reinhorn and R.L. Ketter, to be published.

NCEER-87-0004 "The System Characteristics and Performance of a Shaking Table," by J.S. Hwang, K.C. Chang and G.C. Lee, 6/1/87, (PB88-134259, A03, MF-A01). This report is available only through NTIS (see address given above).

NCEER-87-0005 "A Finite Element Formulation for Nonlinear Viscoplastic Material Using a Q Model," by O. Gyebi and G. Dasgupta, 11/2/87, (PB88-213764, A08, MF-A01).

NCEER-87-0006 "Symbolic Manipulation Program (SMP) - Algebraic Codes for Two and Three Dimensional Finite Element Formulations," by X. Lee and G. Dasgupta, 11/9/87, (PB88-218522, A05, MF-A01).

NCEER-87-0007 "Instantaneous Optimal Control Laws for Tall Buildings Under Seismic Excitations," by J.N. Yang, A. Akbarpour and P. Ghaemmaghami, 6/10/87, (PB88-134333, A06, MF-A01). This report is only available through NTIS (see address given above).

NCEER-87-0008 "IDARC: Inelastic Damage Analysis of Reinforced Concrete Frame - Shear-Wall Structures," by Y.J. Park, A.M. Reinhorn and S.K. Kunnath, 7/20/87, (PB88-134325, A09, MF-A01). This report is only available through NTIS (see address given above).

NCEER-87-0009 "Liquefaction Potential for New York State: A Preliminary Report on Sites in Manhattan and Buffalo," by M. Budhu, V. Vijayakumar, R.F. Giese and L. Baumgras, 8/31/87, (PB88-163704, A03, MF-A01). This report is available only through NTIS (see address given above).

NCEER-87-0010 "Vertical and Torsional Vibration of Foundations in Inhomogeneous Media," by A.S. Veletsos and K.W. Dotson, 6/1/87, (PB88-134291, A03, MF-A01). This report is only available through NTIS (see address given above).

NCEER-87-0011 "Seismic Probabilistic Risk Assessment and Seismic Margins Studies for Nuclear Power Plants," by Howard H.M. Hwang, 6/15/87, (PB88-134267, A03, MF-A01). This report is only available through NTIS (see address given above).

NCEER-87-0012 "Parametric Studies of Frequency Response of Secondary Systems Under Ground-Acceleration Excitations," by Y. Yong and Y.K. Lin, 6/10/87, (PB88-134309, A03, MF-A01). This report is only available through NTIS (see address given above).

NCEER-87-0013 "Frequency Response of Secondary Systems Under Seismic Excitation," by J.A. HoLung, J. Cai and Y.K. Lin, 7/31/87, (PB88-134317, A05, MF-A01). This report is only available through NTIS (see address given above).

NCEER-87-0014 "Modelling Earthquake Ground Motions in Seismically Active Regions Using Parametric Time Series Methods," by G.W. Ellis and A.S. Cakmak, 8/25/87, (PB88-134283, A08, MF-A01). This report is only available through NTIS (see address given above).

NCEER-87-0015 "Detection and Assessment of Seismic Structural Damage," by E. DiPasquale and A.S. Cakmak, 8/25/87, (PB88-163712, A05, MF-A01). This report is only available through NTIS (see address given above).

NCEER-87-0016 "Pipeline Experiment at Parkfield, California," by J. Isenberg and E. Richardson, 9/15/87, (PB88-163720, A03, MF-A01). This report is available only through NTIS (see address given above).

NCEER-87-0017 "Digital Simulation of Seismic Ground Motion," by M. Shinozuka, G. Deodatis and T. Harada, 8/31/87, (PB88-155197, A04, MF-A01). This report is available only through NTIS (see address given above).

NCEER-87-0018 "Practical Considerations for Structural Control: System Uncertainty, System Time Delay and Truncation of Small Control Forces," J.N. Yang and A. Akbarpour, 8/10/87, (PB88-163738, A08, MF-A01). This report is only available through NTIS (see address given above).

NCEER-87-0019 "Modal Analysis of Nonclassically Damped Structural Systems Using Canonical Transformation," by J.N. Yang, S. Sarkani and F.X. Long, 9/27/87, (PB88-187851, A04, MF-A01).

NCEER-87-0020 "A Nonstationary Solution in Random Vibration Theory," by J.R. Red-Horse and P.D. Spanos, 11/3/87, (PB88-163746, A03, MF-A01).

NCEER-87-0021 "Horizontal Impedances for Radially Inhomogeneous Viscoelastic Soil Layers," by A.S. Veletsos and K.W. Dotson, 10/15/87, (PB88-150859, A04, MF-A01).

NCEER-87-0022 "Seismic Damage Assessment of Reinforced Concrete Members," by Y.S. Chung, C. Meyer and M. Shinozuka, 10/9/87, (PB88-150867, A05, MF-A01). This report is available only through NTIS (see address given above).

NCEER-87-0023 "Active Structural Control in Civil Engineering," by T.T. Soong, 11/11/87, (PB88-187778, A03, MF-A01).

NCEER-87-0024 "Vertical and Torsional Impedances for Radially Inhomogeneous Viscoelastic Soil Layers," by K.W. Dotson and A.S. Veletsos, 12/87, (PB88-187786, A03, MF-A01).

NCEER-87-0025 "Proceedings from the Symposium on Seismic Hazards, Ground Motions, Soil-Liquefaction and Engineering Practice in Eastern North America," October 20-22, 1987, edited by K.H. Jacob, 12/87, (PB88-188115, A23, MF-A01). This report is available only through NTIS (see address given above).

NCEER-87-0026 "Report on the Whittier-Narrows, California, Earthquake of October 1, 1987," by J. Pantelic and A. Reinhorn, 11/87, (PB88-187752, A03, MF-A01). This report is available only through NTIS (see address given above).

NCEER-87-0027 "Design of a Modular Program for Transient Nonlinear Analysis of Large 3-D Building Structures," by S. Srivastav and J.F. Abel, 12/30/87, (PB88-187950, A05, MF-A01). This report is only available through NTIS (see address given above).

NCEER-87-0028 "Second-Year Program in Research, Education and Technology Transfer," 3/8/88, (PB88-219480, A04, MF-A01).

NCEER-88-0001 "Workshop on Seismic Computer Analysis and Design of Buildings With Interactive Graphics," by W. McGuire, J.F. Abel and C.H. Conley, 1/18/88, (PB88-187760, A03, MF-A01). This report is only available through NTIS (see address given above).

NCEER-88-0002 "Optimal Control of Nonlinear Flexible Structures," by J.N. Yang, F.X. Long and D. Wong, 1/22/88, (PB88-213772, A06, MF-A01).

NCEER-88-0003 "Substructuring Techniques in the Time Domain for Primary-Secondary Structural Systems," by G.D. Manolis and G. Juhn, 2/10/88, (PB88-213780, A04, MF-A01).

NCEER-88-0004 "Iterative Seismic Analysis of Primary-Secondary Systems," by A. Singhal, L.D. Lutes and P.D. Spanos, 2/23/88, (PB88-213798, A04, MF-A01).

NCEER-88-0005 "Stochastic Finite Element Expansion for Random Media," by P.D. Spanos and R. Ghanem, 3/14/88, (PB88-213806, A03, MF-A01).

NCEER-88-0006 "Combining Structural Optimization and Structural Control," by F.Y. Cheng and C.P. Pantelides, 1/10/88, (PB88-213814, A05, MF-A01).

NCEER-88-0007 "Seismic Performance Assessment of Code-Designed Structures," by H.H-M. Hwang, J-W. Jaw and H-J. Shau, 3/20/88, (PB88-219423, A04, MF-A01). This report is only available through NTIS (see address given above).

NCEER-88-0008 "Reliability Analysis of Code-Designed Structures Under Natural Hazards," by H.H-M. Hwang, H. Ushiba and M. Shinozuka, 2/29/88, (PB88-229471, A07, MF-A01). This report is only available through NTIS (see address given above).

NCEER-88-0009 "Seismic Fragility Analysis of Shear Wall Structures," by J-W Jaw and H.H-M. Hwang, 4/30/88, (PB89-102867, A04, MF-A01).

NCEER-88-0010 "Base Isolation of a Multi-Story Building Under a Harmonic Ground Motion - A Comparison of Performances of Various Systems," by F-G Fan, G. Ahmadi and I.G. Tadjbakhsh, 5/18/88, (PB89-122238, A06, MF-A01). This report is only available through NTIS (see address given above).

NCEER-88-0011 "Seismic Floor Response Spectra for a Combined System by Green's Functions," by F.M. Lavelle, L.A. Bergman and P.D. Spanos, 5/1/88, (PB89-102875, A03, MF-A01).

NCEER-88-0012 "A New Solution Technique for Randomly Excited Hysteretic Structures," by G.Q. Cai and Y.K. Lin, 5/16/88, (PB89-102883, A03, MF-A01).

NCEER-88-0013 "A Study of Radiation Damping and Soil-Structure Interaction Effects in the Centrifuge," by K. Weissman, supervised by J.H. Prevost, 5/24/88, (PB89-144703, A06, MF-A01).

NCEER-88-0014 "Parameter Identification and Implementation of a Kinematic Plasticity Model for Frictional Soils," by J.H. Prevost and D.V. Griffiths, to be published.

NCEER-88-0015 "Two- and Three- Dimensional Dynamic Finite Element Analyses of the Long Valley Dam," by D.V. Griffiths and J.H. Prevost, 6/17/88, (PB89-144711, A04, MF-A01).

NCEER-88-0016 "Damage Assessment of Reinforced Concrete Structures in Eastern United States," by A.M. Reinhorn, M.J. Seidel, S.K. Kunnath and Y.J. Park, 6/15/88, (PB89-122220, A04, MF-A01). This report is only available through NTIS (see address given above).

NCEER-88-0017 "Dynamic Compliance of Vertically Loaded Strip Foundations in Multilayered Viscoelastic Soils," by S. Ahmad and A.S.M. Israil, 6/17/88, (PB89-102891, A04, MF-A01).

NCEER-88-0018 "An Experimental Study of Seismic Structural Response With Added Viscoelastic Dampers," by R.C. Lin, Z. Liang, T.T. Soong and R.H. Zhang, 6/30/88, (PB89-122212, A05, MF-A01). This report is available only through NTIS (see address given above).

NCEER-88-0019 "Experimental Investigation of Primary - Secondary System Interaction," by G.D. Manolis, G. Juhn and A.M. Reinhorn, 5/27/88, (PB89-122204, A04, MF-A01).

NCEER-88-0020 "A Response Spectrum Approach For Analysis of Nonclassically Damped Structures," by J.N. Yang, S. Sarkani and F.X. Long, 4/22/88, (PB89-102909, A04, MF-A01).

NCEER-88-0021 "Seismic Interaction of Structures and Soils: Stochastic Approach," by A.S. Veletsos and A.M. Prasad, 7/21/88, (PB89-122196, A04, MF-A01). This report is only available through NTIS (see address given above).

NCEER-88-0022 "Identification of the Serviceability Limit State and Detection of Seismic Structural Damage," by E. DiPasquale and A.S. Cakmak, 6/15/88, (PB89-122188, A05, MF-A01). This report is available only through NTIS (see address given above).

NCEER-88-0023 "Multi-Hazard Risk Analysis: Case of a Simple Offshore Structure," by B.K. Bhartia and E.H. Vanmarcke, 7/21/88, (PB89-145213, A05, MF-A01).

NCEER-88-0024 "Automated Seismic Design of Reinforced Concrete Buildings," by Y.S. Chung, C. Meyer and M. Shinozuka, 7/5/88, (PB89-122170, A06, MF-A01). This report is available only through NTIS (see address given above).

NCEER-88-0025 "Experimental Study of Active Control of MDOF Structures Under Seismic Excitations," by L.L. Chung, R.C. Lin, T.T. Soong and A.M. Reinhorn, 7/10/88, (PB89-122600, A04, MF-A01).

NCEER-88-0026 "Earthquake Simulation Tests of a Low-Rise Metal Structure," by J.S. Hwang, K.C. Chang, G.C. Lee and R.L. Ketter, 8/1/88, (PB89-102917, A04, MF-A01).

NCEER-88-0027 "Systems Study of Urban Response and Reconstruction Due to Catastrophic Earthquakes," by F. Kozin and H.K. Zhou, 9/22/88, (PB90-162348, A04, MF-A01).

NCEER-88-0028 "Seismic Fragility Analysis of Plane Frame Structures," by H.H-M. Hwang and Y.K. Low, 7/31/88, (PB89-131445, A06, MF-A01).

NCEER-88-0029 "Response Analysis of Stochastic Structures," by A. Kardara, C. Bucher and M. Shinozuka, 9/22/88, (PB89-174429, A04, MF-A01).

NCEER-88-0030 "Nonnormal Accelerations Due to Yielding in a Primary Structure," by D.C.K. Chen and L.D. Lutes, 9/19/88, (PB89-131437, A04, MF-A01).

NCEER-88-0031 "Design Approaches for Soil-Structure Interaction," by A.S. Veletsos, A.M. Prasad and Y. Tang, 12/30/88, (PB89-174437, A03, MF-A01). This report is available only through NTIS (see address given above).

NCEER-88-0032 "A Re-evaluation of Design Spectra for Seismic Damage Control," by C.J. Turkstra and A.G. Tallin, 11/7/88, (PB89-145221, A05, MF-A01).

NCEER-88-0033 "The Behavior and Design of Noncontact Lap Splices Subjected to Repeated Inelastic Tensile Loading," by V.E. Sagan, P. Gergely and R.N. White, 12/8/88, (PB89-163737, A08, MF-A01).

NCEER-88-0034 "Seismic Response of Pile Foundations," by S.M. Mamoon, P.K. Banerjee and S. Ahmad, 11/1/88, (PB89-145239, A04, MF-A01).

NCEER-88-0035 "Modeling of R/C Building Structures With Flexible Floor Diaphragms (IDARC2)," by A.M. Reinhorn, S.K. Kunnath and N. Panahshahi, 9/7/88, (PB89-207153, A07, MF-A01).

NCEER-88-0036 "Solution of the Dam-Reservoir Interaction Problem Using a Combination of FEM, BEM with Particular Integrals, Modal Analysis, and Substructuring," by C-S. Tsai, G.C. Lee and R.L. Ketter, 12/31/88, (PB89-207146, A04, MF-A01).

NCEER-88-0037 "Optimal Placement of Actuators for Structural Control," by F.Y. Cheng and C.P. Pantelides, 8/15/88, (PB89-162846, A05, MF-A01).

NCEER-88-0038 "Teflon Bearings in Aseismic Base Isolation: Experimental Studies and Mathematical Modeling," by A. Mokha, M.C. Constantinou and A.M. Reinhorn, 12/5/88, (PB89-218457, A10, MF-A01). This report is available only through NTIS (see address given above).

NCEER-88-0039 "Seismic Behavior of Flat Slab High-Rise Buildings in the New York City Area," by P. Weidlinger and M. Ettouney, 10/15/88, (PB90-145681, A04, MF-A01).

NCEER-88-0040 "Evaluation of the Earthquake Resistance of Existing Buildings in New York City," by P. Weidlinger and M. Ettouney, 10/15/88, to be published.

NCEER-88-0041 "Small-Scale Modeling Techniques for Reinforced Concrete Structures Subjected to Seismic Loads," by W. Kim, A. El-Attar and R.N. White, 11/22/88, (PB89-189625, A05, MF-A01).

NCEER-88-0042 "Modeling Strong Ground Motion from Multiple Event Earthquakes," by G.W. Ellis and A.S. Cakmak, 10/15/88, (PB89-174445, A03, MF-A01).

NCEER-88-0043 "Nonstationary Models of Seismic Ground Acceleration," by M. Grigoriu, S.E. Ruiz and E. Rosenblueth, 7/15/88, (PB89-189617, A04, MF-A01).

NCEER-88-0044 "SARCF User's Guide: Seismic Analysis of Reinforced Concrete Frames," by Y.S. Chung, C. Meyer and M. Shinozuka, 11/9/88, (PB89-174452, A08, MF-A01).

NCEER-88-0045 "First Expert Panel Meeting on Disaster Research and Planning," edited by J. Pantelic and J. Stoyle, 9/15/88, (PB89-174460, A05, MF-A01).

NCEER-88-0046 "Preliminary Studies of the Effect of Degrading Infill Walls on the Nonlinear Seismic Response of Steel Frames," by C.Z. Chrysostomou, P. Gergely and J.F. Abel, 12/19/88, (PB89-208383, A05, MF-A01).

NCEER-88-0047 "Reinforced Concrete Frame Component Testing Facility - Design, Construction, Instrumentation and Operation," by S.P. Pessiki, C. Conley, T. Bond, P. Gergely and R.N. White, 12/16/88, (PB89-174478, A04, MF-A01).

NCEER-89-0001 "Effects of Protective Cushion and Soil Compliancy on the Response of Equipment Within a Seismically Excited Building," by J.A. HoLung, 2/16/89, (PB89-207179, A04, MF-A01).

NCEER-89-0002 "Statistical Evaluation of Response Modification Factors for Reinforced Concrete Structures," by H.H-M. Hwang and J-W. Jaw, 2/17/89, (PB89-207187, A05, MF-A01).

NCEER-89-0003 "Hysteretic Columns Under Random Excitation," by G-Q. Cai and Y.K. Lin, 1/9/89, (PB89-196513, A03, MF-A01).

NCEER-89-0004 "Experimental Study of `Elephant Foot Bulge' Instability of Thin-Walled Metal Tanks," by Z-H. Jia and R.L. Ketter, 2/22/89, (PB89-207195, A03, MF-A01).

NCEER-89-0005 "Experiment on Performance of Buried Pipelines Across San Andreas Fault," by J. Isenberg, E. Richardson and T.D. O'Rourke, 3/10/89, (PB89-218440, A04, MF-A01). This report is available only through NTIS (see address given above).

NCEER-89-0006 "A Knowledge-Based Approach to Structural Design of Earthquake-Resistant Buildings," by M. Subramani, P. Gergely, C.H. Conley, J.F. Abel and A.H. Zaghw, 1/15/89, (PB89-218465, A06, MF-A01).

NCEER-89-0007 "Liquefaction Hazards and Their Effects on Buried Pipelines," by T.D. O'Rourke and P.A. Lane, 2/1/89, (PB89-218481, A09, MF-A01).

NCEER-89-0008 "Fundamentals of System Identification in Structural Dynamics," by H. Imai, C-B. Yun, O. Maruyama and M. Shinozuka, 1/26/89, (PB89-207211, A04, MF-A01).

NCEER-89-0009 "Effects of the 1985 Michoacan Earthquake on Water Systems and Other Buried Lifelines in Mexico," by A.G. Ayala and M.J. O'Rourke, 3/8/89, (PB89-207229, A06, MF-A01).

NCEER-89-R010 "NCEER Bibliography of Earthquake Education Materials," by K.E.K. Ross, Second Revision, 9/1/89, (PB90-125352, A05, MF-A01). This report is replaced by NCEER-92-0018.

NCEER-89-0011 "Inelastic Three-Dimensional Response Analysis of Reinforced Concrete Building Structures (IDARC-3D), Part I - Modeling," by S.K. Kunnath and A.M. Reinhorn, 4/17/89, (PB90-114612, A07, MF-A01). This report is available only through NTIS (see address given above).

NCEER-89-0012 "Recommended Modifications to ATC-14," by C.D. Poland and J.O. Malley, 4/12/89, (PB90-108648, A15, MF-A01).

NCEER-89-0013 "Repair and Strengthening of Beam-to-Column Connections Subjected to Earthquake Loading," by M. Corazao and A.J. Durrani, 2/28/89, (PB90-109885, A06, MF-A01).

NCEER-89-0014 "Program EXKAL2 for Identification of Structural Dynamic Systems," by O. Maruyama, C-B. Yun, M. Hoshiya and M. Shinozuka, 5/19/89, (PB90-109877, A09, MF-A01).

NCEER-89-0015 "Response of Frames With Bolted Semi-Rigid Connections, Part I - Experimental Study and Analytical Predictions," by P.J. DiCorso, A.M. Reinhorn, J.R. Dickerson, J.B. Radziminski and W.L. Harper, 6/1/89, to be published.

NCEER-89-0016 "ARMA Monte Carlo Simulation in Probabilistic Structural Analysis," by P.D. Spanos and M.P. Mignolet, 7/10/89, (PB90-109893, A03, MF-A01).

NCEER-89-P017 "Preliminary Proceedings from the Conference on Disaster Preparedness - The Place of Earthquake Education in Our Schools," Edited by K.E.K. Ross, 6/23/89, (PB90-108606, A03, MF-A01).

NCEER-89-0017 "Proceedings from the Conference on Disaster Preparedness - The Place of Earthquake Education in Our Schools," Edited by K.E.K. Ross, 12/31/89, (PB90-207895, A012, MF-A02). This report is available only through NTIS (see address given above).

NCEER-89-0018 "Multidimensional Models of Hysteretic Material Behavior for Vibration Analysis of Shape Memory Energy Absorbing Devices, by E.J. Graesser and F.A. Cozzarelli, 6/7/89, (PB90-164146, A04, MF-A01).

NCEER-89-0019 "Nonlinear Dynamic Analysis of Three-Dimensional Base Isolated Structures (3D-BASIS)," by S. Nagarajaiah, A.M. Reinhorn and M.C. Constantinou, 8/3/89, (PB90-161936, A06, MF-A01). This report has been replaced by NCEER-93-0011.

NCEER-89-0020 "Structural Control Considering Time-Rate of Control Forces and Control Rate Constraints," by F.Y. Cheng and C.P. Pantelides, 8/3/89, (PB90-120445, A04, MF-A01).

NCEER-89-0021 "Subsurface Conditions of Memphis and Shelby County," by K.W. Ng, T-S. Chang and H-H.M. Hwang, 7/26/89, (PB90-120437, A03, MF-A01).

NCEER-89-0022 "Seismic Wave Propagation Effects on Straight Jointed Buried Pipelines," by K. Elhmadi and M.J. O'Rourke, 8/24/89, (PB90-162322, A10, MF-A02).

NCEER-89-0023 "Workshop on Serviceability Analysis of Water Delivery Systems," edited by M. Grigoriu, 3/6/89, (PB90-127424, A03, MF-A01).

NCEER-89-0024 "Shaking Table Study of a 1/5 Scale Steel Frame Composed of Tapered Members," by K.C. Chang, J.S. Hwang and G.C. Lee, 9/18/89, (PB90-160169, A04, MF-A01).

NCEER-89-0025 "DYNA1D: A Computer Program for Nonlinear Seismic Site Response Analysis - Technical Documentation," by Jean H. Prevost, 9/14/89, (PB90-161944, A07, MF-A01). This report is available only through NTIS (see address given above).

NCEER-89-0026 "1:4 Scale Model Studies of Active Tendon Systems and Active Mass Dampers for Aseismic Protection," by A.M. Reinhorn, T.T. Soong, R.C. Lin, Y.P. Yang, Y. Fukao, H. Abe and M. Nakai, 9/15/89, (PB90-173246, A10, MF-A02). This report is available only through NTIS (see address given above).

NCEER-89-0027 "Scattering of Waves by Inclusions in a Nonhomogeneous Elastic Half Space Solved by Boundary Element Methods," by P.K. Hadley, A. Askar and A.S. Cakmak, 6/15/89, (PB90-145699, A07, MF-A01).

NCEER-89-0028 "Statistical Evaluation of Deflection Amplification Factors for Reinforced Concrete Structures," by H.H.M. Hwang, J-W. Jaw and A.L. Ch'ng, 8/31/89, (PB90-164633, A05, MF-A01).

NCEER-89-0029 "Bedrock Accelerations in Memphis Area Due to Large New Madrid Earthquakes," by H.H.M. Hwang, C.H.S. Chen and G. Yu, 11/7/89, (PB90-162330, A04, MF-A01).

NCEER-89-0030 "Seismic Behavior and Response Sensitivity of Secondary Structural Systems," by Y.Q. Chen and T.T. Soong, 10/23/89, (PB90-164658, A08, MF-A01).

NCEER-89-0031 "Random Vibration and Reliability Analysis of Primary-Secondary Structural Systems," by Y. Ibrahim, M. Grigoriu and T.T. Soong, 11/10/89, (PB90-161951, A04, MF-A01).

NCEER-89-0032 "Proceedings from the Second U.S. - Japan Workshop on Liquefaction, Large Ground Deformation and Their Effects on Lifelines, September 26-29, 1989," Edited by T.D. O'Rourke and M. Hamada, 12/1/89, (PB90-209388, A22, MF-A03).

NCEER-89-0033 "Deterministic Model for Seismic Damage Evaluation of Reinforced Concrete Structures," by J.M. Bracci, A.M. Reinhorn, J.B. Mander and S.K. Kunnath, 9/27/89, (PB91-108803, A06, MF-A01).

NCEER-89-0034 "On the Relation Between Local and Global Damage Indices," by E. DiPasquale and A.S. Cakmak, 8/15/89, (PB90-173865, A05, MF-A01).

NCEER-89-0035 "Cyclic Undrained Behavior of Nonplastic and Low Plasticity Silts," by A.J. Walker and H.E. Stewart, 7/26/89, (PB90-183518, A10, MF-A01).

NCEER-89-0036 "Liquefaction Potential of Surficial Deposits in the City of Buffalo, New York," by M. Budhu, R. Giese and L. Baumgrass, 1/17/89, (PB90-208455, A04, MF-A01).

NCEER-89-0037 "A Deterministic Assessment of Effects of Ground Motion Incoherence," by A.S. Veletsos and Y. Tang, 7/15/89, (PB90-164294, A03, MF-A01).

NCEER-89-0038 "Workshop on Ground Motion Parameters for Seismic Hazard Mapping," July 17-18, 1989, edited by R.V. Whitman, 12/1/89, (PB90-173923, A04, MF-A01).

NCEER-89-0039 "Seismic Effects on Elevated Transit Lines of the New York City Transit Authority," by C.J. Costantino, C.A. Miller and E. Heymsfield, 12/26/89, (PB90-207887, A06, MF-A01).

NCEER-89-0040 "Centrifugal Modeling of Dynamic Soil-Structure Interaction," by K. Weissman, Supervised by J.H. Prevost, 5/10/89, (PB90-207879, A07, MF-A01).

NCEER-89-0041 "Linearized Identification of Buildings With Cores for Seismic Vulnerability Assessment," by I-K. Ho and A.E. Aktan, 11/1/89, (PB90-251943, A07, MF-A01).

NCEER-90-0001 "Geotechnical and Lifeline Aspects of the October 17, 1989 Loma Prieta Earthquake in San Francisco," by T.D. O'Rourke, H.E. Stewart, F.T. Blackburn and T.S. Dickerman, 1/90, (PB90-208596, A05, MF-A01).

NCEER-90-0002 "Nonnormal Secondary Response Due to Yielding in a Primary Structure," by D.C.K. Chen and L.D. Lutes, 2/28/90, (PB90-251976, A07, MF-A01).

NCEER-90-0003 "Earthquake Education Materials for Grades K-12," by K.E.K. Ross, 4/16/90, (PB91-251984, A05, MF-A05). This report has been replaced by NCEER-92-0018.

NCEER-90-0004 "Catalog of Strong Motion Stations in Eastern North America," by R.W. Busby, 4/3/90, (PB90-251984, A05, MF-A01).

NCEER-90-0005 "NCEER Strong-Motion Data Base: A User Manual for the GeoBase Release (Version 1.0 for the Sun3)," by P. Friberg and K. Jacob, 3/31/90 (PB90-258062, A04, MF-A01).

NCEER-90-0006 "Seismic Hazard Along a Crude Oil Pipeline in the Event of an 1811-1812 Type New Madrid Earthquake," by H.H.M. Hwang and C-H.S. Chen, 4/16/90, (PB90-258054, A04, MF-A01).

NCEER-90-0007 "Site-Specific Response Spectra for Memphis Sheahan Pumping Station," by H.H.M. Hwang and C.S. Lee, 5/15/90, (PB91-108811, A05, MF-A01).

NCEER-90-0008 "Pilot Study on Seismic Vulnerability of Crude Oil Transmission Systems," by T. Ariman, R. Dobry, M. Grigoriu, F. Kozin, M. O'Rourke, T. O'Rourke and M. Shinozuka, 5/25/90, (PB91-108837, A06, MF-A01).

NCEER-90-0009 "A Program to Generate Site Dependent Time Histories: EQGEN," by G.W. Ellis, M. Srinivasan and A.S. Cakmak, 1/30/90, (PB91-108829, A04, MF-A01).

NCEER-90-0010 "Active Isolation for Seismic Protection of Operating Rooms," by M.E. Talbott, Supervised by M. Shinozuka, 6/8/9, (PB91-110205, A05, MF-A01).

NCEER-90-0011 "Program LINEARID for Identification of Linear Structural Dynamic Systems," by C-B. Yun and M. Shinozuka, 6/25/90, (PB91-110312, A08, MF-A01).

NCEER-90-0012 "Two-Dimensional Two-Phase Elasto-Plastic Seismic Response of Earth Dams," by A.N. Yiagos, Supervised by J.H. Prevost, 6/20/90, (PB91-110197, A13, MF-A02).

NCEER-90-0013 "Secondary Systems in Base-Isolated Structures: Experimental Investigation, Stochastic Response and Stochastic Sensitivity," by G.D. Manolis, G. Juhn, M.C. Constantinou and A.M. Reinhorn, 7/1/90, (PB91-110320, A08, MF-A01).

NCEER-90-0014 "Seismic Behavior of Lightly-Reinforced Concrete Column and Beam-Column Joint Details," by S.P. Pessiki, C.H. Conley, P. Gergely and R.N. White, 8/22/90, (PB91-108795, A11, MF-A02).

NCEER-90-0015 "Two Hybrid Control Systems for Building Structures Under Strong Earthquakes," by J.N. Yang and A. Danielians, 6/29/90, (PB91-125393, A04, MF-A01).

NCEER-90-0016 "Instantaneous Optimal Control with Acceleration and Velocity Feedback," by J.N. Yang and Z. Li, 6/29/90, (PB91-125401, A03, MF-A01).

NCEER-90-0017 "Reconnaissance Report on the Northern Iran Earthquake of June 21, 1990," by M. Mehrain, 10/4/90, (PB91-125377, A03, MF-A01).

NCEER-90-0018 "Evaluation of Liquefaction Potential in Memphis and Shelby County," by T.S. Chang, P.S. Tang, C.S. Lee and H. Hwang, 8/10/90, (PB91-125427, A09, MF-A01).

NCEER-90-0019 "Experimental and Analytical Study of a Combined Sliding Disc Bearing and Helical Steel Spring Isolation System," by M.C. Constantinou, A.S. Mokha and A.M. Reinhorn, 10/4/90, (PB91-125385, A06, MF-A01). This report is available only through NTIS (see address given above).

NCEER-90-0020 "Experimental Study and Analytical Prediction of Earthquake Response of a Sliding Isolation System with a Spherical Surface," by A.S. Mokha, M.C. Constantinou and A.M. Reinhorn, 10/11/90, (PB91-125419, A05, MF-A01).

NCEER-90-0021 "Dynamic Interaction Factors for Floating Pile Groups," by G. Gazetas, K. Fan, A. Kaynia and E. Kausel, 9/10/90, (PB91-170381, A05, MF-A01).

NCEER-90-0022 "Evaluation of Seismic Damage Indices for Reinforced Concrete Structures," by S. Rodriguez-Gomez and A.S. Cakmak, 9/30/90, PB91-171322, A06, MF-A01).

NCEER-90-0023 "Study of Site Response at a Selected Memphis Site," by H. Desai, S. Ahmad, E.S. Gazetas and M.R. Oh, 10/11/90, (PB91-196857, A03, MF-A01).

NCEER-90-0024 "A User's Guide to Strongmo: Version 1.0 of NCEER's Strong-Motion Data Access Tool for PCs and Terminals," by P.A. Friberg and C.A.T. Susch, 11/15/90, (PB91-171272, A03, MF-A01).

NCEER-90-0025 "A Three-Dimensional Analytical Study of Spatial Variability of Seismic Ground Motions," by L-L. Hong and A.H.-S. Ang, 10/30/90, (PB91-170399, A09, MF-A01).

NCEER-90-0026 "MUMOID User's Guide - A Program for the Identification of Modal Parameters," by S. Rodriguez-Gomez and E. DiPasquale, 9/30/90, (PB91-171298, A04, MF-A01).

NCEER-90-0027 "SARCF-II User's Guide - Seismic Analysis of Reinforced Concrete Frames," by S. Rodriguez-Gomez, Y.S. Chung and C. Meyer, 9/30/90, (PB91-171280, A05, MF-A01).

NCEER-90-0028 "Viscous Dampers: Testing, Modeling and Application in Vibration and Seismic Isolation," by N. Makris and M.C. Constantinou, 12/20/90 (PB91-190561, A06, MF-A01).

NCEER-90-0029 "Soil Effects on Earthquake Ground Motions in the Memphis Area," by H. Hwang, C.S. Lee, K.W. Ng and T.S. Chang, 8/2/90, (PB91-190751, A05, MF-A01).

NCEER-91-0001 "Proceedings from the Third Japan-U.S. Workshop on Earthquake Resistant Design of Lifeline Facilities and Countermeasures for Soil Liquefaction, December 17-19, 1990," edited by T.D. O'Rourke and M. Hamada, 2/1/91, (PB91-179259, A99, MF-A04).

NCEER-91-0002 "Physical Space Solutions of Non-Proportionally Damped Systems," by M. Tong, Z. Liang and G.C. Lee, 1/15/91, (PB91-179242, A04, MF-A01).

NCEER-91-0003 "Seismic Response of Single Piles and Pile Groups," by K. Fan and G. Gazetas, 1/10/91, (PB92-174994, A04, MF-A01).

NCEER-91-0004 "Damping of Structures: Part 1 - Theory of Complex Damping," by Z. Liang and G. Lee, 10/10/91, (PB92-197235, A12, MF-A03).

NCEER-91-0005 "3D-BASIS - Nonlinear Dynamic Analysis of Three Dimensional Base Isolated Structures: Part II," by S. Nagarajaiah, A.M. Reinhorn and M.C. Constantinou, 2/28/91, (PB91-190553, A07, MF-A01). This report has been replaced by NCEER-93-0011.

NCEER-91-0006 "A Multidimensional Hysteretic Model for Plasticity Deforming Metals in Energy Absorbing Devices," by E.J. Graesser and F.A. Cozzarelli, 4/9/91, (PB92-108364, A04, MF-A01).

NCEER-91-0007 "A Framework for Customizable Knowledge-Based Expert Systems with an Application to a KBES for Evaluating the Seismic Resistance of Existing Buildings," by E.G. Ibarra-Anaya and S.J. Fenves, 4/9/91, (PB91-210930, A08, MF-A01).

NCEER-91-0008 "Nonlinear Analysis of Steel Frames with Semi-Rigid Connections Using the Capacity Spectrum Method," by G.G. Deierlein, S-H. Hsieh, Y-J. Shen and J.F. Abel, 7/2/91, (PB92-113828, A05, MF-A01).

NCEER-91-0009 "Earthquake Education Materials for Grades K-12," by K.E.K. Ross, 4/30/91, (PB91-212142, A06, MF-A01). This report has been replaced by NCEER-92-0018.

NCEER-91-0010 "Phase Wave Velocities and Displacement Phase Differences in a Harmonically Oscillating Pile," by N. Makris and G. Gazetas, 7/8/91, (PB92-108356, A04, MF-A01).

NCEER-91-0011 "Dynamic Characteristics of a Full-Size Five-Story Steel Structure and a 2/5 Scale Model," by K.C. Chang, G.C. Yao, G.C. Lee, D.S. Hao and Y.C. Yeh," 7/2/91, (PB93-116648, A06, MF-A02).

NCEER-91-0012 "Seismic Response of a 2/5 Scale Steel Structure with Added Viscoelastic Dampers," by K.C. Chang, T.T. Soong, S-T. Oh and M.L. Lai, 5/17/91, (PB92-110816, A05, MF-A01).

NCEER-91-0013 "Earthquake Response of Retaining Walls; Full-Scale Testing and Computational Modeling," by S. Alampalli and A-W.M. Elgamal, 6/20/91, to be published.

NCEER-91-0014 "3D-BASIS-M: Nonlinear Dynamic Analysis of Multiple Building Base Isolated Structures," by P.C. Tsopelas, S. Nagarajaiah, M.C. Constantinou and A.M. Reinhorn, 5/28/91, (PB92-113885, A09, MF-A02).

NCEER-91-0015 "Evaluation of SEAOC Design Requirements for Sliding Isolated Structures," by D. Theodossiou and M.C. Constantinou, 6/10/91, (PB92-114602, A11, MF-A03).

NCEER-91-0016 "Closed-Loop Modal Testing of a 27-Story Reinforced Concrete Flat Plate-Core Building," by H.R. Somaprasad, T. Toksoy, H. Yoshiyuki and A.E. Aktan, 7/15/91, (PB92-129980, A07, MF-A02).

NCEER-91-0017 "Shake Table Test of a 1/6 Scale Two-Story Lightly Reinforced Concrete Building," by A.G. El-Attar, R.N. White and P. Gergely, 2/28/91, (PB92-222447, A06, MF-A02).

NCEER-91-0018 "Shake Table Test of a 1/8 Scale Three-Story Lightly Reinforced Concrete Building," by A.G. El-Attar, R.N. White and P. Gergely, 2/28/91, (PB93-116630, A08, MF-A02).

NCEER-91-0019 "Transfer Functions for Rigid Rectangular Foundations," by A.S. Veletsos, A.M. Prasad and W.H. Wu, 7/31/91, to be published.

NCEER-91-0020 "Hybrid Control of Seismic-Excited Nonlinear and Inelastic Structural Systems," by J.N. Yang, Z. Li and A. Danielians, 8/1/91, (PB92-143171, A06, MF-A02).

NCEER-91-0021 "The NCEER-91 Earthquake Catalog: Improved Intensity-Based Magnitudes and Recurrence Relations for U.S. Earthquakes East of New Madrid," by L. Seeber and J.G. Armbruster, 8/28/91, (PB92-176742, A06, MF-A02).

NCEER-91-0022 "Proceedings from the Implementation of Earthquake Planning and Education in Schools: The Need for Change - The Roles of the Changemakers," by K.E.K. Ross and F. Winslow, 7/23/91, (PB92-129998, A12, MF-A03).

NCEER-91-0023 "A Study of Reliability-Based Criteria for Seismic Design of Reinforced Concrete Frame Buildings," by H.H.M. Hwang and H-M. Hsu, 8/10/91, (PB92-140235, A09, MF-A02).

NCEER-91-0024 "Experimental Verification of a Number of Structural System Identification Algorithms," by R.G. Ghanem, H. Gavin and M. Shinozuka, 9/18/91, (PB92-176577, A18, MF-A04).

NCEER-91-0025 "Probabilistic Evaluation of Liquefaction Potential," by H.H.M. Hwang and C.S. Lee," 11/25/91, (PB92-143429, A05, MF-A01).

NCEER-91-0026 "Instantaneous Optimal Control for Linear, Nonlinear and Hysteretic Structures - Stable Controllers," by J.N. Yang and Z. Li, 11/15/91, (PB92-163807, A04, MF-A01).

NCEER-91-0027 "Experimental and Theoretical Study of a Sliding Isolation System for Bridges," by M.C. Constantinou, A. Kartoum, A.M. Reinhorn and P. Bradford, 11/15/91, (PB92-176973, A10, MF-A03).

NCEER-92-0001 "Case Studies of Liquefaction and Lifeline Performance During Past Earthquakes, Volume 1: Japanese Case Studies," Edited by M. Hamada and T. O'Rourke, 2/17/92, (PB92-197243, A18, MF-A04).

NCEER-92-0002 "Case Studies of Liquefaction and Lifeline Performance During Past Earthquakes, Volume 2: United States Case Studies," Edited by T. O'Rourke and M. Hamada, 2/17/92, (PB92-197250, A20, MF-A04).

NCEER-92-0003 "Issues in Earthquake Education," Edited by K. Ross, 2/3/92, (PB92-222389, A07, MF-A02).

NCEER-92-0004 "Proceedings from the First U.S. - Japan Workshop on Earthquake Protective Systems for Bridges," Edited by I.G. Buckle, 2/4/92, (PB94-142239, A99, MF-A06).

NCEER-92-0005 "Seismic Ground Motion from a Haskell-Type Source in a Multiple-Layered Half-Space," A.P. Theoharis, G. Deodatis and M. Shinozuka, 1/2/92, to be published.

NCEER-92-0006 "Proceedings from the Site Effects Workshop," Edited by R. Whitman, 2/29/92, (PB92-197201, A04, MF-A01).

NCEER-92-0007 "Engineering Evaluation of Permanent Ground Deformations Due to Seismically-Induced Liquefaction," by M.H. Baziar, R. Dobry and A-W.M. Elgamal, 3/24/92, (PB92-222421, A13, MF-A03).

NCEER-92-0008 "A Procedure for the Seismic Evaluation of Buildings in the Central and Eastern United States," by C.D. Poland and J.O. Malley, 4/2/92, (PB92-222439, A20, MF-A04).

NCEER-92-0009 "Experimental and Analytical Study of a Hybrid Isolation System Using Friction Controllable Sliding Bearings," by M.Q. Feng, S. Fujii and M. Shinozuka, 5/15/92, (PB93-150282, A06, MF-A02).

NCEER-92-0010 "Seismic Resistance of Slab-Column Connections in Existing Non-Ductile Flat-Plate Buildings," by A.J. Durrani and Y. Du, 5/18/92, (PB93-116812, A06, MF-A02).

NCEER-92-0011 "The Hysteretic and Dynamic Behavior of Brick Masonry Walls Upgraded by Ferrocement Coatings Under Cyclic Loading and Strong Simulated Ground Motion," by H. Lee and S.P. Prawel, 5/11/92, to be published.

NCEER-92-0012 "Study of Wire Rope Systems for Seismic Protection of Equipment in Buildings," by G.F. Demetriades, M.C. Constantinou and A.M. Reinhorn, 5/20/92, (PB93-116655, A08, MF-A02).

NCEER-92-0013 "Shape Memory Structural Dampers: Material Properties, Design and Seismic Testing," by P.R. Witting and F.A. Cozzarelli, 5/26/92, (PB93-116663, A05, MF-A01).

NCEER-92-0014 "Longitudinal Permanent Ground Deformation Effects on Buried Continuous Pipelines," by M.J. O'Rourke, and C. Nordberg, 6/15/92, (PB93-116671, A08, MF-A02).

NCEER-92-0015 "A Simulation Method for Stationary Gaussian Random Functions Based on the Sampling Theorem," by M. Grigoriu and S. Balopoulou, 6/11/92, (PB93-127496, A05, MF-A01).

NCEER-92-0016 "Gravity-Load-Designed Reinforced Concrete Buildings: Seismic Evaluation of Existing Construction and Detailing Strategies for Improved Seismic Resistance," by G.W. Hoffmann, S.K. Kunnath, A.M. Reinhorn and J.B. Mander, 7/15/92, (PB94-142007, A08, MF-A02).

NCEER-92-0017 "Observations on Water System and Pipeline Performance in the Limón Area of Costa Rica Due to the April 22, 1991 Earthquake," by M. O'Rourke and D. Ballantyne, 6/30/92, (PB93-126811, A06, MF-A02).

NCEER-92-0018 "Fourth Edition of Earthquake Education Materials for Grades K-12," Edited by K.E.K. Ross, 8/10/92, (PB93-114023, A07, MF-A02).

NCEER-92-0019 "Proceedings from the Fourth Japan-U.S. Workshop on Earthquake Resistant Design of Lifeline Facilities and Countermeasures for Soil Liquefaction," Edited by M. Hamada and T.D. O'Rourke, 8/12/92, (PB93-163939, A99, MF-E11).

NCEER-92-0020 "Active Bracing System: A Full Scale Implementation of Active Control," by A.M. Reinhorn, T.T. Soong, R.C. Lin, M.A. Riley, Y.P. Wang, S. Aizawa and M. Higashino, 8/14/92, (PB93-127512, A06, MF-A02).

NCEER-92-0021 "Empirical Analysis of Horizontal Ground Displacement Generated by Liquefaction-Induced Lateral Spreads," by S.F. Bartlett and T.L. Youd, 8/17/92, (PB93-188241, A06, MF-A02).

NCEER-92-0022 "IDARC Version 3.0: Inelastic Damage Analysis of Reinforced Concrete Structures," by S.K. Kunnath, A.M. Reinhorn and R.F. Lobo, 8/31/92, (PB93-227502, A07, MF-A02).

NCEER-92-0023 "A Semi-Empirical Analysis of Strong-Motion Peaks in Terms of Seismic Source, Propagation Path and Local Site Conditions, by M. Kamiyama, M.J. O'Rourke and R. Flores-Berrones, 9/9/92, (PB93-150266, A08, MF-A02).

NCEER-92-0024 "Seismic Behavior of Reinforced Concrete Frame Structures with Nonductile Details, Part I: Summary of Experimental Findings of Full Scale Beam-Column Joint Tests," by A. Beres, R.N. White and P. Gergely, 9/30/92, (PB93-227783, A05, MF-A01).

NCEER-92-0025 "Experimental Results of Repaired and Retrofitted Beam-Column Joint Tests in Lightly Reinforced Concrete Frame Buildings," by A. Beres, S. El-Borgi, R.N. White and P. Gergely, 10/29/92, (PB93-227791, A05, MF-A01).

NCEER-92-0026 "A Generalization of Optimal Control Theory: Linear and Nonlinear Structures," by J.N. Yang, Z. Li and S. Vongchavalitkul, 11/2/92, (PB93-188621, A05, MF-A01).

NCEER-92-0027 "Seismic Resistance of Reinforced Concrete Frame Structures Designed Only for Gravity Loads: Part I - Design and Properties of a One-Third Scale Model Structure," by J.M. Bracci, A.M. Reinhorn and J.B. Mander, 12/1/92, (PB94-104502, A08, MF-A02).

NCEER-92-0028 "Seismic Resistance of Reinforced Concrete Frame Structures Designed Only for Gravity Loads: Part II - Experimental Performance of Subassemblages," by L.E. Aycardi, J.B. Mander and A.M. Reinhorn, 12/1/92, (PB94-104510, A08, MF-A02).

NCEER-92-0029 "Seismic Resistance of Reinforced Concrete Frame Structures Designed Only for Gravity Loads: Part III - Experimental Performance and Analytical Study of a Structural Model," by J.M. Bracci, A.M. Reinhorn and J.B. Mander, 12/1/92, (PB93-227528, A09, MF-A01).

NCEER-92-0030 "Evaluation of Seismic Retrofit of Reinforced Concrete Frame Structures: Part I - Experimental Performance of Retrofitted Subassemblages," by D. Choudhuri, J.B. Mander and A.M. Reinhorn, 12/8/92, (PB93-198307, A07, MF-A02).

NCEER-92-0031 "Evaluation of Seismic Retrofit of Reinforced Concrete Frame Structures: Part II - Experimental Performance and Analytical Study of a Retrofitted Structural Model," by J.M. Bracci, A.M. Reinhorn and J.B. Mander, 12/8/92, (PB93-198315, A09, MF-A03).

NCEER-92-0032 "Experimental and Analytical Investigation of Seismic Response of Structures with Supplemental Fluid Viscous Dampers," by M.C. Constantinou and M.D. Symans, 12/21/92, (PB93-191435, A10, MF-A03). This report is available only through NTIS (see address given above).

NCEER-92-0033 "Reconnaissance Report on the Cairo, Egypt Earthquake of October 12, 1992," by M. Khater, 12/23/92, (PB93-188621, A03, MF-A01).

NCEER-92-0034 "Low-Level Dynamic Characteristics of Four Tall Flat-Plate Buildings in New York City," by H. Gavin, S. Yuan, J. Grossman, E. Pekelis and K. Jacob, 12/28/92, (PB93-188217, A07, MF-A02).

NCEER-93-0001 "An Experimental Study on the Seismic Performance of Brick-Infilled Steel Frames With and Without Retrofit," by J.B. Mander, B. Nair, K. Wojtkowski and J. Ma, 1/29/93, (PB93-227510, A07, MF-A02).

NCEER-93-0002 "Social Accounting for Disaster Preparedness and Recovery Planning," by S. Cole, E. Pantoja and V. Razak, 2/22/93, (PB94-142114, A12, MF-A03).

NCEER-93-0003 "Assessment of 1991 NEHRP Provisions for Nonstructural Components and Recommended Revisions," by T.T. Soong, G. Chen, Z. Wu, R-H. Zhang and M. Grigoriu, 3/1/93, (PB93-188639, A06, MF-A02).

NCEER-93-0004 "Evaluation of Static and Response Spectrum Analysis Procedures of SEAOC/UBC for Seismic Isolated Structures," by C.W. Winters and M.C. Constantinou, 3/23/93, (PB93-198299, A10, MF-A03).

NCEER-93-0005 "Earthquakes in the Northeast - Are We Ignoring the Hazard? A Workshop on Earthquake Science and Safety for Educators," edited by K.E.K. Ross, 4/2/93, (PB94-103066, A09, MF-A02).

NCEER-93-0006 "Inelastic Response of Reinforced Concrete Structures with Viscoelastic Braces," by R.F. Lobo, J.M. Bracci, K.L. Shen, A.M. Reinhorn and T.T. Soong, 4/5/93, (PB93-227486, A05, MF-A02).

NCEER-93-0007 "Seismic Testing of Installation Methods for Computers and Data Processing Equipment," by K. Kosar, T.T. Soong, K.L. Shen, J.A. HoLung and Y.K. Lin, 4/12/93, (PB93-198299, A07, MF-A02).

NCEER-93-0008 "Retrofit of Reinforced Concrete Frames Using Added Dampers," by A. Reinhorn, M. Constantinou and C. Li, to be published.

NCEER-93-0009 "Seismic Behavior and Design Guidelines for Steel Frame Structures with Added Viscoelastic Dampers," by K.C. Chang, M.L. Lai, T.T. Soong, D.S. Hao and Y.C. Yeh, 5/1/93, (PB94-141959, A07, MF-A02).

NCEER-93-0010 "Seismic Performance of Shear-Critical Reinforced Concrete Bridge Piers," by J.B. Mander, S.M. Waheed, M.T.A. Chaudhary and S.S. Chen, 5/12/93, (PB93-227494, A08, MF-A02).

NCEER-93-0011 "3D-BASIS-TABS: Computer Program for Nonlinear Dynamic Analysis of Three Dimensional Base Isolated Structures," by S. Nagarajaiah, C. Li, A.M. Reinhorn and M.C. Constantinou, 8/2/93, (PB94-141819, A09, MF-A02).

NCEER-93-0012 "Effects of Hydrocarbon Spills from an Oil Pipeline Break on Ground Water," by O.J. Helweg and H.H.M. Hwang, 8/3/93, (PB94-141942, A06, MF-A02).

NCEER-93-0013 "Simplified Procedures for Seismic Design of Nonstructural Components and Assessment of Current Code Provisions," by M.P. Singh, L.E. Suarez, E.E. Matheu and G.O. Maldonado, 8/4/93, (PB94-141827, A09, MF-A02).

NCEER-93-0014 "An Energy Approach to Seismic Analysis and Design of Secondary Systems," by G. Chen and T.T. Soong, 8/6/93, (PB94-142767, A11, MF-A03).

NCEER-93-0015 "Proceedings from School Sites: Becoming Prepared for Earthquakes - Commemorating the Third Anniversary of the Loma Prieta Earthquake," Edited by F.E. Winslow and K.E.K. Ross, 8/16/93, (PB94-154275, A16, MF-A02).

NCEER-93-0016 "Reconnaissance Report of Damage to Historic Monuments in Cairo, Egypt Following the October 12, 1992 Dahshur Earthquake," by D. Sykora, D. Look, G. Croci, E. Karaesmen and E. Karaesmen, 8/19/93, (PB94-142221, A08, MF-A02).

NCEER-93-0017 "The Island of Guam Earthquake of August 8, 1993," by S.W. Swan and S.K. Harris, 9/30/93, (PB94-141843, A04, MF-A01).

NCEER-93-0018 "Engineering Aspects of the October 12, 1992 Egyptian Earthquake," by A.W. Elgamal, M. Amer, K. Adalier and A. Abul-Fadl, 10/7/93, (PB94-141983, A05, MF-A01).

NCEER-93-0019 "Development of an Earthquake Motion Simulator and its Application in Dynamic Centrifuge Testing," by I. Krstelj, Supervised by J.H. Prevost, 10/23/93, (PB94-181773, A-10, MF-A03).

NCEER-93-0020 "NCEER-Taisei Corporation Research Program on Sliding Seismic Isolation Systems for Bridges: Experimental and Analytical Study of a Friction Pendulum System (FPS)," by M.C. Constantinou, P. Tsopelas, Y-S. Kim and S. Okamoto, 11/1/93, (PB94-142775, A08, MF-A02).

NCEER-93-0021 "Finite Element Modeling of Elastomeric Seismic Isolation Bearings," by L.J. Billings, Supervised by R. Shepherd, 11/8/93, to be published.

NCEER-93-0022 "Seismic Vulnerability of Equipment in Critical Facilities: Life-Safety and Operational Consequences," by K. Porter, G.S. Johnson, M.M. Zadeh, C. Scawthorn and S. Eder, 11/24/93, (PB94-181765, A16, MF-A03).

NCEER-93-0023 "Hokkaido Nansei-oki, Japan Earthquake of July 12, 1993, by P.I. Yanev and C.R. Scawthorn, 12/23/93, (PB94-181500, A07, MF-A01).

NCEER-94-0001 "An Evaluation of Seismic Serviceability of Water Supply Networks with Application to the San Francisco Auxiliary Water Supply System," by I. Markov, Supervised by M. Grigoriu and T. O'Rourke, 1/21/94, (PB94-204013, A07, MF-A02).

NCEER-94-0002 "NCEER-Taisei Corporation Research Program on Sliding Seismic Isolation Systems for Bridges: Experimental and Analytical Study of Systems Consisting of Sliding Bearings, Rubber Restoring Force Devices and Fluid Dampers," Volumes I and II, by P. Tsopelas, S. Okamoto, M.C. Constantinou, D. Ozaki and S. Fujii, 2/4/94, (PB94-181740, A09, MF-A02 and PB94-181757, A12, MF-A03).

NCEER-94-0003 "A Markov Model for Local and Global Damage Indices in Seismic Analysis," by S. Rahman and M. Grigoriu, 2/18/94, (PB94-206000, A12, MF-A03).

NCEER-94-0004 "Proceedings from the NCEER Workshop on Seismic Response of Masonry Infills," edited by D.P. Abrams, 3/1/94, (PB94-180783, A07, MF-A02).

NCEER-94-0005 "The Northridge, California Earthquake of January 17, 1994: General Reconnaissance Report," edited by J.D. Goltz, 3/11/94, (PB94-193943, A10, MF-A03).

NCEER-94-0006 "Seismic Energy Based Fatigue Damage Analysis of Bridge Columns: Part I - Evaluation of Seismic Capacity," by G.A. Chang and J.B. Mander, 3/14/94, (PB94-219185, A11, MF-A03).

NCEER-94-0007 "Seismic Isolation of Multi-Story Frame Structures Using Spherical Sliding Isolation Systems," by T.M. Al-Hussaini, V.A. Zayas and M.C. Constantinou, 3/17/94, (PB94-193745, A09, MF-A02).

NCEER-94-0008 "The Northridge, California Earthquake of January 17, 1994: Performance of Highway Bridges," edited by I.G. Buckle, 3/24/94, (PB94-193851, A06, MF-A02).

NCEER-94-0009 "Proceedings of the Third U.S.-Japan Workshop on Earthquake Protective Systems for Bridges," edited by I.G. Buckle and I. Friedland, 3/31/94, (PB94-195815, A99, MF-A06).

NCEER-94-0010 "3D-BASIS-ME: Computer Program for Nonlinear Dynamic Analysis of Seismically Isolated Single and Multiple Structures and Liquid Storage Tanks," by P.C. Tsopelas, M.C. Constantinou and A.M. Reinhorn, 4/12/94, (PB94-204922, A09, MF-A02).

NCEER-94-0011 "The Northridge, California Earthquake of January 17, 1994: Performance of Gas Transmission Pipelines," by T.D. O'Rourke and M.C. Palmer, 5/16/94, (PB94-204989, A05, MF-A01).

NCEER-94-0012 "Feasibility Study of Replacement Procedures and Earthquake Performance Related to Gas Transmission Pipelines," by T.D. O'Rourke and M.C. Palmer, 5/25/94, (PB94-206638, A09, MF-A02).

NCEER-94-0013 "Seismic Energy Based Fatigue Damage Analysis of Bridge Columns: Part II - Evaluation of Seismic Demand," by G.A. Chang and J.B. Mander, 6/1/94, (PB95-18106, A08, MF-A02).

NCEER-94-0014 "NCEER-Taisei Corporation Research Program on Sliding Seismic Isolation Systems for Bridges: Experimental and Analytical Study of a System Consisting of Sliding Bearings and Fluid Restoring Force/Damping Devices," by P. Tsopelas and M.C. Constantinou, 6/13/94, (PB94-219144, A10, MF-A03).

NCEER-94-0015 "Generation of Hazard-Consistent Fragility Curves for Seismic Loss Estimation Studies," by H. Hwang and J-R. Huo, 6/14/94, (PB95-181996, A09, MF-A02).

NCEER-94-0016 "Seismic Study of Building Frames with Added Energy-Absorbing Devices," by W.S. Pong, C.S. Tsai and G.C. Lee, 6/20/94, (PB94-219136, A10, A03).

NCEER-94-0017 "Sliding Mode Control for Seismic-Excited Linear and Nonlinear Civil Engineering Structures," by J. Yang, J. Wu, A. Agrawal and Z. Li, 6/21/94, (PB95-138483, A06, MF-A02).

NCEER-94-0018 "3D-BASIS-TABS Version 2.0: Computer Program for Nonlinear Dynamic Analysis of Three Dimensional Base Isolated Structures," by A.M. Reinhorn, S. Nagarajaiah, M.C. Constantinou, P. Tsopelas and R. Li, 6/22/94, (PB95-182176, A08, MF-A02).

NCEER-94-0019 "Proceedings of the International Workshop on Civil Infrastructure Systems: Application of Intelligent Systems and Advanced Materials on Bridge Systems," Edited by G.C. Lee and K.C. Chang, 7/18/94, (PB95-252474, A20, MF-A04).

NCEER-94-0020 "Study of Seismic Isolation Systems for Computer Floors," by V. Lambrou and M.C. Constantinou, 7/19/94, (PB95-138533, A10, MF-A03).

NCEER-94-0021 "Proceedings of the U.S.-Italian Workshop on Guidelines for Seismic Evaluation and Rehabilitation of Unreinforced Masonry Buildings," Edited by D.P. Abrams and G.M. Calvi, 7/20/94, (PB95-138749, A13, MF-A03).

NCEER-94-0022 "NCEER-Taisei Corporation Research Program on Sliding Seismic Isolation Systems for Bridges: Experimental and Analytical Study of a System Consisting of Lubricated PTFE Sliding Bearings and Mild Steel Dampers," by P. Tsopelas and M.C. Constantinou, 7/22/94, (PB95-182184, A08, MF-A02).

NCEER-94-0023 “Development of Reliability-Based Design Criteria for Buildings Under Seismic Load,” by Y.K. Wen, H. Hwang and M. Shinozuka, 8/1/94, (PB95-211934, A08, MF-A02).

NCEER-94-0024 “Experimental Verification of Acceleration Feedback Control Strategies for an Active Tendon System,” by S.J. Dyke, B.F. Spencer, Jr., P. Quast, M.K. Sain, D.C. Kaspari, Jr. and T.T. Soong, 8/29/94, (PB95-212320, A05, MF-A01).

NCEER-94-0025 “Seismic Retrofitting Manual for Highway Bridges,” Edited by I.G. Buckle and I.F. Friedland, published by the Federal Highway Administration (PB95-212676, A15, MF-A03).

NCEER-94-0026 “Proceedings from the Fifth U.S.-Japan Workshop on Earthquake Resistant Design of Lifeline Facilities and Countermeasures Against Soil Liquefaction,” Edited by T.D. O’Rourke and M. Hamada, 11/7/94, (PB95-220802, A99, MF-E08).

NCEER-95-0001 "Experimental and Analytical Investigation of Seismic Retrofit of Structures with Supplemental Damping: Part 1 - Fluid Viscous Damping Devices," by A.M. Reinhorn, C. Li and M.C. Constantinou, 1/3/95, (PB95-266599, A09, MF-A02).

NCEER-95-0002 "Experimental and Analytical Study of Low-Cycle Fatigue Behavior of Semi-Rigid Top-And-Seat Angle Connections," by G. Pekcan, J.B. Mander and S.S. Chen, 1/5/95, (PB95-220042, A07, MF-A02).

NCEER-95-0003 "NCEER-ATC Joint Study on Fragility of Buildings," by T. Anagnos, C. Rojahn and A.S. Kiremidjian, 1/20/95, (PB95-220026, A06, MF-A02).

NCEER-95-0004 "Nonlinear Control Algorithms for Peak Response Reduction," by Z. Wu, T.T. Soong, V. Gattulli and R.C. Lin, 2/16/95, (PB95-220349, A05, MF-A01).

NCEER-95-0005 "Pipeline Replacement Feasibility Study: A Methodology for Minimizing Seismic and Corrosion Risks to Underground Natural Gas Pipelines," by R.T. Eguchi, H.A. Seligson and D.G. Honegger, 3/2/95, (PB95-252326, A06, MF-A02).

NCEER-95-0006 "Evaluation of Seismic Performance of an 11-Story Frame Building During the 1994 Northridge Earthquake," by F. Naeim, R. DiSulio, K. Benuska, A. Reinhorn and C. Li, to be published.

NCEER-95-0007 "Prioritization of Bridges for Seismic Retrofitting," by N. Basöz and A.S. Kiremidjian, 4/24/95, (PB95-252300, A08, MF-A02).

NCEER-95-0008 "Method for Developing Motion Damage Relationships for Reinforced Concrete Frames," by A. Singhal and A.S. Kiremidjian, 5/11/95, (PB95-266607, A06, MF-A02).

NCEER-95-0009 "Experimental and Analytical Investigation of Seismic Retrofit of Structures with Supplemental Damping: Part II - Friction Devices," by C. Li and A.M. Reinhorn, 7/6/95, (PB96-128087, A11, MF-A03).

NCEER-95-0010 "Experimental Performance and Analytical Study of a Non-Ductile Reinforced Concrete Frame Structure Retrofitted with Elastomeric Spring Dampers," by G. Pekcan, J.B. Mander and S.S. Chen, 7/14/95, (PB96-137161, A08, MF-A02).

NCEER-95-0011 "Development and Experimental Study of Semi-Active Fluid Damping Devices for Seismic Protection of Structures," by M.D. Symans and M.C. Constantinou, 8/3/95, (PB96-136940, A23, MF-A04).

NCEER-95-0012 "Real-Time Structural Parameter Modification (RSPM): Development of Innervated Structures," by Z. Liang, M. Tong and G.C. Lee, 4/11/95, (PB96-137153, A06, MF-A01).

NCEER-95-0013 "Experimental and Analytical Investigation of Seismic Retrofit of Structures with Supplemental Damping: Part III - Viscous Damping Walls," by A.M. Reinhorn and C. Li, 10/1/95, (PB96-176409, A11, MF-A03).

NCEER-95-0014 "Seismic Fragility Analysis of Equipment and Structures in a Memphis Electric Substation," by J-R. Huo and H.H.M. Hwang, 8/10/95, (PB96-128087, A09, MF-A02).

NCEER-95-0015 "The Hanshin-Awaji Earthquake of January 17, 1995: Performance of Lifelines," Edited by M. Shinozuka, 11/3/95, (PB96-176383, A15, MF-A03).

NCEER-95-0016 "Highway Culvert Performance During Earthquakes," by T.L. Youd and C.J. Beckman, available as NCEER-96-0015.

NCEER-95-0017 "The Hanshin-Awaji Earthquake of January 17, 1995: Performance of Highway Bridges," Edited by I.G. Buckle, 12/1/95, to be published.

NCEER-95-0018 "Modeling of Masonry Infill Panels for Structural Analysis," by A.M. Reinhorn, A. Madan, R.E. Valles, Y. Reichmann and J.B. Mander, 12/8/95, (PB97-110886, MF-A01, A06).

NCEER-95-0019 "Optimal Polynomial Control for Linear and Nonlinear Structures," by A.K. Agrawal and J.N. Yang, 12/11/95, (PB96-168737, A07, MF-A02).

NCEER-95-0020 "Retrofit of Non-Ductile Reinforced Concrete Frames Using Friction Dampers," by R.S. Rao, P. Gergely and R.N. White, 12/22/95, (PB97-133508, A10, MF-A02).

NCEER-95-0021 "Parametric Results for Seismic Response of Pile-Supported Bridge Bents," by G. Mylonakis, A. Nikolaou and G. Gazetas, 12/22/95, (PB97-100242, A12, MF-A03).

NCEER-95-0022 "Kinematic Bending Moments in Seismically Stressed Piles," by A. Nikolaou, G. Mylonakis and G. Gazetas, 12/23/95, (PB97-113914, MF-A03, A13).

NCEER-96-0001 "Dynamic Response of Unreinforced Masonry Buildings with Flexible Diaphragms," by A.C. Costley and D.P. Abrams," 10/10/96, (PB97-133573, MF-A03, A15).

NCEER-96-0002 "State of the Art Review: Foundations and Retaining Structures," by I. Po Lam, to be published.

NCEER-96-0003 "Ductility of Rectangular Reinforced Concrete Bridge Columns with Moderate Confinement," by N. Wehbe, M. Saiidi, D. Sanders and B. Douglas, 11/7/96, (PB97-133557, A06, MF-A02).

NCEER-96-0004 "Proceedings of the Long-Span Bridge Seismic Research Workshop," edited by I.G. Buckle and I.M. Friedland, to be published.

NCEER-96-0005 "Establish Representative Pier Types for Comprehensive Study: Eastern United States," by J. Kulicki and Z. Prucz, 5/28/96, (PB98-119217, A07, MF-A02).

NCEER-96-0006 "Establish Representative Pier Types for Comprehensive Study: Western United States," by R. Imbsen, R.A. Schamber and T.A. Osterkamp, 5/28/96, (PB98-118607, A07, MF-A02).

NCEER-96-0007 "Nonlinear Control Techniques for Dynamical Systems with Uncertain Parameters," by R.G. Ghanem and M.I. Bujakov, 5/27/96, (PB97-100259, A17, MF-A03).

NCEER-96-0008 "Seismic Evaluation of a 30-Year Old Non-Ductile Highway Bridge Pier and Its Retrofit," by J.B. Mander, B. Mahmoodzadegan, S. Bhadra and S.S. Chen, 5/31/96, (PB97-110902, MF-A03, A10).

NCEER-96-0009 "Seismic Performance of a Model Reinforced Concrete Bridge Pier Before and After Retrofit," by J.B. Mander, J.H. Kim and C.A. Ligozio, 5/31/96, (PB97-110910, MF-A02, A10).

NCEER-96-0010 "IDARC2D Version 4.0: A Computer Program for the Inelastic Damage Analysis of Buildings," by R.E. Valles, A.M. Reinhorn, S.K. Kunnath, C. Li and A. Madan, 6/3/96, (PB97-100234, A17, MF-A03).

NCEER-96-0011 "Estimation of the Economic Impact of Multiple Lifeline Disruption: Memphis Light, Gas and Water Division Case Study," by S.E. Chang, H.A. Seligson and R.T. Eguchi, 8/16/96, (PB97-133490, A11, MF-A03).

NCEER-96-0012 "Proceedings from the Sixth Japan-U.S. Workshop on Earthquake Resistant Design of Lifeline Facilities and Countermeasures Against Soil Liquefaction, Edited by M. Hamada and T. O'Rourke, 9/11/96, (PB97-133581, A99, MF-A06).

NCEER-96-0013 "Chemical Hazards, Mitigation and Preparedness in Areas of High Seismic Risk: A Methodology for Estimating the Risk of Post-Earthquake Hazardous Materials Release," by H.A. Seligson, R.T. Eguchi, K.J. Tierney and K. Richmond, 11/7/96, (PB97-133565, MF-A02, A08).

NCEER-96-0014 "Response of Steel Bridge Bearings to Reversed Cyclic Loading," by J.B. Mander, D-K. Kim, S.S. Chen and G.J. Premus, 11/13/96, (PB97-140735, A12, MF-A03).

NCEER-96-0015 "Highway Culvert Performance During Past Earthquakes," by T.L. Youd and C.J. Beckman, 11/25/96, (PB97-133532, A06, MF-A01).

NCEER-97-0001 "Evaluation, Prevention and Mitigation of Pounding Effects in Building Structures," by R.E. Valles and A.M. Reinhorn, 2/20/97, (PB97-159552, A14, MF-A03).

NCEER-97-0002 "Seismic Design Criteria for Bridges and Other Highway Structures," by C. Rojahn, R. Mayes, D.G. Anderson, J. Clark, J.H. Hom, R.V. Nutt and M.J. O'Rourke, 4/30/97, (PB97-194658, A06, MF-A03).

NCEER-97-0003 “Proceedings of the U.S.-Italian Workshop on Seismic Evaluation and Retrofit,” Edited by D.P. Abrams and G.M. Calvi, 3/19/97, (PB97-194666, A13, MF-A03).

NCEER-97-0004 "Investigation of Seismic Response of Buildings with Linear and Nonlinear Fluid Viscous Dampers," by A.A. Seleemah and M.C. Constantinou, 5/21/97, (PB98-109002, A15, MF-A03).

NCEER-97-0005 "Proceedings of the Workshop on Earthquake Engineering Frontiers in Transportation Facilities," edited by G.C. Lee and I.M. Friedland, 8/29/97, (PB98-128911, A25, MR-A04).

NCEER-97-0006 "Cumulative Seismic Damage of Reinforced Concrete Bridge Piers," by S.K. Kunnath, A. El-Bahy, A. Taylor and W. Stone, 9/2/97, (PB98-108814, A11, MF-A03).

NCEER-97-0007 "Structural Details to Accommodate Seismic Movements of Highway Bridges and Retaining Walls," by R.A. Imbsen, R.A. Schamber, E. Thorkildsen, A. Kartoum, B.T. Martin, T.N. Rosser and J.M. Kulicki, 9/3/97, (PB98-108996, A09, MF-A02).

NCEER-97-0008 "A Method for Earthquake Motion-Damage Relationships with Application to Reinforced Concrete Frames," by A. Singhal and A.S. Kiremidjian, 9/10/97, (PB98-108988, A13, MF-A03).

NCEER-97-0009 "Seismic Analysis and Design of Bridge Abutments Considering Sliding and Rotation," by K. Fishman and R. Richards, Jr., 9/15/97, (PB98-108897, A06, MF-A02).

NCEER-97-0010 "Proceedings of the FHWA/NCEER Workshop on the National Representation of Seismic Ground Motion for New and Existing Highway Facilities," edited by I.M. Friedland, M.S. Power and R.L. Mayes, 9/22/97, (PB98-128903, A21, MF-A04).

NCEER-97-0011 "Seismic Analysis for Design or Retrofit of Gravity Bridge Abutments," by K.L. Fishman, R. Richards, Jr. and R.C. Divito, 10/2/97, (PB98-128937, A08, MF-A02).

NCEER-97-0012 "Evaluation of Simplified Methods of Analysis for Yielding Structures," by P. Tsopelas, M.C. Constantinou, C.A. Kircher and A.S. Whittaker, 10/31/97, (PB98-128929, A10, MF-A03).

NCEER-97-0013 "Seismic Design of Bridge Columns Based on Control and Repairability of Damage," by C-T. Cheng and J.B. Mander, 12/8/97, (PB98-144249, A11, MF-A03).

NCEER-97-0014 "Seismic Resistance of Bridge Piers Based on Damage Avoidance Design," by J.B. Mander and C-T. Cheng, 12/10/97, (PB98-144223, A09, MF-A02).

NCEER-97-0015 “Seismic Response of Nominally Symmetric Systems with Strength Uncertainty,” by S. Balopoulou and M. Grigoriu, 12/23/97, (PB98-153422, A11, MF-A03).

NCEER-97-0016 “Evaluation of Seismic Retrofit Methods for Reinforced Concrete Bridge Columns,” by T.J. Wipf, F.W. Klaiber and F.M. Russo, 12/28/97, (PB98-144215, A12, MF-A03).

NCEER-97-0017 “Seismic Fragility of Existing Conventional Reinforced Concrete Highway Bridges,” by C.L. Mullen and A.S. Cakmak, 12/30/97, (PB98-153406, A08, MF-A02).

NCEER-97-0018 “Loss Asssessment of Memphis Buildings,” edited by D.P. Abrams and M. Shinozuka, 12/31/97, (PB98-144231, A13, MF-A03).

NCEER-97-0019 “Seismic Evaluation of Frames with Infill Walls Using Quasi-static Experiments,” by K.M. Mosalam, R.N. White and P. Gergely, 12/31/97, (PB98-153455, A07, MF-A02).

NCEER-97-0020 “Seismic Evaluation of Frames with Infill Walls Using Pseudo-dynamic Experiments,” by K.M. Mosalam, R.N. White and P. Gergely, 12/31/97, (PB98-153430, A07, MF-A02).

NCEER-97-0021 “Computational Strategies for Frames with Infill Walls: Discrete and Smeared Crack Analyses and Seismic Fragility,” by K.M. Mosalam, R.N. White and P. Gergely, 12/31/97, (PB98-153414, A10, MF-A02).

NCEER-97-0022 "Proceedings of the NCEER Workshop on Evaluation of Liquefaction Resistance of Soils," edited by T.L. Youd and I.M. Idriss, 12/31/97, (PB98-155617, A15, MF-A03).

MCEER-98-0001 "Extraction of Nonlinear Hysteretic Properties of Seismically Isolated Bridges from Quick-Release Field Tests," by Q. Chen, B.M. Douglas, E.M. Maragakis and I.G. Buckle, 5/26/98, (PB99-118838, A06, MF-A01).

MCEER-98-0002 "Methodologies for Evaluating the Importance of Highway Bridges," by A. Thomas, S. Eshenaur and J. Kulicki, 5/29/98, (PB99-118846, A10, MF-A02).

MCEER-98-0003 "Capacity Design of Bridge Piers and the Analysis of Overstrength," by J.B. Mander, A. Dutta and P. Goel, 6/1/98, (PB99-118853, A09, MF-A02).

MCEER-98-0004 "Evaluation of Bridge Damage Data from the Loma Prieta and Northridge, California Earthquakes," by N. Basoz and A. Kiremidjian, 6/2/98, (PB99-118861, A15, MF-A03).

MCEER-98-0005 "Screening Guide for Rapid Assessment of Liquefaction Hazard at Highway Bridge Sites," by T. L. Youd, 6/16/98, (PB99-118879, A06, not available on microfiche).

MCEER-98-0006 "Structural Steel and Steel/Concrete Interface Details for Bridges," by P. Ritchie, N. Kauhl and J. Kulicki, 7/13/98, (PB99-118945, A06, MF-A01).

MCEER-98-0007 "Capacity Design and Fatigue Analysis of Confined Concrete Columns," by A. Dutta and J.B. Mander, 7/14/98, (PB99-118960, A14, MF-A03).

MCEER-98-0008 "Proceedings of the Workshop on Performance Criteria for Telecommunication Services Under Earthquake Conditions," edited by A.J. Schiff, 7/15/98, (PB99-118952, A08, MF-A02).

MCEER-98-0009 "Fatigue Analysis of Unconfined Concrete Columns," by J.B. Mander, A. Dutta and J.H. Kim, 9/12/98, (PB99-123655, A10, MF-A02).

MCEER-98-0010 "Centrifuge Modeling of Cyclic Lateral Response of Pile-Cap Systems and Seat-Type Abutments in Dry Sands," by A.D. Gadre and R. Dobry, 10/2/98, (PB99-123606, A13, MF-A03).

MCEER-98-0011 "IDARC-BRIDGE: A Computational Platform for Seismic Damage Assessment of Bridge Structures," by A.M. Reinhorn, V. Simeonov, G. Mylonakis and Y. Reichman, 10/2/98, (PB99-162919, A15, MF-A03).

MCEER-98-0012 "Experimental Investigation of the Dynamic Response of Two Bridges Before and After Retrofitting with Elastomeric Bearings," by D.A. Wendichansky, S.S. Chen and J.B. Mander, 10/2/98, (PB99-162927, A15, MF-A03).

MCEER-98-0013 "Design Procedures for Hinge Restrainers and Hinge Sear Width for Multiple-Frame Bridges," by R. Des Roches and G.L. Fenves, 11/3/98, (PB99-140477, A13, MF-A03).

MCEER-98-0014 "Response Modification Factors for Seismically Isolated Bridges," by M.C. Constantinou and J.K. Quarshie, 11/3/98, (PB99-140485, A14, MF-A03).

MCEER-98-0015 "Proceedings of the U.S.-Italy Workshop on Seismic Protective Systems for Bridges," edited by I.M. Friedland and M.C. Constantinou, 11/3/98, (PB2000-101711, A22, MF-A04).

MCEER-98-0016 "Appropriate Seismic Reliability for Critical Equipment Systems: Recommendations Based on Regional Analysis of Financial and Life Loss," by K. Porter, C. Scawthorn, C. Taylor and N. Blais, 11/10/98, (PB99-157265, A08, MF-A02).

MCEER-98-0017 "Proceedings of the U.S. Japan Joint Seminar on Civil Infrastructure Systems Research," edited by M. Shinozuka and A. Rose, 11/12/98, (PB99-156713, A16, MF-A03).

MCEER-98-0018 "Modeling of Pile Footings and Drilled Shafts for Seismic Design," by I. PoLam, M. Kapuskar and D. Chaudhuri, 12/21/98, (PB99-157257, A09, MF-A02).

MCEER-99-0001 "Seismic Evaluation of a Masonry Infilled Reinforced Concrete Frame by Pseudodynamic Testing," by S.G. Buonopane and R.N. White, 2/16/99, (PB99-162851, A09, MF-A02).

MCEER-99-0002 "Response History Analysis of Structures with Seismic Isolation and Energy Dissipation Systems: Verification Examples for Program SAP2000," by J. Scheller and M.C. Constantinou, 2/22/99, (PB99-162869, A08, MF-A02).

MCEER-99-0003 "Experimental Study on the Seismic Design and Retrofit of Bridge Columns Including Axial Load Effects," by A. Dutta, T. Kokorina and J.B. Mander, 2/22/99, (PB99-162877, A09, MF-A02).

MCEER-99-0004 "Experimental Study of Bridge Elastomeric and Other Isolation and Energy Dissipation Systems with Emphasis on Uplift Prevention and High Velocity Near-source Seismic Excitation," by A. Kasalanati and M. C. Constantinou, 2/26/99, (PB99-162885, A12, MF-A03).

MCEER-99-0005 "Truss Modeling of Reinforced Concrete Shear-flexure Behavior," by J.H. Kim and J.B. Mander, 3/8/99, (PB99-163693, A12, MF-A03).

MCEER-99-0006 "Experimental Investigation and Computational Modeling of Seismic Response of a 1:4 Scale Model Steel Structure with a Load Balancing Supplemental Damping System," by G. Pekcan, J.B. Mander and S.S. Chen, 4/2/99, (PB99-162893, A11, MF-A03).

MCEER-99-0007 "Effect of Vertical Ground Motions on the Structural Response of Highway Bridges," by M.R. Button, C.J. Cronin and R.L. Mayes, 4/10/99, (PB2000-101411, A10, MF-A03).

MCEER-99-0008 "Seismic Reliability Assessment of Critical Facilities: A Handbook, Supporting Documentation, and Model Code Provisions," by G.S. Johnson, R.E. Sheppard, M.D. Quilici, S.J. Eder and C.R. Scawthorn, 4/12/99, (PB2000-101701, A18, MF-A04).

MCEER-99-0009 "Impact Assessment of Selected MCEER Highway Project Research on the Seismic Design of Highway Structures," by C. Rojahn, R. Mayes, D.G. Anderson, J.H. Clark, D'Appolonia Engineering, S. Gloyd and R.V. Nutt, 4/14/99, (PB99-162901, A10, MF-A02).

MCEER-99-0010 "Site Factors and Site Categories in Seismic Codes," by R. Dobry, R. Ramos and M.S. Power, 7/19/99, (PB2000-101705, A08, MF-A02).

MCEER-99-0011 "Restrainer Design Procedures for Multi-Span Simply-Supported Bridges," by M.J. Randall, M. Saiidi, E. Maragakis and T. Isakovic, 7/20/99, (PB2000-101702, A10, MF-A02).

MCEER-99-0012 "Property Modification Factors for Seismic Isolation Bearings," by M.C. Constantinou, P. Tsopelas, A. Kasalanati and E. Wolff, 7/20/99, (PB2000-103387, A11, MF-A03).

MCEER-99-0013 "Critical Seismic Issues for Existing Steel Bridges," by P. Ritchie, N. Kauhl and J. Kulicki, 7/20/99, (PB2000-101697, A09, MF-A02).

MCEER-99-0014 "Nonstructural Damage Database," by A. Kao, T.T. Soong and A. Vender, 7/24/99, (PB2000-101407, A06, MF-A01).

MCEER-99-0015 "Guide to Remedial Measures for Liquefaction Mitigation at Existing Highway Bridge Sites," by H.G. Cooke and J. K. Mitchell, 7/26/99, (PB2000-101703, A11, MF-A03).

MCEER-99-0016 "Proceedings of the MCEER Workshop on Ground Motion Methodologies for the Eastern United States," edited by N. Abrahamson and A. Becker, 8/11/99, (PB2000-103385, A07, MF-A02).

MCEER-99-0017 "Quindío, Colombia Earthquake of January 25, 1999: Reconnaissance Report," by A.P. Asfura and P.J. Flores, 10/4/99, (PB2000-106893, A06, MF-A01).

MCEER-99-0018 "Hysteretic Models for Cyclic Behavior of Deteriorating Inelastic Structures," by M.V. Sivaselvan and A.M. Reinhorn, 11/5/99, (PB2000-103386, A08, MF-A02).

MCEER-99-0019 "Proceedings of the 7th U.S.- Japan Workshop on Earthquake Resistant Design of Lifeline Facilities and Countermeasures Against Soil Liquefaction," edited by T.D. O'Rourke, J.P. Bardet and M. Hamada, 11/19/99, (PB2000-103354, A99, MF-A06).

MCEER-99-0020 "Development of Measurement Capability for Micro-Vibration Evaluations with Application to Chip Fabrication Facilities," by G.C. Lee, Z. Liang, J.W. Song, J.D. Shen and W.C. Liu, 12/1/99, (PB2000-105993, A08, MF-A02).

MCEER-99-0021 "Design and Retrofit Methodology for Building Structures with Supplemental Energy Dissipating Systems," by G. Pekcan, J.B. Mander and S.S. Chen, 12/31/99, (PB2000-105994, A11, MF-A03).

MCEER-00-0001 "The Marmara, Turkey Earthquake of August 17, 1999: Reconnaissance Report," edited by C. Scawthorn; with major contributions by M. Bruneau, R. Eguchi, T. Holzer, G. Johnson, J. Mander, J. Mitchell, W. Mitchell, A. Papageorgiou, C. Scaethorn, and G. Webb, 3/23/00, (PB2000-106200, A11, MF-A03).

MCEER-00-0002 "Proceedings of the MCEER Workshop for Seismic Hazard Mitigation of Health Care Facilities," edited by G.C. Lee, M. Ettouney, M. Grigoriu, J. Hauer and J. Nigg, 3/29/00, (PB2000-106892, A08, MF-A02).

MCEER-00-0003 "The Chi-Chi, Taiwan Earthquake of September 21, 1999: Reconnaissance Report," edited by G.C. Lee and C.H. Loh, with major contributions by G.C. Lee, M. Bruneau, I.G. Buckle, S.E. Chang, P.J. Flores, T.D. O'Rourke, M. Shinozuka, T.T. Soong, C-H. Loh, K-C. Chang, Z-J. Chen, J-S. Hwang, M-L. Lin, G-Y. Liu, K-C. Tsai, G.C. Yao and C-L. Yen, 4/30/00, (PB2001-100980, A10, MF-A02).

MCEER-00-0004 "Seismic Retrofit of End-Sway Frames of Steel Deck-Truss Bridges with a Supplemental Tendon System: Experimental and Analytical Investigation," by G. Pekcan, J.B. Mander and S.S. Chen, 7/1/00, (PB2001-100982, A10, MF-A02).

MCEER-00-0005 "Sliding Fragility of Unrestrained Equipment in Critical Facilities," by W.H. Chong and T.T. Soong, 7/5/00, (PB2001-100983, A08, MF-A02).

MCEER-00-0006 "Seismic Response of Reinforced Concrete Bridge Pier Walls in the Weak Direction," by N. Abo-Shadi, M. Saiidi and D. Sanders, 7/17/00, (PB2001-100981, A17, MF-A03).

MCEER-00-0007 "Low-Cycle Fatigue Behavior of Longitudinal Reinforcement in Reinforced Concrete Bridge Columns," by J. Brown and S.K. Kunnath, 7/23/00, (PB2001-104392, A08, MF-A02).

MCEER-00-0008 "Soil Structure Interaction of Bridges for Seismic Analysis," I. PoLam and H. Law, 9/25/00, (PB2001-105397, A08, MF-A02).

MCEER-00-0009 "Proceedings of the First MCEER Workshop on Mitigation of Earthquake Disaster by Advanced Technologies (MEDAT-1), edited by M. Shinozuka, D.J. Inman and T.D. O'Rourke, 11/10/00, (PB2001-105399, A14, MF-A03).

MCEER-00-0010 "Development and Evaluation of Simplified Procedures for Analysis and Design of Buildings with Passive Energy Dissipation Systems, Revision 01," by O.M. Ramirez, M.C. Constantinou, C.A. Kircher, A.S. Whittaker, M.W. Johnson, J.D. Gomez and C. Chrysostomou, 11/16/01, (PB2001-105523, A23, MF-A04).

MCEER-00-0011 "Dynamic Soil-Foundation-Structure Interaction Analyses of Large Caissons," by C-Y. Chang, C-M. Mok, Z-L. Wang, R. Settgast, F. Waggoner, M.A. Ketchum, H.M. Gonnermann and C-C. Chin, 12/30/00, (PB2001-104373, A07, MF-A02).

MCEER-00-0012 "Experimental Evaluation of Seismic Performance of Bridge Restrainers," by A.G. Vlassis, E.M. Maragakis and M. Saiid Saiidi, 12/30/00, (PB2001-104354, A09, MF-A02).

MCEER-00-0013 "Effect of Spatial Variation of Ground Motion on Highway Structures," by M. Shinozuka, V. Saxena and G. Deodatis, 12/31/00, (PB2001-108755, A13, MF-A03).

MCEER-00-0014 "A Risk-Based Methodology for Assessing the Seismic Performance of Highway Systems," by S.D. Werner, C.E. Taylor, J.E. Moore, II, J.S. Walton and S. Cho, 12/31/00, (PB2001-108756, A14, MF-A03).

MCEER-01-0001 "Experimental Investigation of P-Delta Effects to Collapse During Earthquakes," by D. Vian and M. Bruneau, 6/25/01, (PB2002-100534, A17, MF-A03).

MCEER-01-0002 "Proceedings of the Second MCEER Workshop on Mitigation of Earthquake Disaster by Advanced Technologies (MEDAT-2)," edited by M. Bruneau and D.J. Inman, 7/23/01, (PB2002-100434, A16, MF-A03).

MCEER-01-0003 "Sensitivity Analysis of Dynamic Systems Subjected to Seismic Loads," by C. Roth and M. Grigoriu, 9/18/01, (PB2003-100884, A12, MF-A03).

MCEER-01-0004 "Overcoming Obstacles to Implementing Earthquake Hazard Mitigation Policies: Stage 1 Report," by D.J. Alesch and W.J. Petak, 12/17/01, (PB2002-107949, A07, MF-A02).

MCEER-01-0005 "Updating Real-Time Earthquake Loss Estimates: Methods, Problems and Insights," by C.E. Taylor, S.E. Chang and R.T. Eguchi, 12/17/01, (PB2002-107948, A05, MF-A01).

MCEER-01-0006 "Experimental Investigation and Retrofit of Steel Pile Foundations and Pile Bents Under Cyclic Lateral Loadings," by A. Shama, J. Mander, B. Blabac and S. Chen, 12/31/01, (PB2002-107950, A13, MF-A03).

MCEER-02-0001 "Assessment of Performance of Bolu Viaduct in the 1999 Duzce Earthquake in Turkey" by P.C. Roussis, M.C. Constantinou, M. Erdik, E. Durukal and M. Dicleli, 5/8/02, (PB2003-100883, A08, MF-A02).

MCEER-02-0002 "Seismic Behavior of Rail Counterweight Systems of Elevators in Buildings," by M.P. Singh, Rildova and L.E. Suarez, 5/27/02. (PB2003-100882, A11, MF-A03).

MCEER-02-0003 "Development of Analysis and Design Procedures for Spread Footings," by G. Mylonakis, G. Gazetas, S. Nikolaou and A. Chauncey, 10/02/02, (PB2004-101636, A13, MF-A03, CD-A13).

MCEER-02-0004 "Bare-Earth Algorithms for Use with SAR and LIDAR Digital Elevation Models," by C.K. Huyck, R.T. Eguchi and B. Houshmand, 10/16/02, (PB2004-101637, A07, CD-A07).

MCEER-02-0005 "Review of Energy Dissipation of Compression Members in Concentrically Braced Frames," by K.Lee and M. Bruneau, 10/18/02, (PB2004-101638, A10, CD-A10).

MCEER-03-0001 "Experimental Investigation of Light-Gauge Steel Plate Shear Walls for the Seismic Retrofit of Buildings" by J. Berman and M. Bruneau, 5/2/03, (PB2004-101622, A10, MF-A03, CD-A10).

MCEER-03-0002 "Statistical Analysis of Fragility Curves," by M. Shinozuka, M.Q. Feng, H. Kim, T. Uzawa and T. Ueda, 6/16/03, (PB2004-101849, A09, CD-A09).

MCEER-03-0003 "Proceedings of the Eighth U.S.-Japan Workshop on Earthquake Resistant Design f Lifeline Facilities and Countermeasures Against Liquefaction," edited by M. Hamada, J.P. Bardet and T.D. O'Rourke, 6/30/03, (PB2004-104386, A99, CD-A99).

MCEER-03-0004 "Proceedings of the PRC-US Workshop on Seismic Analysis and Design of Special Bridges," edited by L.C. Fan and G.C. Lee, 7/15/03, (PB2004-104387, A14, CD-A14).

MCEER-03-0005 "Urban Disaster Recovery: A Framework and Simulation Model," by S.B. Miles and S.E. Chang, 7/25/03, (PB2004-104388, A07, CD-A07).

MCEER-03-0006 "Behavior of Underground Piping Joints Due to Static and Dynamic Loading," by R.D. Meis, M. Maragakis and R. Siddharthan, 11/17/03, (PB2005-102194, A13, MF-A03, CD-A00).

MCEER-04-0001 "Experimental Study of Seismic Isolation Systems with Emphasis on Secondary System Response and Verification of Accuracy of Dynamic Response History Analysis Methods," by E. Wolff and M. Constantinou, 1/16/04 (PB2005-102195, A99, MF-E08, CD-A00).

MCEER-04-0002 "Tension, Compression and Cyclic Testing of Engineered Cementitious Composite Materials," by K. Kesner and S.L. Billington, 3/1/04, (PB2005-102196, A08, CD-A08).

MCEER-04-0003 "Cyclic Testing of Braces Laterally Restrained by Steel Studs to Enhance Performance During Earthquakes," by O.C. Celik, J.W. Berman and M. Bruneau, 3/16/04, (PB2005-102197, A13, MF-A03, CD-A00).

MCEER-04-0004 "Methodologies for Post Earthquake Building Damage Detection Using SAR and Optical Remote Sensing: Application to the August 17, 1999 Marmara, Turkey Earthquake," by C.K. Huyck, B.J. Adams, S. Cho, R.T. Eguchi, B. Mansouri and B. Houshmand, 6/15/04, (PB2005-104888, A10, CD-A00).

MCEER-04-0005 "Nonlinear Structural Analysis Towards Collapse Simulation: A Dynamical Systems Approach," by M.V. Sivaselvan and A.M. Reinhorn, 6/16/04, (PB2005-104889, A11, MF-A03, CD-A00).

MCEER-04-0006 "Proceedings of the Second PRC-US Workshop on Seismic Analysis and Design of Special Bridges," edited by G.C. Lee and L.C. Fan, 6/25/04, (PB2005-104890, A16, CD-A00).

MCEER-04-0007 "Seismic Vulnerability Evaluation of Axially Loaded Steel Built-up Laced Members," by K. Lee and M. Bruneau, 6/30/04, (PB2005-104891, A16, CD-A00).

MCEER-04-0008 "Evaluation of Accuracy of Simplified Methods of Analysis and Design of Buildings with Damping Systems for Near-Fault and for Soft-Soil Seismic Motions," by E.A. Pavlou and M.C. Constantinou, 8/16/04, (PB2005-104892, A08, MF-A02, CD-A00).

MCEER-04-0009 "Assessment of Geotechnical Issues in Acute Care Facilities in California," by M. Lew, T.D. O'Rourke, R. Dobry and M. Koch, 9/15/04, (PB2005-104893, A08, CD-A00).

MCEER-04-0010 "Scissor-Jack-Damper Energy Dissipation System," by A.N. Sigaher-Boyle and M.C. Constantinou, 12/1/04 (PB2005-108221).

MCEER-04-0011 "Seismic Retrofit of Bridge Steel Truss Piers Using a Controlled Rocking Approach," by M. Pollino and M. Bruneau, 12/20/04 (PB2006-105795).

MCEER-05-0001 "Experimental and Analytical Studies of Structures Seismically Isolated with an Uplift-Restraint Isolation System," by P.C. Roussis and M.C. Constantinou, 1/10/05 (PB2005-108222).

MCEER-05-0002 "A Versatile Experimentation Model for Study of Structures Near Collapse Applied to Seismic Evaluation of Irregular Structures," by D. Kusumastuti, A.M. Reinhorn and A. Rutenberg, 3/31/05 (PB2006-101523).

MCEER-05-0003 "Proceedings of the Third PRC-US Workshop on Seismic Analysis and Design of Special Bridges," edited by L.C. Fan and G.C. Lee, 4/20/05, (PB2006-105796).

MCEER-05-0004 "Approaches for the Seismic Retrofit of Braced Steel Bridge Piers and Proof-of-Concept Testing of an Eccentrically Braced Frame with Tubular Link," by J.W. Berman and M. Bruneau, 4/21/05 (PB2006-101524).

MCEER-05-0005 "Simulation of Strong Ground Motions for Seismic Fragility Evaluation of Nonstructural Components in Hospitals," by A. Wanitkorkul and A. Filiatrault, 5/26/05 (PB2006-500027).

MCEER-05-0006 "Seismic Safety in California Hospitals: Assessing an Attempt to Accelerate the Replacement or Seismic Retrofit of Older Hospital Facilities," by D.J. Alesch, L.A. Arendt and W.J. Petak, 6/6/05 (PB2006-105794).

MCEER-05-0007 "Development of Seismic Strengthening and Retrofit Strategies for Critical Facilities Using Engineered Cementitious Composite Materials," by K. Kesner and S.L. Billington, 8/29/05 (PB2006-111701).

MCEER-05-0008 "Experimental and Analytical Studies of Base Isolation Systems for Seismic Protection of Power Transformers," by N. Murota, M.Q. Feng and G-Y. Liu, 9/30/05 (PB2006-111702).

MCEER-05-0009 "3D-BASIS-ME-MB: Computer Program for Nonlinear Dynamic Analysis of Seismically Isolated Structures," by P.C. Tsopelas, P.C. Roussis, M.C. Constantinou, R. Buchanan and A.M. Reinhorn, 10/3/05 (PB2006-111703).

MCEER-05-0010 "Steel Plate Shear Walls for Seismic Design and Retrofit of Building Structures," by D. Vian and M. Bruneau, 12/15/05 (PB2006-111704).

MCEER-05-0011 "The Performance-Based Design Paradigm," by M.J. Astrella and A. Whittaker, 12/15/05 (PB2006-111705).

MCEER-06-0001 "Seismic Fragility of Suspended Ceiling Systems," H. Badillo-Almaraz, A.S. Whittaker, A.M. Reinhorn and G.P. Cimellaro, 2/4/06 (PB2006-111706).

MCEER-06-0002 "Multi-Dimensional Fragility of Structures," by G.P. Cimellaro, A.M. Reinhorn and M. Bruneau, 3/1/06 (PB2007-106974, A09, MF-A02, CD A00).

MCEER-06-0003 "Built-Up Shear Links as Energy Dissipators for Seismic Protection of Bridges," by P. Dusicka, A.M. Itani and I.G. Buckle, 3/15/06 (PB2006-111708).

MCEER-06-0004 "Analytical Investigation of the Structural Fuse Concept," by R.E. Vargas and M. Bruneau, 3/16/06 (PB2006-111709).

MCEER-06-0005 "Experimental Investigation of the Structural Fuse Concept," by R.E. Vargas and M. Bruneau, 3/17/06 (PB2006-111710).

MCEER-06-0006 "Further Development of Tubular Eccentrically Braced Frame Links for the Seismic Retrofit of Braced Steel Truss Bridge Piers," by J.W. Berman and M. Bruneau, 3/27/06 (PB2007-105147).

MCEER-06-0007 "REDARS Validation Report," by S. Cho, C.K. Huyck, S. Ghosh and R.T. Eguchi, 8/8/06 (PB2007-106983).

MCEER-06-0008 "Review of Current NDE Technologies for Post-Earthquake Assessment of Retrofitted Bridge Columns," by J.W. Song, Z. Liang and G.C. Lee, 8/21/06 (PB2007-106984).

MCEER-06-0009 "Liquefaction Remediation in Silty Soils Using Dynamic Compaction and Stone Columns," by S. Thevanayagam, G.R. Martin, R. Nashed, T. Shenthan, T. Kanagalingam and N. Ecemis, 8/28/06 (PB2007-106985).

MCEER-06-0010 "Conceptual Design and Experimental Investigation of Polymer Matrix Composite Infill Panels for Seismic Retrofitting," by W. Jung, M. Chiewanichakorn and A.J. Aref, 9/21/06 (PB2007-106986).

MCEER-06-0011 "A Study of the Coupled Horizontal-Vertical Behavior of Elastomeric and Lead-Rubber Seismic Isolation Bearings," by G.P. Warn and A.S. Whittaker, 9/22/06 (PB2007-108679).

MCEER-06-0012 "Proceedings of the Fourth PRC-US Workshop on Seismic Analysis and Design of Special Bridges: Advancing Bridge Technologies in Research, Design, Construction and Preservation," Edited by L.C. Fan, G.C. Lee and L. Ziang, 10/12/06 (PB2007-109042).

MCEER-06-0013 "Cyclic Response and Low Cycle Fatigue Characteristics of Plate Steels," by P. Dusicka, A.M. Itani and I.G. Buckle, 11/1/06 06 (PB2007-106987).

MCEER-06-0014 "Proceedings of the Second US-Taiwan Bridge Engineering Workshop," edited by W.P. Yen, J. Shen, J-Y. Chen and M. Wang, 11/15/06 (PB2008-500041).

MCEER-06-0015 "User Manual and Technical Documentation for the REDARS^{TM} Import Wizard," by S. Cho, S. Ghosh, C.K. Huyck and S.D. Werner, 11/30/06 (PB2007-114766).

MCEER-06-0016 "Hazard Mitigation Strategy and Monitoring Technologies for Urban and Infrastructure Public Buildings: Proceedings of the China-US Workshops," edited by X.Y. Zhou, A.L. Zhang, G.C. Lee and M. Tong, 12/12/06 (PB2008-500018).

MCEER-07-0001 "Static and Kinetic Coefficients of Friction for Rigid Blocks," by C. Kafali, S. Fathali, M. Grigoriu and A.S. Whittaker, 3/20/07 (PB2007-114767).

MCEER-07-0002 "Hazard Mitigation Investment Decision Making: Organizational Response to Legislative Mandate," by L.A. Arendt, D.J. Alesch and W.J. Petak, 4/9/07 (PB2007-114768).

MCEER-07-0003 "Seismic Behavior of Bidirectional-Resistant Ductile End Diaphragms with Unbonded Braces in Straight or Skewed Steel Bridges," by O. Celik and M. Bruneau, 4/11/07 (PB2008-105141).

MCEER-07-0004 "Modeling Pile Behavior in Large Pile Groups Under Lateral Loading," by A.M. Dodds and G.R. Martin, 4/16/07(PB2008-105142).

MCEER-07-0005 "Experimental Investigation of Blast Performance of Seismically Resistant Concrete-Filled Steel Tube Bridge Piers," by S. Fujikura, M. Bruneau and D. Lopez-Garcia, 4/20/07 (PB2008-105143).

MCEER-07-0006 "Seismic Analysis of Conventional and Isolated Liquefied Natural Gas Tanks Using Mechanical Analogs," by I.P. Christovasilis and A.S. Whittaker, 5/1/07.

MCEER-07-0007 "Experimental Seismic Performance Evaluation of Isolation/Restraint Systems for Mechanical Equipment – Part 1: Heavy Equipment Study," by S. Fathali and A. Filiatrault, 6/6/07 (PB2008-105144).

MCEER-07-0008 "Seismic Vulnerability of Timber Bridges and Timber Substructures," by A.A. Sharma, J.B. Mander, I.M. Friedland and D.R. Allicock, 6/7/07 (PB2008-105145).

MCEER-07-0009 "Experimental and Analytical Study of the XY-Friction Pendulum (XY-FP) Bearing for Bridge Applications," by C.C. Marin-Artieda, A.S. Whittaker and M.C. Constantinou, 6/7/07 (PB2008-105191).

MCEER-07-0010 "Proceedings of the PRC-US Earthquake Engineering Forum for Young Researchers," Edited by G.C. Lee and X.Z. Qi, 6/8/07.

MCEER-07-0011 "Design Recommendations for Perforated Steel Plate Shear Walls," by R. Purba and M. Bruneau, 6/18/07, (PB2008-105192).

MCEER-07-0012 "Performance of Seismic Isolation Hardware Under Service and Seismic Loading," by M.C. Constantinou, A.S. Whittaker, Y. Kalpakidis, D.M. Fenz and G.P. Warn, 8/27/07, (PB2008-105193).

MCEER-07-0013 "Experimental Evaluation of the Seismic Performance of Hospital Piping Subassemblies," by E.R. Goodwin, E. Maragakis and A.M. Itani, 9/4/07, (PB2008-105194).

MCEER-07-0014 "A Simulation Model of Urban Disaster Recovery and Resilience: Implementation for the 1994 Northridge Earthquake," by S. Miles and S.E. Chang, 9/7/07, (PB2008-106426).

MCEER-07-0015 "Statistical and Mechanistic Fragility Analysis of Concrete Bridges," by M. Shinozuka, S. Banerjee and S-H. Kim, 9/10/07, (PB2008-106427).

MCEER-07-0016 "Three-Dimensional Modeling of Inelastic Buckling in Frame Structures," by M. Schachter and AM. Reinhorn, 9/13/07, (PB2008-108125).

MCEER-07-0017 "Modeling of Seismic Wave Scattering on Pile Groups and Caissons," by I. Po Lam, H. Law and C.T. Yang, 9/17/07 (PB2008-108150).

MCEER-07-0018 "Bridge Foundations: Modeling Large Pile Groups and Caissons for Seismic Design," by I. Po Lam, H. Law and G.R. Martin (Coordinating Author), 12/1/07 (PB2008-111190).

MCEER-07-0019 "Principles and Performance of Roller Seismic Isolation Bearings for Highway Bridges," by G.C. Lee, Y.C. Ou, Z. Liang, T.C. Niu and J. Song, 12/10/07.

MCEER-07-0020 "Centrifuge Modeling of Permeability and Pinning Reinforcement Effects on Pile Response to Lateral Spreading," by L.L Gonzalez-Lagos, T. Abdoun and R. Dobry, 12/10/07 (PB2008-111191).

MCEER-07-0021 "Damage to the Highway System from the Pisco, Perú Earthquake of August 15, 2007," by J.S. O'Connor, L. Mesa and M. Nykamp, 12/10/07, (PB2008-108126).

MCEER-07-0022 "Experimental Seismic Performance Evaluation of Isolation/Restraint Systems for Mechanical Equipment – Part 2: Light Equipment Study," by S. Fathali and A. Filiatrault, 12/13/07 (PB2008-111192).

MCEER-07-0023 "Fragility Considerations in Highway Bridge Design," by M. Shinozuka, S. Banerjee and S.H. Kim, 12/14/07 (PB2008-111193).

MCEER-07-0024 "Performance Estimates for Seismically Isolated Bridges," by G.P. Warn and A.S. Whittaker, 12/30/07 (PB2008-112230).

MCEER-08-0001 "Seismic Performance of Steel Girder Bridge Superstructures with Conventional Cross Frames," by L.P. Carden, A.M. Itani and I.G. Buckle, 1/7/08, (PB2008-112231).

MCEER-08-0002 "Seismic Performance of Steel Girder Bridge Superstructures with Ductile End Cross Frames with Seismic Isolators," by L.P. Carden, A.M. Itani and I.G. Buckle, 1/7/08 (PB2008-112232).

MCEER-08-0003 "Analytical and Experimental Investigation of a Controlled Rocking Approach for Seismic Protection of Bridge Steel Truss Piers," by M. Pollino and M. Bruneau, 1/21/08 (PB2008-112233).

MCEER-08-0004 "Linking Lifeline Infrastructure Performance and Community Disaster Resilience: Models and Multi-Stakeholder Processes," by S.E. Chang, C. Pasion, K. Tatebe and R. Ahmad, 3/3/08 (PB2008-112234).

MCEER-08-0005 "Modal Analysis of Generally Damped Linear Structures Subjected to Seismic Excitations," by J. Song, Y-L. Chu, Z. Liang and G.C. Lee, 3/4/08.

MCEER-08-0006 "System Performance Under Multi-Hazard Environments," by C. Kafali and M. Grigoriu, 3/4/08 (PB2008-112235).

MCEER-08-0007 "Mechanical Behavior of Multi-Spherical Sliding Bearings," by D.M. Fenz and M.C. Constantinou, 3/6/08 (PB2008-112236).

MCEER-08-0008 "Post-Earthquake Restoration of the Los Angeles Water Supply System," by T.H.P. Tabucchi and R.A. Davidson, 3/7/08 (PB2008-112237).

MCEER-08-0009 "Fragility Analysis of Water Supply Systems," by A. Jacobson and M. Grigoriu, 3/10/08.

MCEER-08-0010 "Experimental Investigation of Full-Scale Two-Story Steel Plate Shear Walls with Reduced Beam Section Connections," by B. Qu, M. Bruneau, C-H. Lin and K-C. Tsai, 3/17/08.

MCEER
EARTHQUAKE ENGINEERING TO EXTREME EVENTS
University at Buffalo, The State University of New York
Red Jacket Quadrangle ▪ Buffalo, New York 14261
Phone: (716) 645-3391 ▪ Fax: (716) 645-3399
E-mail: *mceer@buffalo.edu* ▪ WWW Site *http://mceer.buffalo.edu*
University at Buffalo *The State University of New York*

ISSN 1520-295X